INAUGURAL - DISSERTATION

zur
Erlangung der Doktorwürde
der
Naturwissenschaftlich-Mathematischen Gesamtfakultät
der Ruprecht-Karls-Universität
Heidelberg

vorgelegt von
Lindsay J. Murrells

Tag der mündlichen Prüfung: 16. Oktober 2008

DISSERTATION

submitted to the
Combined Faculties for the Natural Sciences and for Mathematics
of the Ruperto-Carola University of Heidelberg, Germany
for the degree of
Doctor of Natural Sciences

presented by

Lindsay J. Murrells

Date of oral examination: 16th October 2008

Microtubule-associated proteins in fission yeast

Referees: Dr. Darren Gilmour
Prof. Elmar Schiebel

Summary

The highly conserved Dis1/XMAP215 family of microtubule-associated proteins (MAPs) play a central role in cytoplasmic microtubule organisation and mitotic spindle formation. The fission yeast *S. pombe* has two family members, Alp14 and Dis1. Both localise to interphase microtubules, spindle pole bodies (the yeast equivalent of the centrosome), and kinetochores. Here we present the characterisation of Alp14 and Dis1 during interphase. We find that Alp14 localisation resembles that of Mal3, a canonical plus end tracking protein. Deletion results in a decrease in the number and length of interphase microtubule bundles at low temperatures. Alp14 is temperature sensitive. At the restrictive temperature we find that an interphasic intranuclear microtubule bundle forms, nucleated from the region of the spindle pole bodies and kinetochores. This intranuclear bundle has a structure and displays dynamics similar to that of a normal interphase bundle and is able to move the nucleus. Dis1 localises to interphase microtubules but does not show plus end tracking behaviour. Deletion has no apparent effect on the organisation of interphase microtubules, but Dis1 is cold sensitive and at the restrictive temperature the cells become blocked in mitosis with aster-like spindles. Deletion of both *alp14* and *dis1* is lethal. We investigate the functional redundancy between Alp14 and Dis1 during interphase. Over-expression of Dis1 in *alp14*Δ cells can partially rescue the mutant microtubule phenotype. Conversely, attenuated expression of Dis1 in an *alp14*Δ background results in almost complete loss of interphase microtubules. We conclude that the presence of at least one of the Dis1/XMAP215 homologues is essential for the maintenance of interphase microtubule arrays.

Similar to Alp14, Tip1 is a microtubule plus-end tracking protein, homologous to human CLIP170. Together with the EB1 homologue, Mal3, Tip1 spatially regulates microtubule dynamics, ensuring that the cylindrical cell shape of *S. pombe is* maintained. In the second part of this thesis the characterisation of the protein SPCC736.15 (Toi4), identified in a screen for Tip1-interacting proteins is presented. During interphase, Toi4p-GFP localises to the central regions of the cell cortex. Shortly before mitosis, Toi4p-GFP begins to accumulate at the cell ends. Concurrent with the onset of mitosis, there is exclusion of Toi4p-GFP from the region of the cell cortex where the actomyosin ring forms and the cell subsequently divides. The *S. cerevisiae* homologue of Toi4p is Pil1p, which is proposed to be the major component of an endocytic organelle termed the eisosome. We tested for such a role for Toi4 in *S. pombe*, however we detect no link between Toi4 and endocytosis, suggesting that the homologues, although they have a similar localisation pattern, may perform different functions.

Zusammenfassung

Die Mitglieder der Dis1/XMAP215 Proteinfamilie gehören zu den Mikrotubuli assoziierten Proteinen (MAPs). Die stark konservierten Proteine spielen eine wichtige Rolle bei der Organisation der Mikrotubuli im Cytoplasma und beim Aufbau der mitotischen Spindel. In der Spalthefe *S. pombe* gibt es zwei Mitglieder dieser Proteinfamilie, Alp14 und Dis1, die beide auf die Mikrotubuli der Interphase, die Spindelpolkörper (SPB) und die Kinetochoren lokalisieren. In dieser Arbeit werden die Eigenschaften dieser beiden Proteine während der Interphase analysiert und beschrieben. Unsere Untersuchungen haben ergeben, dass die Lokalisierung von Alp14 der von Mal3 ähnelt, das für gewöhnlich am wachsenden plus-Ende und im Bereich der minus-Enden der Mikrotubuli sitzt. Die Eliminierung des Proteins durch Gendeletion (*alp14*Δ), resultiert, bei niedriger Temperatur, in einer Abnahme der Anzahl und Länge von Interphasenmikrotubuli-Bündeln. Bei erhöhter Temperatur bildet sich trotz Interphase, ein einzelnes Mikrotubuli-Bündel im Zellkern was normalerweise nur in der Mitose geschieht. Dieses intra-nukleäre Bündel entspringt aus der Region von SPB und Kinetochoren. Es ähnelt in seiner Struktur und Dynamik einem cytoplasmatischen Mikrotubuli-Bündel und hat die Fähigkeit, den Zellkern zu verschieben. Dis1 befindet sich während der Interphase ebenfalls an den Mikrotubuli, ist jedoch entlang der gesamten Mikrotubuli verteilt und beschränkt sich nicht auf das plus- und minus-Ende. Die Eliminierung des *dis1* Genes hat keinen offensichtlichen Einfluss auf die Organisation der Mikrotubuli in der Interphase. Bei tiefen Temperaturen wird jedoch die Mitose der Zelle blockiert und die Spindeln besitzen abnormale, asterförmige Strukturen. Zellen in denen *alp14* und *dis1* gleichzeitig eliminiert wurden, sind nicht überlebensfähig. In dieser Arbeit wird die offensichtliche funkionelle Redundanz von Alp14 und Dis1 in der Interphase untersucht. Wird Dis1 in *alp14*Δ Zellen überexprimiert, so tritt der oben beschriebene Mikrotubulidefekt nicht mehr auf. Im Gegenzug führt eine verminderte Exprimierung von Dis1 in *alp14*Δ Zellen zu einem beinahe vollständigen Verlust der Interphasenmikrotubuli. Wir folgern, dass mindestens eines der beiden Proteine für die Aufrechterhaltung der Interphasenmikrotubuli unverzichtbar ist.

Wie Alp14 ist Tip1 ein Protein, welches sich an den Plus-Enden der Mikrotubuli befindet. Es ist homolog zu humanem CLIP170 und reguliert zusammen mit dem EB1-Homolog Mal3 die Dynamik der Mikrotubuli in Abhängigkeit von ihrer Position. Auf diese Weise wird die Erhaltung der Bipolaritaet der Zelle sicher gestellt. Der zweite Teil dieser Arbeit charakterisiert das Protein SPCC736.15 (Toi4), welches in einem Screen als Interaktionspartner von Tip1 identifiziert werden konnte. Waehrend der Interphase ist Toi4 im zentralen Bereich des Zellkortex lokalisiert, kurz vor Einsetzen der Mitose hingegen, sammelt es sich an den Zellenden. Toi4p-GFP verschwindet an den Stellen im Kortex, wo sich zu Beginn der Mitose der Aktomyosin-Ring ausbildet und anschliessend die Zellteilung stattfindet. Das Protein Pil1p in *S. cerevisiae* ist homolog zu Toi4p. Pil1p ist eine wichtige Komponente in Eisosomen, welche, so vermutet man, endozytotische Organellen sind. Wir untersuchten Toi4 im Hinblick auf diese Funktion in *S. pombe*, konnten jedoch keinen Zusammenhang von Toi4 und Endozytose feststellen. Dieses Ergebnis deutet darauf hin, dass die beiden Homologe trotz ihrer ähnlichen Lokalisierung unterschiedliche Funktionen erfüllen.

Acknowledgements

First and foremost, thanks to my supervisor Dr Damian Brunner, without whom the work presented in this thesis would not have been possible: It's been a lot of fun working in your lab and your enthusiasm for science is contagious. I really appreciate your continuous support! Next, many thanks to the members of my Thesis Advisory Committee, Dr. Darren Gilmour, Dr. Elmar Schiebel and Prof. Iain Mattaj for their helpful input throughout my Ph.D. and additionally to Prof. Jochen Wittbrodt and Dr. Marko Kaksonen for agreeing to be my Ph.D. examiners.

For reagents, equipment and advice, I'm grateful to the Knop, Gilmour, Karsenti, Pepperkok and Surry labs. Many thanks also to members of the EMBL Advanced Light Microscopy Facility. For help with graphics and printing thanks to the members of the EMBL Photolab. Also thanks to Aidan Budd for help with the sequence alignments.

Thanks to Mika Toya and Emanuel Busch for starting off the projects presented here.

A special thanks goes to the members of the Brunner lab, both past and present: (in no particular order!) Aynur Kaya, Linda Sandblad, Ferenc Jankovics, Catarina Resende, Imola Aprill, Andreia Feijao, Paulo Alves, Nadia Dube, Stephen Huisman, Tatyana Makushok, Tanja Georg, Emanuel Busch and Jerome Solon. Also to additional members of the PomPom Club: Dietrich (and Christina) Foethke, Helio Roque and Johanna Höög. You kept me going when things got tough, and supported me throughout my time at EMBL, from cake, to proof reading and formatting my thesis. Words can't express my gratitude and there's certainly not enough space here! I'm going to miss our coffee break discussions and lab fun together.

Throughout my time at EMBL I've enjoyed and appreciated the opportunity to be involved in organising the Student 'Biology at Work' Symposium, several writing competitions and teaching. Thanks to those who made these possible, in particular Julia Willingale-Theune.

Thanks also to my other friends at EMBL and Calvary Chapel Heidelberg for your support, friendship and for helping me to keep things in perspective. You know who you are!

Mum, Dad and Jonny: You've always been there for me and supported my ambitious plans wholeheartedly, to whichever country it lead. Thank you so much. You're the best!!

Soli Deo Gloria

Table of Contents

Abbreviations

ADP	Adenosine diphosphate
APC	Adenomatous Polyposis Coli
ATP	Adenosine priphosphate
ATPase	Adenosine triphosphate hydrolase
CAP-Gly	Cytoskeletal associated protein-gylcine rich
CLIP	Cytoplasmic linker protein
co-IP	Co-immunoprecipation
EB1	End Binding protein 1
DMSO	Dimethylsulphoxide
dNTPs	De-oxynucleotide triphosphase
dsRed	*Discosoma sp*. red fluorescent protein
DTT	Dithriothreitol
EDTA	Ethylendiaminotetraacetic acid
EMM2	Edinburgh minimal medium 2
GDP	Guanosine diphosphate
GFP	Green fluorescent protein
GMPCPP	Guanosine-5'-([α,β]-Methyleno)-triphosphate
GST	Glutathione-S-transferase
GTP	Guanosine triphosphate
HA	Haemagglutinin A
HEPES	N-(2-hydroxyethyl)-piperazine-N'-(2-ethanesulphonic acid)
HRP	Horeseradish peroxidase
HU	Hydroxyurea
IgG	Immunoglobulin
iMTOC	Interphase microtubule organising centre
kDa	Kilo Dalton
M	Molar
mA	Milli Ampere
MAP	Microtubule-associated protein
MBC	Methyl-2-benzimidazole
mm	Millimetre
MTOC	Microtubule organising centre
N.A.	Numerical Aperture
nm	Nanometre
nM	Nanomolar

μm	Micrometre
OD	Optical density
PAGE	Polyacrylamide gel electrophoresis
PBS	Phosphate buffered saline
PCR	Polymerase chain reaction
PIPES	4-(2-hydroxyethyl)-1-piperazineethanesulphonic acid
RFP	Red fluorescent protein
RNAi	RNA interference
SDS	Sodium dodecyl sulphate
SPB	Spindle pole body
TACC protein	Transforming acidic coiled-coil protein
Toi protein	Tip1-interacting protein
Tris	Tris-(hydroxymethyl)-aminomethane
TRITC	Tetramethylrhodamine isothiocyanate
YE5'S	Yeast extract medium containing 5 supplements
+TIP	Microtubule plus end associated protein
μM	Micromolar
γ-TURC	Gamma-Tubulin ring complex

1. Introduction

1.1. Cell Polarity

Cell polarity is an essential feature for all cells and is the basis for most fundamental cellular processes, such as growth, differentiation and migration. Polarity can refer to cell shape, or the arrangement of cellular components such that they have a specific non-symmetrical three-dimensional organisation. The correct placement of polarity factors is essential to enable each cell to carry out its specific functions and often cells are required to respond quickly to external or developmental stimuli through a reorganisation of cell polarity.

Establishment of cell polarity in all organisms proceeds in accordance with the following general principles: *De novo* establishment of polarity requires an initial trigger, such as a signalling event, however polarity is often inherited from a previous cell cycle through pre-localised polarity factors. A landmark protein then marks this site and small GTPases in its vicinity establish polarity. Polarised growth occurs as the result of cytoskeletal reorganisation. Once polarity is established, feedback loops involving signalling and cytoskeletal proteins and membrane components function to stabilise and maintain this polarity (Pringle *et al.*, 1995; Drubin, 1991).

1.1.1. Establishment of polarity as exemplified by bud site positioning in *S. cerevisiae*

The budding yeast, *Saccharomyces cerevisiae* has been extensively used as a model organism for the study of cell polarity and exemplifies the specific stages of polarity establishment outlined above. In haploid cells, which contain only one copy of each chromosome, the 'bud scar' from the previous cell division provides the polar landmark that determines the location of the next bud site. This site is next to the old scar. Septins localised as the bud scar recruit Bud proteins, triggering a phosphorylation cascade that establishes polarity through activation of a further GTPase Cdc42. Cdc42-GTP induces nucleation of actin filaments, which deliver secretory vesicles to the bud site enabling cell membrane distortion and the formation

of a daughter bud (Figure 1.1; reviewed in Irazoqui and Lew, 2004; Pruyne *et al.*, 2004; Chang and Peter, 2003).

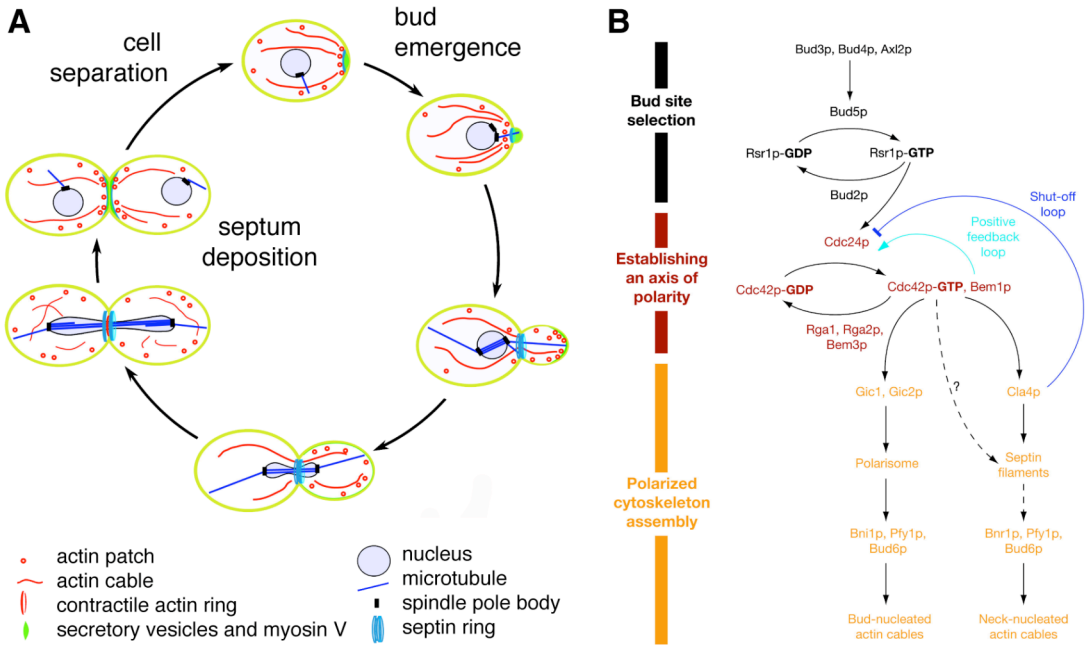

Figure 1.1 Bud formation *in S. cerevisiae*

(A) Organisation of cytoskeletal structures that guide polarised growth during the budding yeast cell cycle. (B) Simplified overview of the signalling pathways that lead to the establishment of a polarised cytoskeleton during the early stages of bud formation in haploid cells. Modified from Pruyne *et al.* (2004).

1.2. The cytoskeleton

In order to create a polarised cell, there exists a filamentous cytoskeletal network that provides a structural and mechanical framework for cells.

The eukaryotic cytoskeleton consists of three filamentous polymers: actin, intermediate filaments and microtubules.

1.2.1. Actin

Actin consists of globular (g-actin) monomers which can polymerise to form a left-handed helical filament of two intertwined strands ~6nm in diameter (f-actin; Figure

1.2A). Actin monomers are polar, therefore filamentous actin has an internal polarity, with a highly dynamic plus (barbed) end, and a less dynamic (pointed) minus end (Steinmetz *et al.*, 1997; Kabsch and Vandekerckhove, 1992).

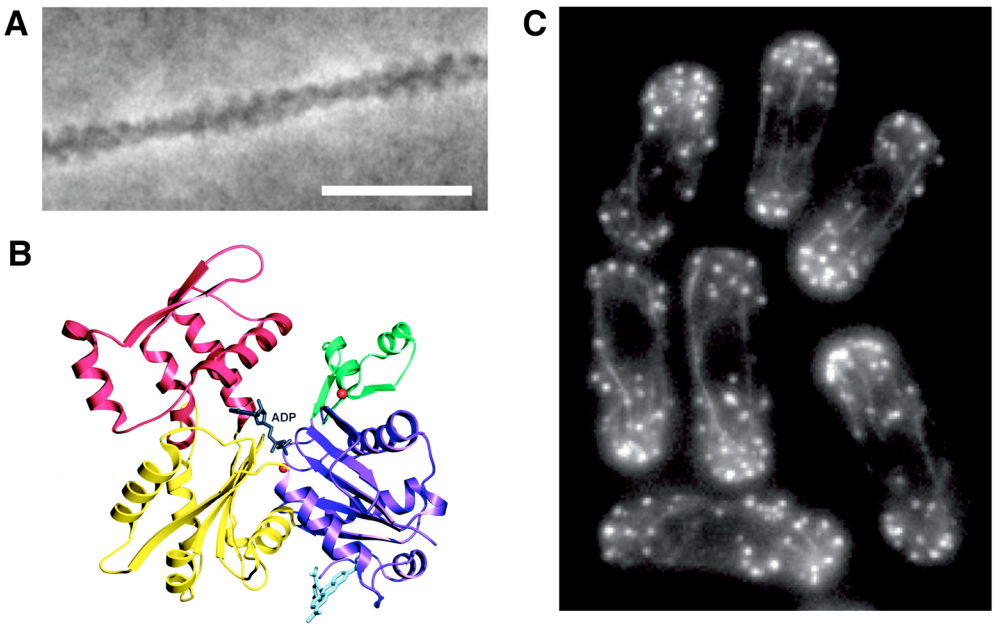

Figure 1.2 The actin cytoskeleton

(A) Electron micrograph of negatively stained actin filaments (Steinmetz *et al.*, 1997). Bar, 25 nm. (B) Ribbon representation of the structure of actin bound to ADP. The four sub domains of actin are represented in different colours. ADP is bound at the centre of the molecule, where the four actin subdomains meet (Otterbein *et al.*, 2001). (C) Actin patches and cables in *S. pombe* cells. Image courtesy of D. Foethke and I. Aprill.

Under physiological conditions, actin polymerisation occurs 12 times faster at the plus end than at the minus end. This, combined with a faster rate of subunit loss at the minus end than at the plus end, generates a flux of actin movement through the filament known as treadmilling: subunits are added at the plus end and then subsequently lost from the minus end (Weger and Isenberg, 1983). The energy for actin polymerisation is acquired through hydrolysis of ATP at a cleft in the centre of the molecule (Figure 1.2B; Carlier *et al.*, 1992). This dynamic assembly and disassembly of actin is crucial to its function and is tightly regulated by numerous actin-binding proteins (reviewed in dos Remedios *et al.*, 2003).

Actin is present in all cells and is essential for all types of motile processes, enriched at sites of growth, where it can exert pushing forces on the cell membrane as a result

of its treadmilling behaviour, to generate membrane protrusions called lamellipodia and filopodia (Pollard and Borisy, 2003). Actin is most abundant in muscle cells where it, together with the motor protein myosin, is responsible for muscle contraction (Squire, 1997). Another example of where actin and myosin together are able to exert a contractile force is constriction of the cytokinetic ring to separate daughter cells at the final stages of cell division (Satterwhite and Pollard, 1992). Actin and actin-binding proteins are also required for endo- and exocytosis and RNA, organelle and vesicle trafficking (dos Remedios *et al.*, 2003). In fission yeast, actin forms patches at the growing cell ends where it interacts with a network of actin- and microtubule-associated proteins to regulate cell growth and polarity. Actin cables are also enriched at the cell poles (Figure 1.2C; Martin and Chang, 2006; Martin *et al.*, 2005).

1.2.2. Intermediate filaments

Intermediate filaments are rope-like fibres with a diameter of ~11nm, so named because they have a diameter intermediate between thin and thick muscle fibres. They constitute a large diverse family of proteins, often expressed tissue specifically and can be identified by their structural, rather than sequence homology (Chang and Goldman, 2004; Herrmann *et al.*, 2003; Herrmann and Foisner, 2003). All intermediate filaments have a central coiled-coil core, with flanking sequences that vary in size and confer the specific functions of this protein family. The intermediate filament monomer is itself rod-shaped, conferred by the central coiled-coil, and can spontaneously polymerise into first dimers and then filaments without the energy required from nucleotide hydrolysis (Strelkov *et al.*, 2003). In contrast to actin and microtubules, intermediate filaments are not polar, however in common with microtubules and actin they can be highly dynamic, with phosphorylation playing a role in their regulation (Helfand *et al.*, 2004). The main role of intermediate filaments seems to be that of a scaffold, providing support to maintain cell and tissue structure; they are flexible but inextensible, thus preventing excessive stretching of tissues (Omary *et al.*, 2004). One of the better-studied examples is the nuclear lamins, which stabilise the nuclear envelope of higher eukaryotes by forming a meshwork under the nuclear membrane. This also serves to anchor the nuclear pores and chromosomes (Dechat *et al.*, 2008). Other common intermediate filament proteins are the vimentins, expressed in fibroblasts and endothelial cells (Figure 1.3). Keratins, the major component of nail and hair and neurofilaments, are found in axons and dendrites. Intermediate filaments have been shown to interact with microtubules and actin and

even to travel along microtubules as cargo of the motors kinesin and dynein, but no molecular motors that travel along intermediate filaments have been identified to date (Helfand *et al.*, 2004; Herrmann and Aebi, 2004).

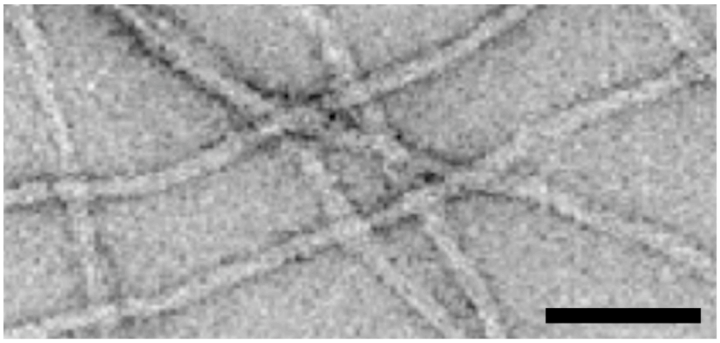

Figure 1.3

Intermediate filaments

Electron micrograph of negatively stained vimentin filaments (Goldie *et al.* 2007). Bar, 50 nm.

1.3. Microtubules

Microtubules are essential for cell polarity, cell division, motility and intracellular transport.

1.3.1. Microtubule structure and polarity

The building blocks of microtubules are ~50 kDa α- and β-tubulin molecules, which share 40% sequence identity and have very similar structures. α- and β-tubulin form heterodimers, which are subsequently arranged head to tail into linear protofilaments. Each microtubule is composed of on average 13 protofilaments, although microtubules with 9-16 protofilaments also exist. Protofilaments associate laterally to form a closed, straight, hollow cylinders of ~25nm (Desai and Mitchison, 1997; Evans *et al.*, 1985; Tilney *et al.*, 1973). Due to the alternation of α- and β-tubulin in the protofilaments, microtubules are intrinsically polar, with β-tubulin at the 'plus' ends and α-tubulin at the 'minus' ends. Like actin, tubulin requires nucleotide binding for polymer assembly. α- and β-tubulin both bind GTP, but only β-tubulin has GTPase activity (Figure 1.4A; Mitchison and Kirschner, 1984).

Microtubules with 13 protofilaments have a predominantly B-lattice structure, in which tubulin homodimers of neighbouring protofilaments form lateral contacts. Cryo-electron microscopy of polymerising microtubules suggests that the protofilaments first associate laterally into a sheet, which then closes to form a tube. At the point at which the tube closes there is a mismatch in the B-lattice structure and

α- and β-tubulin subunits associate laterally to form a local A-lattice structure termed the lattice seam (Figure 1.4B,C; Chretien *et al.*, 1995; Chretien and Wade, 1991; Wade *et al.*, 1990; Mandelkow *et al.*, 1986).

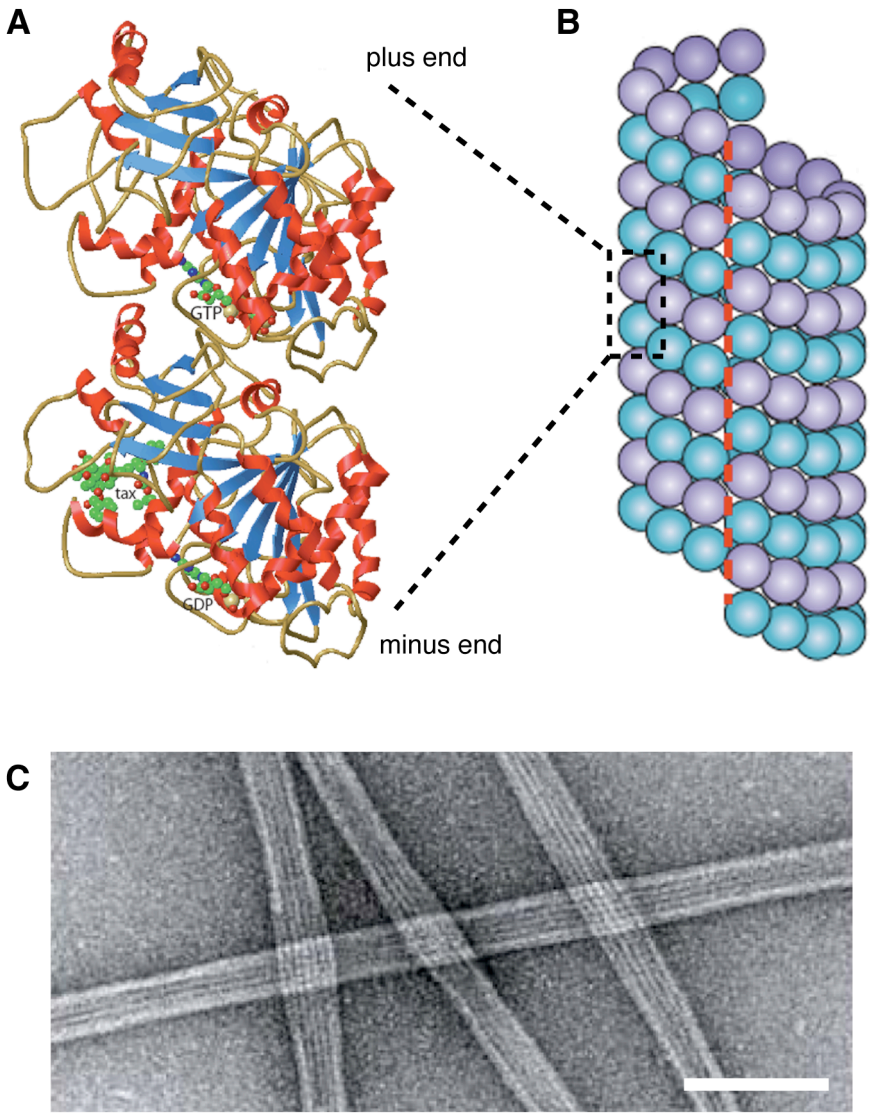

Figure 1.4 Microtubule structure

(A) Ribbon diagram of the structure of a tubulin heterodimer. α-tubulin is shown on top, bound to GTP. β-tubulin on the bottom contains GDP and taxotere, an analogue of taxol that stabilises microtubules against depolymerisation. The structure was obtained by electron crystallography of zinc-induced tubulin sheets (Nogales *et al.*, 1998). (B) Cartoon diagram of a microtubule with 13 parallel protofilaments. A red dashed line indicates the lattice seam. Adapted from Akhmanova and Steinmetz (2008). (C) Electron micrograph of negatively stained microtubules, courtesy of L. Sandblad. Bar, 100 nm.

1.3.2. Dynamic behaviour of microtubules

The functions of microtubules are largely dependent upon their dynamic properties. Microtubule switch stochastically from growth to shrinkage and *vice versa* by addition or loss of tubulin subunits at their ends, a behaviour termed 'dynamic instability' (Mitchison and Kirschner, 1984). This behaviour allows microtubules to rearrange in response to environmental cues and interact with intracellular targets. Observations of the non-equilibrium behaviour of microtubules *in vitro* lead to the following model of dynamic instability.

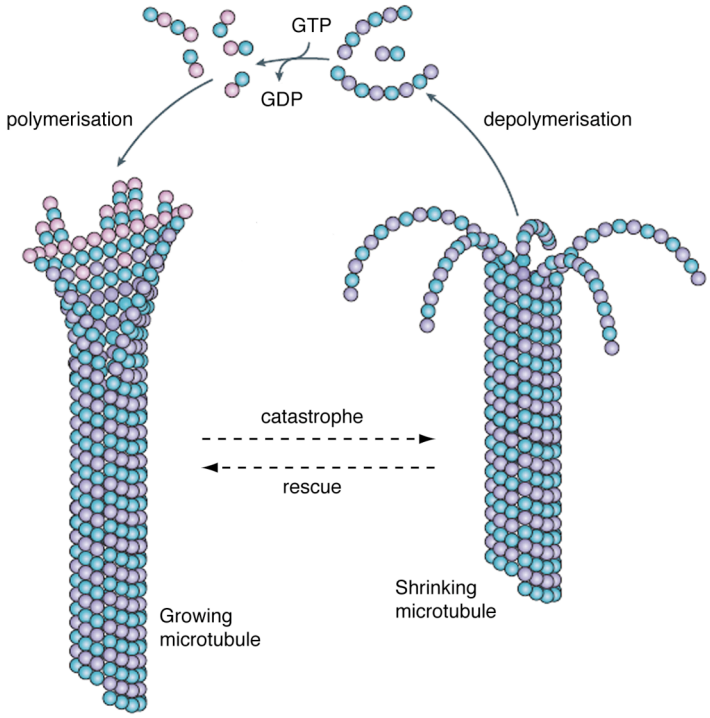

Figure 1.5

Microtubule dynamic instability model

See text for details. Adapted from Akhmanova and Steinmetz, 2008.

The model states that microtubules show phases of polymerisation (growth) and de-polymerisation (shrinkage) and stochastically transition between these two states. Transition from growth to shrinkage is called a 'catastrophe', and from shrinkage to growth is termed 'rescue'. Microtubules can also pause, a state in which they neither grow nor shrink. Four parameters are used to describe microtubule behaviour: the rates of growth and shrinkage and the frequencies of catastrophe and rescue (Figure 1.5). *In vitro,* both the plus and minus ends of microtubule show dynamic instability, however, *in vivo* the minus ends are generally capped and stabilised (see Section 1.3.3.1). Dynamic instability is driven by GTP hydrolysis. Tubulin dimers added to the plus end of microtubules are GTP-bound and form a so-called 'GTP cap' at the plus end. GTP hydrolysis is not required for binding of tubulin dimers to the microtubule, as microtubules polymerise in the presence of a non-hydrolysable GTP

analogue, GMPCPP, rather GTP hydrolysis enables depolymerisation (Amos and Schlieper, 2005; Kirschner, 1978). Upon binding to the microtubule, the GTPase activity of β-tubulin is stimulated and the GTP is hydrolysed to GDP, causing a slight bending of the dimer at the αβ-tubulin interface. The slight bent conformation of the tubulin dimers bound to GDP is proposed to cause mechanical strain, weakening the lattice and resulting in transition from growth to shrinkage when nucleotide hydrolysis catches up with polymerisation and the microtubule loses its GTP cap (Figure 1.5; Amos and Schlieper, 2005; Desai and Mitchison, 1997; Drechsel and Kirschner, 1994; Mitchison and Kirschner, 1984). Consistent with this, cryo-electron microscopy of depolymerising microtubules reveals a 'rams-horn' structure of protofilaments bending away from the tube (Chretien *et al.*, 1995; Chretien and Wade, 1991).

1.3.3. Cellular microtubule organisation and regulation of microtubules

1.3.3.1. Microtubule organising centres

Microtubule nucleation *in vivo* usually occurs at specific structures called microtubule organising centres (MTOCs). MTOCs ensure that microtubules nucleate only at specific sites and also serve to stabilise the minus ends and therefore are important for the spatial control of microtubule organisation. MTOC structure varies considerable between and also within cells, however the universal component of all MTOCs is γ-tubulin, which shares homology to α- and β-tubulin. It exists in a large complex, the γ-tubulin ring complex (γ-TuRC) that forms an open ring structure which caps the minus ends of tubulin heterodimers and acts as a template for microtubule nucleation (Keating and Borisy, 2000; Moritz *et al.*, 2000; Wiese and Zheng, 2000). Microtubule organisation is the key to formation of the different microtubule arrays observed, for example in neurons, yeast and epithelial cells; the positioning of nucleation sites is one important aspect of microtubule organisation. In many animal cells, microtubules are nucleated from a single MTOC called the centrosome, forming a radial array with the plus ends extending throughout the cytoplasm. The centrosome is composed of two centrioles, cylinders assembled from nine triplets of microtubules. These are embedded in an electron dense cloud of proteinaceous pericentriolar material in which the γ-TuRC is found and the microtubule minus ends stabilised (Bornens *et al.*, 2002). Centrioles are not an essential part of the MTOC, indeed both budding and fission

yeast have no centrioles and microtubules are instead nucleated from spindle pole bodies (SPBs), the yeast centrosome equivalent in addition to other MTOCs at the nuclear envelope and along pre-existing microtubules (discussed in Section 1.5.2.1). Additionally, during differentiation epithelial cells contain non-centrosomal microtubule arrays that contribute to their cellular polarity: Microtubules form bundles under the cell cortex, usually oriented with the minus ends at the apical membrane and their plus ends growing towards the basal membrane. This facilitates long-range vesicle transport and therefore sorting of proteins between the two polarised membranes (Musch 2004). Thus, most cells use a combination of centrosomal and non-centrosomal MTOCs to generate the specialised arrays essential for cellular function (Figure 1.6). A further example is in neurons, where axonal microtubules form stable parallel bundles with their plus ends facing away form the cell body and dendrites have antiparallel arrays of microtubules (Baas *et al.*, 1988; Chen *et al.*, 1992).

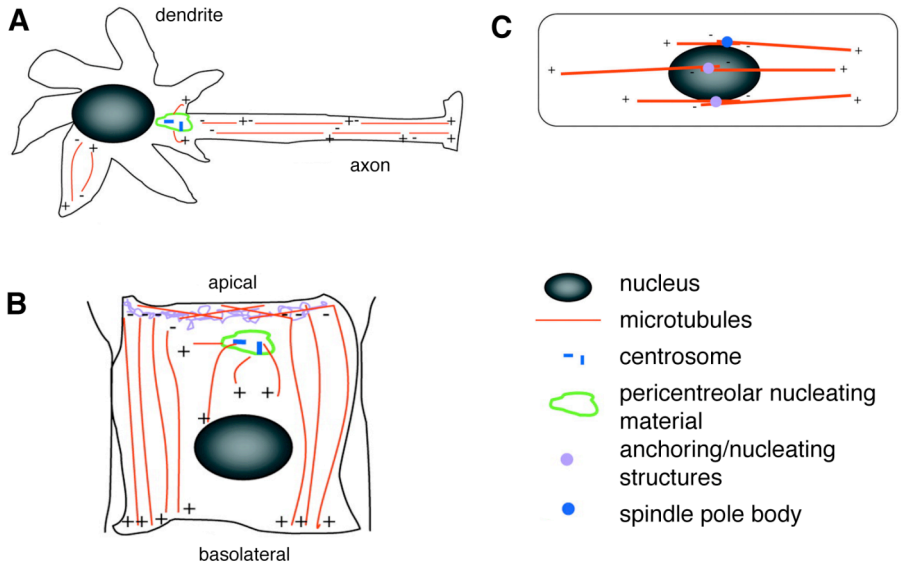

Figure 1.6 Microtubules can be nucleated from centrosomal and non-centrosomal arrays

In addition to nucleation from centrosomes (higher eukaryotes) or their equivalent (SPBs in yeasts), microtubules can be nucleated from non-centrosomal arrays. (A) In neurons non-centrosomal microtubule bundles are arranged parallel in the axons and antiparallel in the dendrites. (B) In epithelial cells microtubules could nucleate in the apical region with their minus ends next to the membrane and their plus end facing towards the basal membrane to facilitate directed transport. (C) Microtubules in fission yeast are nucleated from MTOCs at the nuclear membrane and additionally along microtubules (not shown). Adapted from Bartolini and Gundersen (2006).

1.3.3.2. Regulation of microtubule dynamics

For microtubules to be able to carry out their specialised functions it is essential that their dynamics be regulated. There exist several classes of drugs that can regulate microtubule dynamics and these are important in the treatment of cancer. They are also useful tools for the investigation of microtubule function and structure. There are two main classes of such drugs: stabilising and destabilising. Microtubule destabilising drugs usually bind to free tubulin dimers, preventing them from being incorporated into the microtubule lattice. An example of such a drug is the fungicide methyl-2-benzimidazole carbamate (MBC; Quinlan *et al.*, 1980). Destabilisers can also act by binding to exposed dimers at the ends of the microtubules, destabilising the lattice more directly. Examples of such drugs are colchicine, which prevents the establishment of lateral contacts between tubulin dimers in neighbouring protofilaments; vinblastine, which binds to tubulin at the longitudinal interface between tubulin dimes, forcing them to adopt a curved conformation. Microtubule stabilising drugs promote polymerisation and inhibit microtubule dynamics through stabilisation of the lattice, thus preventing depolymerisation (Ravelli *et al.*, 2004; Gigant *et al.*, 2005). Taxol is one such microtubule stabiliser and is thought to strengthen the lateral contacts between subunits by binding to the inner face of the microtubule lattice. This helps maintain the protofilaments in a straight conformation (Xiao et al, 2006; Andreu *et al.*, 1994; Schiff *et al.*, 1979; Wani *et al.*, 1971).

In vivo microtubule regulation is achieved by the action of **m**icrotubule-**a**ssociated **p**roteins (MAPs). MAPs can act both globally and locally to stabilise or destabilse microtubules, alter the rates of addition or removal of tubulin dimers and mediate interaction with other cellular components, for example the cell membrane (Howard and Hyman, 2007; Cassimeris 1999). As MAPs are the main topic of this thesis they will be discussed in further detail in the following sections.

In addition to regulation by the action of MAPs, physical forces also locally influence microtubule dynamics. When a microtubule contacts a cellular object such as an organelle or the cell membrane, it continues to grow against this barrier, exerting a pushing force against it. This was shown *in vitro* to promote catastrophe: Microtubules were grown against a solid barrier and their growth rate monitored. When the microtubules contacted the barrier their growth rate decreased, they started to buckle and the rate of catastrophe was increased 20-fold. This was attributed to decreased incorporation of tubulin at the plus end based on the observation that microtubules showed slower growth rates in the presence of lower tubulin

concentration (Laan *et al.*, 2008; Jansen *et al.*, 2003; Dogterom and Yurke, 1997). The relevance of this *in vitro* property of microtubules is not fully understood *in vivo*. This is in part due to the presence of MAPs, although there is increasing evidence that a force-based model for microtubule regulation can recapitulate much of the behaviour of microtubules in fission yeast without the action of MAPs (D. Foethke Ph.D Thesis).

1.4. Microtubule-associated proteins

MAPs were discovered through the observation that rates of microtubule polymerisation *in vivo* were much faster than these *in vitro*. They are a diverse group of proteins that bind to and influence the *in vivo* dynamics of microtubules. MAPs can act locally to regulate microtubule dynamics at specific regions of the cell, for example during microtubule-based transport of vesicles, or globally, for example during mitosis when remodelling of the entire microtubule cytoskeleton is required. There are many different MAPs, which can be broadly grouped into microtubule stabilisers, destabilisers and motors.

1.4.1. Microtubule stabilisers

1.4.1.1. Dis1/XMAP215 family

The Dis1/XMAP215 family of microtubule stabilisers are highly conserved, with homologues found in all eukaryotic organisms studied to date. This family has a characteristic N-terminal domain structure consisting of repeating units of ~200 amino acids known as TOG domains. These domains are degenerate at the primary sequence level, but each contains up to five HEAT motifs, curved rows of α-helices, thought to be protein-protein interaction domains. The C-termini of the Dis1/XMAP215 proteins contain coiled-coil regions required for MTOC and microtubule localisation and are generally less conserved (Neuwald and Hirano, 2000). Based on their size and the number of TOG domains, the protein family can be divided into three groups (Figure 1.7; Okhura *et al.*, 2001). The first contains five HEAT repeats at the N-terminus and a non-conserved C-terminus. Members of this group include human ch-TOG, *Xenopus laevis* XMAP215, *Drosophila melanogaster* Minispindles (Msps), *Dictyostelium* DdCP224 and *Arabidopsis thaliana* MOR1 (Whittington *et al.*, 2001; Graf *et al.*, 2000; Cullen *et al.*, 1999; Gard and Kirschner,

1987). The second group has only one member, *Caenorhabditis elegans* ZYG9, which has three TOG domains and a C-terminal domain with no apparent similarity to any of the other homologues (Hirsh and Vanderslice, 1976). Members of the third group have only two N-terminal TOG domains and no conserved C-terminus. To date four members of this group have been identified: *S. cerevisiae* Stu2, *Aspergilus nidulans* AlpA and *Sschizosaccharomyces pombe* Dis1 and Alp14 (Enke *et al.*, 2007; Wang and Huffaker, 1997; Nakeseko *et al.*, 2001). So far, *S. pombe* is the only organism in which two Dis1/XMAP215 homologues have been found. As this is a major topic of this thesis it is discussed in further detail in Section 1.5.3.2.

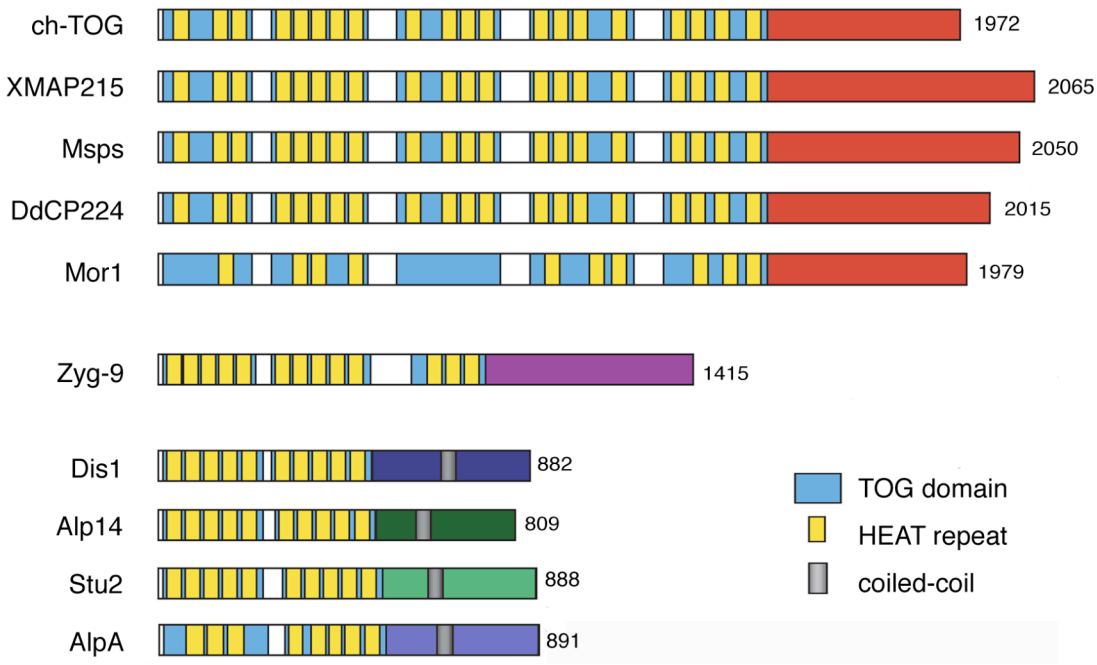

Figure 1.7 Dis1/XMAP protein family

Dis1/XMAP215 homologues can be classified into three different groups according to their structure. Adapted from Okhura *et al.* (2001) and Enke *et al.* (2007).

The Dis1/XMAP215 family members all associate with microtubules, but some are able to track the microtubule tips, showing a specific accumulation at the microtubule plus ends. XMAP215, the founding member of this family, is one of the major regulators of microtubule dynamics in *Xenopus*. It is a flexible monomer of ~60 nm and binds tubulin dimers with a 1:1 stoichiometry (Cassimeris *et al.*, 2001). It is thought to form a ring structure around the dimer, facilitating its addition (or removal) at the microtubule plus end (Figure 1.8A; Brouhard *et al.*, 2008). *In vitro* studies of XMAP215 show that it can bind both the growing and shrinking plus ends of

microtubules and is able to abolish rescues and increase the rate of both polymerisation and depolymerisation. However, the net function of XMAP215 *in vivo* is that of a microtubule stabiliser. It has recently been proposed to act as a processive microtubule polymerase, with properties of a classic catalytic enzyme, being able to accelerate a reaction in both directions, thus reconciling the additional, apparently contradictory *in vitro* data showing that it acts as a microtubule destabiliser (Brouhard *et al.*, 2008; Shirasu-Hiza *et al.*, 2003; Vasquez *et al*., 1999; Gard and Kirschner, 1987). Similar results have also been obtained for the budding yeast homologue, Stu2. Stu2 belongs to the third family of Dis1/XMAP215 homologues, with only two TOG domains, and as such is much shorter than XMAP215. Stu2 functions as a homodimer and transitions from an open structure to a closed on upon binding of a single free tubulin dimer at its first TOG domain. The second TOG domain confers binding to the microtubule ends. Together these two properties lead to the stabilisation of microtubules *in vivo* and both mechanistically and structurally concur with the microtubule polymerase model proposed for XMAP215 (Figure 1.8B; Al-Bassam *et al.*, 2006).

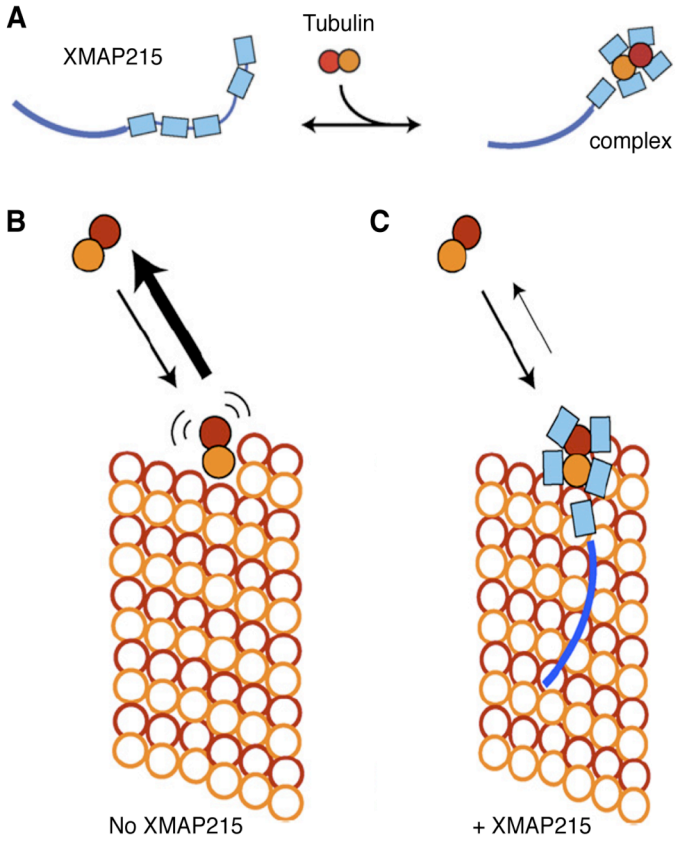

Figure 1.8 Model for tubulin polymerization by XMAP215

(A) Schematic showing XMAP215 enclosing a single tubulin dimer to form a 1:1 complex. (B) Schematic of the plus end of a microtubule (hollow circles). A weakly attached tubulin is shown in full colour. Tubulin dimers collide with the microtubule end in a diffusion-limited reaction, but these collision complexes are short lived, and the tubulin dimer often diffuses away. (C) XMAP215 stabilises the weakly attached tubulin dimer, so that a larger fraction of tubulin is incorporated into the microtubule. Note that the collision complex forms at the same rate with or without XMAP215. Adapted from Brouhard *et al.*, (2008).

Most of the Dis1/XMAP215 family proteins localise to cytoplasmic microtubules and some are additionally able to track the microtubule tips. In *S. cerevisiae,* Stu2 and the EB1 homologue, Bim1 cooperatively regulate microtubule dynamics, although their interaction may be indirect (Wolyniak *et al.*, 2006). Conversely, an interaction between XMAP215 and EB1 in *Xenopus* egg extracts was only observed in mitosis (Niethammer *et al.*, 2007). Thus, the interplay between XMAP215 proteins and other MAPs appears to vary between organisms and cell cycle stage and remains to be fully investigated. Depletion of Dis1/XMAP215 leads to several different cytoplasmic microtubule phenotypes depending on the system studied. For example, in *Dictyostelium*, fewer and shorter cytoplasmic microtubules are observed in DdCP224-depleted cells (Graf *et al.*, 2003). Depletion of *S. cerevisiae* Stu2 leads to fewer microtubules, but these maintain wild type length (Kosco *et al.*, 2001). In *Xenopus* egg extract, depletion of XMAP215 results in a decrease in the microtubule growth rate and microtubules are shorter both in interphase and mitosis (Tournebize *et al*., 2000). Excess of XMAP215 can fully compensate for the absence of EB1 activity, however a higher dosage of EB1 can only partially rescue the phenotype caused by XMAP215 levels (I. Kronja Ph.D. Thesis).

The interphase stabilisation activity of XMAP215 is primarily by its antagonistic activity of the microtubule destabilising kinesin XKCM1 (Tournebize *et al.*, 2000). Common to all the Dis1/XMAP215 homologues is that their depletion leads to defects in spindle morphology and, with the exception of the plant XMAP215 homologues, they all localise to the centrosome/SPB (Garcia *et al.*, 2001; Graf *et al.*, 2000; Tournebize *et al.*, 2000; Cullen *et al.*, 1999; Charrasse *et al.*, 1998; Matthews *et al.*, 1998; Nabeshima *et al.*, 1995; Wang and Huffaker, 1997). This localisation seems to be mediated by the **T**ransforming **A**cidic **C**oiled-**C**oil (TACC) proteins. An interaction between the Dis1/XMAP215 and TACC homologues is also conserved in *Drosophila* (Cullen and Okhura, 2001; Lee *et al.*, 2001), *C. elegans* (Bellanger and Gonczy, 2003; Srayko *et al.*, 2003), *S. pombe* (Sato *et al.*, 2004; Sato and Toda, 2007) and humans (Gergely *et al.*, 2003).

1.4.1.2. +TIPS

Several MAPs have been shown to accumulate specifically at the plus ends of microtubules. Accordingly, these are termed **plus**-end **t**rack**i**ng **p**roteins (+TIPs). CLIP170 was the first +TIP to be identified, but other +TIPs include EB1, Tea1, Dynactin, CLASP, APC and Lis1 (reviewed in Akhmanova and Steinmetz, 2008).

+TIPs have numerous functions, the most important of which is the regulation of plus end dynamics, but they are also involved in targeting and anchoring of specific cellular structures by microtubules, the recruitment of protein complexes to microtubule plus ends and their subsequent delivery to the cell periphery (Vaughan, 2005; Carvalho *et al.*, 2003; Galjart and Perez, 2003).

1.4.1.2.1. EB1 family

End-**B**inding protein **1** (EB1) was originally identified through a screen to identify interactors of Adenomatous Polyposis Coli (APC; see Section 1.4.1.2.3; Su *et al.*, 1995). The family is conserved from yeasts to humans. EB1 family members have a conserved structure with an N-terminal calponin homology domain, which binds microtubules, followed by an unstructured region, a coiled-coil, which confers dimerisation and finally a C-terminal EB1 domain, which interacts with other proteins, including a number of other +TIPs (Honnapa *et al.*, 2005; Slep *et al.*, 2005; Bu and Su, 2003; Hayashi and Ikura, 2003). *In vivo*, EB1 proteins are concentrated in comet-like structures at the growing plus ends of microtubules throughout the cell cycle (Figure 1.9). Additionally, EB1 proteins localise to MTOCs and centrosomes/SPBs, apparently independently of microtubules, as this localisation is maintained in the presence of microtubule depolymerising drugs (Busch and Bruner, 2004; Mimori-Kiyosue *et al.*, 2000; Tirnauer *et al.*, 2000; Tirnauer *et al.*, 1999; Morrison *et al.*, 1998).

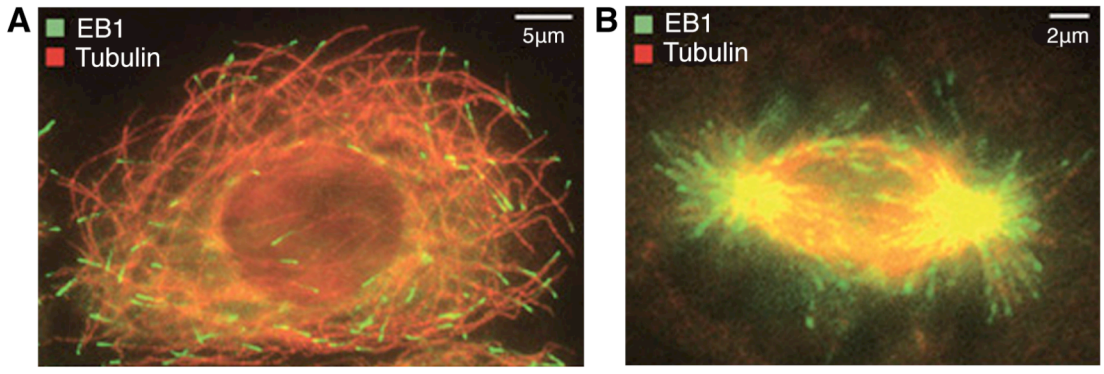

Figure 1.9 EB1 localisation

(A) In interphase cultured mouse kidney epithelial cell stained for EB1 and β-Tubulin. (B) Image of a mitotic cell with the same staining. Adapted from Akhmanova and Steinmetz (2008).

EB1 also binds along the entire length of microtubules. *In vitro* the *S. pombe* homologue of EB1, Mal3, binds the microtubule lattice, specifically at the lattice seam, the weakest point of the microtubule (Sandblad *et al.*, 2006). Thus, binding of Mal3 to the lattice-seam likely contributes to its microtubule stabilising activity. *In vitro* the *S. pombe*, Mal3 was also shown to bind to both the plus and minus ends of microtubules, although as the many of the microtubule minus ends are capped *in vivo*, the relevance of this observation is not yet clear (Bieling *et al.*, 2007). Addition of EB1 increases the rate of tubulin polymerisation in interphase *Xenopus* egg extracts but does not appear to affect the rate in mitotic extracts. In both cases however, the amount of time the microtubules spent in a paused state was increased. Depletion of EB1 from mitotic extract results in dramatic shortening of microtubules nucleated from centrosomes but no effect on interphase microtubule length was observed (Rogers *et al*., 2002; Tirnauer *et al.*, 2002). When the *S. cerevisiae* homologue of Bim1 was deleted, the microtubules were shorter and less dynamic due to a decrease in both growth and shrinkage rates and fewer catastrophe and rescue events (Tirnauer *et al.*, 1999).

1.4.1.2.1.1. EB1 interactions with other MAPS

In addition to its regulation of microtubule dynamics, EB1 is also involved in a variety of other processes, in which it interacts with other MAPs. The dynactin component, $p150^{glued}$ co-localises with EB1 at the microtubule plus ends, along the microtubules and at the centrosomes and this interaction may serve to anchor the microtubule minus ends at the centrosome (Hiyashi *et al.*, 2005; Askham *et al.*, 2002; Berrueta *et al.*, 1999). In Drosophila S2 cells, EB1 has been shown to bind to another minus end directed motor, the kinesin Ncd and is thought to mediate the interaction of centrosomal and kinetochore microtubules (Goshima *et al.*, 2005). EB1 binds to APC and *S. cerevisiae* Bim1 binds to Kar9 where it is implicated in the cortical capture of microtubule plus ends at the bed neck (See Section 1.4.1.2.3; Lee *et al.*, 2000; Liakopoulos *et al.*, 2003). There is also a strong link between EB1 and the CLIP170 protein family, discussed in subsequent sections.

1.4.1.2.2. CLIP170 family

Cytoplasmic **li**nker **p**rotein 170 (CLIP170) was the first +TIP to be discovered and was identified as a linker of endocytic vesicles and microtubules. It also co-localises

with desmosomal plaques that act as a target for microtubules in polarising epithelial cells (Pierre et al, 1992; Wacker *et al.*, 1992; Rickard and Kreis, 1990). CLIP170 has two N-terminal CAP-Gly domains, each followed by a short serine-rich stretch, which mediate its interaction with microtubules. The CAP-Gly domains are followed by a coiled-coil region and then two short metal-binding motifs at the C-terminus, which bind proteins such as $p150^{glued}$ and Lis1. The protein forms homodimers through its coiled-coil region and has a highly elongated form (Pierre *et al.*, 1994). CLIP170 homologues, exist in vertebrates and yeasts, and with the exception of the yeast homologues have a highly conserved structure. The *S. cerevisiae* and *S. pombe* homologues, Bik1 and Tip1 respectively, have only a single CAP-Gly domain and one metal-binding motif (Brunner and Nurse, 2000).

During interphase, CLIP170 specifically localises to microtubule plus ends, forming comets. The size of these comets is determined by the rate of microtubule growth; fast growing microtubules have longer CLIP170 comets. Depolymerising microtubules have no CLIP170 at the plus ends, but upon rescue a new comet appears (Perez *et al.*, 1999; Pierre *et al.*, 1992; Rickard and Kreis, 1990). Analysis of the inhomogeneities in fluorescence intensity in the comet suggested that these are immobile, and that the protein is not actively transported along the microtubules by motors, but rather uses treadmilling to associate with the microtubule plus end: shortly after binding the plus end the affinity of CLIP170 for the microtubule lattice is reduced and the protein disassociates from the older parts of the filament (Folker *et al.*, 2005; Perez *et al.*, 1999). Further work showed that CLIP170 also binds to tubulin oligomers *in vitro.* Arnal *et al.* (2004) suggest that CLIP-170 targets specifically at microtubule plus ends by co-polymerizing with tubulin. Conversely, Dragestein *et al.* (2008) have shown more recently that CLIP170 turns over rapidly on the plus ends of microtubules. They propose that microtubule polymerization generates a vast number of sites that can bind and release CLIP170 molecules several times before disappearing (Figure 1.10; Dragestein *et al.*, 2008). The yeast homologues show a different mechanism of plus end tracking. Bik1 and Tip1 are transported along microtubules by the kinesin motor proteins Kip2 and Tea2 respectively (Busch *et al.*, 2004; Carvalho *et al.*, 2004). The accumulation of Tip1 at the plus ends also depends on the EB1 homologue, Mal3, but this is not seen for Bik1. Other studies *in vitro* and in mammalian cells suggest that interaction with EB1 enhances the affinity of CLIP170 for growing microtubule ends (Ligon *et al.*, 2006; Komarova *et al.*, 2005).

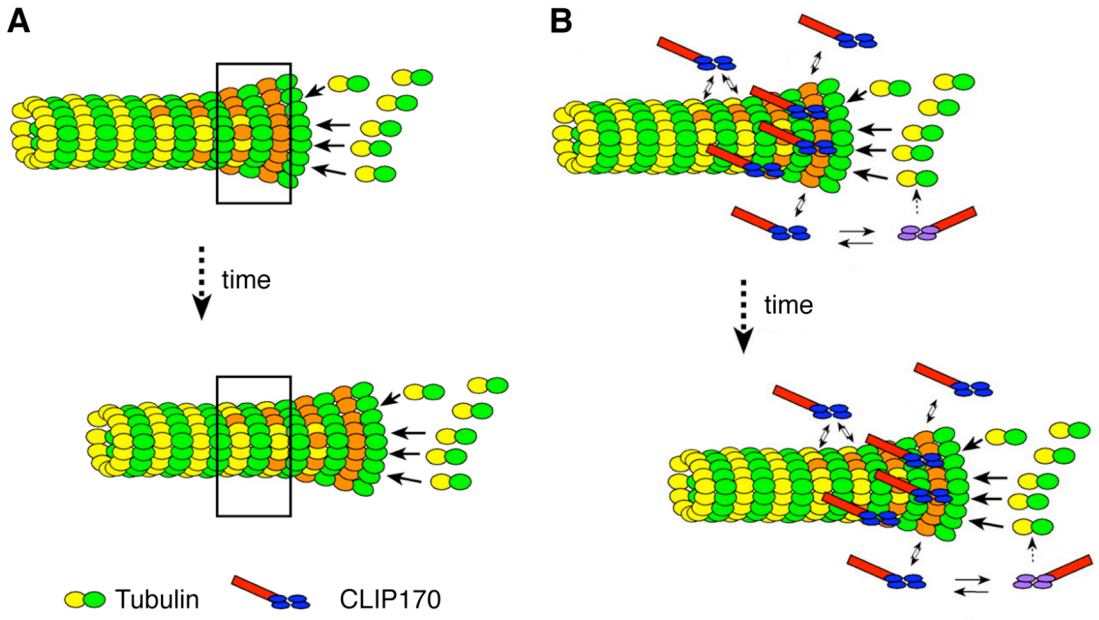

Figure 1.10 Fast exchange model for CLIP170 localisation to the microtubule plus tip

(A) MT polymerization generates a large number of binding sites (orange ellipses), which disappear over time. Thus, as time progresses, less binding sites are present within the depicted rectangle. (B) Dimeric CLIP170 exchanges rapidly on binding sites irrespective of the position on the MT end. Several interactions with CLIP170 molecules can occur during the lifetime of a binding site. Adapted from Dragestein *et al.* (2008).

1.4.1.2.2.1. Functions of CLIP170 in vivo

In addition to linking endosomes to microtubules, CLIP170 is involved in microtubule organisation. When CLIP170 is over-expressed in HeLa cells the microtubules become bundled into thick rings around the nucleus (Pierre *et al.*, 1994). Studies of the *S. pombe* homologue showed that Tip1 is important for the spatial regulation of microtubules during interphase. Tip1 locally influences microtubule dynamics when they contact the central regions of the cell cortex, allowing them to continue growing to the cell ends (Brunner and Nurse, 2000, discussed further in Section 1.5.3.1). CLIP170 has also been shown to be involved in mitosis. It associates with prometaphase kinetochores (Dujardin *et al.*, 1998) and its depletion results in defects in chromosome congression and alignment (Draviam *et al.*, 2006). In addition to interacting with the EB1 family members, CLIP170 proteins function together with a number of additional binding partners (see below).

1.4.1.2.2.2. CLIP170 and p150^{glued}

CLIP-170 binds to p150^{glued}, a component of the Dynactin complex, to recruit the motor protein Dynein and its associated cargo to the plus ends of microtubules. It is thought that the role of CLIP170 in vesicle transport is to facilitate loading of cargo vesicles at the plus ends (Wittmann and Desai, 2005; Vaughan *et al.*, 1999). The interaction of CLIP170 with dynein/dynactin also guides microtubules to specific membrane connections, for example in *S. pombe*, Tip1p together with Ssm4p, a p150^{glued} protein, regulates dynein heavy chain localisation to the cell cortex (Niccoli *et al.*, 2004).

1.4.1.2.2.3. CLIP170 and CLASPs

The **CL**IP-**as**sociated **p**roteins (CLASPs) are important interactors of the CLIP170 protein family members (Akhmanova *et al.*, 2001). CLASPs also show +TIP localisation, however, like APC, they only bind to a subset of microtubule plus ends in polarised cells. They concentrate at the plus ends of microtubules at the leading edge of migrating cells (Galjart, 2005) and in the growth cones of neurons (Lee *et al.*, 2004). CLASPs have recently been shown to be involved in the nucleation of non-centrosomal microtubule arrays from the peripheral Golgi compartments. These microtubules are preferentially oriented towards the leading edge in motile cells and are proposed to play a role in transport of post-Golgi proteins to the leading edge (Efimov *et al.*, 2007). During mitosis, CLASPs localise to the plus ends of spindle microtubules, the centrosomes, the kinetochores and the central region of the spindle. CLASP performs an essential mitotic function, particularly through modulation of the dynamic behaviour of spindle microtubules attached to kinetochores; in the absence of CLASP the centrosomes collapse into a singe aster resulting in chromosome segregation defects (Maiato *et al.*, 2002). Mitotic defects are also seen when the *S. cerevisiae* homologue, Stu1 is inactivated (Pasqualone and Huffaker, 1994). In *S. pombe*, the CLASP homologue, Cls1p/Peg1p, mediates the stabilisation of overlapping microtubules within the mitotic spindle and interphase bundles (Bratman and Chang, 2007) and has also recently been shown to regulate mitochondria distribution (Chiron *et al.*, 2008).

1.4.1.2.3. APC and Kar9

Adenomatous **P**olyposis **C**oli protein (APC) is another +TIP identified in humans as a tumour suppressor protein. APC acts in the Wnt-signalling pathway, degrading β-catenin when Wnt signalling is not activated. APC also plays a role in the regulation of microtubule dynamics and the segregation of chromosomes (Fodde *et al.*, 2001; Zumbrunn *et al.*, 2001). In migrating epithelial cells, APC only localises to a subset of microtubule plus ends, in particular those extending towards growth sites; APC stabilises the microtubules at the leading edge by increasing the rate of microtubule polymerisation and rescue and by decreasing the rate of depolymerisation and catastrophe (Mimori-Kiyosue *et al.*, 2000; Nathke *et al.*, 1996). APC was found to interact with EB1 and probably relies on EB1 for its +TIP accumulation. A role for APC in cross-talk between the actin and microtubule cytoskeletons has also been demonstrated in mammalian cells and *in vitro* (Moseley *et al.*, 2007).

Kar9 was originally thought to be the functional homologue of APC in budding yeast, but this was based on the discovery of only a short region of homology between the two proteins, which was later found in additional, otherwise non-related +TIPS. Kar9 binds to the homologue of EB1, Bim1. Kar9 performs a role in cell division in budding yeast to capturing the microtubule tips at the bud neck and position the mitotic spindle, processes, which also rely on its association with the actin cytoskeleton (Liakopoulos *et al.*, 2003; Lee *et al.*, 2000).

1.4.1.3. Microtubule destabilisers

Microtubule destabilisers perform an important role in remodelling of microtubule organisation during cell division. Their action allows the cell to respond quickly to cell cycle signals. Destabilising MAPs function by either altering plus end microtubule dynamics, for example by increasing the frequency of catastrophe.

1.4.1.3.1. Stathmin

Stathmin, or **O**nco**p**rotein 18 (Op18) has been linked to many types of cancer. Stathmins destabilise microtubules either by sequestering tubulin (Cassimeris, 2002). The activity of Stathmin *in vivo* is regulated by phosphorylation. Stathmin is deactivated by phosphorylation of four serine residues. This is required for formation of the mitotic spindle and to allow local growth of microtubules at the leading edge of

migrating cells. Dephosphorylation re-activates Stathmin and is essential for progression through the cell cycle (Wittmann *et al.*, 2004; Curmi *et al.*, 1999; Marklund *et al.*, 1996).

1.4.1.3.2. Katanin and Spastin

Katanin and Spastin are both AAA proteins, which sever microtubules by cleaving in the middle of the lattice. This forms new microtubule minus ends, which are lacking a γ-tubulin cap and are thus intrinsically more prone to depolymerise (White *et al.*, 2007). Katanins act during meiosis in *C. elegans* to sever microtubules surrounding the chromatin, aiding in the establishment of a short meiotic spindle (Lu *et al.*, 2004; Schneider and Bowerman, 2003).

1.4.1.3.3. Kinesin-13 family members

Rather than using the energy acquired through ATP hydrolysis to move along a microtubule, Kinesin-13 (or Kin I) family members use this energy to bind to the end of microtubules and peel the protofilaments apart (Moores *et al.*, 2003; Moores *et al.*, 2002; Desai *et al.*, 1999). The human Kinesin-13 family member, MCAK (**M**itotic **C**entromere **A**ssociated **K**inesin) localises to both the plus and minus ends of microtubules by diffusing one-dimensionally along the microtubule lattice. In addition, it localises to the spindle poles and kinetochores (Walczak *et al.*, 1996). Depletion of the *Xenopus* homologue, XKCM1 results in four-fold decrease in catastrophe in metaphase extract, resulting in a striking increase in microtubule length and subsequent failure to organise into bipolar spindles (Tournebize *et al.*, 2000; Walczak *et al.*, 1996).

1.4.1.4. Motors

With the exception of the Kinesin I family, microtubule motors use the energy gained from ATP hydrolysis to move along microtubules. Motors are required for the cellular transport of cargoes, are able to move microtubules along each other and can influence microtubule dynamics. As such, they are important organisers of the microtubule cytoskeleton. There exist three types of motors: the kinesins and dyneins move along microtubules and the myosins move along actin. Recently it has been suggested that Myosin V and Kinesin act together to enhance each others processivity

(Ali *et al.*, 2007). As microtubules and actin are both polar structures the movement of molecular motors is polarised in a specific direction. Both plus and minus end-directed motors exist.

1.4.1.4.1. Kinesins

The kinesins are a diverse set of motor proteins, which perform diverse cellular functions. They generally have a globular motor domain, which directly binds the microtubule lattice, a neighbouring flexible region followed by a coiled-coil, which allows them to oligomerise, and a tail region, which binds to the cargo. They can be sub-divided into 14 different families, but more broadly classified into three groups: Class A, which have their motor domain at their N-terminus and show plus-end directed movement; C-type kinesins which have a C-terminal motor domain and move towards the minus end of microtubules and finally M-type kinesin, which have a central motor domain (Marx *et al.*, 2005; Miki *et al.*, 2005; Lawrence *et al.*, 2004). Some of the M-type kinesins are non-motile and have microtubule depolymerising activity (previously discussed in Section 1.4.1.3.3). Kinesins can show processive movement along microtubules, where they take several steps before dissociating, or non-processive movement, where they dissociate after taking a single step (Helenius *et al.*, 2006; Yildiz and Selvin, 2005; Hoenger *et al.*, 2000). Kinesins often interact with other MAPs to influence microtubule dynamics. One example is the *S. pombe* M-type kinesin, Tea2. Tea2 forms a core +TIP complex with the EB1 and CLIP170 homologues, Mal3, and Tip1 respectively. Tea2 transports the CLIP170 homologue Tip1 along microtubules to their plus ends (Busch and Brunner, 2004). Binding of Tea2 to microtubules and stimulation of its ATPase activity requires Mal3. Cells lacking Tea2 have shorter microtubules and altered polarity (see Section 1.5.3.1; Bieling *et al.*, 2007; Browning and Hackney, 2005; Busch *et al.*, 2004).

1.4.1.4.2. Dynein

Dynein is a minus end-directed motor that was first identified in cilia and flagella, (Vale, 2003). Dynein is an AAA ATPase. A globular microtubule-binding domain is connected via a stalk to the ring-shaped motor domain, made up of six AAA domains, followed by a seventh AAA domain of unknown structure. A coiled-coil region, which confers dimerisation, connects the microtubule-binding and motor domains to the N-terminal tail that interacts with accessory peptides known as the light and intermediate chains and cargo (Burgess *et al.*, 2003; Samso *et al.*, 1998). Animals

have multiple genes for dynein heavy chains, multiple splice isoforms of intermediate chains and multiple isoforms of light chains. Therefore there is great diversity in the dynein types found in a single organism, with different cell types expressing different dynein isoforms according to their specialised function. Functions of dynein/dynactin include vesicle transport, nuclear positioning, mitotic chromosome movement and nuclear positioning (Courtheoux *et al.*, 2007; McCarthy and Goldstein, 2006; Cowan and Hyman, 2004). *In vivo*, cytoplasmic dynein usually functions in a complex with dynactin. The $p150^{glued}$ subunit of dynactin binds to the intermediate chains of dynein and also to other MAPs such as CLIP170 (Vaughan *et al.*, 1999; Wittmann and Desai, 2005). The dynein/dynactin complex functions at the plus tips of microtubules where it interacts with other MAPs and also membranes (Vale *et al.*, 2003) and is proposed to act as an anchor for astral microtubules enabling them to generate pulling forces to position the spindle (Yeh *et al.*, 2000) and also to direct vesicle transport on microtubules to specific membrane regions (Shaw *et al.*, 2007).

1.5. The Fission yeast, Schizosaccharomyces pombe

The fission yeast *S. pombe* has become an important model organism for the study of cell polarity. It has a cylindrical shape with a diameter of 3-4 μm and a length of 7-15 μm depending on its stage in the cell cycle. The cells retain their cylindrical shape by positioning and maintenance of the growth sites at the cell poles (Figure 1.11; Hayles and Nurse, 2001; Mitchison and Nurse, 1985).

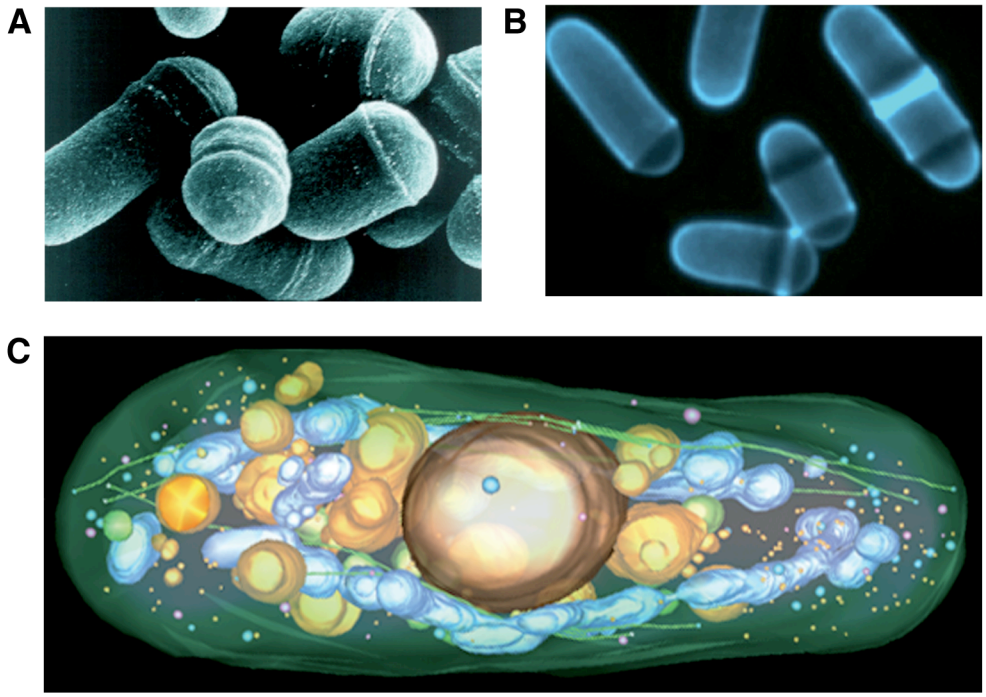

Figure 1.11 The fission yeast, *S. pombe*

(A) Scanning electron micrograph. (B) Fluorescent microscopy image of cells stained with the cell wall marker, calcofluor. (C) Model of electron tomogram of an entire cell volume showing microtubules, the nucleus, mitochondria and membrane structures. (A) and (B) courtesy of D. Brunner; (C) Hoog *et al.* (2007).

1.5.1. The cell division cycle

The manner by which *S. pombe* divides in the middle of the cell led to the name fission yeast. After cell division the cell grows initially only at one pole, but after reaching a certain size they switch from mono- to bipolar growth, an event termed new end take-off (NETO). NETO involves the accumulation of actin patches at the new cell pole. The cell then continues to grow from both cell poles until a critical size

is reached and the cell has synthesised all the components necessary for cell division and the chromosomes have separated. A cytokinetic ring of actin and myosin then forms at the cell centre and contracts. First a septum and then new cell walls form, which subsequently become the new cell ends (Mitchison and Nurse, 1985). In contrast to higher eukaryotes, but common to other fungi, the nuclear envelope remains intact during cell division, thus *S. pombe* is said to undergo a closed mitosis (see Section 1.5.4). Common to all morphogenetic processes, cell division in *S. pombe* requires a dramatic remodelling of the cytoskeleton (Figure 1.12).

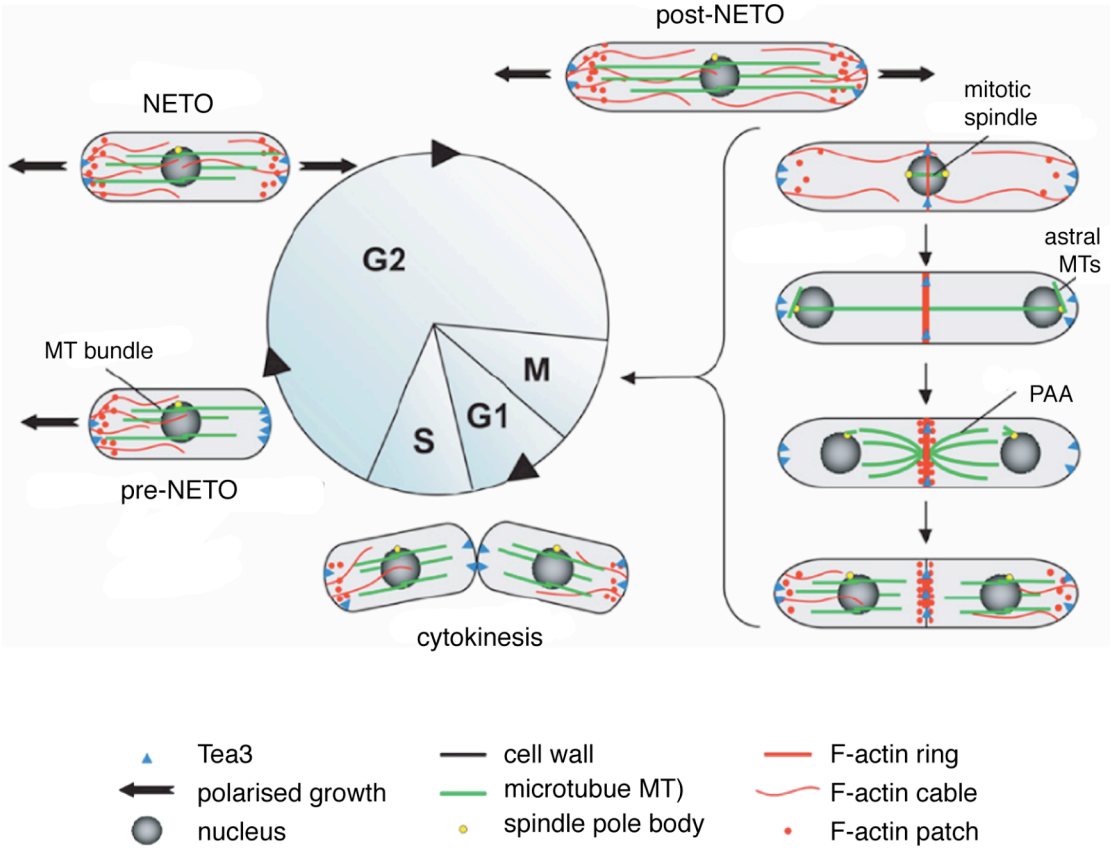

Figure 1.12 The fission yeast cell cycle

Model showing the cytoskeletal changes during the different stages of the cell cycle, shown in a clockwise order. Thick arrows represent a growing cell pole. NETO; new end take off. Adapted from La Carbona *et al.* (2006).

1.5.2. Organisation of the microtubule cytoskeleton

1.5.2.1. Interphase microtubule arrays

During interphase the microtubules in *S. pombe* are organised into 2-7 bundles, which extend along the longitudinal axis of the cell. Each bundle is composed of 2-9 microtubules which extend from their minus ends in the cell centre towards the cell poles, with their plus ends facing the poles (Figure 1.13). The microtubules form an anti-parallel overlap zone at the cell centre (Hoog *et al.*, 2007; Carazo-Salas *et al.*, 2005; Drummond and Cross, 2000). Ase1, a member of the MAP65/PRC1/ASE1 family of microtubule bundling proteins binds to and stabilises regions of anti-parallel overlap (Loiodice, 2005).

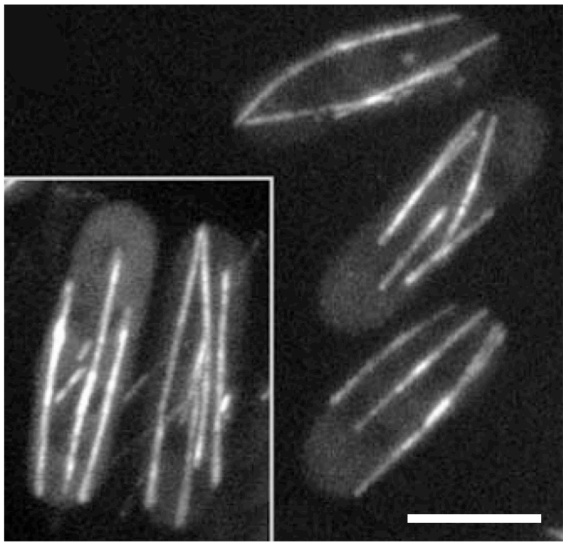

Figure 1.13

Fission yeast interphase microtubules

Fluorescent image *of S. pombe* cells expressing GFP-tubulin. Bar, 4 μm.

The interphase microtubule bundles are highly dynamic; they grow out from the centre of the cell towards the cell ends. Growth at the plus end of a bundle is usually that of a single microtubule, which grows at a rate of 2-3 μm/min. When the bundles reach the cell cortex in the central regions of the cell they continue to grow, sliding along the cortex. This serves to re-align the microtubules along the long axis of the cells and also enables the microtubules to grow until they reach the cell poles. When microtubules reach the cell poles their growth rate decreases to ~1.3 μm/min and they start to bend (Loiodice *et al.*, 2005; Behrens and Nurse, 2002; Tran *et al.*, 2001). After ~1.5 sec at the cell pole they undergo catastrophe and depolymerise with a rate of ~9 μm/min (Tran *et al.*, 2001; Busch and Brunner, 2004). This dynamic behaviour is important for the maintenance of polarity in *S. pombe*, as the microtubules are

responsible for the transport of cell polarity factors, such as the protein Tea1, to the cell poles, which determines the position of growth sites (Mata and Nurse, 1997). This behaviour of microtubules is mediated by the Mal3/Tip1/Tea2 +TIP complex (discussed in Section 1.5.3.1). An additional role of the interphase microtubule array is to position the nucleus in the centre of the cell. This is important as the position of the nucleus at the onset of mitosis determines the site at which the septum forms and thus the point at which the cell subsequently divides (Daga and Chang, 2005). Microtubules are attached to the nuclear envelope in the region of their overlap zones. When the ends of the bundles encounter the cell poles and continue to grow, they can exert a pushing force on the nuclear envelope, as the region of the microtubule bundle attached to the nuclear envelope is moved (Daga *et al.*, 2006; Dogterom *et al.*, 2005; Tran *et al.*, 2001). Mutants in which the microtubule organisation is disrupted, for example in *ase1*Δ or γ-tubulin complex mutants, are unable to centre the nucleus, often leading to unequally sized daughter cells following cell division (Janson *et al.*, 2005; Loiodice *et al.*, 2005; Sawin *et al.*, 2004).

The centrosome equivalent of *S. pombe* is the **s**pindle **p**ole **b**ody (SPB), which is found at the nuclear envelope and nucleates microtubules throughout the cell cycle. In interphase it is found on the cytoplasmic side of the nuclear envelope (Ding *et al.*, 1997). During interphase there are additional MTOCs. These are found at the nuclear envelope where, in addition to the SPB, they nucleate antiparallel bundles (Janson *et al.*, 2005; Sawin *et al.*, 2004; Drummond and Cross, 2000). Microtubules can also be nucleated along existing microtubules and are subsequently transported towards the cell centre to the overlap zones by the action of the kinesin, Klp2. It is believed that the bundling action of Ase1 is responsible for determining the antiparallel orientation of the newly nucleated microtubule along the lattice of the pre-existing one, thus Ase1 and Klp2 collaborate in the maintenance of the anti-parallel overlap zone (Janson *et al.*, 2005; Zimmerman and Chang, 2005; Loiodice, 2005; Sawin *et al.*, 2004; Zimmerman *et al.*, 2004).

1.5.2.2. Microtubule organisation during mitosis

At the onset of mitosis new microtubules are nucleated within the nucleoplasm from the duplicated SPBs forming the mitotic spindle, which functions to separate the sister chromosomes into the daughter cells. Shortly after the spindle begins to form, the interphase microtubule arrays depolymerise. It is unclear exactly when the SPB duplicates. Originally it was thought to be during late G2 phase, but more recently it has been proposed to occur during the G1/S transition (Uzawa *et al.*, 2004; Ding *et*

al., 1997). At the onset of mitosis, the SPBs become embedded in the nuclear envelope, which at this point has a fenestrated appearance. The SPBs are separated to opposite sides of the nucleus and organise the bipolar spindle. The spindle is composed of a single bundle of more than 20 microtubules. Each of the six kinetochores (three duplicated chromosomes) is captured by 3-4 microtubules. The remaining microtubules interdigitate in the spindle midzone or extend to the other SPB (Sagolla *et al.*, 2003; Ding *et al.*, 1993). At the onset of anaphase A the spindle extends, pulling apart the sister chromosomes to opposite ends of the cell. During this time the number of microtubules decreases and during anaphase B cytoplasmic astral microtubules are nucleated from the SPBs. These interact with the cell cortex to align the spindle along the long axis of the cell; their absence results in misaligned spindles (Oliferenko and Balasubramanian, 2002). During spindle elongation, an equatorial MTOC forms at the division site. It nucleates a ring of microtubules that grow towards both cell ends, forming a post-anaphase array, which is proposed to push the nucleus away from the site of division to prevent them being cut as the cells fission (Pardo and Nurse, 2003). The spindle then breaks down and the SPBs begin to nucleate a new interphase microtubule array (Figure 1.14; Hagan, 1998).

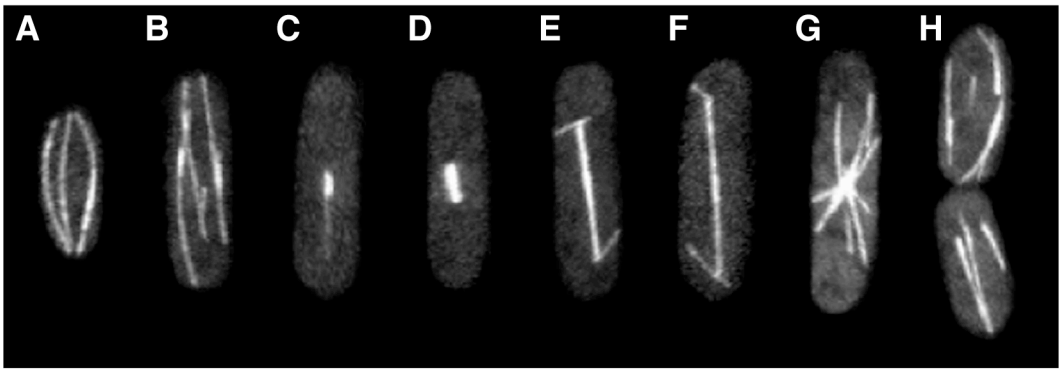

Figure 1.14 Microtubule organization during mitosis

Fluorescent images of *S. pombe* cells expressing GFP-tubulin. (A) Pre-NETO. (B) Pos-NETO (C) Beginning of mitosis. (D) Metaphase. (E) Early anaphase. (F) Late anaphase. (G) Post-anaphase array. (H) Cytokinesis. Images provided courtesy of H. Roque.

1.5.2.3. Microtubule organisation during meiosis

Unlike the higher eukaryotes, *S. pombe* can exist either as a haploid, with only one copy of each chromosome, or as a diploid cell, with two copies. In conditions where

nutrients become limiting, two haploid cells of opposite mating type conjugate to form a diploid cell. Diploids will undergo mitosis, resulting in the formation of four haploid spores, the *S. pombe* gametes.

There are two rounds of nuclear division in meiosis, each of which involves DNA duplication. During the first reductional division (Meiosis I), the duplicated chromosomes are separated from each other. During the second nuclear division (Meiosis II) the nucleus again divides, this time in a more similar way to a mitotic division. This second equatorial division serves to halve the number of chromatids such that each daughter is a haploid. Importantly, during Meiosis I, recombination between the sister chromosomes occurs, which results in genetic diversity between the parent and daughters. In higher eukaryotes the haploid gametes from each parent fuse during fertilisation to form a zygote. However, in *S. pombe* the gametes are packaged as four spores, which are then able to germinate to generate haploid cells when conditions become more favourable.

Before Meiosis I in *S. pombe* the nucleus becomes highly dynamic and oscillates back and forth along the long cell axis for several hours. This process, known as horsetail movement, aids pairing of homologous chromosomes and recombination and requires a specialised microtubule organisation (Davis and Smith, 2005; Ding *et al.*, 2004; Niwa *et al.*, 2000; Yamamoto *et al.*, 1999; Chikashige *et al.*, 1994). The SPB leads horsetail movement of the nucleus through its attachment to the chromosome telomeres. Movement of the SPB is driven by the cytoplasmic dynein/dynactin complex (Figure 1.15; Yamamoto *et al.*, 1999; Miki *et al.*, 2002; Niccoli *et al.*, 2004). The dynein heavy chain and the $p150^{glued}$ dynactin subunit homologue, Ssm4, localise to the SPBs and microtubules during horsetail movement and Ssm4 and the CLIP170 homologue, Tip1 regulate dynein recruitment to the cell cortex (Niccoli *et al.*, 2004). Dynein also localises to the points where the astral microtubule plus ends interact with the cell cortex (Niccoli *et al.*, 2004; Yamamoto *et al.*, 1999). The protein Num1 functions as a cortical-anchoring factor for dynein, allowing dynein to pull on the astral microtubules, generating forces that drive nuclear oscillation (Yamashita and Yamamoto, 2006; Miki *et al.*, 2002; Yamamoto *et al.*, 1999).

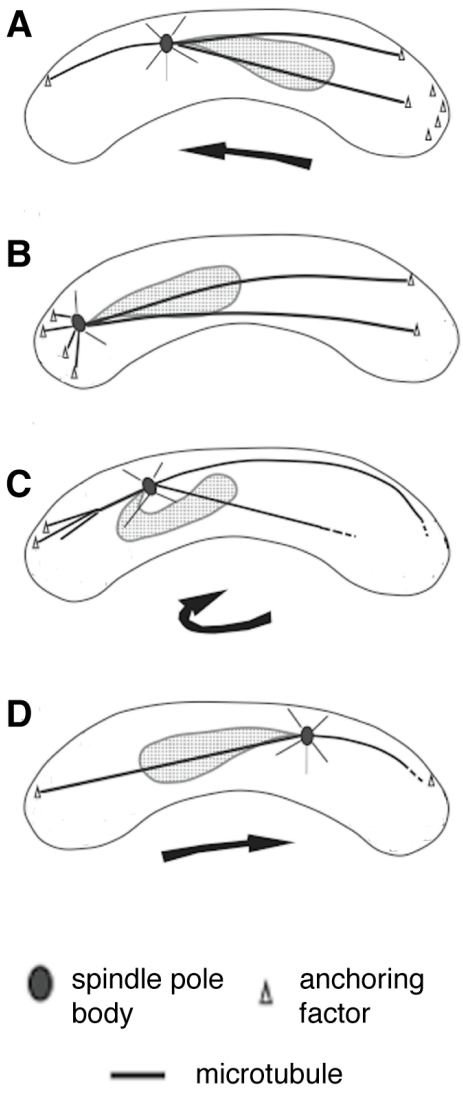

Figure 1.15 Horsetail movement during meiosis

A model by which nuclear movement is directed by selective stabilization of microtubules. (A) The horsetail nucleus moves forward, accompanied by the elongation of the rearward-extending microtubule bundles that are anchored at the rear end of the cell. (B) When the nucleus reaches the end of a half-oscillation it often pauses, presumably due to the balanced forces between forward- and rearward-extending arrays of microtubules. (C) After the rearward-extending microtubules disengage from their cortical anchors, the nucleus reverses direction and begins to move toward the opposite end of the cell. The forces generated by the microtubules driving the nucleus to traverse the cell also cause the unanchored ends of the forward-extending microtubules to bend, curving along the cell cortex. (D) The horsetail nucleus continues moving in the new direction. Repeated cycles of microtubule reorganization, as shown in A-D, result in oscillatory movement of the horsetail nucleus during meiotic prophase, typically lasting for 2-3 hours. Adapted from Ding *et al.* (1998).

1.5.3. MAPs involved in the regulation of interphase microtubules in *S. pombe*

1.5.3.1. The Mal3/Tip1/Tea2 +TIP complex

Important regulators of interphase microtubules are the EB1 and CLIP170 homologues, Mal3 and Tip1 respectively. During interphase, Mal3 autonomously binds to the SPBs, the plus ends of microtubules and also along the lattice at the lattice seam (Busch *et al.*, 2004; Sandblad *et al.*, 2007; Beinhauer *et al.*, 1997). Loss of Mal3 results in short microtubules and Mal3 was shown to act as a general stabiliser of microtubules when they growth through the cytoplasm (Busch and

Brunner, 2004; Beinhauer *et al.*, 1997). Tip1 localises to the microtubules by binding to the Kinesin 7 family member, Tea2 (Busch *et al.*, 2004). Tea2 is a plus end-directed kinesin, homologous to *S. cerevisiae* Kip2. Binding of Tea2 and thus Tip1 to microtubules *in vitro* is also dependent on Mal3 (Bieling *et al.*, 2007). Tip1, through its Tea2-mediated plus end localisation acts to prevent microtubules undergoing catastrophe when they contact the central regions of the cell cortex, allowing them to grow long enough to reach the cell poles where they can deliver factors such as Tea1, which are essential for maintenance of cell polarity (Busch *et al.*, 2004; Brunner and Nurse, 2000). Thus, together Mal3, Tip1 and Tea2 act to maintain a wild type microtubule organisation where the microtubules extend to the cell ends and catastrophes are restricted to the cell poles (Figure 1.16; Busch and Brunner, 2004).

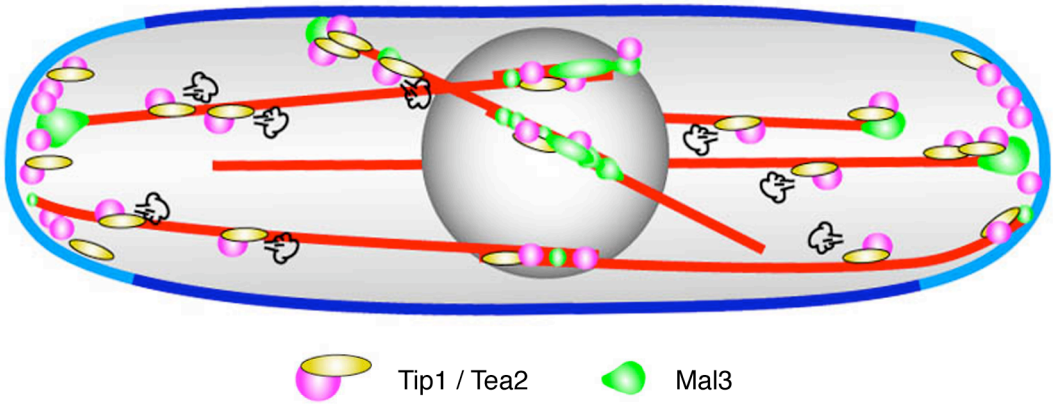

Figure 1.16 Model for interphase microtubule regulation in fission yeast

Tip1 is transported to the plus ends of microtubules by the kinesin Tea2, where it is important for the spatial regulation of microtubule dynamics, suppressing catastrophe at the cortex in the central region but not at the cell ends. Mal3 is a general promoter of microtubule growth, suppressing catastrophe in the cytoplasm. Mal1 is also required for loading of Tip1 and Tea2 onto the microtubules. Model courtesy of D. Brunner.

1.5.3.2. The fission yeast Dis1/XMAP215 homologues

S. pombe provides a unique system to study the functions of the Dis1/XMAP215 family members, as it is the only system known to date in which more than one XMAP215 homologue exists. Both Alp14 and Dis1 localise to microtubules, SPBs and kinetochores, although their localisation pattern differs in a cell cycle specific

manner (Garcia *et al.*, 2001; Nakaseko *et al.*, 2001; Okahura *et al.*, 2001). Alp14 is essential for growth at high temperatures, and Dis1 at low temperatures. Deletion of both *alp14* and *dis1* is lethal at all temperatures, highlighting the essential role of the Dis1/XMAP215 homologues in fission yeast (Garcia *et al.*, 2001). Furthermore, the phenotypes of the deletion mutants are different, suggesting that they function by non-redundant mechanisms.

1.5.3.2.1. Alp14

Alp14 is reported to localise to interphase microtubule arrays as moving particles (Garcia *et al.*, 2001; Nakaseko *et al.*, 2001; Okahura *et al.*, 2001). The interphase localisation of Alp14 to microtubules is dependent upon the Transforming Acidic Coiled-Coil (TACC) protein Alp7, as Alp14 fails to localise to microtubules in *alp7*Δ cells (Sato *et al.*, 2004). Alp7 is also required for transport of Alp14 into the nucleus (see Section 1.5.4). When *alp14* is deleted the cells are unviable at high temperatures and at low temperatures the cells often have shape and mitotic abnormalities (Garcia *et al.*, 2001; Nakaseko *et al.*, 2001; Okhura *et al.*, 2001). There is some disagreement about the effect of *alp14*Δ on the microtubule arrays in *alp14*Δ cells: One group reports normal interphase microtubules (Garcia *et al.* (2001), however two groups report fewer or no microtubules (Nakaseko *et al.*, 2001; Okhura *et al.*, 2001).

During mitosis, Alp14 is associated with the SPB and the peripheral regions of the kinetochores and is involved in the bivalent attachment of the kinetochores to the spindle (Garcia *et al.*, 2001; Garcia *et al.*, 2002b). Alp14 is a component of the Mad2-dependent spindle checkpoint; *alp14*Δ cells fail to correctly assemble bipolar spindles (Garcia *et al.*, 2001). The kinetochore attachment of Alp14 is reduced in the absence of the kinesin Klp5 and conversely, deletion of *alp14* reduces localisation of Klp5 to the kinetochore. In addition, any combination of mutations in *alp14/dis1* and *klp5/klp6* were synthetically lethal, suggesting that these proteins collaborate in bipolar spindle formation (Garcia *et al.*, 2002b).

1.5.3.2.2. Dis1

During interphase, Dis1 localises to microtubules with a localisation and dynamic behaviour indistinguishable from the movement of control tubulin. Unlike Alp14, this localisation is independent of Alp7 (Nabeshima *et al.*, 1995; Nakaseko *et al.*, 1996; Nakaseko *et al.*, 2001). In mitosis, Dis1 localises to, and interacts with the

kinetochores and SPBs. This localisation is regulated during metaphase and anaphase by phosphorylation of Dis1 by Cdc2 and is required to ensure high-fidelity chromosome segregation (Aoki *et al.*, 2006; Nabeshima *et al.*, 1995). In contrast to Dis1, which has six Cdc phosphorylation sites, Alp14 only has one site and the two proteins appear to be subject to different regulatory signals (Nakaseko *et al.*, 2001).

When *dis1* is deleted the cells have a cold-sensitive phenotype. Interphase microtubules in *dis1*Δ cells at the permissive temperature have a wild type appearance and behaviour (Nabeshima *et al.*, 1995) but mitotic *dis1*Δ cells have abnormal spindles. Dis1 was also shown to co-operate with Klp5/6 for the establishment of bivalent attachment of the kinetochores to the mitotic spindles (Garcia *et al.*, 2002b).

1.5.3.2.3. A redundant role for Alp14 and Dis1?

Deletion of *alp14* and dis1 together results in synthetic lethality, however when a multi-copy plasmid over-expressing Dis1 is transformed into *alp14*Δ cells it confers viability on culture plates at the restrictive temperature. Conversely, Alp14 over-expressed from a multi-copy plasmid is able to partly rescue the *dis1*Δ cold-sensitive growth phenotype (Garcia *et al.*, 2001). It therefore appears that there is at least some degree of functional redundancy between Alp14 and Dis1, but that together they perform an essential function. A major part of the work presented in this thesis addresses this issue.

1.5.4. Fission yeast closed mitosis vs. open mitosis in higher eukaryotes

In higher eukaryotes, the nuclear envelope breaks down during mitosis allowing cytoplasmic factors to easily access the chromosomes and spindle. The chromosome-associated RanGEF generates a RanGTP gradient around the chromosomes. Away from the chromosomes, microtubule nucleation and stabilising factors, such as TPX2 and NumA are bound by Importin, preventing them from nucleating microtubules. In the vicinity of the chromosomes, RanGTP binds to Importin, resulting in the release of the factors that promote microtubule formation around the chromosomes (Figure 1.17A).

As a consequence of a closed mitosis in *S. pombe*, it is necessary that nuclear import and export pathways exist to allow the nuclear accumulation of mitotic factors and their subsequent removal from the nucleus following mitosis. In a series of elegant experiments it was recently shown that during spindle formation Alp7 acts as the chaperone for transport of Alp14 into the nucleus. This is dependent on the Ran-Importin nuclear import machinery. Alp7 failed to accumulate in the nucleus in a *pim1* mutant, the Ran GTP exchange factor, but when Alp7 was targeted to the nucleus via the Ran-independent nuclear import pathway, the mutant defects were suppressed. An Alp7/Alp14/Importin complex forms in the cytoplasm, which is then transported through the nuclear pore complex. Once in the nucleus, like in higher eukaryotes, there is an increase in the levels of RanGTP, generated at the chromosomes, which results in the release of Alp7/Alp14 from Importin (Figure 1.17B; Sato and Toda, 2007).

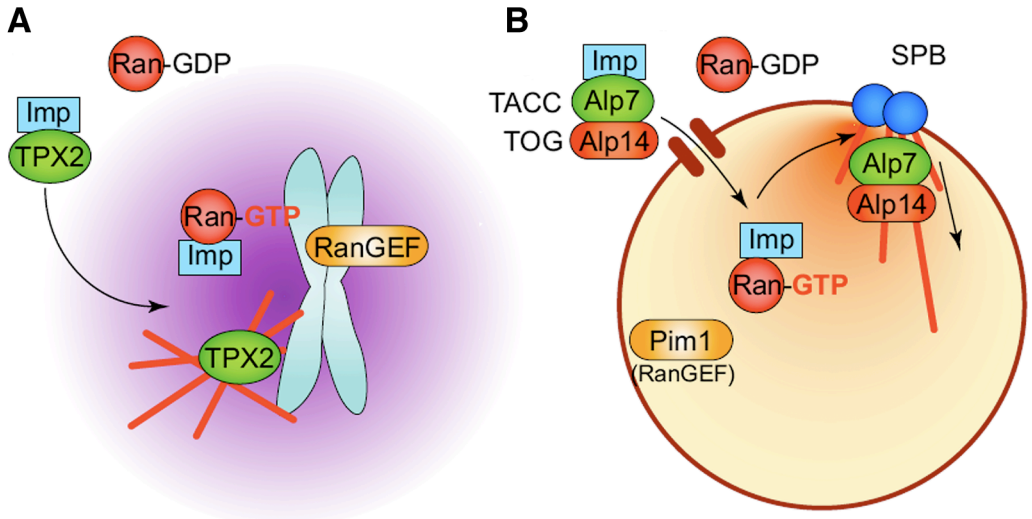

Figure 1.17 Ran-mediated spindle formation in closed and open mitosis

(A) *Xenopus* egg extract. In higher eukaryotes the nuclear envelope breaks down during mitosis, allowing access of cytosolic factors to the chromosomes. (B) In contrast, the nuclear envelope remains intact during mitosis in yeast, requiring a nuclear import pathway to enable cytosolic factors to access the chromosomes. In fission yeast, Alp7 acts a chaperone to import Alp14 into the nucleus via the Ran-Importin system. See text for further details. Figure from Sato *et al.* (2007).

1.6. Aims of this thesis

Although much is already known about the roles of the microtubule cytoskeleton and the regulation of its dynamic rearrangement during the cell cycle, there are still many open questions. Analysis of the role of microtubule-associated proteins is key to understanding these processes. This unifying theme presented this thesis is the investigation of microtubule-associated proteins in fission yeast.

The highly conserved fission yeast members of the Dis1/XMAP215 family of microtubule-associated proteins (MAPs) play a central role in cytoplasmic microtubule organisation and mitotic spindle formation. In Part I of this thesis we present an investigation of the role of the *S. pombe* homologues Alp14 and Dis1 during interphase. We also address the significance of the presence of two Dis1/XMAP215 homologues in fission yeast and characterise the interphase deletion phenotypes.

Together with the EB1 homologue, Mal3, Tip1, the CLIP170 homologue spatially regulates microtubule dynamics, ensuring the maintenance of *S. pombe* bipolarity. In Part II of this thesis we present the characterisation of the protein SPCC736.15 (Toi4), identified in a screen for Tip1-interacting proteins.

2. Materials and Methods

All reagents were obtained from Sigma unless otherwise stated.

2.1. *S. pombe* cell culture techniques

Standard methods were used for the maintenance of fission yeast strains (Moreno *et al.*, 1991). Cells were either grown in rich yeast extract medium (YE5'S) or Edinburgh Minimal Medium (EMM2) containing the appropriate amino acid supplements (Forsburg and Rhind, 2006). Briefly, yeast cells were stored in glycerol-containing medium and then woken on YE5'S or EMM2 agar plates and incubated at 25°C or 30°C for 1-3 days until colonies formed. Liquid pre-cultures (10ml) of the appropriate medium were inoculated and grown for 8-16 hours with constant agitation and then used to inoculate a larger culture volume. These cultures were grown for 16-20 hours to an optical density OD_{595} of 0.4-0.7 to ensure cells were in exponential growth phase and subsequently used for strain construction or imaging experiments. All medium and solutions used for cell culture were autoclaved or filter sterilised before use.

2.1.1. Strains under control of the *nmt1* promoter

When strains containing GFP-atb2 under the control of the nmt1 promoter were used the strains were grown and imaged in the presence of 15 μM thiamine to prevent over-expression from this promoter. For the shut-off experiments the strains were generated and maintained in EMM2 without thiamine. To shut-off expression from the *81nmt1* promoter, the cells were first grown form a pre-culture to exponential phase and then thiamine added at a concentration of 30 μM to ensure that the promoter was fully repressed. Cells were maintained in exponential phase by diluting with thiamine-containing medium.

2.2. Construction of strains by homologous recombination

2.2.1. Generation of PCR fragments for transformation

Strains were constructed using the homologous recombination-based transformation method described by Bahler *et al.,* 1998. Briefly, ~100 bp PCR primers (Biospring) containing 80 bp gene-specific sequence followed by 20-24 bp sequence, corresponding to the plasmid template (Table 1) were used to amplify a transformation cassette containing a selection marker (Uracil, Kanamycin resistance: Bahler *et al.*, 1998; hygromycin B resistance: Sato *et al.*, 2005) for creating deletion strains and an additional promoter or tag sequence for 5' or 3' modification of the target gene. See Table 2.1 for a list of primer sequences and plasmid templates. This PCR fragment was extracted using phenol/chloroform and resuspended in 10 mM Tris-HCL at 1 µg/µl. 50 ml exponentially-growing cells (OD_{595} = 0.5) cultured in rich medium were transformed.

2.2.2. Construction of a new transformation plasmid template

To improve selection efficiency of crosses with multiple gene modifications we modified an existing plasmid template so that it contained a hygromycin B resistance gene instead of the kanamycin resistance gene. A 1.6 Kb SacI-BglII hph fragment was purified from plasmid pFA6a-hphMX6 (Sato *et al.*, 2005) and sub-cloned into the same site of the plasmid cassette pFA6a-KanMX6-*81nmt1* (Bahler *et al.*, 1998), which was digested with the same enzymes to remove the 1.6 Kb fragment. This new plasmid was designated pFA6a-HphMX6-*81nmt1*.

2.2.3. Transformation protocol

50 ml exponentially growing cells were transferred to a 50 ml Falcon tube and pelleted by centrifugation at 2500 xg. Cells were then washed twice with 50 ml water and the cell pellet resuspended in 1 ml of 0.1 M LiAc/TE pH 7.5. Cells were transferred to a 1.5 ml Eppendorf tube, and resuspended in LiAc/TE at $2x10^9$ cells/ml. 100 µl of the concentrated cells were mixed with 2 µl sheared herring testes DNA (10

mg/ml) and 10 µl of the transforming DNA. After 10 min incubation at room temperature, 260 µl of 40% PEG/0.1M LiAc/TE was added. The cell suspension was mixed gently and incubated for 1 hour at 30ºC (or 25ºC for temperature sensitive strains). 43 µl of DMSO was added, and the cells were heat shocked for 5 min at 42ºC. Cells were then washed once with 1 ml of water, resuspended in 0.5 ml of water, and plated onto 2 rich medium non-selective plates. These plates were incubated for 1 day at 25ºC or 30ºC, resulting in a lawn of cells. The cells were then replica plated onto selective plates. Cells transformed with fragments carrying the *kanMX6* marker were plated onto YE5'S containing 100 mg/l Geneticin. Cells transformed with fragments carrying the Hygromycin B *hph* marker were plated onto YE5'S containing 300 mg/l Hygromycin B. Cells transformed with fragments carrying the *ura4+* marker were plated onto EMM2 plates without uracil, The replica plates were incubated for 2–3 days at 25ºC or 30ºC, and large colonies were re-streaked onto fresh selective plates.

2.2.4. Screening transformants by colony PCR

Single colonies were checked for stable integration of the DNA fragment by homologous recombination. A toothpick of cells was resuspended in zymolyase solution (2.5 mg/ml zymolyase 20-T, 0.1 M sodium phosphate, 1.2 M sorbitol, pH 7.4) and incubated for 10 mins at 37ºC followed by 95ºC to release the genomic DNA. 2 µl was then used in a PCR reaction to amplify an ~1 Kb region of DNA including the site of integration. One primer corresponded to a sequence within the transforming fragment. For modules containing kanMX6 we used primer 5'-GCTAGGATACAGTTCTCACATCACATCCG-3'. For modules containing hph we used primer 5'- CGCCAACATCTTCTTCTGG-3'. For modules containing ura4+ we used primer 5'-CCAAGCCGATACCAGGGGACATAG-3'. The other confirmation primer annealed to a region of the targeted gene outside the sequences covered by the transforming fragment and is listed in Table 2.1. A PCR product was obtained only for strains in which the transformation fragment was stably integrated.

Table 2.1 ***PCR primers for creation of strains by transformation***

Gene modification	Forward transformation primer	Reverse transformation primer	Plasmid template	Confirmation primer
Nup85-linker-GFP	DPE 275: TCAACTGTAAAGGACCAGCAGCTTTTACT ATCCATTCATGAGCGTCTTTCTTCTGCGAT ATCATGGTATTTTCTTCACTTAAAAAAAAT CCTTGGAGCTCCTTCAGGA	DPE 274: GTATCTTAATAAAAACATGTATGAAGCTT CTATGTTACAGAAAGATTAAAATGTCAA GTAACAGAAATAGCCTAATTTAAATCCC GAATTCGAGCTCGTTTAAAC	pFA6a-linker-GFP(S65T)-KanMX6 (Sandblad et al., 2006)	DPE 277: GCTGGGTTCA CTGATTTTGG ATC
Dis1-GFP	DPE 720: AGGCACGAGACAACTGGAGGGAGAGTCA TGATTTGTCAAGTCATTTGTGGGAGCAAA TCCAAAGGATGAAGAAGGCGATCCTTGGA GCTCCTTCAGGA	DPE 463: GAGTGATTTCAACTCTACCTAATCGACTT TAACAAACACTCCAACAAAAAACTCTAC CAGCATTTCCACGCTTGTGCATTGAATTC GAGCTCGTTTAAAC	pFA6a-GFP(S65T)-KanMX6 (Baehler et al., 1998)	DPE 465: CATTTTCCTA TTCATCTATC C
Dis1-linker-GFP	DPE 720: AGGCACGAGACAACTGGAGGGAGAGTCA TGATTTGTCAAGTCATTTGTGGGAGCAAA TCCAAAGGATGAAGAAGGCGATCCTTGGA GCTCCTTCAGGA	DPE 463: GAGTGATTTCAACTCTACCTAATCGACTT TAACAAACACTCCAACAAAAAACTCTAC CAGCATTTCCACGCTTGTGCATTGAATTC GAGCTCGTTTAAAC	pFA6a-linker-GFP(S65T)-KanMX6 (Sandblad et al., 2006)	DPE 465: CATTTTCCTA TTCATCTATC C
81nmt1-dis1	DPE 460: CTCTACGGTGCTGGCTGTGTGAGTGAAAC ATTGTCGTCCGTAAAGTTAGTCGTCTCTAT TTACACATGTACAACTCCAATGAATTCGA GCTCGTTTAAAC	DPE 461: CTTCTATCTCCATTAATTTGTAAAAAGCT TACCTTATCAAAAATTTGACTGAGAATGC GGCTATTAAAATCGTCCAACTCCATGATT TAACAAAGCGACTATA	pFA6a- KanMX6-P81nmt1 (Baehler et al., 1998)	DPE 464: GCTCTAATAG TGTAATCTTG C
81nmt-alp14	DPE 432: TACTCCGGCCTTGCTAAATCGATATTCTGT AAAGTTTGACAGTGTTGTATTTGCCTACA GGCTTAACGAGTAATTACTTAGAATTCGA GCTCGTTTAAAC	DPE 639: GACGCACTTTCCATACTTTATGTACTATT CTTGATTCTAGAGGAAGTTTGGAGTAGTC TTCTTCTTGATCTTGGCTCATGATTTAACA AAGCGACTATA	pFA6a- HphMX6-P81nmt1 (This study)	DPE 640: GCCTACAGG CTTAACGAG
Toi4-GFP	DPE 214: CCTCATGTCCATGCTGAGCGTATGTCTCGC ATTGCTTCTGAGTCTAGCGATGCCGTTCCT CAGCAAACCGCCGTCCAGGTTGCTCGGAT CCCCGGGTTAATTAA	DPE 215: CGATTGTTTCTGGGATCATCAATCCATCC AAAAAGGAAAAAGTCACGAAAAAGCCC AAATGGGATTACGATAAGCTTTCAAGAA ATTTCTGAATTCGAGCTCGTTTAAAC	pFA6a-GFP(S65T)-KanMX6 (Baehler et al., 1998)	DPE 447: CACCACCTTC CTTCTTCCTT C

Table 2.1 (continued)

Gene modification	Forward transformation primer	Reverse transformation primer	Plasmid template	Confirmation primer
toi4Δ	DPE 433: ATACTACTACTACTACCACTTATTTTTATT **ATTACTACCATCTCTTCTTATTTACCCACA** TCTATTTCTATTTCTGCAAGCGGATCCCCG **GGTTAATTAA**	DPE 578: CAATTATTCTTTAATAAAGAAAATAAATT **ATGACCAAACAAGGACCTGGG** GAAAAGAGTAGTAAAAAAGAGTCGACAA **ACGGAATTCGAGCTCGTTTAAAC**	pFA6a-KanMX6 (Baehler et al., 1998)	DPE 560: GCT CAT ACC TGT CAC TGA CG
Toi4-HA	DPE 576: CCTCATGTCCATGCTGAGCGTATGTCTCGC **ATTGCTTCTGAGTCTAGCGATGCCGTTCCT** CAGCAAACCGCCGTCCAGGTTGCTCGGAT **CCCCGGGTTAATTAA**	DPE 577: CTGGGATCATCAATCCATCCAAAAAGGA **AAAAGTCACGAAAAAGCCCAAATGGGAT** TACGATAAGCTTTCAAGAAATTTCTGAAT **TCGAGCTCGTTTAAAC**	pFA6a-3HA-KanMX6 (Baehler et al., 1998)	DPE 447: CACCACCTTCC TTCTTCCTTC
Alm1(Toi1)-GFP	DPE 190: CACTCTGTTGACACTAATTCTCCTCCTAAA **CGGTCCAGTTCAGACGCTGGTATGGATGT** TTCCAATGATGTTAAGAAAGCCAAACGGA **TCCCCGGGTTAATTAA**	DPE 191: GCTCTTCAAAAAATATCAAAATATTAAAT **TACAATACAAAGCTTTTTATTATAATAAA** ATTAAAGTCGTTTTTTTTATTGGAAACCA **GGAATTCGAGCTCGTTTAAAC**	pFA6a-GFP(S65T)-KanMX6 (Baehler et al., 1998)	DPE 193: GACCACAAGG AAAACTCACC GC
Toi3-GFP	DPE 210: CGGTGAAAACTTTACTACCTGCGTTTAAG **GAGCAAGTATACCCCATTCTTCACAAATTT** GTCAGTGAGAATGAGAAGGATATCCGGAT **CCCCGGGTTAATTAA**	DPE 211: CAAATTTAATTAACTTTGAACTTACGAAA **TATTTAACATCTATTTGTTTAAATATATA** CATACAATATATTATGTATATCGAATTCG **AGCTCGTTTAAAC**	pFA6a-GFP(S65T)-KanMX6 (Baehler et al., 1998)	DPE 231: GCTTGGTTCTA CAATTTGAACG G
Toi9-linker-GFP	DPE 290: GGAGTTTTGATGATAAAGATTTACTTATCG **GTAAACAAAAGAAGGAGATTATTTGTTGT** TGTGATTTTTTACATGATTCTCTGATCCTT **GGAGCTCCTTCAGGA**	DPE 289: CCTGTTCATATTATGTTTTGACAAATATT **AGCTACCAGTTTAGTAACTTCAAATAAAA** ATTCGTATATGATTATATATATGAATTCG **AGCTCGTTTAAAC**	pFA6a-linker-GFP(S65T)-KanMX6 (Sandblad et al., 2006)	DPE : 292 GATGGCAATC GAAAGCGTCG C

Nucleotides in bold correspond to sequences specific for the plasmid used as templates to amplify the transformation fragment. Nucleotides in normal font correspond to the gene specific sequences required to allow homologous recombination (Baehler et al., 1998).

2.3. Construction of strains by crossing

Strains were crossed by mixing a toothpick of equal amounts of each parent strain of opposite mating type together on malt extract (MEA, Forsburg and Rhind, 2006) or minimal glutamate (EMMG; EMM2 containing 1 g/L sodium glutamate instead of Na_4Cl) with 20 µl water. Plates were incubated at 25ºC or 30ºC depending on the temperature sensitivity of the strains. After 48 hours the presence of spores was checked by microscopy and tetrads were dissected using a micromanipulator on appropriate non-selective medium. Plates were incubated at 25ºC or 30ºC until colonies were formed. Plates were replica-plated onto selective medium to assign markers and/or checked by colony PCR where no appropriate selection markers could be used to determine genotypes.

Table 2.2 Strains used in this study

Strain ID	Genotype
DB 337	*h- alp14-GFP-kanr leu1 ura4 his7*
DB 1224	*h- mal3::his3 alp14-GFP::kanr his7 leu1*
DB 1832	*h? klp5::ura4+ alp14-GFP-kanr his3-D1 leu1-32 ura4-D18*
DB 1830	*h- alp14-GFP-kanr klp6::ura4 his-(3 or 7) ura4 leu1*
DB 1843	*h? klp5::ura4 klp6::ura4 alp14-GFP-kanr his leu1 ura4*
DB 1469	*h- dis1-GFP::kanr*
DB 1822	*h- dis1-linker-GFP::kanr ade6-M216 leu1 ura4-D18*
DB 1862	*h- alp14-rRFP-kanR dis1-linker-GFP::kanr ura4 leu1 ade6-M216?*
DB 336	*h- alp14::kanr leu1 ura4*
DB 1197	*h- lys1+::nmt1-GFP-α2tub ura4-D18*
DB 1206	*h- alp14::kanr lys1+::nmt1-GFP-α2tub leu1-32 ura4-D18*
DB 2088	*h? nup85-GFP::kanr alp14::kan leu1-32::pSV40-GFP-atb2[leu1+] leu1-32 ade6? ura4-D18?*
DB 1454	*h- lys1+::nmt1-GFP-α2tub (integrated) nup85-GFP::kanr alp14::kanr ura4? leu1-32*
DB 1451	*h- sad1-dsRed::leu2 lys1+::nmt1-GFP-α2tub (integrated) nup85-GFP::kanr alp14::kanr ura4 leu1-32?*
DB 2037	*h+ alp14::kanr mal3-linker-GFP::kanR leu1 ura4*
DB 2036	*h? alp14::kanr mal3-linker-GFP::kanR leu1 sad1-dsRed::leu2/Sad1+ ura4 leu1-32*
DB 1783	*h- sad1-dsRed::leu2/Sad1+ mis6-GFP::kanr leu1 ura4 also maybe his2 and/or lys1-131*
DB 1663	*h- alp14::kanr mis6-GFP::kan sad1-dsRed::leu2/Sad1+*
DB 2065	*h? alp7::ura4+ nup85-GFP::kanr leu1-32::pSV40-GFP-atb2[leu1+] leu1-32 ura4 ade6?*
DB 2063	*h? alp7::ura4+ nup85-GFP::kanr alp14::kan leu1-32::pSV40-GFP-atb2[leu1+] leu1-32 ura4 ade6?*

Strain ID	Genotype
DB 1827	*H? dis1::hph sad1-dsRed::leu2 lys1+::nmt1-GFP-α2tub (integrated) nup85-GFP::kanr leu1? ura4?*
DB 2091	*h? leu1-32::pSV40-GFP-atb2[leu1+] 81nmt1-dis1::kanr Nup85-GFP::Kan leu1-32 ade6? ura4-D18?*
DB 2088	*h? nup85-GFP::kanr alp14::kan leu1-32::pSV40-GFP-atb2[leu1+] leu1-32 ade6? ura4-D18?*
DB 2089	*h? alp14::kan leu1-32::pSV40-GFP-atb2[leu1+] 81nmt1-dis1::kanr Nup85-GFP::Kn leu1-32 ade6? ura4-D18?*
DB 2092	*h? leu1-32::pSV40-GFP-atb2[leu1+] Nup85-GFP::Kan leu1-32*
DB 2101	*h- leu1-32::pSV40-GFP-atb2[leu1+] Nup85-GFP::Kan 81nmt1-alp14::hph leu1-32*
DB 2104	*h? leu1-32::pSV40-GFP-atb2[leu1+] Nup85-GFP::Kan dis1::hph 81nmt1-alp14::hph*
DB 2103	*h? leu1-32::pSV40-GFP-atb2[leu1+] Nup85-GFP::Kan dis1::hph*
DB 1636	*h- nmt1-GFP-dis1::kanr*
DB 1065	*h- alm1-GFP-KanR leu1 ura4*
LM 1	*h+ toi3-GFP::kanr adeM210 (or 216)*
LM 5	*h- toi4-GFP::kanr adeM210(or 216)*
DB 934	*h- toi9-GFP::kanr ade6-M216 leu1*
LM 231	*h- toi4-3HA::kanr*
DB 437	*h? crb3-3HA::kanr ura4-D18 leu1-32 ade6-M21(0 or 6)*
DB 427	*h- tip1::kanr ade6-M210 leu1-32 ura4-D18*
DB 588	*h-*
LM 142	*h- toi4-GFP::kanr cdc25-22*
LM 137	*h- toi4-GFP::kanr cdc10-129*
LM 149	*h- toi4-GFP::kanr spn1-1::kanMX6*
LM 179	*Toi4::kanr*
LM 196	*Toi4::kanr lys1+::nmt1-GFP-α2tub*
DB 1203	*h+ tip1::kanr lys1+::nmt1-GFP-α2tub*
LM 203	*toi4::kanr tip1::kanr lys1+::nmt1-GFP-α2tub*
DB 417	*h- tip1-GFP::kanr ura4-D18 leu1-32 ade6-M216*
LM 249	*toi4::kanr tip1-GFP::kanr ura4-D18? leu1-32? ade6-M216?*
DB 417	*h- tip1-GFP::kanr ura4-D18 leu1-32 ade6-M216*

2.4. Live Imaging

2.4.1. Cell preparation

Cells were grown from overnight pre-cultures to exponential phase (OD_{595} ~ 0.5) in 20 ml EMM2 containing the necessary amino acid supplements. Cells were transferred to plasma-treated glass bottom microwell dishes (MatTek Corporation, MA, USA) coated with 1 µl 2 mg/ml lectin BS-1 in H_2O (Sigma, #L2380). Dishes

were spun at 300 xg for 1 min in a bench-top centrifuge to attach the cells to the bottom of the MatTek dish. Unattached cells were washed away and 2 ml fresh medium was added.

2.4.2. Temperature shift experiments

For experiments in which the cells were imaged at 30ºC or for the 36ºC *alp14*Δ temperature shift experiments, the temperature shift was performed in the microscope environment box (see below). For cold shift experiments the cells were incubated at 18ºC in a cooled water bath and then imaged in a room maintained at 18ºC.

2.4.3. Cell cycle arrest with hydroxyurea

To arrest the cells in interphase they were first grown to exponential phase in EMM2. 1.2 mM hydroxyurea (HU) stock was added to a final concentration of 12 μM and the cells incubated with constant agitation for 3-4 hours (see figure legends for details for each individual experiment). For experiments in which a HU block was maintained throughout imaging, after transfer of the cells to MatTeK dishes they were washed and imaged with culture medium that had been passed through a 0.45 μm filter to remove any cells. When cells were imaged with a HU washout, they were washed and imaged in medium that did not contain HU.

2.4.4. FM4-64 endocytosis assay

The protocol for the endocytosis assays, performed using FM4-64 was adapted from Walther *et al.* (2006), Gachet and Hyams (2005) and Vida and Emr (1995).
Toi4-GFP, *toi4*Δ or wild type cells were grown to exponential phase at 25ºC in EMM2 overnight and transferred to lectin-coated MatTek dishes. Sufficient EMM2 added to cover the cells. Dual colour time lapse imaging using 488 nm and 568 nm excitation filters was started with a 30 sec delay between frames. After several images had been acquired, FM4-64 (Molecular Probes, #T-3166) was added to a final concentration of 2 μM from a 16 μM stock in DMSO. After 1 minute the FM4-64 was washed out with EMM2 and imaging continued for several minutes to visualise endocytic vesicle formation and consumption. When methyl-2-benzimidazole carbamate (MBC) was added to depolymerise the microtubules, the protocol remained the same, except for the following: Two minutes before addition of the FM4-64, MBC

(Sigma, #378674) was added to a final concentration of 25 µg/ml from a 10 mg/ml stock in DMSO. In all subsequent solutions added to the cells, MBC was added to a final concentration of 25 µg/ml to maintain the microtubules in a depolymerised state. The same concentration of MBC was used in the control wild type cells expressing GFP-tubulin to initially determine the parameters for the endocytosis assays.

2.4.5. Actin staining

Cells were stained for actin according to a protocol modified from Arai *et al.*, (1998). Cells were grown to exponential phase in YE5S at 25ºC and then shifted to 36ºC. Cells were fixed at the time-points indicated in pre-warmed 3% paraformaldehyde (PFA; Electron Microscopy Sciences #15710, EM-grade) and 0.24 M sorbitol for 30 min. Subsequent steps were performed at room temperature. Cells were then pelleted in a 15 ml Falcon tube by centrifuging for 3 minutes at 3200 xg and transferred to a 1.5 ml Eppendorf tube. Cells were washed 3 times with 1 ml PEM (100 mM PIPES, 1 mM EGTA, 1 mM Mg_2SO_4, pH 6.9 (NaOH)), centrifuging at 3000 xg for 1 minute. Cells were permeabilised by incubating in 1 ml PEM containing 1.2M Sorbitol and 1% Triton X-100 for 1 minute. Cells were washed 3 times and then blocked for 1 hour in 1 ml PEMBAL (PEM containing 1% BSA (FA and globulin-free), 0.1% NaN_3 and 100 mM lysine hydrochloride). To stain the actin, a volume of resuspended cells corresponding to an approximately 2µl cell pellet was transferred to a fresh Eppendorf tube. Cells were pelleted and then resuspended in 50µl PEMBAL. 15 µl BODIPY-Phallacidin containing 0.2 units/µl (Molecular Probes, #B607) was added and the cells were incubated for 30 min at room temperature, protected from the light, and then washed 3 times with PEMBAL. Cells were imaged immediately using an EGFP filter set.

2.4.6. TRITC-lectin and Calcofluor staining

The protocol for staining cells with TRITC-lectin and calcofluor was adapted from Bahler and Pringle (1998). Toi4-GFP cells were grown in YE5'S to exponential growth phase overnight at 25ºC and maintained at 25ºC throughout the experiment. 10 ml culture was transferred to a 15 ml Falcon tube. TRITC-lectin (Sigma, #L5264) was added to a final concentration of 5 µg/ml from a 100X stock in EMM2 and incubated for 5 minutes with gentle agitation. Cells were filtered onto a 47 mm filter (pore size, 0.8 µm; Whatman International Ltd, Maidstone, England) and washed with 20 ml YE5'S. The filter was transferred to a small conical flask containing 10 ml

YE5'S and incubated with gentle agitation for 45 minutes. 1 ml cell culture was transferred to a 1.5 ml Eppendorf tube and calcofluor white (Sigma, #18909) was added to a final concentration of approximately 1 mg/ml to counter-stain the cells. Cells were then imaged immediately using GFP and Cy3 filter sets.

2.4.7. Microscopes used for imaging

Cells were imaged using the microscope stated in the figure. The microscope set-ups are outlined below. All microscopes were fitted with an environment box (Mechanical Workshop, EMBL) that allowed the microscope stage to be maintained at a constant temperature throughout imaging.

2.4.7.1. PerkinElmer UltraView LCI spinning disc confocal system

An Argon Krypton was used for imaging GFP (488 nm excitation) and dsRed (568 nm excitation). The spinning disc system was coupled to a Nikon Eclipse TE200 microscope with a 100X oil immersion objective (Plan Fluor, NA 1.3). Images were acquired with a Hamamatsu Orca ER camera with a pixel size of 6.45 μm. Z-stacks were taken with 13-20 planes per stack, with a distance of 0.5 μm between planes.

2.4.7.2. PerkinElmer UltraView RS spinning disc confocal system

A 488 nm Argon Krypton was used to image GFP-tagged strains. The spinning disc system was coupled to a Carl Zeiss Axiovert 200 M microscope with a 100X oil immersion objective (Plan Fluor NA 1.3). Images were acquired with a Hamamatsu Orca ER camera with a pixel size of 6.45 μm. Z-stacks were taken with 13-20 planes per stack, with a distance of 0.5 μm between planes.

2.4.7.3. PerkinElmer UltraView ERS spinning disc confocal system

An Argon Krypton dual laser line was used for imaging GFP (488 nm excitation) and dsRed (568 nm excitation). The PerkinElmer UltraView ERS dual spinning disc system was coupled to a Carl Zeiss Axiovert 200 M microscope with a 100X oil immersion objective (Plan Fluor, NA 1.3). Images were acquired with a Hamamatsu

C9199-50 EMCCD camera with a pixel size of 8 µm. Z-stacks were taken with 13-20 planes per stack, with a distance of 0.5 µm between planes.

2.4.7.4. Carl Zeiss Axiovert 200 M Widefield system

A mercury lamp was used in combination with EGFP (F41-017) and Cy3 (F41-007) filter sets (AHF Analysentechnik). Images were acquired with a Coolsnap HQ camera (Roper Scientific) with a 100X oil immersion objective (Plan-XX, NA XX). Pixel size was 6.28 µm. Z-stacks were taken with 13-20 planes per stack, with a distance of 0.5 µm between planes, controlled by a XX piezo system.

2.4.8. Image analysis

Images from the confocal spinning disc microscope systems were acquired using PerkinElmer software. Images from the Carl Zeiss wide field microscope was acquired and Z-stacks generated using Metamorph software. Data was analysed using ImageJ (NIH, USA). Data acquired with the PerkinElmer systems was imported into ImageJ using a plug-in written by A. Seitz (EMBL) and Z-stacks were maximum-projected using a custom routine written by T. Zimmerman, EMBL. Frames of time-lapse movies were aligned using the StackReg plug-in (Thevenaz *et al.*, 1998) Movement of Alp14-GFP was quantified from kymographs, generated using a plug-in written by J. Reitdorf (EMBL). Image series were processed with Adobe Photoshop and Adobe ImageReady. Plotting of numerical data was done with Microsoft Excel.

2.5. Biochemistry

2.5.1. Cell extract preparation

For immuno-precipitation and pulldown experiments *S. pombe* yeast extracts were prepared as previously described (Moreno *et al.*, 1991). 50 ml cells were cultured at 25°C in YE5'S or EMM2 medium to OD_{595}= 0.5 and harvested by centrifugation at 2000 xg for 2 minutes at 4°C. The pellet was resuspended in10 ml of STOP buffer (150 mM NaCl, 50 mM NaF, 10 mM EDTA, 10 mM NaN_3), to terminate cell growth, enzymatic reactions and protect the extract from protein degradation,

followed by another round of centrifugation. The pellet was resuspended in 1 ml HEPES buffer (25 mM HEPES 50 mM Potassium Acetate, 1 mM $MgCl_2$, 1 mM EDTA, 1% CHAPS) containing protease inhibitors (1 mM DTT, 40 µg/ml Aprotinin, 20 µg/ml Leupeptin, 1 mM MSF, 2 mM Benzamidine, 1 µg/ml Pepstatin A, Roche EDTA-free protease inhibitor mix, 0.1 mM Sodium Vanadate, and 15 mM p-Nitrophenylphosphate) and transferred to a 1.5 ml Eppendorf tube. Cells were centrifuged again at 3,800 xg for 1 minute at 4°C and resuspended in 1 ml HEPES buffer. Cells walls and membranes were disrupted by vortexing with 0.5 ml glass beads (Sigma) in the FastPrep vortex (SAVANT, GMI, Minnesota, USA). A further 200 µl of HEPES buffer was added and a small hole in the bottom of the Eppendorf tube was made with a hot 27GA3/4 needle so the cell extract could be separated from the glass beads by a brief centrifugation. The extract was then centrifuged for 10 minutes at 3,800 xg and the supernatant fraction was recovered, taking care not to disturb the pellet. The pellet was the resuspended in 200 µl HEPES buffer. Samples of the supernatant and pellet fraction were mixed with protein loading buffer (100 mM Tris, HCl pH 6.8, 4% SDS, 0.2% bromophenol blue, 20% glycerol, 0.2 M DTT) and stored at -80°C for SDS-PAGE. The supernatant fraction was subsequently used for co-immunoprecipitation or pulldown experiments.

For extraction of Toi4-GFP with different detergents the HEPES buffer contained either 0.1% or 1% Triton X-100, 1% CHAPS, 1% NP-40 or 1% Tween-20. Otherwise, the protocol was identical.

2.5.2. Co-immunoprecipitation and pulldown experiments

Co-immunoprecipitation (co-IP) experiments were performed with monoclonal anti-GFP antibody (Roche Applied Science, Indianapolis, USA) bound to ProteinG-Dynabeads (Dynal Biotech, Hamburg, Germany) or polyclonal anti-Tip1 antibody (Brunner and Nurse, 2000) bound to ProteinA-Dynabeads (Dynal Biotech, Hamburg, Germany): 10 µl of beads were transferred to 1.5 ml Eppendorf tubes and washed 3 times with 1 ml PBS containing 0.1% Triton X-100. 1 µl antibody and 200 µl PBS-Triton were added to the beads and incubated for 1 hour at 4ºC. Beads were then washed 3 times with 1 ml HEPES buffer containing inhibitors. For the pulldowns, 33 µl Glutathione-Sepharose beads were used per sample. These were washed 3 times in 1 ml HEPES buffer. To this end Dynabeads were separated from the buffer using a

magnet (Dynal Biotech, Hamburg, Germany) and Sepharose beads by a 2 minute centrifugation step at 1700 xg. For both pulldowns and co-IPs the beads were incubated with 250 µl soluble yeast extract in 1.5 ml Eppendorf tubes for 1 hour, rotating at 4ºC. The beads were briefly washed 3 times in HEPES buffer and then mixed with protein loading buffer and stored at -80ºC for SDS-PAGE. Samples of the extracts before and after incubation with the beads were also collected for analysis.

2.5.3. Membrane localisation

For testing whether Toi4-GFP was membrane-associated 50 ml cells were harvested and extract collect as previously described (See Section 2.6.1) with the exception that HEPES Buffer was replaced by TNE buffer (50 mM Tris-HCl pH 7.4, 150 mM NaCl, 5 mM EDTA plus the same inhibitors as used for cell extract preparation). The soluble extract was transferred to 1 ml Beckman centrifuge tubes (Beckman Instruments Inc., CA, USA, #343778) and centrifuged for 1 hour at 100,000 xg to pellet the membranes. The supernatant fraction was removed and a sample collected for analysis. The membranes were washed with 400 µl TNE buffer on ice and re-centrifuged at 100,000 xg for 30 minutes. The membranes were then resuspended in 130 µl TNE buffer and 20 µl resuspended membranes added to 6 tubes. Cells were re-centrifuged at 100,000 xg for 30 minutes and the supernatant removed. Protein loading buffer was added to one tube and stored at -80ºC as a control. The remaining pellets were then resuspended in 400 µl TNE buffer containing either 1 M urea, 0.1 M sodium carbonate, 10 mM DTT or 0.5 M NaCl. A buffer-only control was also included. Membranes were incubated on ice for 30 minutes, and then centrifuged for 1 hour at 100,000 xg at 4ºC. The pellet fractions were resuspended in protein loading buffer and stored at -80ºC for SDS-PAGE. The supernatant fractions were removed and 25 µg BSA added. The proteins present in this fraction were precipitated with 100% TCA overnight on ice. The tubes were centrifuged at 20,800 xg and the pellet overlaid with 100% ice-cold acetone. The pellets were then dried, resuspended in protein loading buffer and stored at -80ºC for SDS-PAGE.

2.5.4. SDS-PAGE and Western blotting

Proteins were separated according to size by SDS polyacrylamide gel electrophoresis (SDS-PAGE) (Laemmli, 1970). Pre-cast 10% acrylamide gels (Invitrogen, CA, USA)

were used with MOPS-SDS buffer (2.5 mM MOPS, 2.5 mM Tris, 0.05 mM EDTA, 0.1% SDS) and run at 100 V. PageRuler Plus Molecular weight markers (Fermentas, St. Leon-Rot, Germany) were used to indicate protein molecular weight.

Proteins were detected by standard Western blotting techniques. Proteins separated by SDS-PAGE were transferred to an Immobilin-P transfer membrane (MILLIPORE), which had been pre-equilibrated in 100% methanol for 15 seconds followed by 10 minutes incubation in ice-cold transfer buffer (2.5 mM Tris base, 25 mM glycine, 20% methanol). The gel and membrane were assembled in a wet blotting setup operated at 4°C for 5 hours with a transfer current of 250 mA. The membrane was then rinsed in water and even transfer confirmed by staining with Ponceau S (SERVA Electrophoresis GmbH, Heidelberg, Germany). Membranes were then blocked with 5% skimmed milk powder in PBS-T (PBS plus 0.1% Tween-20) for 1 hour at room temperature. Primary antibodies (monoclonal anti-GFP (1:2000; Roche Applied Science, Indianapolis, USA), monoclonal anti-HA (1:2000; Sigma, #H3663) or polyclonal anti-Tip1 (1:500; Brunner and Nurse, 2000)) were diluted in 5% milk PBS-T. Membranes were incubated for 2.5 hours with the primary antibody and washed 3 x 10 min in PBS-T. The membranes were then incubated with secondary antibodies, coupled to horseradish peroxidase (ELC anti-mouse IgG, # NA931 or ELC anti-rabbit IgG, # NA934, Amersham Biosciences, Amersham, England) diluted 1:2000 in 5% milk PBS-T for 30 minutes and washed the same way. Western Lightning Enhanced Luminal reagent (PerkinElmer Life Sciences, MA, USA) was added to the membranes and membranes were exposed to BioMax MR film (KODAK, Stuttgart, Germany) to detect specific signals arising from chemo-luminescence catalysed by HRP coupled to the secondary antibodies

2.6. Electron microscopy of *alp14*Δ cells

2.6.1. High pressure freezing

At the time of freezing, 10 ml of cell culture at OD_{595} ~0.5 was filtered using a Millipore 15 ml filtration set-up with a polycarbonate filter (0.4 μm pore size) (Millipore, MA, USA). Cell paste was loaded into a Leica slot specimen carrier and

frozen in a Leica EMPACTII high-pressure freezer (Leica Microsystems GmbH, Wetzlar, Germany).

2.6.2. Fixation and freeze substitution

Fixation occurred during freeze substitution using anhydrous acetone containing 0.1% dehydrated glutaraldehyde (Electron Microscopy Sciences, Hatfield, PA, USA) 0.25% uranyl acetate (SERVA Electrophoresis GmbH, Heidelberg, Germany), and 0.01% osmium tetroxide (OsO4) (SERVA Electrophoresis GmbH, Heidelberg, Germany). Substitution took place over 56 hours at -90ºC in an EM AFS (Leica Microsystems GmbH, Wetzlar, Germany). the temperature was then increased 5ºC per hour to -45ºC. Plastic infiltration was carried out in steps (3:1 acetone:lowicryl [HM20] ratio (HM20; Polysciences Inc, PA, USA) and then 1:1, 1:3, and finally two times Lowicryl, each step lasting 1–3 hr) at this temperature followed by UV polymerization. Polymerization continued for 45 hours at this temperature and then increased to room temperature at 10ºC per hour. Once room temperature had been reached then samples were then illuminated for a further 12 hours.

2.6.3. Serial sectioning

Serial semi-thick sections (210–250 nm) were cut with a Leica Ultracut UCT microtome (Leica Microsystems GmbH, Wetzlar, Germany). Sections were collected on Formvar-coated, palladium-copper slot grids (Agar Scientific GmbH, Wetzlar, Germany) and post-stained with 2% UA in 70% methanol (MERCK, Darmstadt, Germany), followed by Reyonolds lead citrate (Electron Microscopy Sciences, Hatfield, Pa, USA). Cationic gold particles (15 nm; British Biocell, Cardiff, UK) were applied to both sides of the grid to be used as fiducial markers.

2.6.4. Tomogram acquisition

For tomography, the grids were placed in either high-tilt holder (Model 2020; Fischione Instruments, Corporate Circle, PA) or high-tilt rotate holder (Model 650; Gatan, Pleasanton, CA). Cells were selected by low magnification visual inspection of the grids. Serial tilt series were acquired for the selected cells, which spanned several serial sections. Montage tomographic datasets were collected using a FEI Tecnai TF20 or a FEI Tecnai TF30 (FEI Company, Oregon, USA) at a magnification of

~14,500X or ~15,500X, respectively using the tilt-series acquisition software, SerialEM (Mastronarde, 2005). Images were acquired every 1º over a ± 65º range using a Gatan 4K x 4K CCD camera. Image processing was performed on a Sun Opteron workstation (Sun Microsystems GmbH, Kirchheim, Germany). Images were aligned using the fiducial marker positions and tomograms computed using the R-weighted back-projection based FFS algorithm (Gilbert, 1972; Sandberg, 2003) and joined using eTomo graphical interphase (Mastronade, 1997).

2.6.5. Tomogram modelling

The IMOD software package (Kremer *et al.*, 1996) was used to display, model, and analyze tomograms and models. Relevant structures were modelled as reported in Hoog *et al.* (2007). Microtubules were tracked and ends morphology analyzed using the "slicer" tool. Microtubule ends were marked in different colours to allow distinction (Hoog *et al.*, 2007 and O'Toole *et al.*, 2003).

2.7. Bioinformatic analysis

2.7.1. Sequence alignment

To determine the extent of similarity between Toi4, its orthologue SPAC3C7.02c and the S. cerevisiae homologues Pil1 and Lsp1 we first aligned the amino acid sequences using the **M**ultiple **A**lignment using **F**ast **F**ourier **T**ransform (MAFFT Programme, EMBL-EBI Website). These multiple sequence alignments were then loaded into ClustalX (version 2.0.9; Larkin *et al.*, 2007). The sequences showed most similarity at their N-terminus (residue 1-264 in the multiple alignment). A pairwise sequence identity matrix of the N-terminal regions of all four proteins was calculated in the context of the MAFFT alignment using ClustalX (Appendix, Figure 7.3).

2.7.2. Prediction of post-translational modifications

To search for predicted post-translational modifications of Toi4 which could confer membrane localisation, we used the proteomics tools hosted by the ExPASY website (www.expasy.org/tools).

PART I

Characterisation of the *Schizosaccharomyces pombe* XMAP215 homologues, Alp14 and Dis1, during interphase

3. Results

3.1. Characterisation of Alp14 and Dis1 interphase localisation and dynamics

Alp14 is reported to localise as discrete patches on interphase microtubules (Garcia *et al.*, 2001). Live cell imaging of Alp14-GFP revealed moving particles that travelled quickly back and forth along microtubules (Nakaseko *et al.*, 2001; Okhura *et al.*, 2001) but quantitative results are lacking. The interphase localisation of Alp14 to microtubules is dependent upon the **T**ransforming **A**cidic **C**oiled-**C**oil (TACC) protein Alp7 (Sato *et al.*, 2004). Dis1, the Alp14 homologue, which localises to microtubules independently of Alp7, was reported to have a localisation and dynamic behaviour indistinguishable from the movement of microtubules (Nakaseko *et al.*, 2001; Nakaseko *et al.*, 1996; Nabeshima *et al.*, 1995). Previous studies of both Alp14 and Dis1 have focused on their roles during mitosis, therefore we sought to investigate the roles of these proteins during interphase.

3.1.1. Alp14 behaves as a microtubule plus-end tracking protein

To determine the precise interphase behaviour of Alp14 we used a strain in which the 3' terminus of the endogenous *alp14* gene was fused to the coding sequence of GFP (gift from T. Toda). The Alp14-GFP was therefore expressed under the control of the native promoter from the native locus. Consistent with previously published results (Nakaseko *et al.*, 2001; Okhura *et al.*, 2001; Garcia *et al.*, 2001) Alp14-GFP localised as particles (Figure 3.1A, and Figure 3.2A). Time-lapse imaging revealed that the particles moved in 2 directions, outbound from the region of the interphase microtubule organising centres (iMTOCs) in the cell centre, where Alp14-GFP was always present, towards the cell ends and inbound towards the cell centre (Figure 3.1A). From the literature we conclude that these particles are moving along microtubules (Garcia *et al.*, 2001; Nakaseko *et al.*, 2001; Okhura *et al.*, 2001). There were two classes of outbound particles: those moving outward with no particles in front of them, presumably at the microtubule tips or those moving behind another particle, presumably along an existing microtubule bundle, as determined using maximum intensity projections of the duration of the imaging.

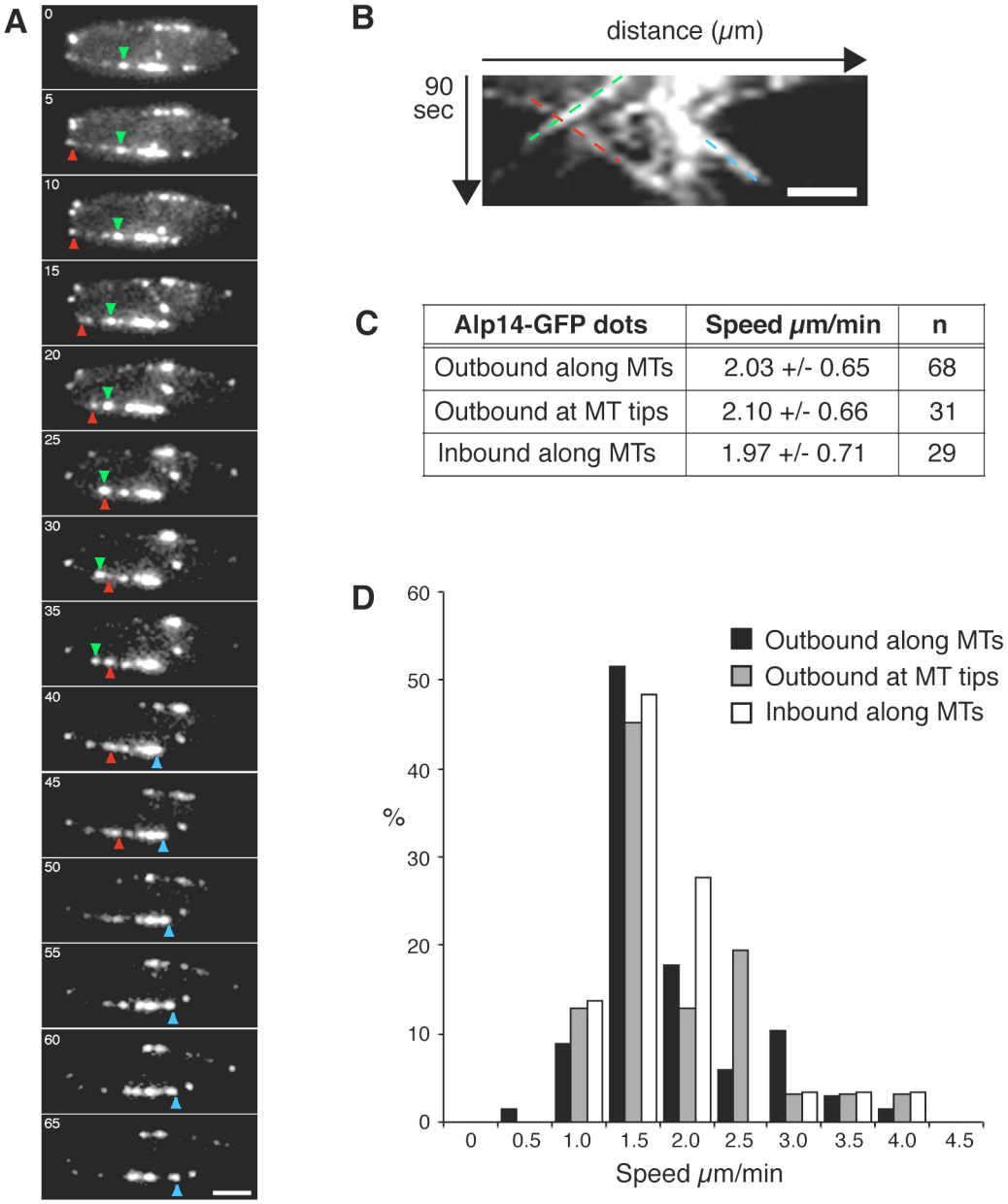

Alp14-GFP dots	Speed μm/min	n
Outbound along MTs	2.03 +/- 0.65	68
Outbound at MT tips	2.10 +/- 0.66	31
Inbound along MTs	1.97 +/- 0.71	29

Figure 3.1 Alp14-GFP particles move along interphase microtubule bundles

(A) Time lapse sequence of Alp14-GFP-expressing wild type cells. Frames show projections of 11 sections covering the entire Z-axis of the cell. Blue arrows mark movement of an outbound particle at the end of a microtubule bundle; green arrows mark outbound movement of a particle along an existing bundle; red arrows mark inbound movement along a bundle. (B) Kymograph of the lower microtubule bundle in (A) illustrating Alp14-GFP particle movement. Colours of dashed lines correspond to the particles marked with arrows in (A). (C) Quantification of the speed of the different types of Alp14-GFP particles moving along microtubules in wild type cells. (D) Distribution of the speed of the different types of particle movement in wild type cells. Bars, 2 μm.

Kymograph analysis showed the average speed of the outbound particles presumed to be moving along existing microtubule bundles was 2.03 +/- 0.65 μm/min (Figure 3.1B,C). This is similar to the speed and behaviour of the canonical +TIP Mal3 moving along microtubules (Busch and Brunner 2004). The speed of outbound particles presumed to be at the microtubule tips was 2.10 +/- 0.66 μm/min, which is slightly less than the reported value for Mal3. The speed of inbound particles was 1.97 +/- 0.71 μm/min (Figure 3.1B,C). There was no significant difference between the speed of particles moving outwards or inwards from the cell centre, as shown in Figure 3.1C,D.

3.1.2. Alp14 +TIP behaviour does not depend on Mal3

Due to the similarity between Alp14-GFP behaviour and that of Mal3, we checked whether the +TIP activity of Alp14 was Mal3-dependent. In addition, it was reported that the *S. cerevisiae* Alp14 homologue Stu2 and the Mal3 homologue Bim1 interact *in vivo*, although this interaction may be indirect (Wolyniak *et al.*, 2006). We created an Alp14-GFP strain in which the *mal3* gene was deleted. Live imaging of Alp14-GFP in this strain revealed shorter microtubules, as expected for *mal3*Δ cells (Beinhauer *et al.*, 1997) but Alp14-GFP still localised to the microtubules and displayed +TIP behaviour (Figure 3.2D). We therefore conclude that Alp14 +TIP behaviour is independent of Mal3 and also probably of the microtubule localisation of Tip1 and Tea2; localisation of Tip1 and Tea2 to interphase microtubules is dependent upon Mal3 (Browning *et al.*, 2003; Busch and Brunner, 2004). It remains possible, however that Tip1 and Tea2 play a role independent of Alp14 +TIP behaviour, for example loading of Alp14 onto microtubules.

3.1.3. Alp14 +TIP behaviour does not depend on Klp5 or Klp6

We then wanted to determine whether the +TIP behaviour of Alp14 was a property intrinsic to the protein itself, or whether Alp14 was being transported on growing plus ends by another protein(s), as is the case for the *S. pombe* CLIP170 homologue, Tip1, which is transported by the kinesin 7 family member, Tea2 (Busch *et al.*, 2004). However, based on the results with the *mal3*Δ strain, we can exclude transport of Alp14-GFP by Tea2.

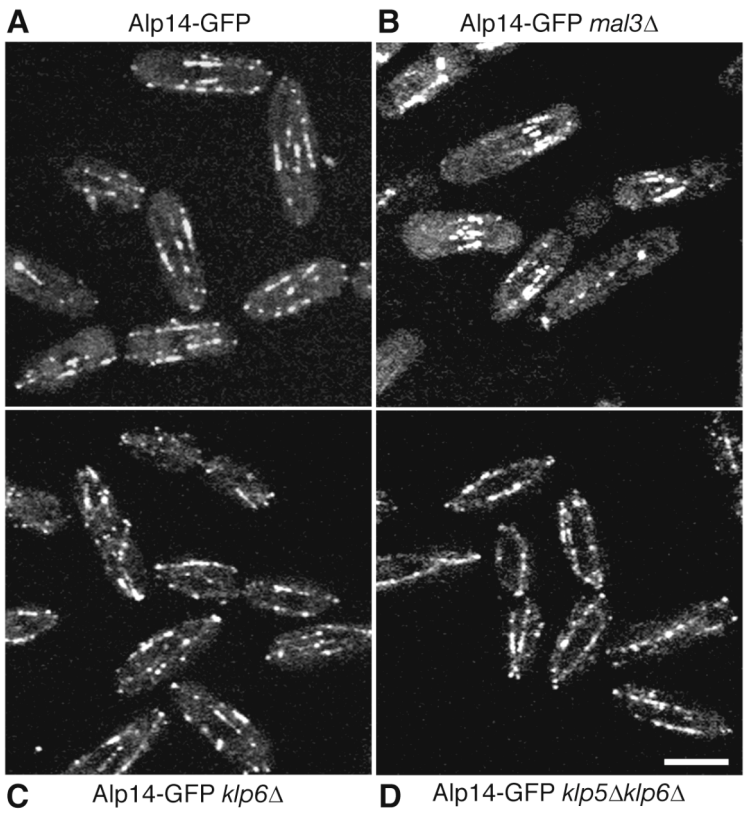

Figure 3.2

Alp14-GFP shows wild type localisation in *mal3Δ* and *klp5/6Δ* cells

(A) Alp14-GFP localisation in wild type cells. Alp14-GFP localisation along microtubules is unaffected in *mal3Δ* cells (B) and *klp6Δ* cells either as a single mutant (C) or as a *klp5Δ klp6Δ* double mutant (D). Images are projections of confocal sections covering the entire Z-axis of the cell. Bar, 5 *μ*m.

Only one other kinesin family in *S. pombe,* the kinesin 8 family members Klp5 and Klp6, are reported to localise to the plus ends of microtubules and show +TIP behaviour (West *et al.*, 2001). Despite the fact that Klp5 and Klp6 are depolymerising kinesins, they share an essential function with Alp14 and Dis1; any combination of mutants in *alp14/dis1* and *klp5/klp6* is synthetically lethal (West *et al.*, 2002; Garcia *et al.*, 2001b). In addition, Klp5/Klp6 cooperate with Alp14/Dis1 during mitosis to establish bivalent attachment of the kinetochores to the mitotic spindle. Furthermore, Klp5 localisation to the kinetochore is substantially decreased in the absence of Alp14 (Garcia *et al.*, 2002b). Given the link between Alp14 and Klp5/Klp6 during mitosis, we decided to test whether Klp5/Klp6 mediated the interphase +TIP behaviour of Alp14.

Alp14-GFP strains were constructed in which either the *klp5 or klp6* gene was deleted. Live imaging of these strains showed that the behaviour of Alp14-GFP *klp5*Δ and Alp14-GFP *klp6*Δ was the same and was indistinguishable from Alp14-GFP alone (Figure 3.2A,C). Although Klp5 and Klp6 co-localise and function together as a heterodimer *in vivo* (Garcia *et al.*, 2002a), it remains possible that single deletion of either gene could be compensated for by the activity of the remaining protein. We therefore constructed an Alp14-GFP strain in which both *klp5* and *klp6* genes were deleted. Alp14-GFP behaviour on interphase microtubules in this double deletion

strain was again identical to control cells (Figure 3.2C). Alp14 thus functions as a +TIP independently of Klp5 and Klp6.

3.1.4. Dis1 also associates with microtubules but does not show tip-tracking behaviour

To test whether Dis1 expressed at endogenous levels also shows +TIP behaviour we introduced the GFP coding sequence at the 3′ end of the *dis1* gene locus. The resulting chimeric protein localised to interphase microtubules but with a different pattern to Alp14. We found that Dis1-GFP gave a strong microtubule signal in the central region of the cell where the overlap zones are found (Drummond and Cross, 2000). Although the Dis1-GFP signals oscillated within these regions (Figure 3.3A,B), this resembled the movement of the overlap regions when the microtubule bundle is pushed to centre the nucleus by forces generated by contact with one of the cell poles (Tran *et al.*, 2001; Daga *et al.*, 2006). When longer exposures were used it became clear that in addition to localisation at the overlap regions, Dis1GFP also localised along the entire length of the microtubules. Unlike Alp14, Dis1-GFP did not show +TIP behaviour or movement along the microtubules (Figure 3.3A,B). The brighter Dis1-GFP signal in the overlap region is probably a consequence of an increase in the number of short microtubules in this region (Hoog *et al.*, 2007). Thus our results are similar to previous localisation studies of Dis1-GFP, which report Dis1-GFP dynamics as being indistinguishable from control tubulin-GFP expressing cells (Nakaseko *et al.*, 2001).

3.1.5. Addition of a linker sequence between the C-terminus and the GFP tag does not change Dis1 dynamic behaviour at 30°C

C-terminal tagging of the +TIP Mal3 causes abnormal microtubule behaviour (Beinhauer *et al.*, 1997; Browning *et al.*, 2003) so we wanted to check whether this could also be the cause of the absence of +TIP behaviour of Dis1-GFP. Addition of a 22 amino acid linker sequence between the C-terminus and the GFP tag rescued the abnormal behaviour of Mal3 (Sandblad *et al.*, 2007) so we added this linker-GFP sequence to the *dis1* gene locus. The resulting chimeric protein showed the same behaviour as the non-linker construct at 30°C but cells expressing this protein at 25°C grew very slowly (Figure 3.3C).

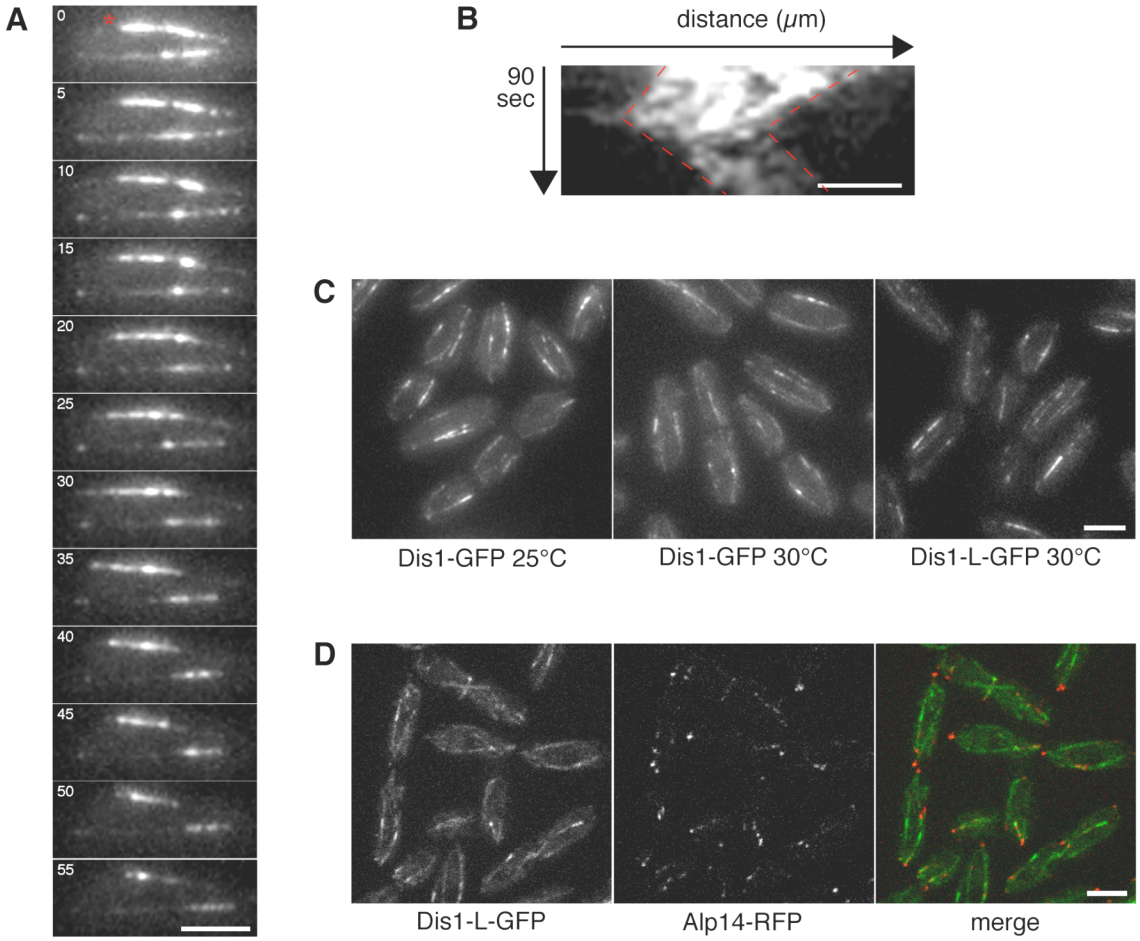

Figure 3.3 Dis1 does not actively move along microtubule bundles

(A) Movie sequence of Dis1-GFP-expressing wild type cells. (B) Kymograph of the microtubule bundle marked with an asterisk in (A) illustrating Dis1-GFP oscillation at the cell centre. Dashed lines highlight that Dis1 remains localised to the central region of the bundles. (C) Addition of a linker sequence between the GFP tag and the C-terminus of Dis1 does not change Dis1 behaviour at 30ºC. (D) Dis1-GFP and Alp14-rRFP show very little co-localisation. Images are projections of sections covering the entire Z-axis of the cell. Bars, 4 μm.

3.1.6. Alp14 and Dis1 show very limited co-localisation

Given the apparent difference in localisation and dynamics of Alp14 and Dis1, we were interested to know whether there was any co-localisation of these proteins. A strain was constructed in which Alp14 was C-terminally tagged with RFP and Dis1 with linker-GFP. Fluorescence microscopy of both Dis1 and Alp14 at 30°C gave identical results to Figure 3.1 and Figure 3.3A,B,C respectively, indicating that the

tags were not interfering with protein localisation. Dual colour imaging revealed occasional co-localisation of Alp14 and Dis1 in central regions of the cell, but only Alp14-RFP localised to the microtubule tips (Figure 3.3D). This suggests that Alp14 and Dis1 localise to microtubules independently of each other.

3.2. *alp14*Δ

3.2.1. *alp14*Δ cells have compromised interphase microtubules at the permissive temperature

In order to characterise the phenotype of *alp14*Δ cells with respect to microtubule function in interphase we constructed a strain in which *alp14* was deleted and microtubules were labelled with GFP-tubulin expressed from the repressed *nmt1* promoter. Live imaging revealed that at 25°C the cells appeared longer, and many had shape abnormalities, as previously described (Garcia *et al.*, 2001; Nakaseko *et al.*, 2001; Okhura *et al.*, 2001). In addition, interphase cells had fewer microtubule bundles, which appeared shorter (Figure 3.4B). This is in disagreement with Garcia *et al.* (2001), who reported normal interphase arrays as determined by immunostaining. However, it is in partial agreement with Nakaseko *et al.* (2001), who reported that interphase microtubules in *alp14*Δ cells were rarely observed. Only Okhura *et al.* (2001) report a similar phenotype. We therefore quantified the interphase microtubules in *alp14*Δ cells and found an average of 2.53 +/- 1.14 microtubule bundles per cell (Figure 3.4C inset), which had an average length of 3.57 +/- 2.03 μm (Figure 3.4C). This is fewer than wild type cells, which have an average of 3.49 +/- 0.98 microtubule bundles per cell with an average length of 6.34 +/- 2.41 μm (Figure 3.4C). We also quantified the percentage of microtubule bundles where one or both of the ends of the bundle were touching the cell poles and found that in *alp14*Δ cells only 27% of the bundles reached at least one of the cell poles, in contrast to 76% in wild type cells. This reduction in the percentage of microtubule bundles reaching the cell poles, in addition to reflecting a decrease in the average bundle length, may also reflect the increase in the length of *alp14*Δ cells. In addition, many cells showed mitotic abnormalities (Garcia *et al.*, 2001, Nakaseko *et al.*, 2001, Okhura *et al.*, 2001).

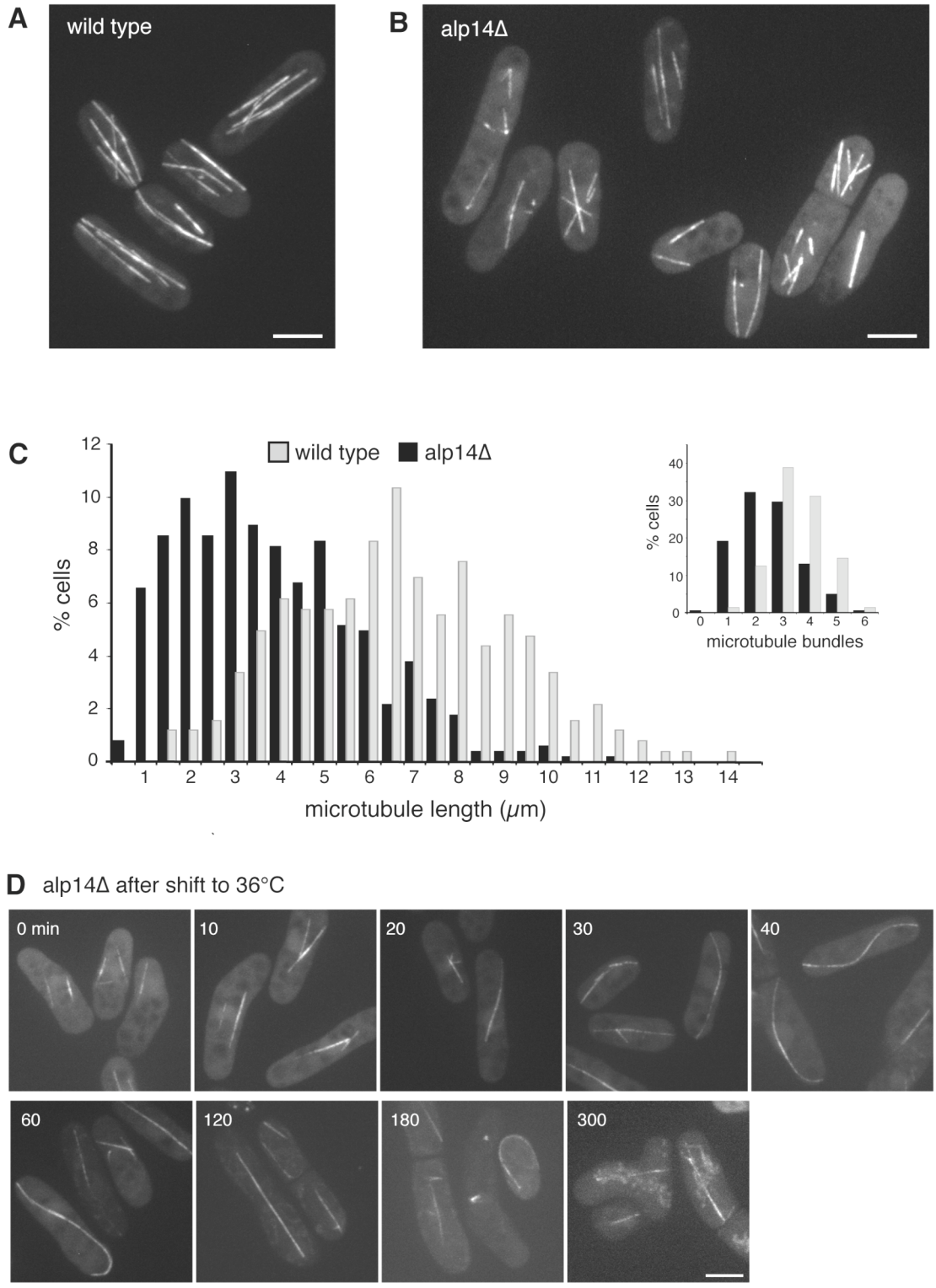

Figure 3.4 Interphase microtubule arrays are abnormal in *alp14Δ* cells

Microtubules in wild type control (A) and *alp14Δ* cells (B) expressing GFP-tubulin at 25ºC. (C) Quantification of microtubule bundle length and bundle number in wild type and *alp14Δ* cells. (D) Microtubules in *alp14Δ* cells at 36ºC. Images are projections of confocal sections covering the entire Z-axis of the cell. Bars, 4 μm.

3.2.2. The behaviour of microtubules in *alp14*Δ cells changes when the cells are moved to the restrictive temperature

We then monitored the microtubules when *alp14*Δ cells were shifted to the restrictive temperature of 36°C. Previous studies had focused mainly on the mitotic phenotypes of *alp14*Δ cells under these conditions. We however, followed specifically the interphase phenotype. In agreement with previous studies (Garcia *et al.*, 2001; Nakaseko *et al.* 2001) we observed that after 4-6 hours many of the cells showed highly abnormal mitotic phenotypes and had what appeared to be an elongated spindle, although astral microtubules were absent. In addition we observed a large number of shape abnormalities and dead cells (Figure 3.4D, t=180 and 300 min). We also looked at the cells at earlier time points. After shifting to the restrictive temperature many of the cells lost all but one of their bundles; after 40 mins most cells had a single microtubule array (Figure 3.4D). In contrast, the wild type control cells maintained a normal interphase microtubule array throughout. The behaviour of the *alp14*Δ microtubule array at the restrictive temperature was different to those at the permissive temperature; it grew to the cell poles, sometimes curling around them (Figure 3.4D, t=40 min and t=60 min). This shows that microtubules display altered dynamic behaviour in *alp14*Δ cells at higher temperatures.

3.2.3. The microtubule array is intranuclear and interphasic

Upon careful examination of the confocal slices used to create the maximum projection images of *alp14*Δ cells at the restrictive temperature, we noticed that the single microtubule structure consistently passed through the centre of the cell. In *S. pombe* cells the nucleus occupies nearly the entire cell centre, so for the microtubules to pass through the central cell region they would have to also pass through the nucleus. Consistent with this, the microtubule array at the restrictive temperature showed similarities to an elongated spindle structure, which forms in the nucleus during closed mitosis in fission yeast, however we never observed astral microtubules. We therefore devised an experiment to test both whether the microtubule array in *alp14*Δ at the restrictive temperature was intranuclear and to confirm whether this structure formed in interphasic or mitotic cells. To test whether the microtubules were intranuclear we created an *alp14*Δ, GFP-tubulin strain in which the nuclear pore complex protein Nup85 was C-terminally tagged to express a linker-GFP to visualise the nuclear envelope.

3.2.3.1. *alp14Δ* cells form intranuclear microtubule arrays at the restrictive temperature

We systematically examined consecutive confocal slices of the synchronised interphase cells in Figure 3.5B after two hours at the restrictive temperature. They clearly revealed that the microtubule array was indeed intranuclear and not cytoplasmic; the array passed through the centre of the nucleus and protruded from either end, without significant deformation of the spherical nuclear mass (Figure 3.5C). These microtubules were obviously deforming the nuclear envelope, as indicated by Nup85-GFP dots spread along the microtubule bundle (Figure 3.7C, arrowheads).

3.2.3.2. The microtubule array forms in interphase cells at the restrictive temperature

The intranuclear microtubule array was reminiscent of mitotic spindles and could indicate a mitotic block. However, recently intranuclear microtubules have also been observed in cells in which the gamma-tubulin ring complex component Mto1 is deleted. In these cells the intranuclear bundle formed during interphase as a result of the microtubules failing to exit the nucleus following mitosis (Zimmerman and Chang, 2005). We therefore checked whether we could exclude this as the reason for intranuclear microtubule formation in *alp14*Δ cells at 36ºC. *alp14*Δ cells were blocked in interphase using hydroxyurea (HU). Treatment with HU inhibits the reduction of ribonucleotides to deoxyribonucleotides by the enzyme ribonucleotide reductase, blocking the cells early S-phase, prior to significant DNA replication (Yarbro, 2002). After 3.5 hours incubation at the permissive temperature in the presence of HU, cells were shifted to the restrictive temperature (36°C) concomitant with HU washout and thus release from the early S-phase block. After 3.5 hours block with HU at the permissive temperature, followed by HU washout and one hour incubation at the restrictive temperature 97% of the wild type cells had cytoplasmic microtubule arrays (Figure 3.5A,B), confirming that the HU was efficiently blocking the cells in interphase. Examination of the similarly treated *alp14*Δ cells showed that 71% had an intranuclear microtubule array, compared with only 3% at the permissive temperature (Figure 3.5A,B). Of those cells that formed an intranuclear microtubule array, at no

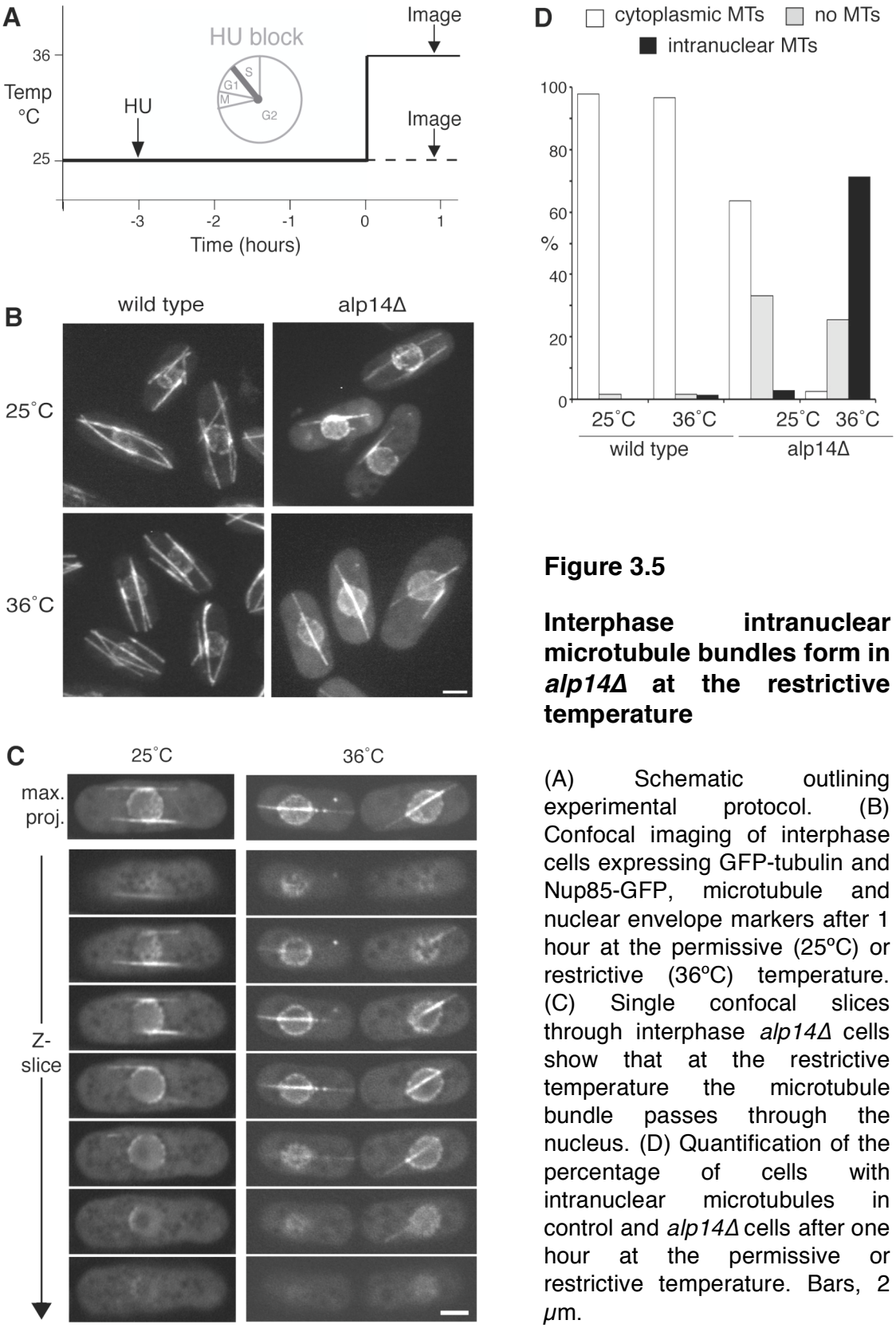

Figure 3.5

Interphase intranuclear microtubule bundles form in *alp14Δ* at the restrictive temperature

(A) Schematic outlining experimental protocol. (B) Confocal imaging of interphase cells expressing GFP-tubulin and Nup85-GFP, microtubule and nuclear envelope markers after 1 hour at the permissive (25ºC) or restrictive (36ºC) temperature. (C) Single confocal slices through interphase *alp14Δ* cells show that at the restrictive temperature the microtubule bundle passes through the nucleus. (D) Quantification of the percentage of cells with intranuclear microtubules in control and *alp14Δ* cells after one hour at the permissive or restrictive temperature. Bars, 2 *μ*m.

time did we observe more than one array per nucleus. These results confirm that the intranuclear microtubule array seen in *alp14*Δ cells at the restrictive temperature is interphasic, and not a mitotic spindle. In addition, as the cells were in interphase before being shifted to the restrictive temperature, it shows that the intranuclear microtubule structure does not form as a result of the cells failing to nucleate cytoplasmic microtubules following mitosis, as in the case of *mto1*Δ cells (Zimmerman and Chang, 2005), but that it forms *de novo* as a consequence of the temperature shift.

3.2.4. The transition temperature at which intranuclear microtubules form is sharp

Given the striking microtubule phenotype of *alp14*Δ cells forming upon shift to the restrictive temperature, we were curious whether there was a critical temperature at which all the microtubules switched from a cytoplasmic to a nuclear nucleation, or whether this occurred gradually over a wider temperature range. To test this, exponentially growing cells were blocked in interphase using HU and then shifted for one hour to a higher temperature. The number of intranuclear microtubules was then quantified for each of the temperatures. As shown in Figure 3.6, a sharp switch occurred between 31°C and 33°C during which the percentage of cells with an intranuclear microtubule array increased from 11% to 84%. This suggests that a defined switch from cytoplasmic to intranuclear microtubule nucleation occurs upon reaching the critical temperature.

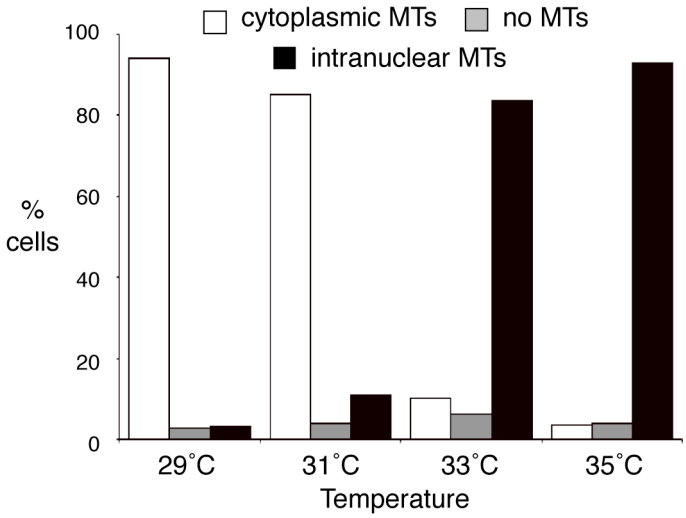

Figure 3.6

The transition temperature at which intranuclear microtubules form in *alp14Δ* cells is sharp

Quantification of the percentage of interphase *alp14Δ* cells with intranuclear microtubules after one hour at the indicated temperature.

3.2.5. At the restrictive temperature the intranuclear microtubule bundle forms concomitant with the loss of cytoplasmic microtubules.

We were interested to see how the intranuclear microtubule arrays formed at the restrictive temperature, and whether they displayed behaviour similar to cytoplasmic interphase microtubules or spindles. We monitored the initial stages of intranuclear microtubule array formation in a strain containing GFP-labelled tubulin and nuclear envelope markers (Figure 3.7A). The cells were blocked with HU and then released from the block 10 minutes before imaging began to ensure all cells were in interphase. Upon shifting to the restrictive temperature the cytoplasmic microtubules gradually depolymerised back to a region next to the nucleus and no new nucleation of cytoplasmic microtubule bundles was observed. During this time an intranuclear microtubule array began to grow from the region of the nuclear envelope with which one of the remaining cytoplasmic microtubules was associated (Figure 3.7A; t=7 min). The cytoplasmic microtubule bundle continued to behave normally for several minutes but eventually depolymerised back to the region of the nuclear envelope from which the intranuclear microtubule array continued to grow. Upon formation of the intranuclear microtubule array we failed to observe an increase in the background fluorescence of GFP in the nucleus (Figure 3.4D).

3.2.6. The intranuclear microtubule array displays very slow dynamics and is able to move the nuclear mass

We then monitored the behaviour of the intranuclear microtubule arrays over a two hour time period in cells released from a HU block. Figure 3.7B shows a typical example of such behaviour. In this cell, the intranuclear microtubule array grew at a rate of approximately 0.075 μm/min, eventually spanning the spherical nucleus. It then continued to grow, protruding mostly from one side of the nucleus. The array appeared not to rupture the nuclear envelope, which seemed to locally deform around the protruding structure, indicated by the presence of discrete patches of GFP signal along the array, which likely corresponded to the nuclear pores, labelled with Nup85-GFP (Figure 3.7A; t=15 min). This is in contrast to the behaviour of the intranuclear microtubule bundle seen in *mto1*Δ cells where the bundle is able to puncture through the nuclear envelope and to re-establish a cytoplasmic microtubule array (Zimmerman and Chang, 2005). Once the array reached one cell pole it continued to grow, now protruding from the other side of the nucleus and both ends of the array contacted the

cell poles (Figure 3.7C; t=20 min). The array continued to grow, bending as a result of the force exerted against the cell poles (Figure 3.7C; t=20-25 min), but then underwent a catastrophe (Figure 3.7C; t=25-35 min). Rather than depolymerising completely, it shrank to half the length of the cell but then rescue occurred and the array began to re-grow, once again reaching the cell poles. We also observed examples where the intranuclear microtubule array, when in contact with a cell pole, exerted force on the nuclear envelope such that the entire nucleus was displaced to one end of the cell (Figure 3.7C; t=25-30 min; t=85-105 min), suggestive of a physical connection between the nuclear envelope and the microtubule array. This type of nuclear movement by microtubules is seen during interphase in wild type cells where the cytoplasmic microtubule bundles exert forces on the nucleus to keep it in the centre of the cell, however the movement seen in the *alp14*Δ cells was more extreme than what is usually observed in wild type cells (Daga *et al.*, 2006; Tran *et al.*, 2001; Tran *et al.*, 2000). In addition, this type of behaviour is not seen in *mto1*Δ cells, providing further evidence that the behaviour of the intranuclear microtubule bundles in the two mutants are very different (Zimmerman and Chang, 2005).

3.2.7. The intranuclear microtubule bundle is associated with the SPB

During interphase one of the cytoplasmic microtubule bundles is nucleated from, and remains associated with the spindle pole body (SPB). We were therefore also interested to know if the intranuclear microtubule formed in *alp14*Δ at the restrictive temperature was associated with the SPB. To test this we created a strain containing the GFP fluorescent markers for the microtubules and nuclear envelope used previously, plus Sad1-dsRed, an SPB marker (Chikashiga and Hiraoka, 2001; Hagan and Yangida, 1995). When interphase cells were shifted from the permissive to the restrictive temperature we observed that the intranuclear microtubules began to grow from the region of the nuclear envelope to which Sad1-dsRed also localised (Figure 3.7C; t=1-5 min). The microtubule bundle grew out from the region of the SPB, which remained associated with one end of the bundle until the other end of the microtubule reached the cell pole (Figure 3.7C; t=0-10 min).

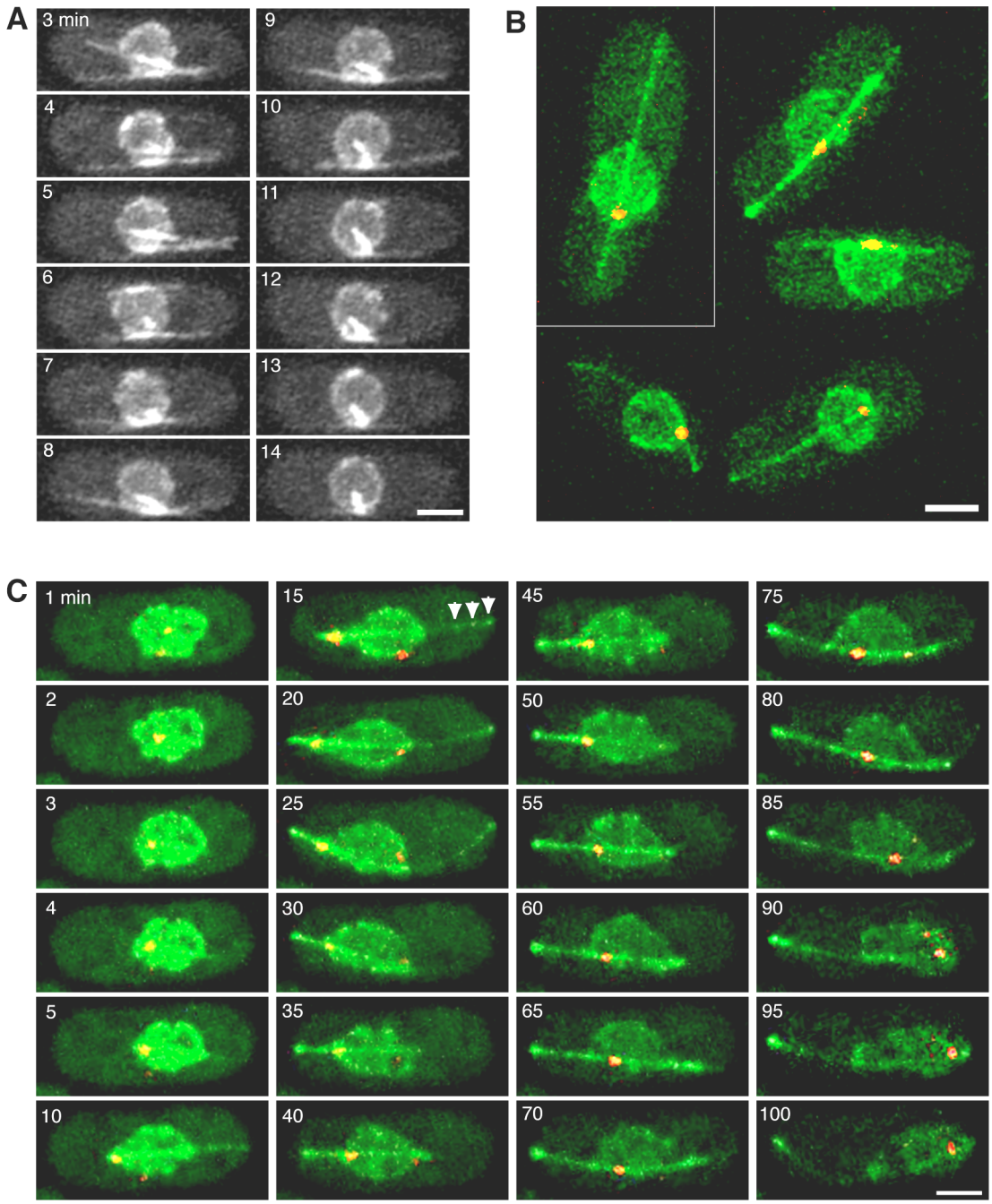

Figure 3.7 Intranuclear microtubule bundle formation and dynamics in *alp14Δ* at the restrictive temperature

Movie sequence of projected confocal images of *alp14Δ* cells expressing GFP-tubulin, Nup85-GFP microtubule and nuclear envelope markers. (A) Upon shifting to the restrictive temperature, cytoplasmic microtubule bundles depolymerise concomitant with intranuclear microtubule bundle formation. (B and C) Imaging of cells additionally expressing the Sad1-dsRed SPB marker. (B) After 1 hour at the restrictive temperature the SPB is always associated with the intranuclear microtubule bundle. (C) The intranuclear microtubule bundle is nucleated from the vicinity of the SPB. The bundle shows shows dynamic behaviour and is able to move the nucleus. White arrows indicate GFP foci that likely correspond to Nup85-GFP. Bars, 2 μm.

The bundle subsequently continued to grow, eventually to span the entire cell length. The SPB was no longer at the microtubule bundle tip, but rather seemed to move along the bundle (Figure 3.7C; t=15-100 min). This SPB behaviour was observed in all cells imaged. The extent of the SPB movement along the region of the bundle protruding from the main nuclear body did vary; in some cells the SPB initially travelled the length of the bundle, but at later time points the SPB localised to the spherical nuclear region rather than along the protruding part of the microtubule array. However, for all cells in which the bundle protruded from only one side of the nuclear envelope, the SPB was found at the non-protruding end of the bundle, at the nuclear periphery and only when the bundle protruded from both sides of the nucleus was the SPB found away from the ends of the bundle. In addition, we never observed duplicated SPBs in cells with intranuclear microtubule bundles, providing further evidence that the cells were in interphase. Further examples are shown in Figure 3.7B.

3.2.8. Electron microscopy of *alp14*Δ cells at the restrictive temperature

As a result of the live cell imaging data we wanted to look in more detail at the intranuclear microtubule array formed in *alp14*Δ at the restrictive temperature. For this we initiated a collaboration with H. Roque and C. Antony (EMBL, Heidelberg) to examine *alp14*Δ cells at high resolution using transmission electron microscopy tomography. *ap14*Δ cells were shifted to the restrictive temperature for two hours and then rapidly cryo-immobilised and fixed. Tomograms were acquired of serial sections through single cells and subsequently tomograms were montaged and the microtubules, nuclear envelope and SPB were modelled.

3.2.8.1. The SPB remains outside the nuclear envelope when cells are shifted to 36ºC

During mitosis, the SPB is embedded into the nuclear envelope, which becomes fenestrated in this region. This allows nucleation of intranuclear microtubules that form the spindle. In contrast, during interphase the SPB remains outside the nuclear envelope, which is intact (Figure 3.8A, Ding *et al.*, 1997). Given the close association of the SPB with the intranuclear microtubule array, as visualised by confocal fluorescence imaging, we examined the position of the SPB in the electron tomograms. In most cases there was a single unduplicated SPB (Figure 3.8B), but in

some cases the SPB had duplicated and an electron dense bridge structure was connecting the 2 SPBs indicating that the cells were in late G2 phase (Figure 3.8C). In all cases (n=8) the nuclear envelope below the SPB was clearly intact (Figure 3.8B,C, Figure 3.9B). We could therefore confirm that although the cell cultures were unsynchronised and fixed after two hours at the restrictive temperature all modelled cases were still in interphase and the microtubule structure was not a mitotic spindle. In all cases we observed microtubules inside the nucleus, in close proximity to the nuclear envelope in the region of the SPB (Figure 3.8B,C; Figure 3.9).

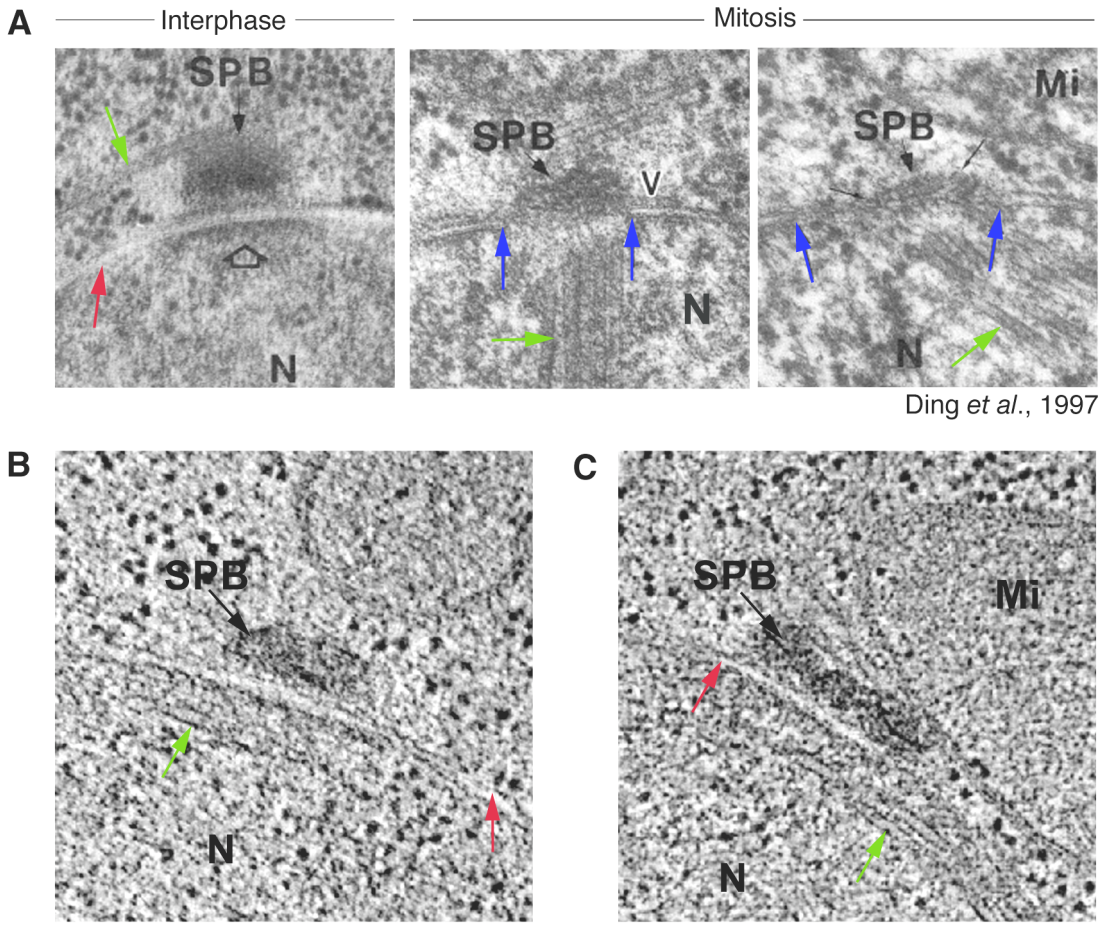

Figure 3.8 The SPB lies outside the nucleus above an intact nuclear envelope in *alp14Δ* cells

(A) Electron microscopy of serial section of wild type cells shows that in interphase the SPB lies outside the nucleus and that the nuclear envelope remains intact. During mitosis, the SPB becomes embedded in the nuclear envelope, which shows fenestrations. (B) and (C) Electron microscopy tomographic slices through *alp14Δ* cells after 2 hours at the restrictive temperature. The SPB remains outside the nucleus and the nuclear envelope is clearly intact below the SPB. (B) and (C) acquired by H. Roque (EMBL). Green arrows show microtubules; red arrows indicate an intact nuclear envelope; blue arrows show nuclear envelope fenestrations. N, nucleus; Mi, mitochondrion; SPB, spindle pole body.

3.2.8.2. The intranuclear microtubule array is a bundle of mixed polarity

We next looked in more detail at the intranuclear microtubule array. We found that it consisted of a bundle of overlapping microtubules arranged with mixed polarity, as determined by examination of the microtubule end structures (O'Toole *et al.*, 1999; O'Toole *et al.*, 2003): The O'Toole studies show that minus ends are capped or closed and often appear pointed, while the majority of microtubules plus ends have flared, open structures. The intranuclear bundle had an arrangement reminiscent of interphasic cytoplasmic SPB-associated bundles, with greater overlap between the microtubules in the region next to the SPB (Figure 3.9C; Höög *et al.*, 2007). There were between 3 and 8 microtubules in the bundle (n=4 complete bundles). In addition, in 6 out of 8 cases (n=4 complete bundles; n=4 partial bundles) the microtubule bundle was found to curve around the inner face of the nuclear envelope such that it passed under the SPB (Figure 3.7B,C; Figure 3.8).

3.2.8.3. The intranuclear microtubule does not pierce the nuclear envelope, which locally deforms around it.

Upon closer examination of the images in Figure 3.7C (t=10 min) we observed punctate staining along the length of the microtubule region protruding from the nucleus, which was presumably the nuclear pore marker Nup85-GFP (See Section 4.2.6; Figure 3.7C). This suggested that the nuclear envelope was still intact around the microtubule structure and that the microtubule bundle was deforming the nuclear envelope rather than piercing it. To confirm this, we examined the region of the nuclear envelope at which the microtubule bundle extended beyond the spherical nuclear mass. Modelling of the microtubules and nuclear envelope in this region revealed that the microtubule bundle remained inside the nuclear envelope, which showed extreme local deformations to maintain an intact structure around the bundle (Figure 3.9C). In all cases where we could model the entire microtubule bundle (n=4) the nuclear envelope was intact around the bundle.

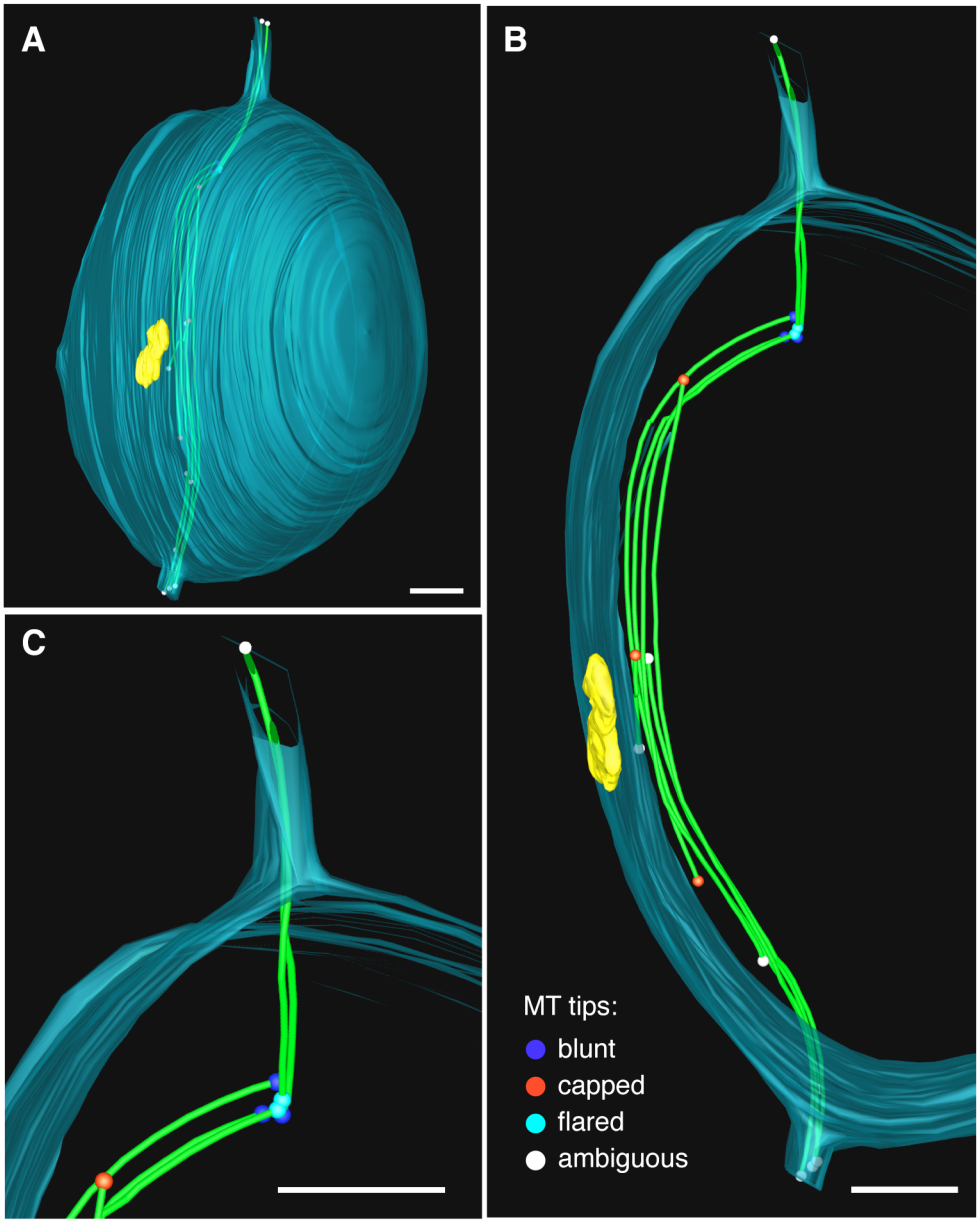

Figure 3.9 3D model of the intranuclear microtubule bundle in *alp14Δ* after two hours at the restrictive temperature

3D modelling of an electron microscopy tomography tilt series. (A) and (B) The intranuclear microtubule array consists of a bundle of microtubules of mixed polarity. The SPB remains outside the nucleus and the nuclear envelope is intact under the SPB. The bundle curves around the inner face of the nuclear envelope (C) Close-up view of the bundle. At the point where the bundle protrudes from the nuclear mass the nuclear envelope remains intact, extending around the bundle. A sharp break in the bundle is clearly visible. The nuclear envelope is shown in transparent turquoise; microtubules are green; the SPB is yellow; microtubule end structures are indicated by coloured caps, according to the legend in (B). Bars, 250 nm. Images acquired by H. Roque (EMBL).

3.2.8.4. The microtubule bundle sometimes appears to have a break, possibly due to increased force from bending

In two of the eight cases we observed a discontinuity in the microtubule bundle close to where it extended beyond the main nuclear mass (n=4 complete bundles; n=4 partial bundles). It appeared that the microtubules had snapped at this point, as there was a joint in the bundle where all the microtubules ended and new microtubules began (Figure 3.9C). This was not seen in all cases and could be an artefact resulting from sample preparation, however the high-pressure freezing technique used to immobilise the cells prior to fixation minimises such artefacts. Also, the snapping of an intranuclear microtubule bundle was never observed *in vivo*. However, as the intranuclear microtubules maintain a close proximity to the inner face of the nuclear envelope it is possible that the bending force exerted on the bundle caused it to snap in the region near to point at which it leaves the main nuclear body, where the angle of bending, and thus the force on the bundle is presumably greatest.

3.2.9. Initial stages of intranuclear microtubule bundle formation revealed an aster-like structure

The results of the live imaging and electron microscopy raised a number of questions about how the intranuclear microtubule bundle was nucleated. Interphase microtubules are nucleated from MTOCs around the nuclear envelope, one of which is the SPB, in the cytoplasm, and along pre-existing microtubules (reviewed in Sawin and Tran, 2006). From the live imaging results it appeared that the intranuclear microtubule was nucleated from a region close to the SPB (Figure 3.7C), however the electron microscopy results revealed that the SPB was outside the nuclear envelope, so could not directly nucleate microtubules inside the nucleus. In contrast, during mitosis the spindle microtubules are nucleated from the SPBs, which are embedded in the fenestrated nuclear envelope (Figure 3.8A; Ding et el., 1997). We therefore sought to determine what was nucleating the intranuclear microtubules.

3.2.9.1. Initially Mal3-GFP moves outwards from the centre of an aster-like structure marked by Sad1-dsRed

We first tried to establish the polarity of the intranuclear microtubule bundle during the initial stages of its formation. We used an *alp14*Δ strain in which the canonical

+TIP Mal3 was C-terminally tagged with a linker-GFP construct (Sandblad *et al.*, 2007). Initial imaging experiments revealed, to our surprise, that upon shifting to the restrictive temperature, prior to bundle formation there was a period of time during which the microtubules formed a dynamic aster-like structure, before coming together as a single bundle (Figure 3.10A).

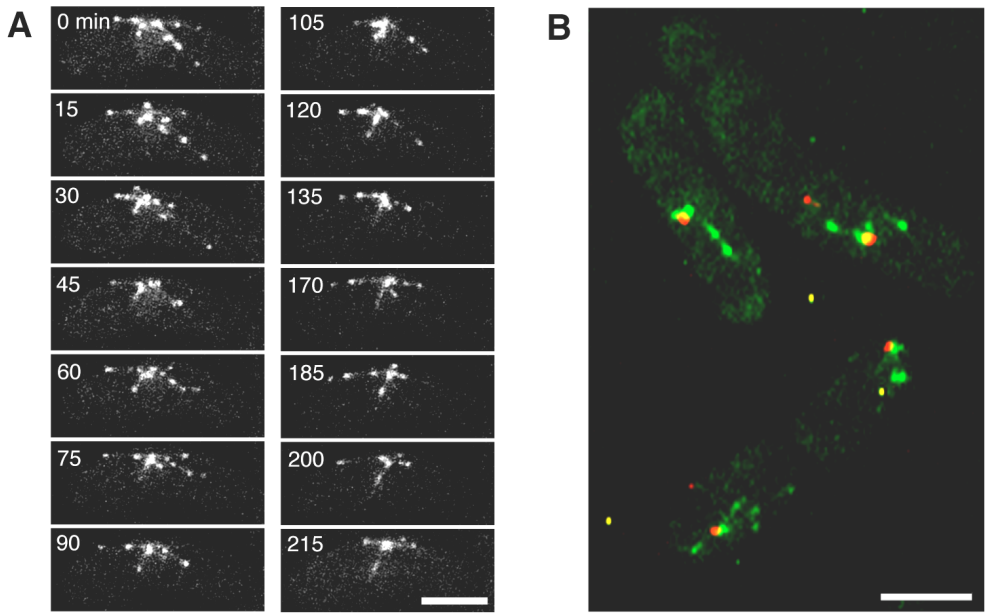

Figure 3.10 Early stages of intranuclear microtubule bundle formation

(A) Movie sequence of projections of confocal images of interphase *alp14Δ* cells expressing Mal3-GFP. Shortly after shift to the restrictive temperature, an aster-like structure is visible, with particles of Mal3-GFP moving outwards from the centre. (B) The SPB marker Sad1-dsRed localises to the centre of the Mal3-GFP aster-like structure. Bars, 4 μm.

That we had not observed this aster-like structure in previous experiments was likely due to the fact that we had always used GFP-labelled tubulin in addition to the nuclear envelope marker Nup85-GFP. The nuclear envelope signal probably masked to some extent the GFP-tubulin such that single microtubules were not easily visible. The initial movies were acquired with a 15 second delay between frames and indicated that Mal3-GFP moved outwards from the centre of the aster-like structure. We initially concluded that the microtubule plus ends were facing outwards and the minus ends were the site of nucleation at the centre of the 'aster'. However, during the time at which we were investigating this it was shown that Mal3 also localises to and tracks free microtubule minus ends *in vitro* (Bieling *et al.*, 2007). As it was unknown whether the minus ends of the intranuclear microtubules were free or associated with the γ-tubulin complex, we did not proceed with acquiring Mal3-GFP movies with a

higher time resolution; paradoxically, the canonical +TIP Mal3 was shown to be an unsuitable marker for distinguishing the microtubule plus ends. Unfortunately, the other +TIPs that are usually used for labelling of the plus ends were also unsuitable as they are only expressed in the cytoplasm. Thus, we were unable to determine the initial polarity of the intranuclear microtubules by live imaging. We were, however able to confirm the location of the SPB with respect to the aster-like structure. To do this we imaged *alp14*Δ Sad1-dsRed Mal3-GFP strain and repeated the experiment above. As expected from the results with Sad1-dsRed and GFP-tubulin, we observed that the Sad1-dsRed signal was consistently found in the focal point of the aster-like structure (Figure 3.10B) and upon formation of a single bundle, was initially located at one end of the bundle, as previously observed (Figure 3.6B). This suggests that, despite the absence of a direct connection between the microtubules and the SPB, the bundle is indeed nucleated from the SPB region.

3.2.9.2. Electron microscopy tomography of the aster-like structure

As we were unable to determine the polarity of the microtubules forming the aster-like structure using live imaging, we decided to use electron microscopy tomography. We used HU-blocked interphase *alp14*Δ cells grown at the permissive temperature, which were high pressure frozen five minutes after being shifted to the restrictive temperature to visualise the aster-like structure seen by live imaging. We found three cells in which an aster-like structure could be seen (Figure 3.11). In all cases there appeared to be no single central point of nucleation from which all microtubules grew, but rather microtubule ends were found in a region next to the nuclear envelope in the vicinity of the SPB. The polarity of the intranuclear microtubules was determined by examining the structure of the microtubule ends. We scored the end structure of the closest tip of each microtubule to the spindle pole body and found three plus ends, three minus ends and two cases in which the structure was ambiguous. This suggests that there was no direct nucleation by the SPB, since we would expect the majority of minus ends to be localised closest to the SPB. In addition there were some open, ambiguous ends, which could indicate free minus ends, not associated with γ-tubulin (Figure 3.11). In addition, no electron dense structure was visible at the ends of the microtubules, which could be responsible for their nucleation.

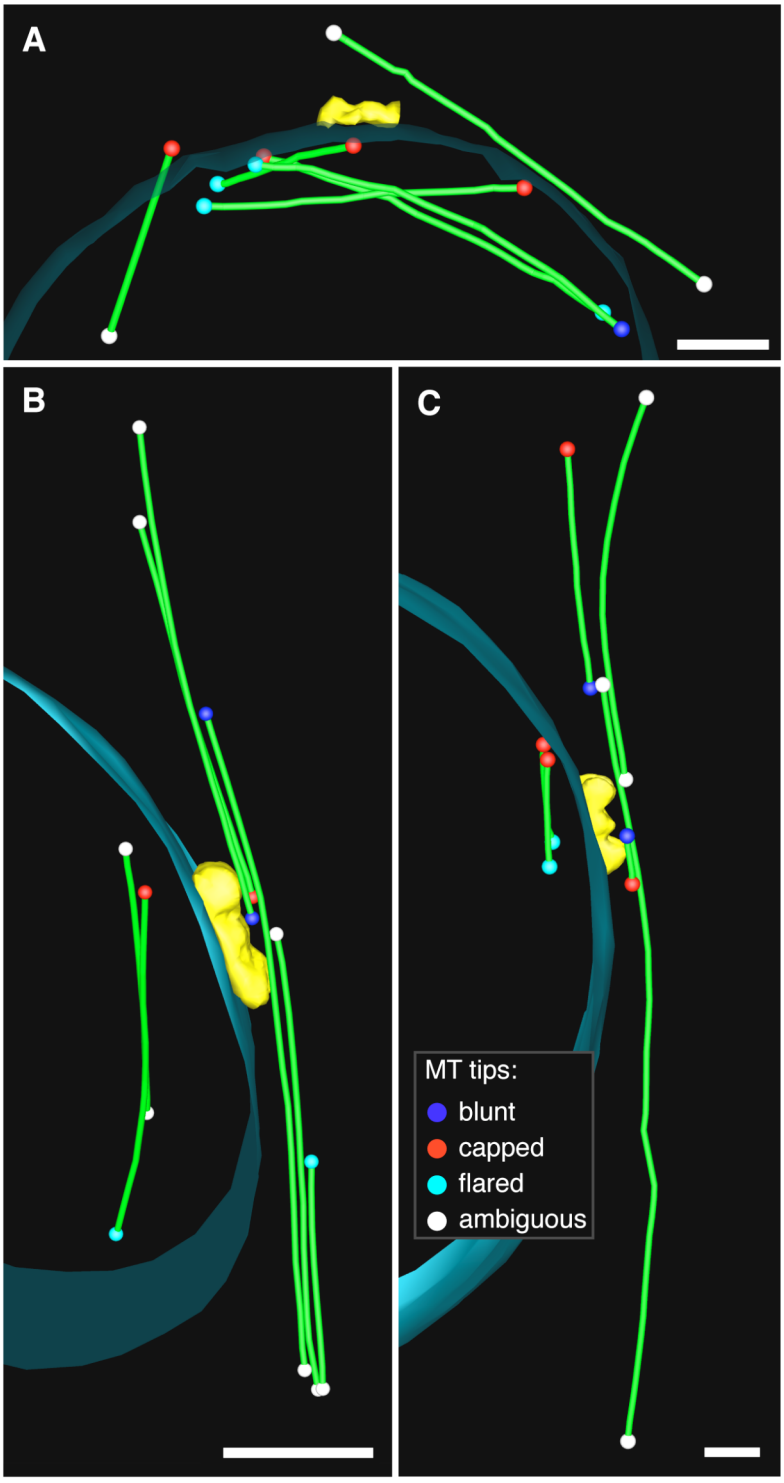

Figure 3.11 3D models of the intranuclear microtubule bundle in *alp14Δ* five minutes after shifting to the restrictive temperature

3D modelling of electron microscopy tomography tilt series. (A), (B) and (C) Three examples of cells where the microtubules form an aster-like structure are shown. The nuclear envelope is shown in transparent turquoise; microtubules are green; the SPB is yellow; microtubule end structures are indicated by coloured caps, detailed in (C). Bars, 250 nm. Images acquired in collaboration with H. Roque (EMBL).

3.2.9.3. The kinetochores and SPB co-localise when *alp14*Δ cells are shifted to the restrictive temperature

It was clear from the electron microscopy data that the microtubules were being nucleated from a region near the SPB, but it was unclear what the nucleating factor(s) was (were). The absence of a visible direct connection between the SPB and the intranuclear microtubule bundle prompted us to search for other possible nuclear microtubule nucleators that localise to the region of the SPB. The proximity of some plus ends in the region where the microtubules of the aster-like structure formed during the initial stages of bundle formation, suggested that maybe the plus ends and not the minus ends were associated with nucleating factor(s). One possible candidate were the kinetochores, which have been shown to nucleate microtubules in higher eukaryotes (Torosantucci *et al.*, 2008; Tulu *et al.*, 2006; Maiato *et al.*, 2004; Khodjakov *et al.*, 2003). Although they have not been shown to be microtubule nucleators in *S. pombe* to date, the kinetochores are tightly clustered adjacent to the SPB during interphase (Funabiki *et al.*, 1993). It might be expected that upon formation of the intranuclear microtubule structure and subsequent growth, the protein(s) responsible for nucleation would remain at the end of the microtubules they nucleated. As the intranuclear bundle shows mixed polarity, this would mean that the nucleator protein(s) might be seen to move away from the SPB region and be spread along the bundle. As a first test of whether the kinetochores were nucleating the intranuclear bundle, we examined whether the kinetochores and SPB co-localised after *alp14*Δ cells were shifted to the restrictive temperature.

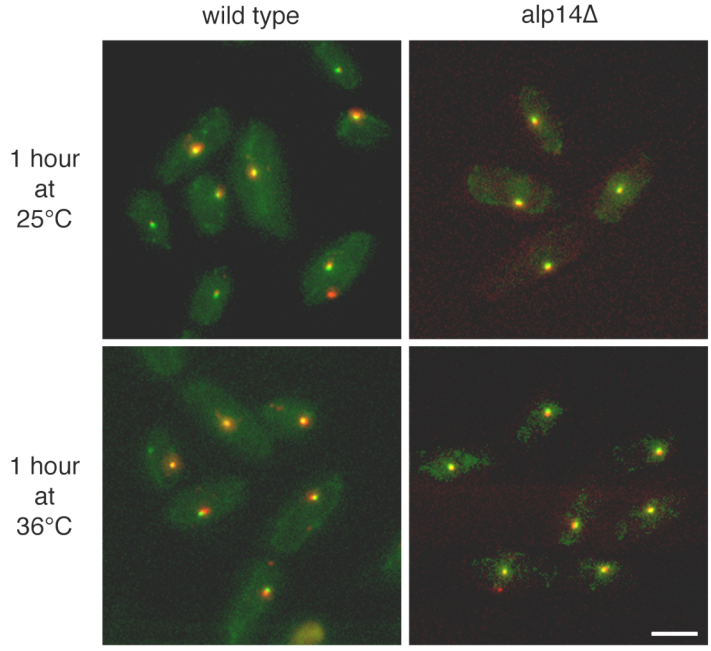

Figure 3.12

The kinetochores co-localise with the SPB in *alp14Δ* cells at the restrictive temperature

Projection of wide field images showing that the kinetochores, labelled by Mis6-GFP co-localise with the Sad1-dsRed in interphase wild type control and *alp14Δ* cells at both the permissive and restrictive temperatures. Bar, 4 μm.

*alp14*Δ cells expressing Sad1-dsRed, the SPB marker, and Mis6-GFP, a kinetochore protein that associates with the inner centromere DNA (Takahashi *et al.*, 2000) were grown at the permissive temperature then blocked in interphase by a three hour treatment with HU. Control and *alp14*Δ cells were then either incubated at 25ºC or shifted to the restrictive temperature for one hour without HU washout. After one hour images were acquired to visualise the extent of co-localisation of the kinetochore and SPB markers. After close examination of the images, we found that the kinetochores and SPB were closely associated in the *alp14*Δ cells at both the restrictive and permissive temperatures (Figure 3.12). This does not exclude that the kinetochores are responsible for nucleating the intranuclear microtubules, however it does show that if they do, the association with the microtubule ends is only transient as the kinetochores remain in the SPB region and the ends of the microtubules in the bundle move away from this region. To determine unambiguously whether the kinetochores or the SPB are nucleating the intranuclear microtubules we would need to separate them. During this investigation, the only system we found to do this in *S. pombe* is to use a *mis6-302* mutant in which the SPBs and kinetochores no longer co-localise after six hours at 36ºC (Saitoh *et al.*, 1997). Unfortunately this is not compatible with the *alp14*Δ phenotype, in which intranuclear microtubules form within five minutes after shifting to 36ºC. More recently, King *et al.*, (2008) identified a protein, Ima1, which links chromatin to the nuclear envelope. They report that in *ima1*Δ cells there is inefficient coupling of centromeric heterochromatin to Sad1. In light of this, it would be interesting to see from where the intranuclear microtubules are nucleated in an *alp14*Δ *ima1*Δ strain at the restrictive temperature.

It would also be interesting to visualise the location of the kinetochores using electron microscopy tomography, but as kinetochores are extremely difficult to visualise by electron microscopy, immuno-localisation using gold particles would be required.

3.2.10. Investigating the role of Alp7 in intranuclear microtubule array formation

The localisation of Alp14, but not Dis1 to interphase microtubules and the SPB is dependent upon the TACC protein Alp7/Mia1 (Sato *et al.*, 2004). In addition, during spindle formation Alp7 transports Alp14 into the nucleus via the Ran-dependent transport machinery (Sato and Toda, 2007). Given this close relationship between Alp14 and Alp7, we wanted to test whether Alp7 also played a role in intranuclear microtubule formation.

3.2.10.1. Intranuclear microtubules do not form in *alp7Δ* cells

We constructed an *alp7*Δ strain with the microtubule and nuclear envelope markers and performed the same temperature shift experiment as for the *alp14*Δ strain (see section 3.2.3). The cells were blocked in interphase with HU as it is known that *alp7*Δ cells have mitotic defects (Zheng *et al.*, 2005; Sato *et al.*, 2004; Sato *et al.*, 2003; Oliferenko and Balasubramanian, 2002), and we wanted to exclude mitotic cells from our analysis. At 25ºC, as previously reported, *alp7*Δ cells had fewer microtubules, which often curled around the cell poles and lost association with the nuclear envelope region (Figure 3.13A; Oliferenko and Balasubramanian, 2002; Zheng *et al.*, 2006). After 1 hour at 36ºC, *alp7*Δ cells did not form intranuclear microtubule arrays (Figure 3.12B). This confirmed that Alp14-dependent maintenance of interphase microtubule arrays in the cytoplasm is not dependent upon Alp7, or Alp14 localisation to interphase microtubules.

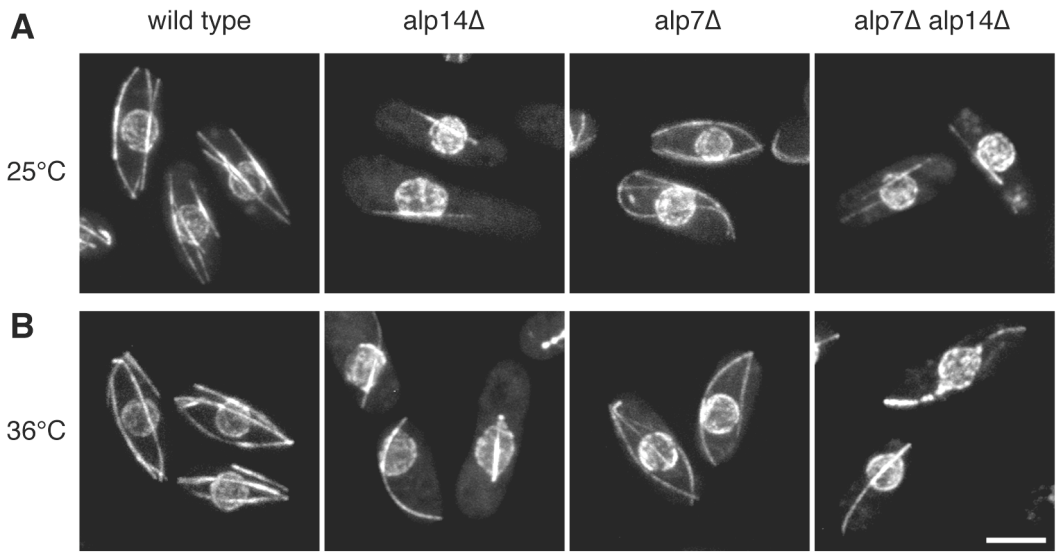

Figure 3.13 Deletion of *alp7* does not affect intranuclear microtubule formation

Interphase cells expressing the microtubule and nuclear envelope markers GFP-tubulin and Nup85-GFP, after one hour at (A) the permissive (25ºC) or (B) the restrictive (36ºC) temperature. Wild type control and *alp14Δ* cells are shown for comparison. *alp7Δ* cells have fewer interphase microtubules, which are longer and show iMTOC attachment defects, but do not form intranuclear microtubules at the restrictive or permissive temperature. The organisation of the microtubule bundles in *alp7Δ alp14Δ* cells is indistinguishable from *alp14Δ* cells. Images are projections of confocal slices. Bar, 4 *μ*m.

3.2.10.2. *alp14Δ alp7Δ* cells still form intranuclear microtubules

Given that Alp7 transports Alp14 into the nucleus during mitosis, we wondered whether the formation of intranuclear microtubules in the *alp14*Δ cells was due to the nuclear transport function of Alp7. It has not been previously reported that Alp7 transports additional cargo across the nuclear envelope, however it has not been ruled out (Sato *et al.*, 2007). We therefore checked whether *alp14*Δ still formed intranuclear microtubules when *alp7* was also deleted. Cells were blocked in interphase using HU and then imaged after one hour at 25ºC or 36ºC. At 25ºC the microtubule arrays in the *alp14*Δ *alp7*Δ cells resembled those in the *alp14*Δ cells (Figure 3.13A). When the cells were shifted to 36ºC for 1 hour *alp14*Δ *alp7*Δ cells formed intranuclear microtubules which had the same appearance as those in the *alp14*Δ cells (Figure 3.13B). We therefore conclude that formation of intranuclear microtubules at 36ºC is due to the absence of a function of Alp14 that is independent of Alp7.

3.3. *dis1*Δ

In addition to Alp14, *S. pombe* has a second XMAP215 protein family member, Dis1. In contrast to *alp14*Δ cells that are temperature sensitive, the *dis1*Δ cells are cold sensitive. It is known that Dis1 has a role in mitosis as *dis1*Δ cells at the permissive temperature have a delay in spindle elongation (Nabeshima *et al.*, 1998; Nabeshima *et al.*, 1995). At the restrictive temperature, mitotic *dis1*Δ cells do not have a delay in spindle elongation, but rather the spindle growth fails to pause. In wild type cells pausing normally occurs during metaphase-anaphase A, but in *alp14*Δ cells, spindle growth continues, resulting in elongated spindles. This suggests a role for Dis1 in completing the formation of the bipolar spindle in metaphase and inhibiting spindle extension in anaphase (Nabeshima *et al.*, 1998). Additionally, *dis1*Δ cells often terminally arrest with short, often V-like wedge-shaped spindles (Nabeshima *et al.*, 1995, Ohkura *et al.*, 1988). No mutant interphase phenotype has been reported for *dis1*Δ cells at either the permissive or the restrictive temperature, suggesting that Dis1 is essential for mitosis at low temperatures, but dispensable during interphase at all temperatures. There is however, an indication that there is some functional overlap or redundancy between Alp14 and Dis1 as the double deletion strain is lethal (Garcia *et al.*, 2001). We sought to further investigate the *dis1*Δ phenotype with respect to the role of Dis1 in interphase.

3.3.1. *dis1Δ* form intranuclear microtubules at the restrictive temperature but with slower dynamics compared to *alp14Δ*

We were interested to know whether *dis1*Δ cells formed intranuclear microtubule bundles at the restrictive temperature. Therefore, we first repeated the cold shift experiments of Nabeshima *et al.* (1995), monitoring the phenotype of *dis1*Δ cells over a period of six hours. Cells were cultured to exponential phase at the permissive temperature of 30ºC and then shifted to 18ºC, the restrictive temperature. In accordance with published observations, *dis1*Δ cells at the permissive temperature had normal morphology and growth rate and the microtubules behaved the same as in wild type cells (Figure 3.14A). When the cells were shifted to 18ºC intranuclear microtubules formed. However, their appearance was very slow, with a clear phenotype only visible after four hours at 18ºC (Figure 3.14B). This is in contrast to *alp14*Δ cells, which formed intranuclear microtubules within minutes of being shifted to 36ºC (See section 3.2). Furthermore, the delay was too slow to be explained by reduced microtubule growth as a consequence of difference in temperature between the two experiments. We therefore conclude that the intranuclear microtubules formed in *dis1*Δ cells at the restrictive temperature probably form via a different, slower mechanism than in *alp14*Δ cells at 36ºC.

3.3.2. *dis1Δ* intranuclear microtubules often form aster-like structures rather than a single microtubule bundle

We then examined the structure of the intranuclear microtubules in *dis1*Δ cells after six hours at the restrictive temperature (Figure 3.14A and Figure 3.15A). We found that many cells had intranuclear microtubules arranged in aster-like structures, reminiscent of the early stages of intranuclear microtubule formation in *alp14*Δ cells at 36ºC (Figure 3.15A). These cells however could correspond to cells terminally arrested in mitosis with V-shaped spindles (Nabeshima *et al.*, 1995, Ohkura *et al.*, 1988). In addition, we observed a number of binucleate cells in which both nuclei contained an aster-like microtubule structure. To investigate these two possibilities we examined the cells with intranuclear microtubules more closely and categorised them according to whether the intranuclear microtubule structure had an aster-like arrangement or was a single bundle. We also noted whether the cells had a single nucleus or were binucleate, and if the nuclei were still connected or separate. Examples of each category are shown in Figure 3.15A.

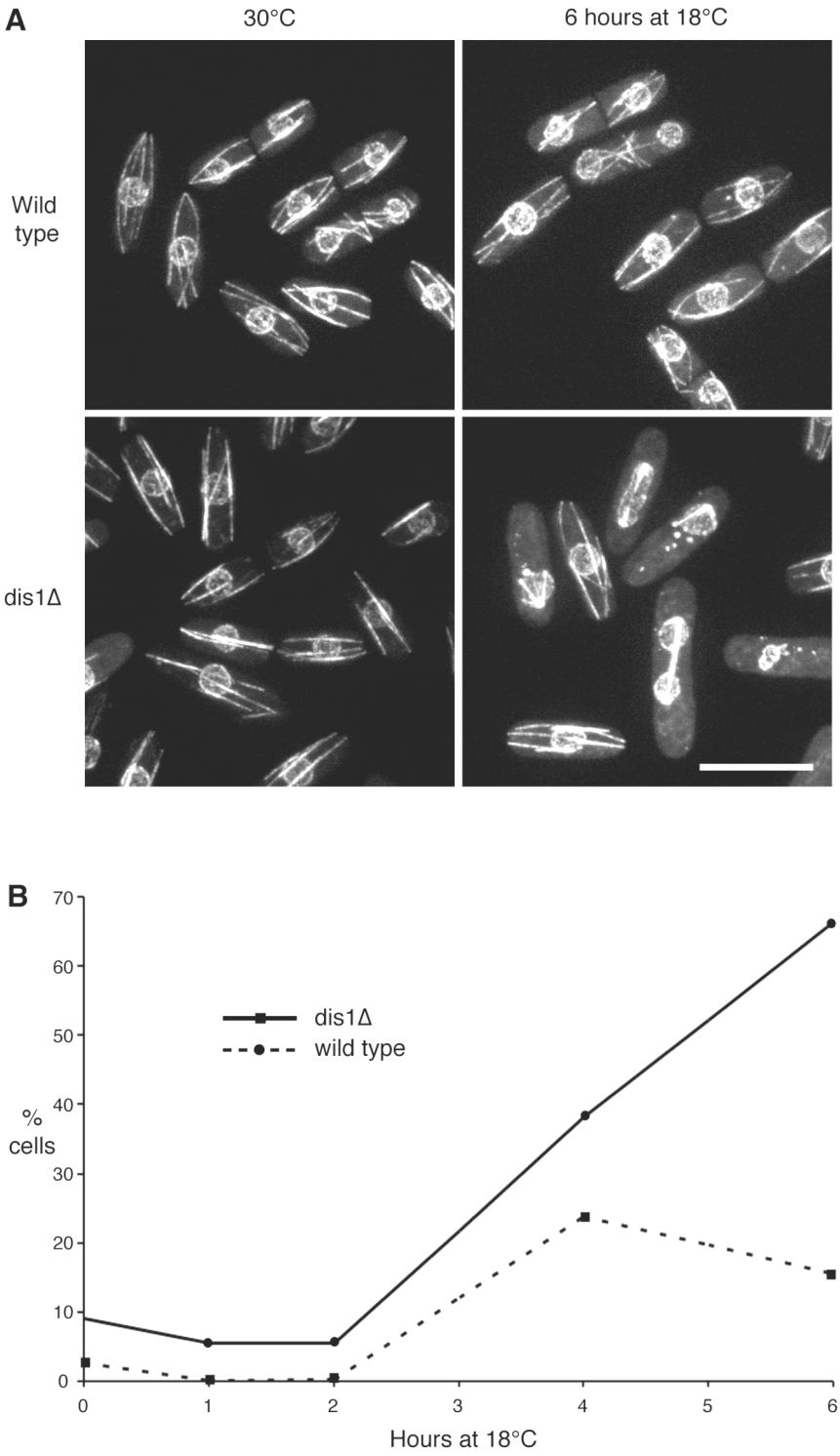

Figure 3.14 Intranuclear microtubules also form in *dis1Δ* cells at the restrictive temperature

(A) Projection of confocal slices of wild type and *dis1Δ* cells at the permissive temperature (30ºC), or after 6 hours at the restrictive temperature (18ºC). Cells express the microtubule and nuclear envelope markers GFP-tubulin and Nup85-GFP. (B) Time course showing the increase in the percentage of cells with intranuclear microtubules in *dis1Δ* and wild type cells after shifting to 18ºC. Bar, 10 μm.

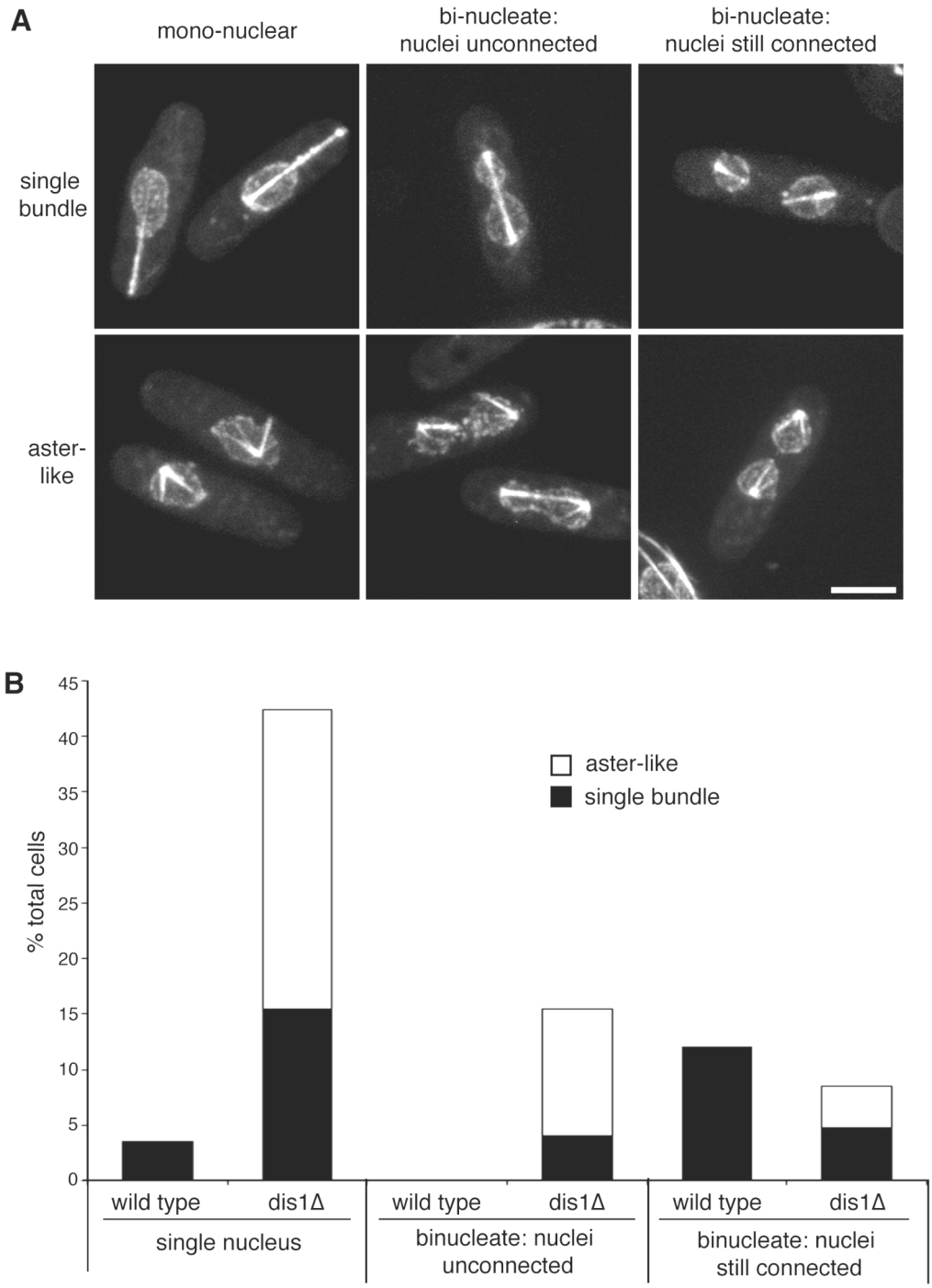

Figure 3.15 *dis1Δ* cells are often binucleate and have multiple intranuclear microtubule bundles

(A) Projection images of confocal slices of *dis1Δ* cells expressing GFP-tubulin and Nup85-GFP microtubule and nuclear envelope markers after 6 hours at the restrictive temperature (30ºC). Cells with intranuclear microtubules can be categorised as mono- or bi-nucleate, where the spherical nuclear masses are connected or unconnected. Cells can be further categorised based on the intranuclear microtubule arrangement: single bundles, similar to those seen in *alp14Δ* cells, or multiple bundles that display an aster-like structure. (B) Quantification of the percentage of cells falling into each of the categories in (A). Bar, 4 μm.

More than half of the *dis1*Δ cells with intranuclear microtubules were mononuclear, 63% of which had an aster-like structure (Figure 3.15B). A number of cells were expected to be binucleate and have an intranuclear microtubule bundle, as the cell cultures were unsynchronised and some cells would be mitotic. This was seen for the wild type control, however what we did not see in the wild type control were binucleate cells, where the nuclei were not connected and had intranuclear microtubules (Figure 3.15B). 23% of the *dis1*Δ cells with intranuclear microtubules were binucleate with unconnected nuclei, 74% of which had an aster-like structure (Figure 3.15B). It is known that *dis1*Δ cells when shifted to the restrictive temperature have an elongated spindle, but cytokinesis defects have not been reported (Nabeshima *et al.*, 1998). These results show that the intranuclear microtubule structure formed in *dis1*Δ cells at the restrictive temperature have a different morphology to those in *alp14*Δ, and suggests that the intranuclear microtubules that formed in *dis1*Δ cells may be as a result of a mitotic defect, and not a cytoplasm to nuclear shift of the interphase microtubule array.

3.3.3. Intranuclear microtubules do not form in interphasic *dis1*Δ cells

We next wanted to confirm whether the intranuclear microtubules found in *dis1*Δ cells at the restrictive temperature formed in mitosis as suggested by the literature, or in interphase as in the case for *alp14*Δ. This was possibly by examining whether the SPBs were duplicated, however that would have required that the cells additionally express an SPB marker. To distinguish between these two possibilities more quickly, we used the same HU interphase block experiment as for *alp14*Δ, with a few modifications. Cells were first grown at the permissive temperature overnight to exponential phase and then shifted to 18ºC with the addition of HU. After three hours additional HU was added to maintain the interphase block and after four hours the cells were imaged and the number of cells with intranuclear microtubules was quantified. We found that when HU was added at the same time as the cells were shifted, nearly 10% of wild type cells still had intranuclear microtubules and ~10% of the cells with cytoplasmic microtubules had a post anaphase array organization (Figure 3.16B). This indicated that the HU block was not working efficiently under these conditions. We therefore sought to establish a protocol in which the HU block was working efficiently in combination with the shift to the restrictive temperature.

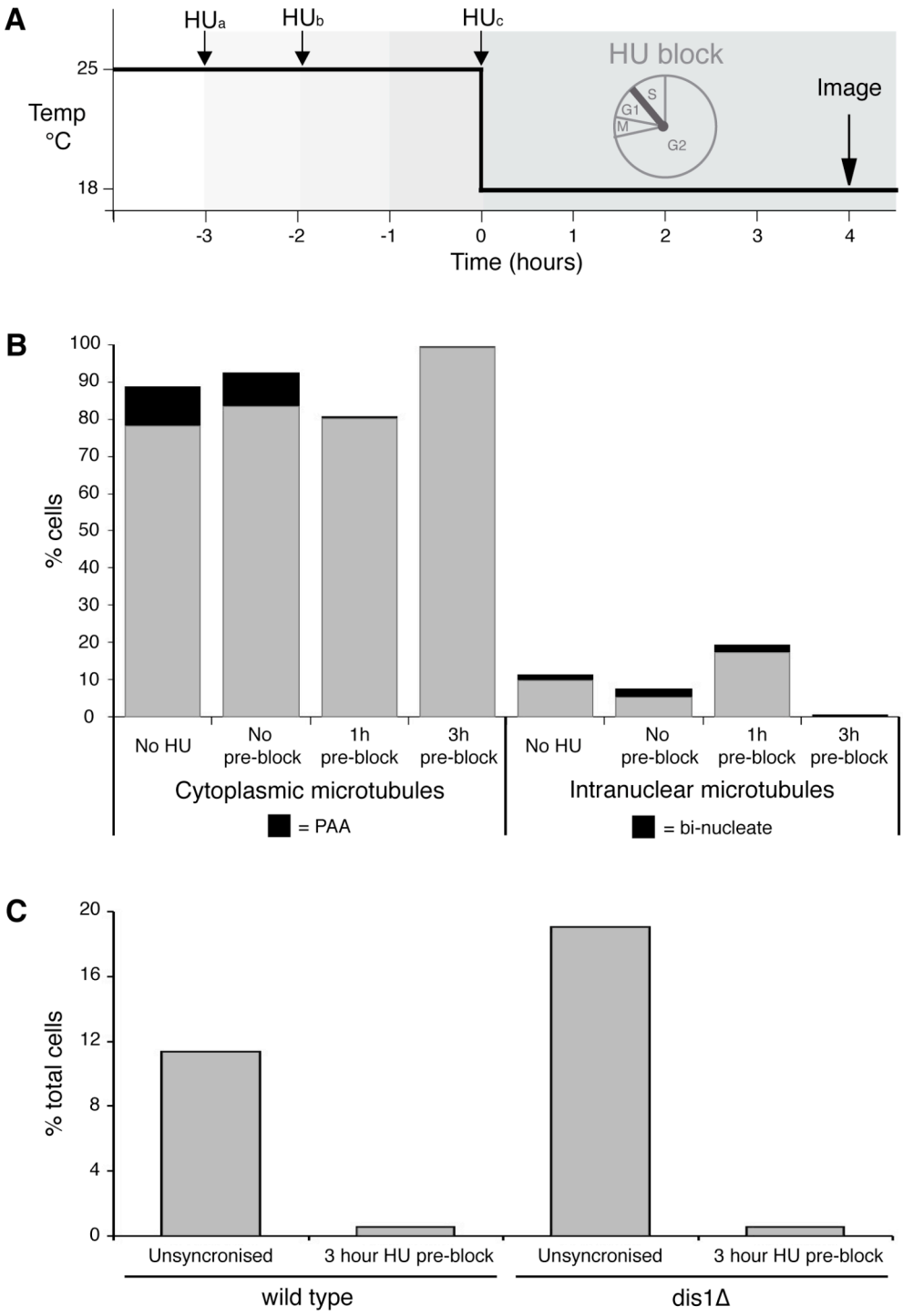

Figure 3.16 Intranuclear microtubules in interphasic *dis1Δ* cells at the restrictive temperature

(A) Schematic outlining the experimental protocol. (B) Quantification of the percentage of wild type cells with cytoplasmic or intranuclear microtubules after incubation with hydroxyurea (HU) for different amounts of time before shifting to 18ºC for 4 hours, as outlined in (A). (C) percentage of *dis1Δ* and wild type cells with intranuclear microtubules with and without a 3 hour pre-block with HU before shifting to 18ºC for 4 hours.

We tried pre-incubating the cells at the permissive temperature in the presence of HU for various lengths of time, before shifting to the restrictive temperature for four hours. Cells release from a HU block after several hours, so although the results using unsynchronised cells (Figure 3.14B) showed only a moderate increase in the number of intranuclear microtubules in *dis1*Δ cells after four hours at the restrictive temperature compared to the after six hours, we wanted to minimise the time the cells were grown in the presence of HU. To maintain the block in the short term, we added additional HU after three hours (Figure 3.16A). We found that after a HU pre-block of three hours, 99% of wild type cells had a cytoplasmic microtubule organization found during interphase, indicating that the HU block was effective. *dis1*Δ cells were therefore treated with a three hour HU pre-block before shifting to the permissive temperature. Quantification revealed that less than 1% of the cells had intranuclear microtubules after four hours, showing that the intranuclear microtubules form in mitotic *dis1*Δ cells at the restrictive temperature and are not as a result of the interphase array switching from the cytoplasm to the nucleus, as is the case for *alp14*Δ (Figure 3.16C).

As the mitotic *dis1*Δ phenotype is already well characterised (Nabeshima *et al.*, 1998; Nabeshima *et al.*, 1995; Ohkura *et al.*, 1988) and clearly different to the *alp14*Δ phenotype at the restrictive temperature we did not pursue the *dis1*Δ analysis further.

3.4. Rescue of *alp14*Δ/*dis1*Δ by over-expression of the reciprocal XMAP215 homologue

The reciprocal temperature sensitivities of the *alp14*Δ and *dis1*Δ strains raised the question of what was conferring viability at the permissive temperature. As the two proteins are homologues, one obvious hypothesis was that in *alp14*Δ cells, Dis1 was conferring viability and in *dis1*Δ cells it was Alp14. The temperature sensitive lethality of the strains could thus result from inactivation of the reciprocal homologue, or the inability to perform a fully redundant function. We therefore wanted to test whether moderate over-expression of Dis1 could rescue the *alp14*Δ interphase microtubule phenotype at both the permissive and restrictive temperatures. It was previously published that *alp14*Δ cells are viable at the restrictive temperature when Dis1 is over-expressed (Garcia *et al.*, 2001) however only growth on agar plates was assayed and the cells were not imaged. In addition, over-expression of Dis1 in this study was achieved using a multi-copy plasmid, which meant each cell was

expressing different amounts of Dis1. We sought to repeat this experiment using more controlled over-expression conditions by replacing the endogenous *dis1* promoter with the *81nmt1* promoter. This promoter is an attenuated version of the *nmt1* promoter, which results in moderate levels of transcription when cells are grown in the absence of thiamine (Basi *et al.*, 1993). This was a convenient system for the moderate over-expression of Dis1 (Figure 3.17), however it required that we used a different expression system for our microtubule marker, GFP-α-Tubulin; cells needed to be grown in the absence of thiamine to over-express Dis1, but this would also have resulted in over-expression of GFP-α-Tubulin, which is lethal. We therefore used the SV40 promoter (Jones *et al.*, 1988), which is not influenced by thiamine. Expression levels of GFP-α-Tubulin using this promoter are comparable to those when the fully repressed *nmt1* promoter is used (Bratman and Chang, 2007; T. Makushok, personal communication).

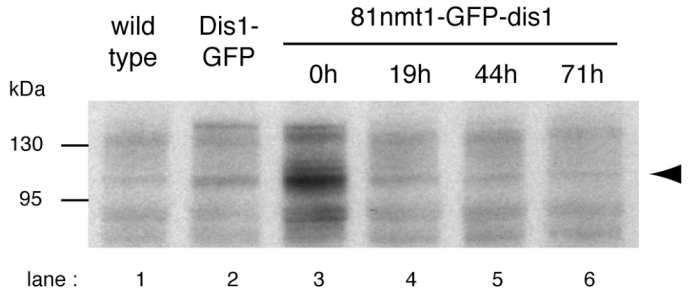

Figure 3.17 Over-expression and shut-down of GFP-Dis1 under the control of the *81nmt1* promoter

Western blot of cell extract from strains expressing GFP-Dis1 under the control of the *81nmt1* promoter. Expression was controlled by addition of thiamine. When cells were grown without thiamine, GFP-Dis1 was moderately over-expressed (lane 3), compared to expression levels from the endogenous promoter (lane 2). When 30 μM thiamine was added the expression of GFP-Dis1 was attenuated (lanes 4-6). Arrow indicates the position of GFP-Dis1 on the membrane. Numbers above lanes 3-6 indicate the amount of time the cells were grown in the presence of thiamine before the extract was prepared. GFP-Dis1 was detected using an anti-GFP antibody.

3.4.1. Over-expression of Dis1 rescues the *alp14*Δ phenotype at the permissive temperature

We first tested whether over-expression of Dis1 could rescue the *alp14*Δ interphase microtubule phenotype at the permissive temperature. An *alp14*Δ, GFP-α-Tubulin, Nup85-GFP, *81nmt1-dis1* strain was created, and cells were grown to exponential

phase at the permissive temperature, always in the absence of thiamine. We found that interphase microtubule arrays appeared wild type in *alp14*Δ cells when Dis1 was over-expressed (Figure 3.18A).

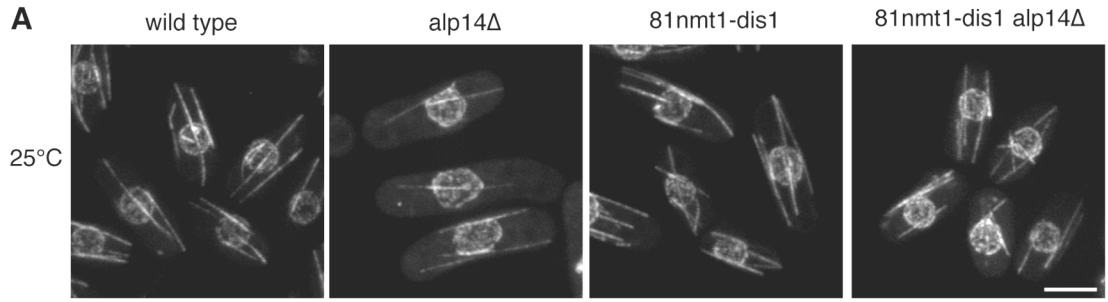

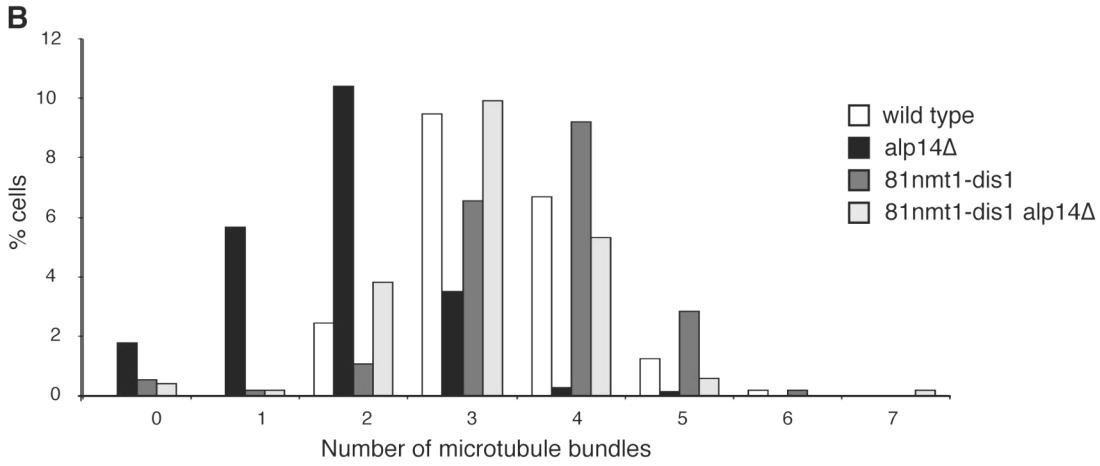

C

	Average number of bundles	Average bundle length
wild type	3.36 +/- 0.81	6.83 +/- 2.28
alp14Δ	1.94 +/- 0.76	5.62 +/- 2.06
81nmt1-dis1	3.70 +/- 0.84	6.31 +/- 2.34
81nmt1-dis1 alp14Δ	3.15 +/- 0.86	5.18 +/- 2.09

Figure 3.18 Over-expression of Dis1 rescues the mutant interphase microtubule phenotype of *alp14Δ* cells at the permissive temperature

(A) Images of control and *alp14Δ 81nmt1dis1* cells expressing GFP-tubulin and Nup85-GFP, microtubule and nuclear envelope markers at 25ºC in the absence of thiamine. Cells express GFP-tubulin and Nup85-GFP, microtubule and nuclear envelope markers. (B) and (C) Quantification of the number of microtubule bundles and bundle length in each of the strains in (A). Images are projections of confocal sections covering the entire Z-axis of the cell. Bar, 4 *μ*m.

Quantification of microtubule bundle number revealed that when Dis1 was over-expressed at the permissive temperature, the cells had a wild type number of bundles (Figure 3.18B,C), in contrast to *alp14*Δ cells, which had fewer bundles (Figure 3.4 B,C and Figure 3.18). Bundle length was measured and found to be similar to wild type values, however no quantitative conclusions about bundle length can be drawn from this data, as very short microtubules, which occur frequently in *alp14*Δ cells (Figure 3.4B,C) were obscured by the nuclear envelope marker so that the apparent bundle length of *alp14*Δ cells was also similar to wild type cells. This also accounts for the decrease in the average number bundles per cell in *alp14*Δ cells when compared to the statistics in cells without the nuclear envelope marker (Figure 3.4C). However, from the wild type bundle number and qualitative examination of the microtubule bundle arrays we conclude that over-expression of Dis1 in *alp14*Δ cells rescues the *alp14*Δ interphase microtubule phenotype.

3.4.2. The intranuclear microtubule phenotype of *alp14*Δ cells at the restrictive temperature is partially rescued by over-expression of Dis1

As previously shown, *alp14*Δ cells form intranuclear microtubule bundles within one hour of being shifted to the restrictive temperature of 36ºC. To further test whether Dis1 was able to fully rescue the *alp14*Δ phenotype we tested whether intranuclear microtubules still formed in *alp14*Δ cells when Dis1 was over-expressed. Exponentially growing *alp14*Δ cells over-expressing Dis1 were shifted to the restrictive temperature and after one hour images were acquired and the microtubule organisation quantified (Figure 3.19). We found that some *alp14*Δ cells over-expressing Dis1 still formed intranuclear microtubules (Figure 3.19A), however quantification clearly showed there were much fewer cells with intranuclear microtubules in *alp14*Δ mutants over-expressing Dis1 (Figure 3.19B; 42% including cells that additionally have cytoplasmic microtubules), as compared to *alp14*Δ alone (Figure 3.19B; 95%). In addition, we found that 30% of the *alp14*Δ cells over-expressing Dis1 had both a cytoplasmic microtubule array and an intranuclear bundle. This suggests that over-expression of Dis1 is able to at least partly rescue the *alp14*Δ intranuclear phenotype at the restrictive temperature. It would be interesting to test whether higher expression levels of Dis1 could achieve a full rescue of *alp14*Δ.

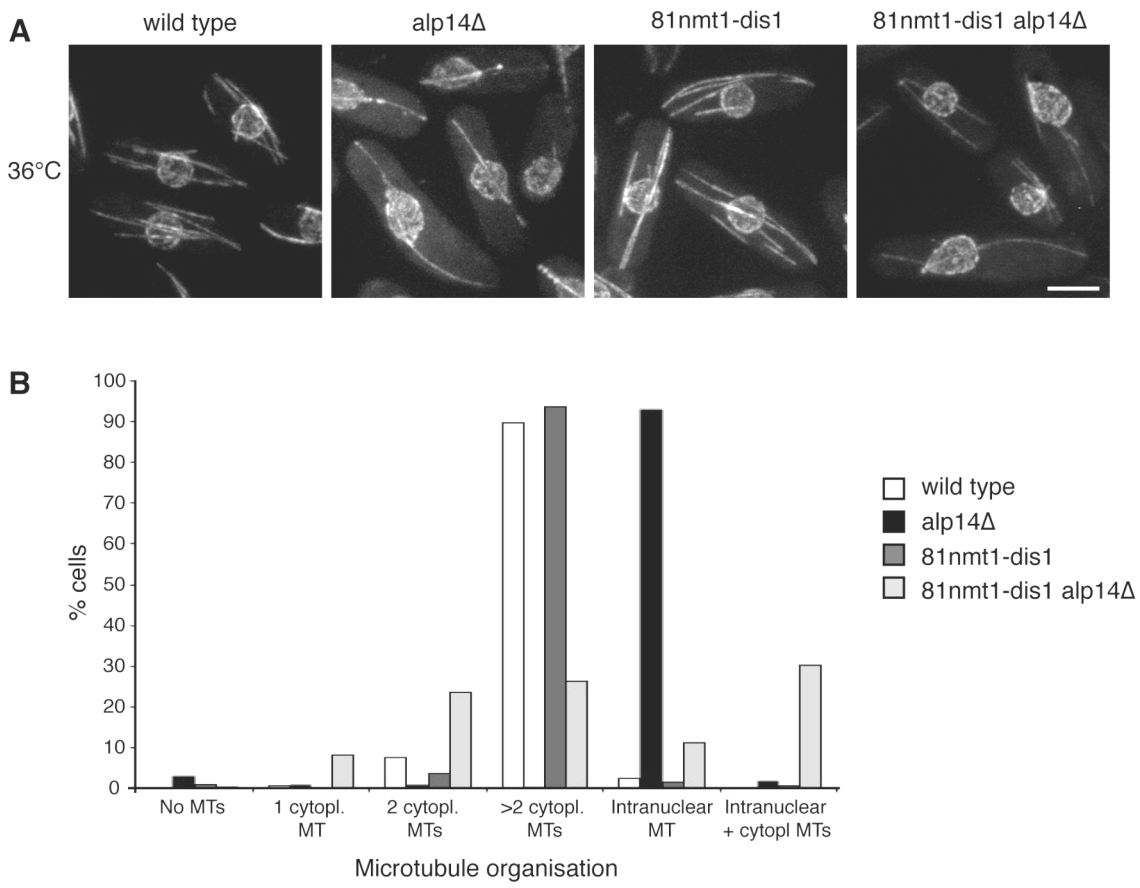

Figure 3.19 Over-expression of Dis1 partially rescues the intranuclear microtubule phenotype of *alp14Δ* cells at the restrictive temperature

(A) Images of control and *alp14Δ81nmt1dis1* cells expressing GFP-tubulin and Nup85-GFP, microtubule and nuclear envelope markers at 36ºC in the absence of thiamine. Cells express GFP-tubulin and Nup85-GFP, microtubule and nuclear envelope markers. (B) Quantification of microtubule organisation in each of the strains in (A). Images are projections of confocal sections covering the entire Z-axis of the cell. Bar, 4 μm.

3.4.3. Over-expression of Alp14 does not rescue the interphase microtubule phenotype of *dis1Δ* at the restrictive temperature

We then carried out the reciprocal experiment with the *dis1*Δ strain, to see if over-expression of Alp14 was able to rescue the *dis1*Δ phenotype at the restrictive temperature. It is reported in the literature that Alp14 over-expression is able to partly rescue the *dis1*Δ phenotype at cold temperatures, however as for the Dis1 over-

expression experiments, this was only assayed in terms of growth on agar plates in the presence of a multi-copy plasmid expressing Alp14 (Garcia *et al.*, 2001). We used the same integrated *81nmt1* promoter to moderately over-express the endogenous copy of *alp14* as for *dis1* over-expression in *dis1*Δ cells, in combination with the GFP microtubule and nuclear envelope markers. Cells were grown to exponential phase at the permissive temperature and then shifted to the restrictive temperature for six hours before images were acquired. At the permissive temperature, microtubules in the cells over-expressing Alp14 appeared the same as wild type (Figure 3.20A). After six hours at the restrictive temperature, the cells over-expressing Alp14 in the *dis1*Δ background formed intranuclear microtubules and were indistinguishable from the *dis1*Δ cells (Figure 3.20A). Quantification confirmed this observation; 74% of *dis1*Δ cells over-expressing Alp14 had intranuclear microtubules (Figure 3.20B). These intranuclear microtubules had the same appearance of those in the *dis1*Δ alone, and frequently had an aster-like organization (Figure 3.20A; Figure 3.15A). It was clear from these results that the level of Alp14 over-expression achieved using the fully active *81nmt1* promoter was not sufficient to rescue the intranuclear microtubule phenotype in *dis1*Δ cells at the restrictive temperature. This does not exclude that higher expression levels of Alp14 could rescue. Together with the results from Garcia *et al.* (2001) using multi-copy plasmid expressing Alp14, these results suggest that Alp14 and Dis1 are probably not functionally redundant with respect to their roles during mitosis at 18ºC.

3.4.4. At least one of the XMAP215 homologues is required for vegetative growth of *S. pombe*.

It is known from previous studies that *alp14*Δ *dis1*Δ cells are synthetic lethal when the double deletion strain is generated by crossing the single deletions (Garcia *et al.*, 2001). We confirmed this result, and examined the double deletion spores to see if the cause of lethality could be established. We found that many of the spores had started to germinate, but had failed to correctly divide (data not shown). We were unsure whether this was a meiotic or mitotic defect, and thus whether cells could survive without both XMAP215 homologues once they had germinated and entered the vegetative life cycle. We therefore attempted to create the double deletion strain by replacing the endogenous *dis1* gene in an *alp14*Δ strain with an antibiotic resistance gene, using standard *S. pombe* transformation techniques. However, we found that no positive transformants grew on the antibiotic plates, at both 25ºC and 30ºC, suggesting that either Alp14 or Dis1 are required for vegetative growth at all temperatures.

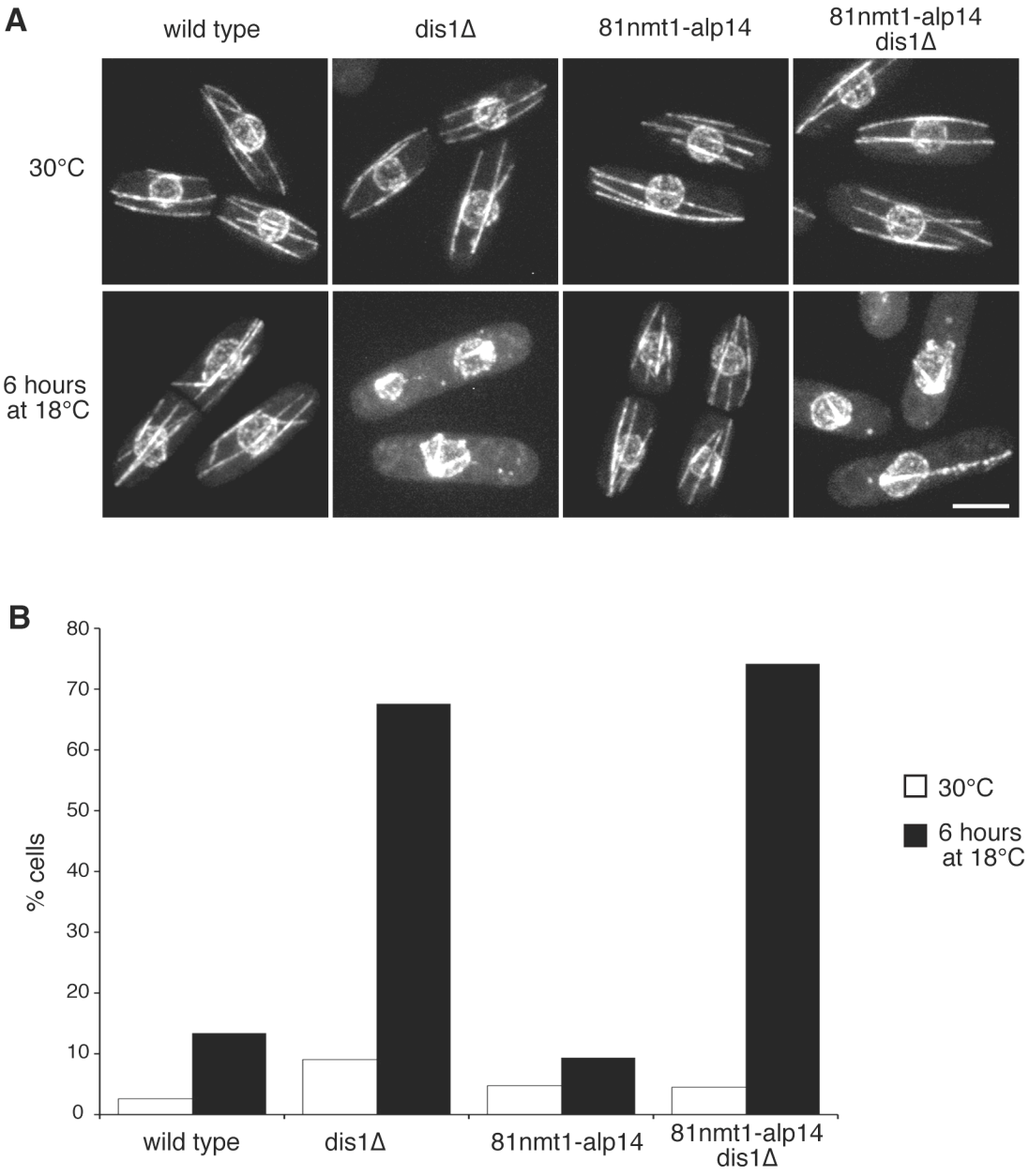

Figure 3.20 Over-expression of Alp14 does not rescue the *dis1Δ* microtubule phenotype at the restrictive temperature

(A) Images of control and *dis1Δ 81nmt1alp14* cells at 30ºC and after 6 hours at 18ºC in the absence of thiamine. (B) Quantification of percentage of cells in (A) with intranuclear microtubules. Cells express GFP-tubulin and Nup85-GFP, microtubule and nuclear envelope markers. Images are projections of confocal sections covering the entire Z-axis of the cell. Bar, 4 μm.

3.5. Dis1 shut-off in *alp14*Δ

We then wanted to establish whether the cause of intranuclear microtubule formation was the result of inactivation of Dis1 when the cells were shifted to the restrictive temperature. Dis1 was a logical candidate, as it is the Alp14 orthologue and we showed previously that over-expression of Dis1 was able to at least partially rescue the *alp14*Δ interphase microtubule phenotype (see section 3.4.2). In addition, it is known from previous studies and confirmed by this study that *alp14*Δ *dis1*Δ cells are synthetic lethal (Section 3.4.4; Garcia *et al.*, 2001). To test the hypothesis that Dis1 was being inactivated by the temperature shift, we used the same strain used in the rescue experiments, where the *dis1* gene was expressed under the control of the *81nmt1* promoter (Section 3.4). The attenuated promoter is much more sensitive to the presence of thiamine than the full strength promoter, such that when cells are grown in the presence of thiamine, expression from the promoter is extremely low (Basi *et al.*, 1993). We aimed to abolish transcription of *dis1* and then observe the microtubule phenotype as the level of Dis1 protein in the cells decreased. Our initial hypothesis was that shutting-off Dis1in *alp14*Δ cells might mimic the effect of the temperature shift to 36ºC, and that we would observe intranuclear microtubules at the permissive temperature.

3.5.1. Expression of Alp14/Dis1 in fission yeast is essential for maintenance of an interphase microtubule array.

3.5.1.1. Dis1 shut-off in *alp14*Δ cells at 25ºC results in a decrease in the number of cytoplasmic interphase microtubules

*81nmt1dis1 alp14*Δ cells were grown to exponential phase at 25ºC in the absence of thiamine as this is the permissive temperature for *alp14*Δ cells. Thiamine was then added to a final concentration of 30μM and cells were maintained in exponential growth by diluting with medium containing 30μM thiamine. The final concentration of thiamine used in this experiment was double that usually used to repress the *81nmt1* promoter, however we wanted to ensure that the promoter remained fully repressed at all times, and the thiamine was not fully depleted by the cells. After the cells had been grown in the presence of thiamine for 72 hours they were imaged.

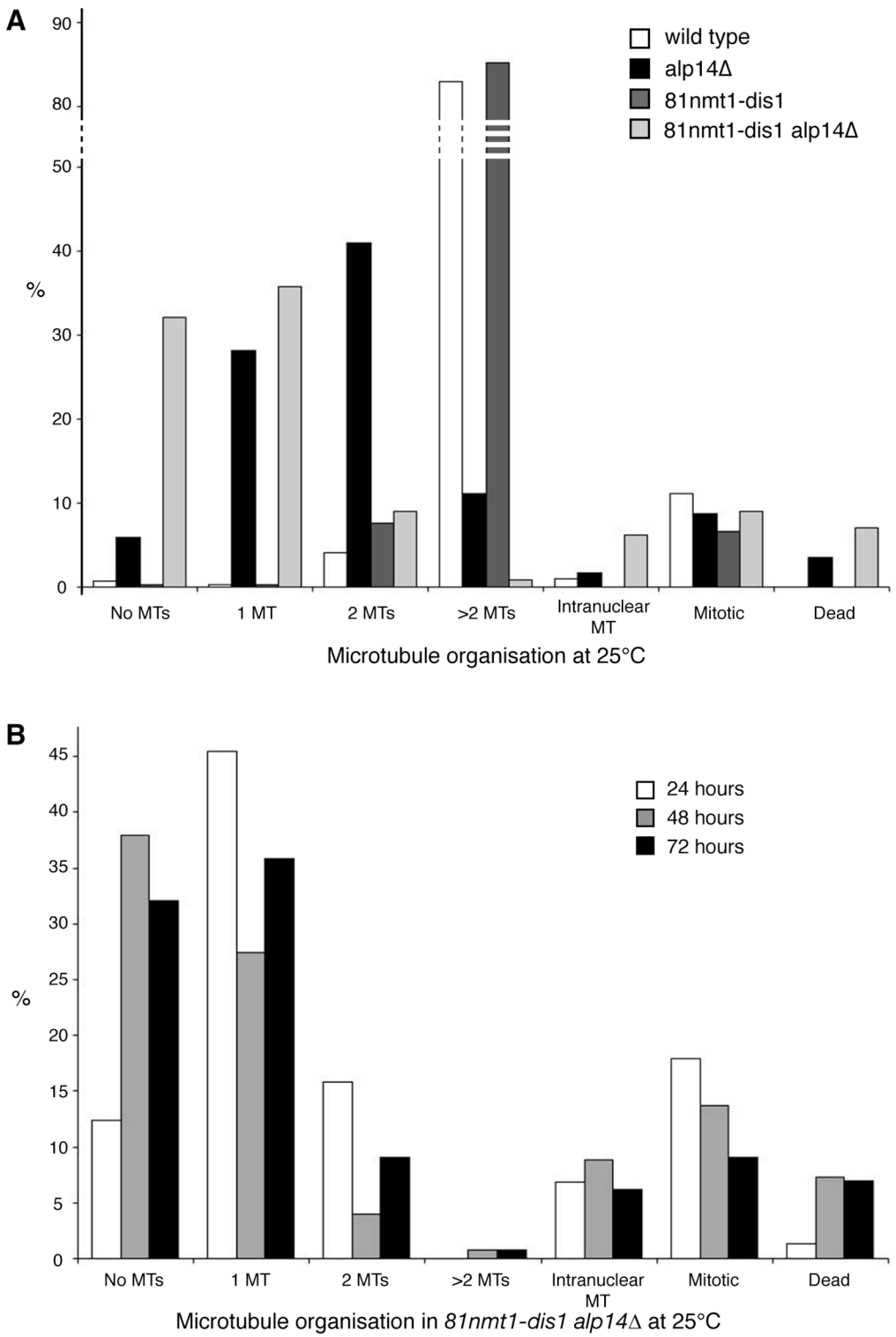

Figure 3.21 Microtubule organisation in *alp14Δ* cells at the permissive temperature when expression of Dis1 is shut off

(A) Quantification of microtubule organisation at 25ºC in control and *alp14Δ 81nmt1dis1* cells after 72 hours growth in the presence of thiamine. (B) Quantification of microtubule organisation in *alp14Δ 81nmt1dis1* cells after 24, 48 and 72 hours growth in the presence of thiamine.

Quantification (Figure 3.21A) showed a significant decrease in the number of cells with two or more microtubule bundles in the *alp14*Δ *dis1* shut-off cells (10%) compared to *alp14*Δ alone (52%). There was a slight increase in the number of dead cells in the *alp14*Δ *dis1* shut-off strain compared to *alp14*Δ alone, however most striking was the increase in the number of cells with no microtubules; 32% of *alp14*Δ *dis1* shut-off cells compared to 6% in the *alp14*Δ strain (Figure 3.21A). When we examined the *alp14*Δ *dis1* shut-off cells at 24, 48 and 72 hours after addition of thiamine we found that the decrease in microtubule bundle number occurred predominantly within the first 24 hours of shut-off, indicating that Dis1 protein levels were being effectively reduced within 24 hours of thiamine addition (Figure 3.21B). This is consistent with Western blotting of extract from GFP-Dis1 cells under the control of the same promoter grown under the same conditions (Figrue 4.17A). Contrary to our prediction that shutting-off *dis1* would lead to intranuclear microtubule formation in the *alp14*Δ background, we saw only a slight increase in the number of cells with intranuclear microtubules (Figure 3.12A; 7% in the *alp14*Δ *dis1* shut-off, compared to 3% in *alp14*Δ). Both Dis1 and Alp14 have roles during mitosis, and the single mutants at the restrictive temperatures have mitotic defects. When we examined the percentage of mitotic cells we found that there was no obvious increase in the *alp14*Δ *dis1* shut-off compared to *alp14*Δ alone or the control cells, suggesting that the cells were not terminally arresting in a mitotic state (Figure 3.21B).

3.5.1.2. Dis1 shut-off in *alp14*Δ cells at 30ºC also results in a decrease in interphase microtubules and increased lethality

As Alp14 is not the only protein that could be inactivated in *dis1*Δ cells by the shift to cold temperature, we repeated this experiment, maintaining the cells at 30ºC, which is the permissive temperature for both *alp14*Δ and *dis1*Δ cells. As for 25ºC, after 72 hours growth in the presence of excess thiamine, *alp14*Δ *dis1* shut-off cells showed a decrease in the number of interphase microtubules but no increase in the number of cells with intranuclear microtubules compared with *alp14*Δ expressing endogenous levels of Dis1 (Figure 3.22A). When the Dis1 shut-off was monitored over time, we found that the number of cells with no microtubules reached approximately 22% within the first 24 hours of *dis1* shut-off, and then remained constant (Figure 3.22B). This suggests that the rate of *dis1* shut-off occurred faster at 30ºC than 25ºC, which is expected since the generation time of *S. pombe* at 30ºC is shorter at 30ºC than at 25ºC.

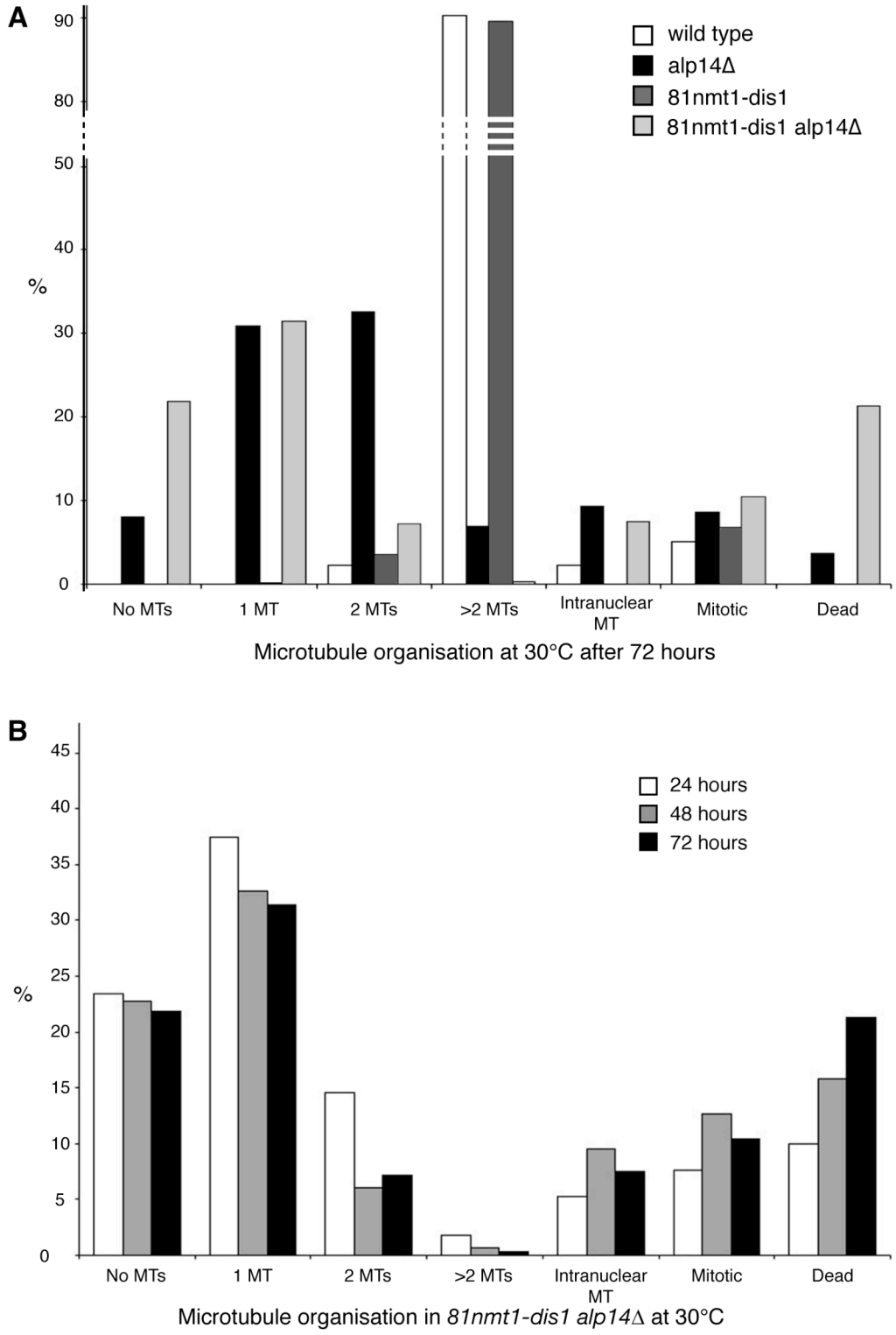

Figure 3.22 Microtubule organisation in *alp14Δ* cells at the restrictive temperature when expression of Dis1 is shut off

(A) Quantification of microtubule organisation at 30ºC in control and *alp14Δ 81nmt1dis1* cells after 72 hours growth in the presence of thiamine. (B) Quantification of microtubule organisation in *alp14Δ 81nmt1dis1* cells after 24, 48 and 72 hours growth in the presence of thiamine.

In contrast to the results at 25ºC, we observed a striking increase in the number of dead cells (21%) compared to both the *alp14*Δ cells alone (4%) (Figure 3.22A) and the *alp14*Δ *dis1* shut-off cells grown at 25ºC (7%; Figure 3.21A). The number of dead cells in the *alp14*Δ *dis1* shut-off culture also increased over time (Figure 3.22B), but the number of mitotic cells remained constant, suggesting that the compromised interphase microtubule array was resulting in lethality rather than a mitotic defect.

4. Discussion

S. Pombe provides a unique system to study the functions of the Dis1/XMAP215 family members, as it is the only system known to date where more than one XMAP215 homologue exists. This suggests that the various functions assigned to this protein class might have been split between the two homologues. Alp14 is essential for growth at high temperatures, and Dis1 at low temperatures. In addition, deletion of both *alp14* and *dis1* was shown to be lethal at all temperatures, highlighting the essential role of the Dis1/XMAP215 homologues in fission yeast. Alp14 and Dis1 perform non-redundant functions, as the phenotypes of the deletion mutants are distinct. A significant amount of data exists about the role of Alp14 and Dis1 during mitosis, but an investigation of their role during interphase is lacking. Here we discuss the data we acquired addressing the role of these proteins in microtubule organisation during interphase and the further implications of these findings.

4.1. Alp14 behaves as an autonomous plus end tracking protein

Alp14 is reported to localise to interphase microtubule arrays as moving particles (Nakaseko *et al.*, 2001; Okahura *et al.*, 2001), however a detailed characterisation of its localisation and dynamics had not previously been performed. We carried out a comprehensive *in vivo* analysis of the dynamics of Alp14-GFP and found that it behaves as a canonical +TIP. We observed Alp14-GFP in the regions of microtubule overlap at the centre of the cell and moving outwards towards the cell tips along microtubules, both at the ends of microtubules and along pre-existing arrays. In addition, we observed movement of Alp14-GFP particles inwards towards the cell centre along pre-existing microtubules (Figure 3.1). This localisation and dynamic behaviour at the plus ends of microtubules resembles that of Mal3, a canonical +TIP (Busch and Brunner, 2004). The lack of a significant difference in the speeds of the two types of Alp14-GFP plus-end directed movement could indicate that movement along apparently pre-existing microtubules is actually plus-tip localisation on new

microtubules growing next to pre-existing ones, however the resolution of this system does not allow us to determine this.

The minus-end directed Alp14-GFP movement, which is also shown for Mal3 and Stu2 (Wolyniak *et al.*, 2006; Busch *et al.*, 2004) occurs at a much slower speed than the rate of microtubule de-polymerization (Figure 3.1C; Busch *et al.*, 2004), making it unlikely that Alp14-GFP also tracks the minus ends of depolymerising microtubules. The minus-end-directed movement of Alp14 however, is slower than that of Mal3, suggesting that certainly in terms of this type of movement along microtubules, the two proteins are either not found in the same complex. Support that Mal3 and Alp14 do not travel along the microtubules together comes from the analysis of the movement of Alp14-GFP along the microtubules in *mal3*Δ cells (Figure 3.2B). This was not abolished, as is the case for Tip1 and Tea2, proteins known to require Mal3 for +TIP tracking (Busch and Brunner, 2004; Browning *et al.*, 2003). This shows that the plus-end directed movement of Alp14-GFP occurs independently of Mal3 and as such Tip1 and Tea2. In turn, *in vitro* experiments with recombinant Mal3 have shown that Mal3 behaves as an autonomous +TIP (Bieling *et al.*, 2007). The plus end association of the *Aspergillus* Dis1/XMAP215 homologue AlpA was also shown to be independent of theTea2 homologue, KipA (Enke *et al.*, 2007). An interaction between Alp14 and Mal3 was not tested biochemically in *S. pombe*, but the *S. cerevisiae* homologue Stu2 was reported to immunoprecipitate with the Mal3 homologue Bim1 only weakly, indicating that this interaction could be indirect, or that only a small amount of the total protein interacts (Wolyniak *et al.*, 2006). Further, in *Xenopus* egg extracts XMAP215 and EB1 interact only indirectly during interphase, through the microtubule destabliser XKCM1 (Niethammer *et al.*, 2007). However the Dictyostelium EB1 and XMAP215 homologues do co-localise and interact (Rehberg and Graf, 2002). The relationship between Mal3 and Alp14 in *S. pombe* therefore needs to be investigated further before firm conclusions can be drawn.

The movement of Alp14-GFP along microtubules also occurred independently of the microtubule destabilising kinesins Klp5 and Klp6, as confirmed by analysis of Alp14-GFP in *klp5*Δ and *klp6*Δ single and double deletion strains (Figure 3.2C,D). A functional relationship between Klp5/Klp6 and Alp14 has previously been demonstrated *in vivo*; it was shown that the kinetochore localisation of Klp5 was reduced in the absence of Alp14. In addition, any combination of mutations in Alp14/Dis1 and Klp5/Klp6 was synthetically lethal (Garcia *et al.*, 2002b). Therefore, despite their apparently opposing activities towards microtubule stability, it might be interesting to examine whether Klp and Klp6 are able to correctly localise during interphase in the absence of Alp14, especially given that Klp5 and Klp6 localise to

microtubules as discrete dots (Garcia *et al.,* 2002a), a localisation similar to Alp14-GFP. In *S. cerevisiae* it was shown that Stu2 localises to microtubules independently of any motor protein (Al Bassam *et al.*, 2006). In addition, the plus end localisation of the *Aspergillus* homologue AlpA is not dependent on the kinesins KipA or KinA, shown to be required for the microtubule plus-end localisation of the homologues of Tip1 and a dynein pathway component respectively (Enke *et al.*, 2007).

The *in vivo* discrete microtubule lattice and plus-end-localisation of Dis1/XMAP215 homologues is characteristic not only of yeast, but is also seen for other family members, for example DdCP224 in *Dictyostelium* (Rehburg and Graf, 2002), *Aspergillus* AlpA (Enke *et al.*, 2007), *Drosophila* Minispindles (Brittle and Okhura, 2005) and *Xenopus* XMAP215 (Brouhard *et al.*, 2008).

4.2. Dis1 and Alp14 localisations are distinct

We examined the localisation and behaviour of Dis1-GFP and found it to be different to Alp14-GFP. Rather than showing +TIP behaviour, Dis1-GFP localised along the microtubules with a stronger signal in the region where the microtubules overlap in the cell centre (Figure 3.3A). The oscillation of these broad Dis1-GFP patches resembled that of the overlap regions (Figure 3.3B) rather than active movement along the microtubules (Daga *et al.*, 2006; Tran *et al.*, 2001). This localisation and behaviour of Dis1 was also seen when a linker sequence was added between the C-terminus of Dis1 and the GFP tag. This makes it less likely that the tag was interfering with Dis1 localisation (Figure 3.3C). These results are similar to previous reports that Dis1-GFP localisation and dynamics were indistinguishable from GFP-tubulin (Nakaseko *et al.*, 2001), and that the brighter Dis1-GFP signal at the overlap regions is probably a consequence of an increase in the number of short microtubules in this region. Interestingly, preliminary results revealed that Dis1-GFP failed to localise correctly when the microtubule bundling protein Ase1, an antiparallel microtubule bundling protein enriched in the overlap zones (Loiodice *et al.*, 2005), was deleted (data not shown). This central region of the cell around the nucleus is the site of interphase microtubule nucleation from the SPB and regions on the nuclear surface (reviewed in Sawin and Tran, 2006). The γ-tubulin complex-associated proteins are also found to localise to these regions (Zimmerman and Chang, 2005; Sawin *et al.*, 2004; Zimmerman *et al.*, 2004; Fujita *et al.*, 2002; Vardy and Toda, 2000; Horio *et al.*, 1991). This raises the possibility that Dis1 plays a role in interphase microtubule nucleation and/or stabilisation of overlap regions. However, taking into consideration the data that cytoplasmic microtubule arrays are not affected by deletion of *dis1*, this

is likely not an essential function unless Alp14 compensates for loss of Dis1. However, when we examined the extent of co-localisation between Alp14-rRFP and Dis1-GFP we found that during interphase they only rarely co-localised in the central regions of the cell (Figure 3.3D).

That Alp14 and Dis1 have different localisation patterns and display different dynamic behaviour demonstrates the diversity of the Dis1/XMAP215 homologues. Although most are reported to show plus-end tracking behaviour (Brouhard *et al.*, 2008; Enke *et al.*, 2007; Brittle and Okhura, 2005; Rehburg and Graf, 2002), the *Arabidopsis* homologue MOR1 localises along microtubules at all stages of the cell cycle (Kawamura *et al.*, 2006), a similar localisation to Dis1. These localisation results taken together indicate that the *S. pombe* orthologues have different roles in interphase microtubule organisation.

4.3. The role of Alp14 with respect to interphase microtubules

Previous studies of the microtubule arrays in *alp14*Δ cells report apparently contradictory data; Garcia *et al.* (2001) reports normal interphase microtubules, however two groups report fewer or no microtubules in *alp14*Δ cells at the permissive temperature (Nakaseko *et al.*, 2001; Okhura *et al.*, 2001). This could be reconciled by the fact that Garcia *et al.* (2001) used immunostaining of fixed cells to determine microtubule organisation, which is an unreliable method in *S. pombe* due to the problems associated with fixation artefacts (D. Brunner, unpublished observation). In all cases however, a quantitative analysis of the microtubule arrays in *alp14*Δ cells was lacking.

4.3.1. *alp14Δ* cells have altered interphase microtubule arrays at the permissive temperature

When we examined the interphase microtubule arrays in *alp14*Δ cells at the permissive temperature by live imaging of GFP-tubulin, we found that in contrast to the measurements of Garcia *et al.* (2001) but in agreement with Okhura *et al.* (2001), that the number of interphase microtubule bundles was reduced and the bundles were shorter, with a lower percentage reaching either or both cell ends (Figure 3.4B,C).

However, this decrease in the percentage of microtubules reaching the cell ends reflected not only that the microtubules were shorter, but that the cells were also longer. In addition, many had shape and mitotic abnormalities (Garcia *et al.*, 2001; Nakaseko *et al.*, 2001; Okhura *et al.*, 2001). The reduction in the number of microtubule bundles points to a function of Alp14 at the minus ends of microtubules, or at the plus ends just as they start growing. A role for Alp14 at the plus ends during mitosis is seen in *alp14*Δ, where it is involved in kinetochore-spindle attachment (Garcia *et al.*, 2002b; Garcia *et al.*, 2001). During interphase in *alp14*Δ at the permissive temperature, one of the remaining bundles is associated with the SPB (data not shown), which indicates an interphase role of Alp14 in particular with respect to maintenance of the non-SPB microtubule bundles. Interestingly though, mutations in proteins associated with the γ-tubulin complex and iMTOC function often have fewer microtubules, but rather than being shorter, as in the case of *alp14*Δ, they are longer and curl around the cell ends. In addition, the microtubules are often unattached to the nucleus, which is not seen in *alp14*Δ (Tange *et al.*, 2004; Fujita *et al.*, 2002; Paluh *et al.*, 2000; Vardy and Toda, 2000;). This suggests that Alp14 plays role in microtubule stabilisation that is different to that of the γ-tubulin complex components or that it plays a dual role at both the plus and minus ends of microtubules.

An additional stabilisation role for Alp14 at the plus ends of the microtubules is indicated by a decrease in the length of the bundles (Figure 3.4C), as seen in *mal3*Δ cells (Beinhauer *et al.*, 1997), although this could also be attributed to a role for Alp14 in stabilisation of microtubules at their minus ends, as indicated by the effect on microtubule length in the γ-tubulin mutants, mentioned previously. This decrease in the number and length of interphase microtubules is also seen in *Dictyostelium* when the Alp14 homologue DdCP224 is depleted (Graf *et al.*, 2003). Interestingly, the effect of Stu2 depletion on the cytoplasmic microtubules in *S. cerevisiae* results in a decrease in the number of cytoplasmic microtubule bundles, but these maintain wild type length. Additionally, quantification of the dynamics of the cytoplasmic microtubules in Stu2-depleted cells revealed normal rates of growth and shrinkage, however the frequency of catastrophes and rescues was decreased and the microtubules spent a longer time in the paused state (Kosco *et al.*, 2001). This increase in pausing time was also seen in Msps-depleted *Drosophila* S2 cells during interphase (Brittle and Okhura, 2005). It would therefore be interesting to analyse the dynamics of interphase microtubules in *alp14*Δ cells at the permissive temperature as it may provide additional insight into the role of Alp14 with respect to microtubule regulation.

The additional microtubule length decrease of *alp14*Δ microtubule bundles compared to the situation in Stu2-depleted cells highlights the more complex interphase function of Alp14 over Stu2, which is not surprising, given the more important role of cytoplasmic microtubules in *S. pombe* than in *S. cerevisiae*.

4.4. *alp14*Δ at the restrictive temperature

4.4.1. Formation of intranuclear microtubules during interphase *alp14Δ* cells at the restrictive temperature

When *alp14*Δ cells were shifted to the restrictive temperature of 36ºC the interphase microtubule array underwent a switch from a cytoplasmic to intranuclear localisation (Figure 3.4D and Figure 3.5). Upon shifting to the restrictive temperature, the interphase array of 1-3 microtubule bundles depolymerised, and at the same time, a single microtubule bundle was nucleated inside the nucleus (Figure 3.7A). Confirmation that the microtubule bundle was intranuclear came from examination of confocal slices through cells in which the microtubules and nuclear envelope were labelled with GFP (Figure 3.5C). Only interphase cells formed intranuclear microtubules, confirmed by experiments where the cells were blocked in interphase with HU prior to being shifted to the restrictive temperature (Figure 3.5B,D). When we tested whether there was a critical temperature at which this transition occurred we found that there was a defined shift from a cytoplasmic organisation at 31ºC to intranuclear microtubule bundle formation at 33ºC, rather than a gradual transition between the 2 states (Figure 3.6). This striking shift from cytoplasmic to nuclear microtubule organisation during interphase has not been reported for mutants of any of the other Dis1/XMAP215 homologues.

4.4.2. Comparison of *alp14Δ* with other examples of intranuclear microtubule formation in interphase *S. pombe* cells

To our knowledge only three reports of nuclear microtubules existing during interphase have been reported in *S. pombe*. The first is in cells lacking Mto1 (also known as Mbo1 or Mod20), which mediates γ-tubulin complex recruitment specifically to cytoplasmic MTOCs (Sawin *et al.*, 2004; Venkatram *et al.*, 2004). It

was shown that *mto1*Δ cells fail to nucleate cytoplasmic microtubules. Many of the cytoplasmic microtubules in *mto1*Δ cells originate from the mitotic spindle. These microtubules escape from the nucleus during spindle breakdown as nuclear envelope fission occurs. It was also shown that following cold shock, which depolymerises the microtubules, small fragments of intranuclear microtubules that re-grow, can break off from the intranuclear bundle. These are able to exit the nucleus by puncturing through the nuclear envelope and propagate within the cytoplasm to form additional cytoplasmic microtubule bundles (Zimmerman and Chang, 2005). The intranuclear microtubules formed in *mto1*Δ cells are different to those formed in *alp14*Δ at the restrictive temperature in two respects. The first is that the *mto1*Δ microtubules do not represent *de novo* nucleation inside the nucleus, rather a failure to nucleate a cytoplasmic array. Secondly, fragments that break off from the intranuclear microtubule bundle in *mto1*Δ cells puncture through the nuclear envelope, an event that we never observed in *alp14*Δ cells at the restrictive temperature.

The second example we found of intranuclear microtubules forming in interphase cells is when the protein Ned1 (**N**uclear **e**longation and **d**eformation 1) is over-expressed (Tange *et al.*, 2002). Ned1 is implicated in the maintenance of nuclear morphology and interacts with components of the Ran GTPase system and the essential nucleoporin Nup189. The behaviour of this microtubule bundle more closely resembled the behaviour of those in *alp14*Δ cells, as discussed in further detail in Section 4.4.4.2.1. Interestingly, the cold-sensitive growth phenotype of *dis1*Δ was enhanced when combined with the *ned1-1* mutation. The lethality resulting from Ned1 over-expression probably occurs as a result of the disruption of the essential interaction of Ned1 with Dis3, another gene implicated in the regulation of mitosis by the Ran system, as a *dis1*Δ *dis3*Δ mutant is also synthetic lethal. Mutations in the Ran GTP-exchange facter *pim1-46* reduced the effect of Ned1 over-expression on nuclear elongation, further suggesting that the Ran system is involved in formation of the nuclear bundle (Tange *et al.*, 2002). In this study no link between Alp14 and Ned1 was examined, but we did investigate the link between Alp14 and Alp7 with respect to intranuclear microtubule formation. We found no effect on intranuclear microtubule formation in *alp7*Δ *alp14*Δ cells (Figure 3.13), showing that Alp7, a target of Ran in spindle formation (Sato *et al.*, 2007), does not contribute to intranuclear formation in *alp14*Δ cells (See Section 4.4.6). However, there may be an additional link between Alp7 and Alp14 that is not related to interphase microtubule behaviour. Thus, it may be interesting to examine this link between Alp14 and the Ran system more directly.

The third example where intranuclear microtubule bundle formation occurs, results from blocking nuclear export by treating the cells with the drug leptomycin B, an inhibitor of the nuclear export protein Crm1 (Kudo *et al.*, 1999; Wolff *et al.*, 1997). This results in the formation of an intranuclear microtubule bundle (Matsuyama *et al.*, 2006). Formation of this intranuclear bundle most likely results from an inhibition of tubulin exported from the nucleus. When we examined images of GFP-tubulin in *alp14*Δ cells we observed no obvious increase in the background of GFP-tubulin in the nucleus (Figure 3.4D). Therefore it is unlikely that a failure to export tubulin from the nucleus is the cause of intranuclear microtubule bundle formation in *alp14*Δ cells at the restrictive temperature.

4.4.3. Arrangement and behaviour of the intranuclear microtubule bundle

Having discovered that *alp14*Δ cells form an intranuclear microtubule array at the restrictive temperature, we examined the behaviour and structure of this array in more detail. We found that the formation of the intranuclear microtubule occurs at the same time as the cytoplasmic microtubules are lost, with a short period in which both types of bundle co-exist (Figure 3.7A). This suggests that rather than active removal of the cytoplasmic microtubule bundles, they become less stable; new microtubules may no longer be formed at the iMTOCs. Once existing microtubules depolymerise, in accordance with the stochastic dynamic behaviour of *S. pombe* microtubules (Drummond and Cross, 2000), if there were no replacement microtubules to maintain the bundle, the result would be in a gradual loss of the cytoplasmic bundles over time.

We show that the *alp14*Δ intranuclear microtubule array consists of a bundle with similar arrangement to cytoplasmic microtubule SPB-associated bundles (Figure 3.9). There is a region in the centre of the bundle with microtubule overlap of mixed polarity and one or more microtubules extend towards the cell ends, deforming the nuclear envelope, but not grossly affecting the shape of the nuclear mass, which retains its spherical shape. The bundle displays an arrangement and dynamic behaviour similar to that observed for interphase microtubules, albeit with much slower dynamics (Figure 3.7C). The bundles grow to reach both ends of the cell. Once a critical length is reached, in which the microtubules bend as a result of forces exerted against the cell ends, the bundle depolymerises, but is able to rescue and re-grow to the cell ends. In addition, as shown by electron microscopy tomography, the bundle bends around the inner face of the nuclear envelope (Figure 3.9).

4.4.3.1. A link between the intranuclear microtubule bundle and the nuclear envelope?

The intranuclear bundle is nucleated from a region next to the SPB (Figure 3.8B,C; Figure 3.9; see Section 4.4.5 for a discussion of intranuclear bundle nucleation). This association of the SPB with the bundle is maintained, and the bundle is able to move the SPB, which can also slide along the bundle (Figure 3.7B,C). At all times the SPB and bundle remain separated from each other by the nuclear envelope, a further indication that the cells are in interphase (Figure 3.8B; Figure 3.9). In addition, we never observed more than one SPB signal in cells with intranuclear microtubule bundles, indicating that the SPBs were not duplicated. The bundle is able to move the nuclear mass (Figure 3.7C), a feature of intranuclear microtubules, which exert forces on the nuclear envelope to keep the nucleus in the centre of the cell (Daga *et al.*, 2006; Tran *et al.*, 2001; Tran *et al.*, 2000). However, the movement of the nucleus in *alp14*Δ is more extreme than that seen in wild type cells. That the bundle can move the nucleus suggests that it retains a connection to the nuclear envelope rather than behaving autonomously within the nucleus. If this is the case, the region around the SPB would be the obvious anchoring point for the bundle, as it bends around the inner surface of the nuclear envelope under the SPB (Figure 3.9), rather than passing directly through the centre of the nuclear mass, which would be the expected arrangement to minimise bending of the bundle. Further evidence for this comes from the observation that the SPB always remains associated with the bundle (Figure 3.7B,C). This connection cannot be directly with the SPB, as the nuclear envelope is situated in between and therefore prevents this (Figure 3.8B; Figure 3.9), but could be, for example, via SPB-associated proteins at the inner surface of the nuclear envelope.

Another possible link between the SPB and the microtubule bundle could be the kinetochores, which localise next to the SPB at the permissive and restrictive temperatures in *alp14*Δ cells (Figure 3.12). Alternatively, the bundle may interact directly with components found dispersed across the nuclear surface. Microtubules are nucleated from points on the nuclear surface (Tran *et al.*, 2001) and in addition, a physical connection was observed between cytoplasmic microtubules and the nuclear envelope in the form of electron dense bridges (Hoog *et al.*, 2007), however the identity of the proteins involved in this interaction is not known. It is possible that such a connection also exists between intranuclear microtubules and the inner surface of the nuclear envelope, although this is not seen with the spindle, except indirectly at their point of attachment to the SPBs (Ding *et al.*, 1997). Another possibility is that

the intranuclear microtubules are interacting with the nuclear pore complexes. A direct interaction between microtubules and the nuclear pore complex has not been proven unequivocally to date, however microtubules lying across the surface of the nuclear envelope are always in close proximity to the nuclear pores (J. Hoog and H. Roque, personal commuication) and a mammalian nucleoporin is known to associate with cytoplasmic microtubules (Joseph and Dasso, 2008).

4.4.4. A consideration of the forces

4.4.4.1. Forces acting on the intranuclear microtubule bundle

Once the intranuclear microtubule bundle is established it shows similar, albeit slower, dynamics to normal interphase microtubule arrays (Figure 3.7C). It grows to reach the cell ends but then continues to grow, curving, until a critical force is exerted on the bundle by the rigid cell wall. It then depolymerises to a region close to the cell centre and rescues, once again reaching the cell ends. When we examined the *alp14*Δ cells after two hours at the restrictive temperature we found that in two of the eight bundles we examined, there was a discontinuity in the bundle. All the microtubules in the bundle in that region ended and new ones began next to these (Figure 3.9C). This had the appearance of an elbow-shaped joint suggesting that the bundles had snapped at this point. This could be a freezing artifact, however the cells were high pressure frozen extremely rapidly so such artifacts are minimised. In addition, it has never been reported that normal interphase microtubule bundles break when processed in the same way. This breakage could therefore be due to the high forces exerted on the bundle as it grows against the cell poles. As the bundle remains in the nucleus it cannot be subject to the same plus-end regulation as cytoplasmic bundles. This is because a number of the +TIP complex components such as Tea2 and Tip1 are not found in the nucleus (Brunner *et al.*, 2000). In addition, the nuclear envelope may prevent the bundle from interacting directly with the cell poles. This could 'protect' the microtubules from catastrophe, for example by maintaining Mal3 at the plus ends, as loss of Mal3 precedes catastrophe of cytoplasmic microtubules (Busch and Brunner, 2004). Increased stability of the microtubules at the cell poles would result in increased bending of the bundle, which could eventually result in the bundle breaking.

In vitro force experiments on microtubules (Janson and Dogeterom, 2004 and references therein) in addition to examination of mutants in which the microtubules

bend around the cell poles, for example mutants of the γ-tubulin complex components (Zimmerman and Chang, 2005; Venkatram *et al.*, 2004; Paluh *et al.*, 2000; Vardy and Toda, 2000) show that microtubules are able to bend considerably before they break. Given that the extent of bending of the intranuclear microtubule bundle that we observed was less extreme than the other *in vivo* examples, it is likely that the degree of long range bending alone is not sufficient to result in microtubule breakage. In both cases the break in the bundle was next to the region where the bundle protrudes from the region of the nuclear body. This could result in a local increase in bending force in this region, which in addition to the long range bending exerted from the cell poles, could have exceeded the bending capacity of the bundle, resulting in a break in this region. This idea is consistent with the hypothesis that the intranuclear microtubule bundle is in some way anchored to the nuclear envelope, forcing it to bend around the inner surface of the nuclear surface.

4.4.4.2. Forces acting on the nucleus

4.4.4.2.1. Nuclear envelope protrusions

The extension of the nuclear envelope around the microtubule bundle (Figure 3.9) shows limited similarities to the extension of the mitotic spindle during anaphase/telophase. The nuclear mass retains a roughly spherical shape and the nuclear envelope deforms, maintaining close proximity to the bundle, resulting in a spherical shape with a thin protrusion, rather than an ovoid (Figure 3.5; Figure 3.9). The significant difference between the shape of the protrusions in the *alp14*Δ cells and in mitosis, is that there is only one spherical nuclear mass in *alp14*Δ, whereas in mitosis the nucleus duplicates and the spindle connects the two spherical nuclear masses. The extension of the nuclear envelope around the protruding microtubule represents a large increase in the surface area of the nuclear envelope and requires that it be coupled to an external membrane reservoir, most likely the endoplasmic reticulum. Lim *et al.*, (2007) modelled the changes in nuclear shape accompanying elongation of the intranuclear microtubule bundle formed when Ned1 is over-expressed (Tange *et al.*, 2002). They found that these closely resemble those of a lipid vesicle in response to microtubule elongation (Kaneko *et al.*, 1998; Hotani and Miyamoto, 1990).

Unlike in higher eukaryotes, *S. pombe* does not have nuclear lamins, which form a nuclear scaffold to maintain nuclear shape (reviewed in Rowat *et al.*, 2008).

Interestingly, in the model of Lim *et al.* (2007), a term that would be provided by a nuclear scaffold protein is not required to maintain the nuclear mass in a spherical shape when the length of the intranuclear microtubule bundle exceeds the diameter of the nuclear mass. This suggests that even if an as yet undiscovered nuclear lamina analogue exists in *S. pombe,* it does not influence nuclear geometry during interphase. As *alp14*Δ cells show the same changes in nuclear shape at the restrictive temperature as were observed when Ned1 was over-expressed, we can conclude that the same forces likely govern the nuclear shape changes resulting from intranuclear microtubule elongation in *alp14*Δ.

4.4.4.2.2. Movement of the nucleus

As discussed previously, the intranuclear microtubule bundle is able to move the nuclear mass (Figure 3.7C), but this movement is more extreme than that conferred by the cytoplasmic microtubule arrays during nuclear centring in interphase (Daga *et al.*, 2006; Tran *et al.*, 2001; Tran *et al.*, 2000). This movement raised the possibility of a link existing between the bundle and the nuclear envelope (see section 4.4.3.1). In mitosis, the mitotic spindle separates the duplicated chromosomes to opposite ends of the cell. During mitosis, the spindle is anchored to the duplicated SPBs. As the spindle grows, the SPBs are moved apart to opposite sides of the nucleus and then as the spindle continues to grow, the nucleus extends and the homologous chromosomes are moved to opposite ends of the cell as two separate, approximately spherical nuclear masses. Given that the function of the spindle is to move apart the nuclear mass, it is possible that the intranuclear bundle in *alp14*Δ is also able to perform this function. As the *alp14*Δ cells are in interphase, the SPB is unduplicated, which explains why the nucleus remains as a single spherical mass, however one property of the bundle argues against an active role for movement of the nuclear mass specifically to the cell ends as is seen in mitosis. This is that the nuclear mass is moved to the end of the cell, but that it then can return to the cell centre (Figure 3.7C). This is not seen in mitosis, where the nuclear masses are retained at the cell ends until the cell divides.

We observed that at the early stages of intranuclear microtubule bundle formation, the SPB was found at one end of the bundle. As the bundle grew and contacted both cell poles, the SPB moved away from the end of the bundle and remained associated with the bundle along its length (Figure 3.7B). Once the SPB was no longer associated with one end of the microtubule bundle, movement of the nucleus was no longer observed. This nuclear movement, lead by the SPB is reminiscent of the situation in meiosis when the nucleus oscillates in a process called horsetail movement. This

requires that a physical connection exists between the nuclear mass and the SPB. Recently, a protein that could perform such a function in interphase *alp14*Δ cells at the restrictive temperature has been identified: Ima1, an inner nuclear membrane protein, specifically binds to heterochromatic regions and couples the heterochromatin to the SPB on the other side of the nuclear envelope (King *et al.*, 2008). One major difference between horsetail movement and the movement of the nuclear mass observed in *alp14*Δ cells at the restrictive temperature is that during meiosis, cytoplasmic, not intranuclear microtubules are moving the SPB. This implies that the similarity between the two processes is in the movement itself, lead by the SPB, rather than the mechanism of force generation: Growth of the intranuclear microtubule moves the SPB in *alp14*Δ cells, but in meiosis the SPB is moved by pulling forces generated by interaction of cytoplasmic microtubules with dynein at the cell cortex.

4.4.5. What is nucleating the intranuclear microtubules?

When we took a closer look at the initial stages of intranuclear microtubule bundle formation we found that prior to bundle formation, the microtubules formed an aster-like structure (Figure 3.10). Mal3-GFP dots were observed radiating from a central point at the nuclear envelope, which co-localised with the SPB marker Sad1-dsRed (Figure 3.10A,B). We initially believed that the movement of the Mal3-GFP dots outwards from the centre of the aster-like structure indicated that the minus ends were at the centre and the plus ends moved outwards. However, during the course of these experiments a paper was published showing that Mal3-GFP also localises to and tracks uncapped microtubule minus ends *in vitro* (Bieling *et al.*, 2007). This paradoxically means that the canonical marker for microtubule plus ends may not reliable. We therefore used electron microscopy tomography to examine the organisation of this aster-like structure in more detail with the hope that we could determine what was nucleating the intranuclear microtubules. We found that rather than having a central point of nucleation typical of an aster, the microtubules were emanating from different points next to the nuclear envelope in the vicinity of the SPB. Examination of the ends of the microtubules revealed no electron-dense structures associated with the microtubules ends and additionally no consensus in their polarity (Figure 3.11). This suggested that the SPB was not nucleating the microtubules, firstly because it remained outside the nucleus; secondly, if the SPB was nucleating the microtubules then predominantly minus ends would be expected to be found at the SPB; finally, because the ends of the microtubules were not closely clustered at the nuclear envelope below the SPB.

This evidence that the SPB was not the direct nucleator of the intranuclear microtubules prompted us to examine the localisation of the kinetochores in *alp14*Δ cells. Although kinetochores have not been shown to nucleate microtubules in yeasts to date, they are clustered adjacent to the SPB during interphase (Funabiki *et al.*, 1993). We showed that the kinetochores co-localise with the SPB both at the permissive and restrictive temperature in *alp14*Δ cells (Figure 3.12), however the kinetochores are not visible by electron tomography in *S. pombe* so we were unable to see if they were physically associated with the microtubules. To determine unambiguously whether the kinetochores, and not (indirectly) the SPB, are indeed nucleating the intranuclear microtubules a system is required which can separate the kinetochores from each other and the SPB. The only such system we found in *S. pombe* during the course of our experiments was to use a *mis6-302* mutant in which the SPBs and kinetochores no longer co-localise after six hours at 36ºC (Saitoh *et al.*, 1997). Unfortunately this was not compatible with the *alp14*Δ phenotype as intranuclear microtubules form within five minutes of shifting to 36ºC. As previously mentioned, Ima1, which links heterochromatin to the nuclear envelope/SPB, was recently discovered. The *ima1*Δ strain, in which the heterochromatin and nuclear envelope are no longer physically coupled, may prove a useful tool to further investigate this (King *et al.*, 2008).

If indeed the kinetochores nucleate the intranuclear microtubules, their subsequent role may be similar to that of the SPB with respect to SPB-associated microtubule bundle maintenance during interphase. Evidence for this comes from the observation that the kinetochores remain associated with the SPB during the formation and subsequent growth of the bundle; from examination of the position of the SPB signal with respect to the bundle we can infer that the kinetochores are localised initially at one end and then as the bundle grows they move along the bundle, remaining laterally associated with it (Figure 3.7B,C; Figure 3.12). Electron microscopy of intranuclear microtubule bundles after two hours at the restrictive temperature shows an arrangement similar to that of a cytoplasmic SPB-associated bundle (Höög *et al.*, 2007); there is a microtubule overlap region in the centre of the intranuclear microtubule bundle next to the kinetochores/SPB (Figure 3.9). As is suggested for the cytoplasmic SPB-associated bundle (Hoog *et al.*, 2007; Masuda *et al.*, 1992), new microtubules could be nucleated from the kinetochores in this overlap region of the intranuclear microtubule bundle and grow out towards the cell ends. Consistent with this, several microtubule ends are clustered in the region of the SPB in the bundle (Figure 3.9).

4.4.6. Alp7 does not have a role in intranuclear microtubule bundle formation

The TACC protein Alp7 is closely involved in the function of Alp14. Alp14 localisation to interphase microtubules and SPBs requires Alp7 (Sato *et al.*, 2004) and during spindle formation Alp7 is the chaperone for transport of Alp14 into the nucleus (Sato and Toda, 2007). Conversely, localisation of Alp7 to the spindle requires Alp14 (Sato *et al.*, 2004). Further, Sato *et al.*, (2008) showed that in the absence of Alp7, Alp14 fails to accumulate in the nucleus, suggesting that Alp7-dependent nuclear import of Alp14 is the only pathway by which Alp14 enters the nucleus. An interaction between the Alp14/Dis1 and Alp7 homologues is also conserved in *Drosophila* (Cullen and Okhura, 2001; Lee *et al.*, 2001), *C. elegans* (Bellanger and Gonczy, 2003; Srayko *et al.*, 2003) and human cells (Gergely *et al.*, 2003).

Given this close relationship between Alp14 and Alp7, we tested whether Alp7 also plays a role in intranuclear microtubule formation in *alp14*Δ cells. We found that *alp7*Δ cells did not form intranuclear microtubules at either the permissive or restrictive temperature (Figure 3.13). This suggests that the role of Alp14 as a stabiliser of interphase microtubules occurs independently of its Alp7-dependent functions, i.e. the loss of the import machinery that transports Alp14 into the nucleus does not influence intranuclear microtubule formation. Additionally, it seems that nucleation/stabilisation of interphase microtubules by Alp14 does not require its localisation to the microtubule lattice or the SPBs, since this localisation is lost in the absence of Alp7 (Sato *et al.*, 2004).

The *alp7*Δ *alp14*Δ double mutant showed identical behaviour to the *alp14*Δ single mutant with respect to intranuclear microtubule bundle formation (Figure 3.13). This indicated that the temperature shift in *alp14*Δ cells does not result in activation of Alp7-dependent nuclear import of an additional factor that causes intranuclear microtubule formation in the absence of Alp14.

4.5. Dis1 is not required for cytoplasmic microtubule maintenance at any temperature

In contrast to the abnormal interphase microtubule arrays in *alp14*Δ cells at the permissive temperature and the intranuclear microtubule phenotype at the restrictive temperature, we found that the interphase microtubules in *dis1*Δ cells at the permissive temperature had a wild type appearance and behaviour (Figure 3.14A; Nabeshima *et al.*, 1995, Ohkura *et al.*, 1988). Intranuclear microtubules did form at the restrictive temperature in *dis1*Δ cells, but that they formed with much slower dynamics than in *alp14*Δ cells (Figure 3.14B). In addition, the intranuclear microtubule structures often had an aster-like appearance (Figure 3.14A; Figure 3.15A). We found that these intranuclear microtubule arrays did not form in *dis1*Δ when they were blocked in interphase, indicating that it was a mitotic phenotype (4.16). Consistent with published results (Nabeshima *et al.*, 1995, Ohkura *et al.*, 1988), our data indicates an essential function for Dis1 during mitosis at the restrictive temperature.

Unlike in wild type cells, we observed binucleate cells in *dis1*Δ at the restrictive temperature, which also had intranuclear microtubule bundles but no connection between the two nuclei (Figure 3.15A). This is indicative that the cells were in S phase, and therefore interphasic. Thus, abnormal mitotic intranuclear microtubule bundles in *dis1*Δ cells at the restrictive temperature are able to persist into interphase. This indicates that Dis1 may be involved in the removal of the microtubule bundles from the nucleus following mitosis and also in the prevention of the formation of binucleate cells. Thus, Dis1 could act as a destabliser during mitotic exit and a stabiliser in metaphase and possibly interphase. Although Dis1 does not appear to have an essential role in interphase microtubule nucleation in wild type cells it may have an essential role in *alp14*Δ cells.

4.6. Dis1 and Alp14 have partially overlapping function with respect to a role in interphase

Despite the different interphase functions of Alp14 and Dis1, we were interested whether over-expression of Dis1 could rescue the *alp14*Δ microtubule defects. When a multi-copy plasmid over-expressing Dis1 was transformed into *alp14*Δ cells it conferred viability on plates at the restrictive temperature (Garcia *et al.*, 2001). Replacement of the endogenous promoter of *dis1* with the *81nmt1* promoter results in

moderate over-expression of Dis1 (Basi *et al.*, 1993; Western blot of Dis1-GFP (Figure 3.17*)*. When Dis1 was over-expressed in *alp14*Δ cells at the permissive temperature we found that both the number of microtubule bundles and their length was restored to that of wild type cells (Figure 3.18). This suggests that, although the primary role of Dis1 is during mitosis, it does share some functional overlap with Alp14 with respect to interphase microtubule organisation.

There are a number of explanations for the appearance of interphase microtubules in *alp14*Δ cells at the restrictive temperature. One is that the increase in temperature results in the sequestration of tubulin in the nucleus, resulting in preferential nucleation inside the nucleus simply as a result of a shift in the equilibrium of tubulin concentration. This could suggest a role for Alp14 at higher temperatures in maintaining tubulin in the cytoplasm. We believe that this is not the case, as we did not observe an obvious increase in nuclear tubulin signal in *alp14*Δ cells expressing GFP-tubulin (Figure 3.4D). The second is that the temperature increase inactivates another protein, possibly by causing it to fold incorrectly, which maintains microtubule nucleation in the cytoplasm in the absence of Alp14. One obvious candidate for such a role is the Alp14 orthologue, Dis1, supported by the observation that the *alp14*Δ *dis1*Δ strain is lethal (Garcia *et al.*, 2001, confirmed by our data). We tested this by over-expressing Dis1 in *alp14*Δ cells: Fewer than half the *alp14*Δ cells over-expressing Dis1 had intranuclear microtubule bundles after 1 hour at the restrictive temperature (Figure 3.19). This partial rescue of the *alp14*Δ phenotype by Dis1 again points to a degree of functional redundancy of Alp14 and Dis1 during interphase and suggests that Dis1 may be the factor that is being inactivated by a shift to higher temperatures, which in wild type cells would not give a phenotype due to the presence of Alp14. This could also explain the reason for an incomplete rescue, because if the temperature increase inactivates Dis1, only high levels of over-expression would achieve a large enough pool of functional Dis1 to fully rescue the *alp14*Δ phenotype. This could be tested by over-expressing Dis1 from a stronger promoter and observing whether the number of cells with intranuclear microtubules decreases when the amount of Dis1 increases.

A further possibility is that an increase in temperature leads to a more complex phenotype of *alp14*Δ involving the inactivation of additional factors, however given the degree of sequence homology between Alp14 and Dis1 the former explanation is more likely to be correct.

4.7. The presence of at least one of the Dis1/XMAP215 homologues is essential for the maintenance of interphase microtubule arrays

To further test the interaction between Dis1 and Alp14 we attempted to shut-off expression of Dis1 in *alp14*Δ cells, in effect creating a conditional *alp14*Δ*dis1*Δ strain, which is known to be synthetically lethal (Garcia *et al.*, 2001, confirmed by our data). We found that when the cells were grown at both 25ºC and 30ºC the most striking effect of a decrease in the amount of Dis1 was that the number of interphase microtubule bundles further decreased compared to the *alp14*Δ cells (Figure 3.21; Figure 3.22). This effect was more striking at 25º (Figure 3.21), probably because *dis1*Δ cells already show defects at 25ºC and both single deletions are viable at 30ºC. We did see a small increase in the number of intranuclear microtubules in the shut-off strain at 30ºC compared to in the *alp14*Δ single deletion, however this was not striking (Figure 3.21). The lack of a striking increase in the number of cells with intranuclear microtubules when Dis1 is shut-off in *alp14*Δ cells does not exclude that Dis1 is the factor that is being inactivated when *alp14*Δ cells are moved to the restrictive temperature. It is possible that only small amounts of Dis1 are required to maintain the interphase arrays and that shut-off of Dis1 by attenuation of the *81nmt1* promoter is not complete. Support from this comes from our observation that when *alp14*Δ *81nmt1dis1* cells are grown on plates in the presence of thiamine, they are viable at both 25ºC and 30ºC, even after repeated rounds of re-streaking onto fresh thiamine-containing plates (data not shown). This is surprising, as the *alp14*Δ *dis1*Δ double deletion is synthetically lethal at all temperatures (Garcia *et al.*, 2001, confirmed by our data). This indicates that Dis1 protein still remains, either because there is still low levels of transcription or that the *dis1* mRNA or protein is exceptionally stable.

Reduction of Dis1 levels in *alp14*Δ cells decreases the number of interphase microtubule bundles. Rather than causing a switch from cytoplasmic to intranuclear microtubules, decreasing *dis1* expression too much causes lethality, as seen in the *alp14*Δ *dis1*Δ strain. Consistent with the literature, it does seem that interphase microtubules can be removed without immediate lethality, however it is unclear what additional roles Dis1 may play. It is possible that low levels of Dis1 are still needed for intranuclear microtubule nucleation and that the degree of reduction achieved in our shut-off strain is simply resulting in lethality. Taken together, the results of *dis1* shut-off at 25ºC and 30ºC suggest that the presence of Alp14 or Dis1 is essential for the maintenance of interphase microtubule arrays.

4.8. Dis1 and Alp14 do not appear to show function redundancy with respect to the role of Dis1 in mitosis

To test whether Alp14 and Dis1 also show functional redundancy during mitosis we over-expressed Alp14 in the *dis1*Δ background. Previously, this was tested by assaying the growth on plates of cells over-expressing a multi-copy plasmid. Alp14 over-expression was found to only partly rescue the *dis1*Δ phenotype at the restrictive temperature (Garcia *et al.*, 2001). Cells moderately over-expressing Alp14 did not even partly rescue the *dis1*Δ cold-sensitive phenotype (Figure 3.20). This suggests that Dis1 and Alp14 do not show an overlap in function with respect to the role played by Dis1 in mitosis. This may be due to differential regulation of Alp14 and Dis1 by phosphorylation. Cdc2 phosphorylates Dis1 during mitosis and this is essential for regulation of Dis1 localisation, both in metaphase and anaphase, to ensure high-fidelity chromosome segregation (Aoki *et al.*, 2006; Nabeshima *et al.*, 1995). Interestingly, a Dis1^{6A} mutant, in which the six serine/threonine residues phosphorylated by Cdc2 were changed to alanine, is able to weakly rescue the *alp14*Δ temperature sensitive phenotype, but in an otherwise wild type background shows mitotic defects (Aoki *et al.*, 2006). This suggests that the role of Dis1 can be separated into phosphorylation-dependent and -independent roles. Phosphorylation of Alp14 is either not required for its role in interphase, or Alp14 itself is not subject to phosphorylation at all; in contrast to Dis1, Alp14 only has one predicted Cdc2 phosphorylation site (Nakaseko *et al.*, 2001). This may explain why Alp14 is unable to rescue the *dis1*Δ temperature sensitive phenotype, which results from the loss of the phosphorylation-dependent role of Dis1.

An alternative explanation is that the temperature-sensitive phenotype of *dis1*Δ results from the inactivation of Alp14 at low temperatures and that the levels of Alp14 simply need to be much higher to achieve sufficient levels of functional Alp14 to rescue the intranuclear microtubule phenotype of *dis1*Δ. Support for this comes from the study where Alp14 over-expressed from a multi-copy plasmid was able to partly rescue the *dis1*Δ temperature sensitive growth phenotype (Garcia *et al.*, 2001). This could be tested by over-expression of Alp14 from a stronger promoter. However, when Alp14 is deleted, the microtubules show interphase defects, therefore it would follow that if the shift to low temperatures in the *dis1*Δ cells results in inactivation of Alp14, then such interphase defects would also be seen. We cannot exclude that at cold temperatures Alp14 function is only compromised with respect to its role in mitosis, or that an interphase defect in *dis1*Δ cells would only be seen at later time

points after shifting to the restrictive temperature, which is masked because the cells become blocked in mitosis. However, taken together, it seems more likely that Alp14 and Dis1 do not have much functional redundancy with respect to their roles in mitosis.

4.9. Model for Alp14 and Dis1 function during interphase

Taking all this data into consideration, we conclude that the presence of one of the Dis1/XMAP215 homologues is essential for maintenance of normal interphase microtubule arrays and we propose the following model for the interphase role of the Dis1/XMAP215 homologues in fission yeast (Figure 4.1).

During interphase in wild type cells, both Alp14 and Dis1 are localised to the microtubules at temperatures below 33ºC (Figure 4.1A), which is the temperature at which intranuclear microtubules form in *alp14*Δ cells (Figure 4.1C). Alp14 localises as particles which display +TIP behaviour (Figure 3.1), but in contrast Dis1 is localised all along the microtubules, with a brighter signal at the overlap zones and does not display +TIP behaviour (Figure 3.3A,B). When the temperature increases above 33ºC, Dis1 function in the cytoplasm is compromised, however Alp14 is not affected by the temperature increase so the microtubule arrays remain stable (Figure 4.1B). In *alp14*Δ cells at the permissive temperature (less than 33ºC) the number and length of the microtubule bundles is decreased because the stabilisation/nucleation role of Alp14 is absent, however, some cytoplasmic microtubule bundles still remain due to the ability of Dis1 to maintain these bundles in the cytoplasm (Figure 4.1C). At temperatures above 33ºC Dis1 function in the cytoplasm is compromised and it can no longer maintain the cytoplasmic microtubules. As a result the cytoplasmic microtubules depolymerise and a microtubule bundle forms in the nucleus (Figure 4.1D). This bundle has dynamic properties similar to a cytoplasmic bundle, deforming the nuclear envelope as it grows (Figure 3.7C) In *dis1*Δ cells at 30ºC or above the cytoplasmic microtubules have a normal arrangement (Figure 3.13A) but during mitosis they have a slight delay in spindle elongation. At temperatures below 30ºC the interphase microtubules also behave as in the wild type as Alp14 is not affected by the temperature shift (Figure 4.1E). However, the temperature decrease results in the inactivation of unidentified proteins, which partly compensate for the absence of Dis1 at the permissive temperature (Figure 4.1F). The result is that the cells have more

severe mitotic defects and become blocked in mitosis and the spindles have an aster-like appearance (Figure 3.14A and Figure 3.15A). Although the details of this model remain to be elucidated, it can be reconciled with previously published data and the results presented in this thesis.

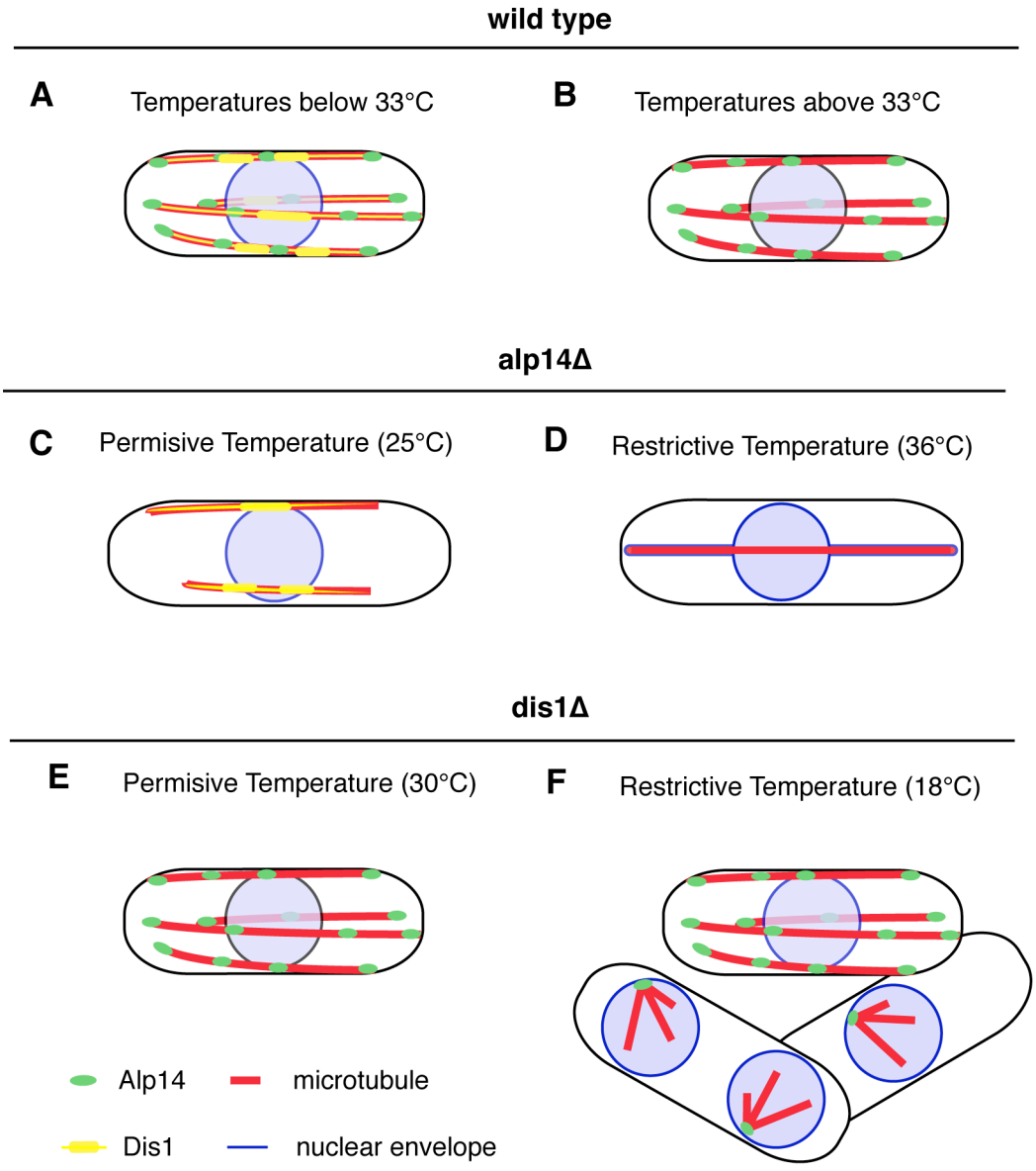

Figure 3.1 Model for Alp14 and Dis1 function during interphase

4.10. Alp14 acts as a stabiliser of interphase microtubules

The results from *alp14*Δ cells at both the permissive and restrictive temperature points towards a role for Alp14 as a microtubule stabiliser. In addition, the localisation of Alp14 at both the plus ends of microtubules and at the cell centre places it in a position where it could perform such a microtubule stabilisation role. In addition to the data from *S. cerevisiae* Stu2 discussed previously (Kosco *et al.*, 2001) such a role for Dis1/XMAp215 is found in other systems: In *Xenopus* egg extract, depletion of XMAP215 results in a decrease in the microtubule growth rate and microtubules are shorter both in interphase and mitosis. The interphase stabilisation activity of XMAP215 acts primarily by its antagonistic activity of the microtubule destabilizing kinesin XKCM1 (Tournebize *et al.*, 2000). Although there are a number of depolymerising kinesins in *S. pombe*, there is no XKCM1 homologue, raising the question of whether such an antagonistic role exists for Alp14.

XMAP215 is also a key component for the microtubule nucleating activity of centrosomes (Popov *et al.*, 2002). In *Dictyostelium*, reduced expression of DdCP224 leads to a decrease in the number and length of astral microtubules. Microtubule re-growth following treatment by the microtubule depolymerising drug nocodazole was also dependent upon DdCP224. Additionally, when DdCP224 was over-expressed there was an increase in the number of MTOCs (Graf *et al.*, 2003). RNAi of ZYG-9 in *C. elegans* results in shorter astral microtubules, mitotic and meiotic spindles and clusters of short microtubules in the cytoplasm during meiosis (Srayko *et al.*, 2003; Kemphues *et al.*, 1986). *Drosophila* Msps mutant embryos have fewer and disorganised microtubules (Cullen *et al.*, 1999; Moon and Hazelrigg, 2004) and RNAi of Msps in *Drosophila* S2 cells results in shorter, often bundled interphase microtubules and abnormal spindles (Brittle and Okhura, 2005). *Arabidopsis mor1* mutants at the restrictive temperature cells have disorganised interphase cortical microtubules, resulting in numerous morphological defects (Whittington *et al.*, 2001). Depletion of chTOG in HeLa cells slightly decreased the length of spindle microtubules and spindle density and caused centrosome fragmentation (Cassimeris and Morabito, 2004). In addition, it was shown that chTOG is required for MT aster formation in HeLa mitotic extracts (Dionne *et al.*, 2000).

There also exists data suggesting that XMAP215 acts as a microtubule destabliser *in vitro* (Shirasu-Hiza *et al.*, 2003) however, this can be reconciled by the proposal that when tubulin dimer concentration is limiting, XMAP215 cannot promote microtubule

growth and instead it promotes depolymerisation. Thus, XMAP215 could act as a classic catalytic enzyme in that can accelerate a reaction in both directions (Figure 1.8; Howard and Hyman, 2007). Recent *in vitro* work has confirmed that XMAP215 does indeed act as a microtubule polymerase (Brouhard *et al.*, 2008) and this hypothesis is also consistent with the *in vitro* data for Stu2, although it was not directly tested (Al Bassam *et al.*, 2006). It will be interesting to see in the future if Alp14 also functions in such a way at the plus ends of microtubules, and whether it has a direct stabilisation role at the minus ends of microtubules.

4.11. An essential interphase role for the Dis1/XMAP215 homologues in fission yeast

Fission yeast occupies the unique position in that it has two homologues of the Dis1/XMAP215 family. This raises the question to what extent do they functionally overlap, and what are their unique functions? Both Alp14 and Dis1 belong to the third group of the Dis1/XMAP215 family members. Other homologues belonging to this group are *S. cerevisiae* Stu2 and *Aspergillus nidulans* AlpA. The family 3 homologues are only approximately half the length of the other proteins, therefore we wondered if Alp14 and Dis1 functionally interacted to perform the equivalent roles of the other homologues. A strain in which both *alp14* and *dis1* are deleted is synthetically lethal and the single deletions both show lethal temperature sensitive phenotypes in addition to defects at the permissive temperatures confirming an essential role. We found that moderate Dis1 over-expression rescues the *alp14*Δ phenotype at the permissive temperature and partially rescues it at the restrictive temperature. Interestingly, the converse was not true, and Alp14 over-expression did not reduce the severity of the *dis1*Δ phenotype. This suggests that Dis1 plays a more complex role than Alp14, specifically in mitosis, which could be attributed to its regulation by Cdc2, but that it still retains a function in the cytoplasm. Dis1 rescue of the *alp14*Δ phenotype points towards an overlap in function with respect to interphase microtubule stabilisation, When Dis1 levels were decreased in *alp14*Δ cells at the permissive temperature the number of interphase microtubule bundles decreased further, and many cells had no bundles. This shows that Dis1 and Alp14 together are required for maintenance of interphase microtubule arrays, with Alp14 playing the primary role. That even moderate over-expression of Dis1 is able to rescue *alp14*Δ suggests that if Dis1 is responsible, very little additional Dis1 is able to compensate for this second function of Alp14, namely maintaining microtubule nucleation in the cytoplasm. Even if Dis1 is not the factor being affected by the shift to the restrictive

temperature in *alp14*Δ cells, formation of intranuclear microtubules suggests that the default localisation of microtubule nucleation is nuclear, rather than cytoplasmic.

4.12. Perspectives

The work here raises a number of questions that merit further investigation. The presence of one of the XMAP215 homologues is essential for *S. pombe* viability. Due to a number of technical limitations, our attempts to create a conditional double deletion strain by shutting off Dis1 expression were inconclusive. To further address the question of functional redundancy between Alp14 and Dis1, it would be interesting to examine the effect of fully removing Dis1 from the cells. Unfortunately, the only method to quickly and effectively knock down protein expression in yeast cells takes advantage of temperature sensitive strains. This is a problem for knocking down Dis1 expression, as we believe Dis1 is naturally temperature sensitive. Another method for knocking down protein levels in higher eukaryotes is RNAi, however this is not very fast and does not work in yeast. A faster way to knock down Dis1 would be to destroy the protein, rather than preventing transcription and translation, however this technology in S. *pombe* is not compatible with use for Dis1 inactivation in *alp14*Δ cells as it requires head induction.

Our initial hypothesis was that shifting the cells to 36ºC inactivated Dis1, resulting in the formation of intranuclear microtubules. When *dis1*was shut down in *alp14*Δ cells intranuclear microtubules were not observed, but there was an increase in lethality. This raised the question of whether Dis1 has separable functions with respect to maintaining interphase microtubules in the cytoplasm and cell viability, the former being a temperature-dependent function and the latter temperature-independent. Therefore, in addition to investigating the effects of complete depletion of Dis1 in *alp14*Δ cells, the controlled, partial depletion of Dis1 to different extents could prove informative. As is the case for full depletion, this is technically difficult to accomplish, due to the lack of suitable inducible and repressible promoter systems available for use in *S. pombe*. Additionally, it may be hard to get the levels of expression right, as the *alp14*Δ *dis1*Δ strain is lethal and little Dis1 may still rescue.

A more straightforward way in to investigate this and to gain more information about the function of the individual TOG domains of Alp14 and Dis1 would be to generate chimeric proteins. In contrast to the XMAP215 homologues found in higher eukaryotes, which have four TOG domains, the yeast XMAP215 homologues have

only two TOG domains. It would be interesting to see if a single chimeric protein, that is able to fully perform the functions of both Alp14 and Dis1, could be created by fusing and/or exchanging Alp14 and Dis1 TOG domains; XMAP215 itself would also be an interesting candidate. Conversely, these chimeric proteins could be systematically added to XMAP215-depleted *Xenopus* egg extract to test the extent of functional homology between the family members.

In summary, our results yield an insight into the essential role of Alp14 and Dis1 in the maintenance of interphase microtubule arrays in *S. pombe*. Together with the existing data provided by XMAP215 homologues in other organisms this provides a further step towards a more complete understanding of the function of this protein family *in vivo*.

PART II

Identification and characterisation of Toi4, a putative Tip1-interacting protein *in Schizosaccharomyces pombe*

5. Results

5.1. Screens to identify Tip1-interacting proteins

Although we now have a good understanding of how Tip1p regulates microtubule dynamics, the mechanisms and proteins that modulate the activity of Tip1p are not yet understood. Tip1p could be a component of many different protein complexes, for example, the human homologue of Tip1p, CLIP170, has been shown to link endocytic vesicles to microtubules (Pierre *et al.*, 1992). Such additional roles for Tip1p, involving interactions with different cellular structures, are therefore likely. In addition to its microtubule plus-end localisation, Tip1p is also found at the cell ends, where turnover is rapid. This points towards the existence of a turnover and anchoring mechanism, involving, as yet, unidentified proteins. To identify such proteins and also additional roles of Tip1p, screens were carried out in the lab by M. Toya to identify proteins that interact with Tip1p *in vitro*.

5.1.1. Classic GST-Tip1 Pulldown

Potential **T**ip **o**ne-**i**nteracting proteins were identified from a pulldown using bacterially-expressed GST-Tip1p, chemically cross-linked to ProteinA beads using an anti-GST antibody, as bait. Proteins binding specifically to GST-Tip1 beads were isolated from an SDS gel and identified using mass spectrometry (Appendix Figure 7.2). Four **T**ip **o**ne-**i**nteracting (Toi) proteins were identified (Table 5.1).

Table 5.1 Tip1 interactors identified by a classic GST-pulldown screen

Screen name	Name / gene ID[1]	Function
Toi1	Alm1	Medial ring conserved Tpr protein.
Toi2	Spt5	Conserved transcription elongation factor.
Toi3	SPCC1450.12	Unknown.
Toi4	SPCC736.15	Predicted protein kinase inhibitor. Similar to *S. cerevisiae* Pil1 and Lsp1.

[1] Nomenclature used by *S. pombe* genome sequencing project (Wood *et al.*, 2002)

5.1.2. GST-Tip1 pulldown in combination with Isotope Coded Affinity Tagging

It is possible that Tip1p could be a component of many different protein complexes, therefore interactors may only be bound to Tip1p at low stoichiometry. In addition, turnover of Tip1p at microtubule ends is rapid and interactions with other proteins could only be transient. Such interactors may not be detected by a classic GST pulldown screen, as identification by mass spectrometry requires that protein bands be isolated from a stained acrylamide gel, and these interactors may not be visible above background protein levels. In order to more sensitively detect Tip1p interactors, an **i**sotope-**c**oded **a**ffinity **t**ag (ICAT) method was employed (Figure 7.3, Appendix; Gygi *et al.*, 1999). Briefly, two ICAT variants, which differ in their hydrogen isotope content and therefore have different molecular weights, were used. Isotopically heavy ICAT tags were attached to the cysteine residues of proteins eluted from GST-Tip1p beads, and light ICAT tags to proteins eluted from GST-only control beads. The two samples were mixed and enzymatically cleaved to generate peptide fragments, some of which were tagged. ICAT-bearing fragments were isolated using avidin affinity chromatography by virtue of a biotin tag incorporated into the ICAT molecule, and their identity determined by mass spectrometry. Due to the different mass of the tags, the relative amounts of each of the labelled proteins in the GST-Tip1p eluate, or the control, GST eluate were calculated. In this way, femtomolar differences in protein levels between the two samples could be detected and six additional candidate Tip1p-interactors were identified (Table 5.2, M. Toya in collaboration with E. Brunner and R. Aebersold, University of Zurich).

Table 5.2 Tip1 interactors identified by a GST-pulldown in combination with ICAT

Screen name	Name / gene ID[1]	Function
Toi5	Mok1/ Ags1	β-glucan synthase.
Toi6	SPAC30C2.08	Unknown. Similar to *S. cerevisiae* YPL260W.
Toi7	Nup85	Nuclear pore complex component.
Toi8	Num1	Predicted involvement in nuclear migration. Similar to *S. cerevisiae* Num1p.
Toi9	SPCC1235.09	LisH domain protein. Similar to *S. cerevisiae* Sif2p.
Toi10	Moe1	eIF3 translation initiation factor involved in microtubule disassembly.

[1] Nomenclature used by *S. pombe* genome sequencing project (Wood *et al.*, 2002)

5.1.3. Localisation of Toi proteins

As with all screens, it is necessary to select a subset of hits for further analysis. Therefore we chose the Toi proteins listed in Tables 5.1 and 5.2 for further analysis. Toi proteins were C-terminally tagged with GFP to visualise their *in vivo* localisation. Not all of the Toi proteins were viable when C-terminally tagged with GFP and additionally some Toi proteins showed no GFP signal. Figure 5.1 shows the localisation of the Toi proteins in which a GFP signal was visible.

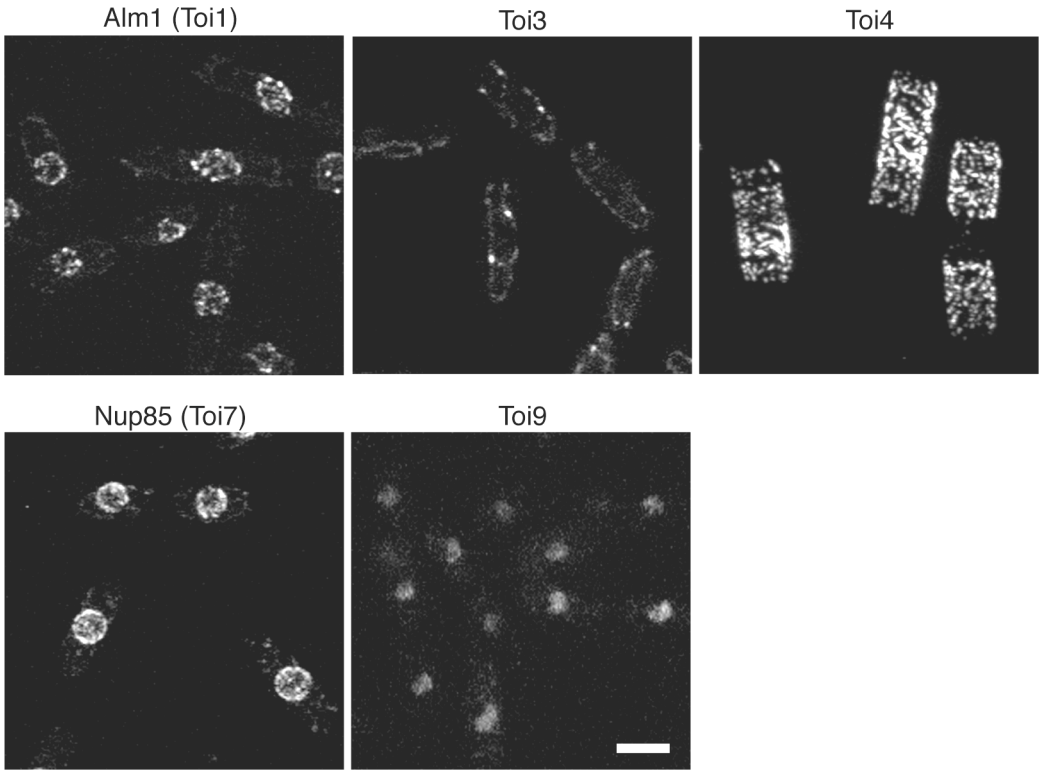

Figure 5.1 Localisation of Toi-GFP proteins

Images of cells endogenously expressing Toi-GFP. Images are projections of confocal sections covering the entire Z-axis of the cell. Bar, 4 μm.

5.2. Toi4 identified as a potential Tip1-interacting protein

Given the interesting localisation of the protein product of the predicted open reading frame designated SPCC736.15 by the *S. pombe* sequencing project (Wood *et al.*, 2002), we chose to pursue characterisation of this protein. SPCC736.15 will

subsequently be referred to as Toi4 (**T**ip **o**ne **i**nteracting protein **4**). The Toi4 open reading frame is 1056 base pairs, with no predicted introns. The translated product of this open reading frame is predicted to be 39.8 kDa. Sequence analysis of the Toi4 open reading frame revealed no recognisable functional domains, except a coiled-coil in the central region of the coding sequence. A BLAST query of the Toi4 predicted open reading frame against the *S. cerevisiae* sequence database (Saccharomyces Genome Database, http://www.yeastgenome.org) identified two homologues, Pil1 and Lsp1. We created a multiple sequence alignment of the three sequences, which revealed them to be most similar at the N-terminus. We then measured the pairwise identity of the more conserved N-terminal region and found Toi4 to have 63% sequence identity to both Pil1 and Lsp1 (Appendix Figure 7.3). Pil1 and Lsp1 are targets of the 3-phosphoinositide-dependent protein kinases Pkh1 and Pkh2 and are differentially phosphorylated depending on the concentration and type of sphingolipid long chain bases (Zhang *et al.*, 2004). One target of Pkh1p is the Pkc1p-MAP kinase pathway that regulates cell wall maintenance and integrity and repolarisation of the actin cytoskeleton during heat stress (Delley and Hall, 1999 Inagaki *et al.*, 1999; Levin and Bartlett-Heubusch, 1992; Paravicini *et al.*, 1992). Deletion of *PIL1* or *LSP1* enhances heat stress resistance; both single and double mutants were more resistant to heat stress than wild type, but the double mutants to a lesser extent, suggesting that they regulate the same or similar processes that mediate heat stress (Zhang *et al.*, 2004). In addition, Pil1 and Lsp1 were proposed to be the major constituents of endocytic organelles termed eisosomes (Walther *et al.*, 2006; see Section 5.5)

5.2.1. Seeking to confirm the interaction between Toi4 and Tip1

As Toi4 was identified in a large-scale screen using bacterially expressed GST-Tip1 present at a non-physiological concentration, we first sought to confirm whether Toi4 was a genuine Tip1 interactor. As an internal control for the validity of the screen, it was previously confirmed that the known Tip1-interactor Mal3 was enriched in the pulldown fraction (M. Toya, data not shown). The standard method of detecting protein-protein interaction in *S. pombe* is to perform co- immunoprecipitation experiments (co-IPs) in *S. pombe* cell extract where one of the proteins is attached to beads and is the bait. If the target protein interacts with the bait it will then be detected by Western blot of the proteins bound to the beads. To be able to perform such an experiment we needed both a way of detecting Toi4-GFP by Western blot and a way to couple Toi4 to the beads. We therefore created strains in which the endogenous copy of Toi4 was C-terminally tagged with either GFP or HA. We chose a C-terminal tag so that the protein was still expressed from the endogenous promoter.

5.2.1.1. Toi4 is modified in vivo

Before testing the interaction between Toi4 and Tip1 we first optimised the conditions for preparation of *S. pombe* cell extract from strains expressing Toi4-GFP, which we wanted to use in subsequent experiments. This was important as the standard protocol for yeast extract preparation uses a buffer containing 0.1% Triton X-100, a non-ionic detergent, to maintain the protein in solution. We found that 0.1% Triton X-100 did not effectively solubilise Toi4 as large amounts remained in the non-soluble pellet fraction (Figure 5.2A compare lanes 1 and 2). We therefore tested a range of different detergents in the extract buffer, including non-ionic and zwitterionic detergents and observed the extraction efficiency qualitatively by Western blot of the extract pellet and supernatant fractions.

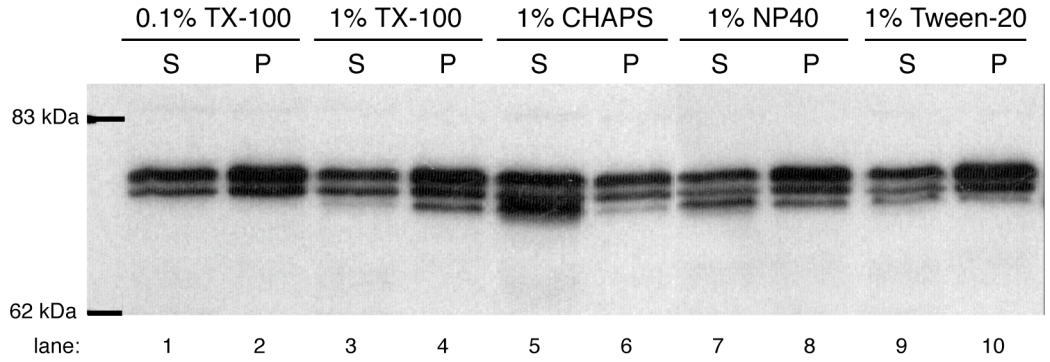

Figure 5.2 Extract of cells expressing Toi4-GFP, prepared with different detergents

Western blot of extract of cells expressing Toi4-GFP prepared in the presence of the indicated detergents. Supernatant (S) and pellet (P) fractions represent the soluble and insoluble extract fractions respectively. Toi4-GFP detected with anti-GFP antibody.

We found that for all detergents tested, three molecular weight species of Toi4-GFP of approximately 70 kDa were found in the cell extract, indicating that Toi4-GFP is modified *in vivo* (Figure 5.2). Interestingly, the relative amounts of each species in the supernatant fraction differed in the presence of different detergents: When the non-ionic detergents Triton X-100, NP-40 and Tween-20 were used there was very little of the lowest molecular weight species of Toi4. In contrast, when the zwitterionic detergent CHAPS was used, there was a large increase in the relative amount of the lowest molecular weight species. This suggests that the increased ionic strength of the CHAPS detergent resulted in more effective solubilisation of all species, but particularly the lowest molecular species compared to the non-ionic detergents.

Therefore we chose to use a buffer containing this detergent for extract preparation to test for an interaction between Toi4 and Tip1.

5.2.1.2. The interaction between Toi4 and Tip1 is not reproducible

Having optimised the conditions for Toi4 solubilisation in *S. pombe* cell extract, we then tested whether the interaction between Toi4 and Tip1 could be confirmed. To do this, smaller-scale experiments were carried out in cell extract using either endogenously expressed Tip1 or Toi4 attached to beads as the bait. Subsequent Western blot analysis of the proteins bound to the beads allowed us to see whether the reciprocal protein could be co-immunoprecipitated. Toi4 was tagged with either GFP or HA in a wild type background or in a strain containing C-terminally GST-tagged Tip1 to allow co-immunoprecipitation (co-IP) and detection of Tip using either anti-Tip1 or anti-GST antibodies or glutathione-sepharose beads for pulldown via the GST tag. We performed a number of co-IP and pulldown experiments using Toi4-GFP, Tip or Tip1-GST as bait. Toi4-GFP and Toi4-HA were coupled to ProteinG-coated Dyna- or Sepharose beads via anti-GFP or anti-HA antibodies respectively; Tip1 was coupled to ProteinA-coated Dyna- or Sepharose beads via anti-Tip1 antibody; Tip1-GST was coupled to Glutathione-Sepharose beads. We experienced a lot of problems with non-specific binding of Toi4-GFP and Toi4-HA to the beads and antibodies (e.g. Figure 5.3; lanes 1-4). A representative example of the problems experienced with non-specific binding is shown in Figure 5.3. Cell lysates were incubated with anti-HA antibody coupled to ProteinG beads. Proteins were co-immunoprecipitated and analysed by Western blot with anti-Tip1 antibody. As a control, Toi4-HA cell extract was incubated with beads alone (Figure 5.3; lane 1). As an additional control, extract from a strain expressing Crb3-HA, a protein with no known link to Tip1, was also incubated with beads coupled to anti-HA antibody (Figure 5.3; lane 4). From the Western blot we found that Tip1 in the Toi-HA cell extract bound to the beads even in the absence of anti-HA antibody (Figure 5.3; lane 1) and bound equally well to beads coupled to anti-HA antibody (Figure 5.3; compare lanes 1 and 2). Despite this non-specific binding of Tip1 to Toi4-HA, we failed to see a reproducible increase in the amount of binding of Tip1 to Toi4 compared to non-specific binding in the controls (e.g. Figure 5.3; lane 2 compared to lanes 3 and 4). This would be expected if a specific interaction between Toi4 and Tip1 occurs. On the contrary, we qualitatively observed the same amount of binding of Tip1 to the beads even in the absence of the anti-HA antibody, showing that this binding was not Toi4-dependent (Figure 5.3; lane 1). Thus, under our experimental conditions we could not detect significant binding of Toi4 to Tip1.

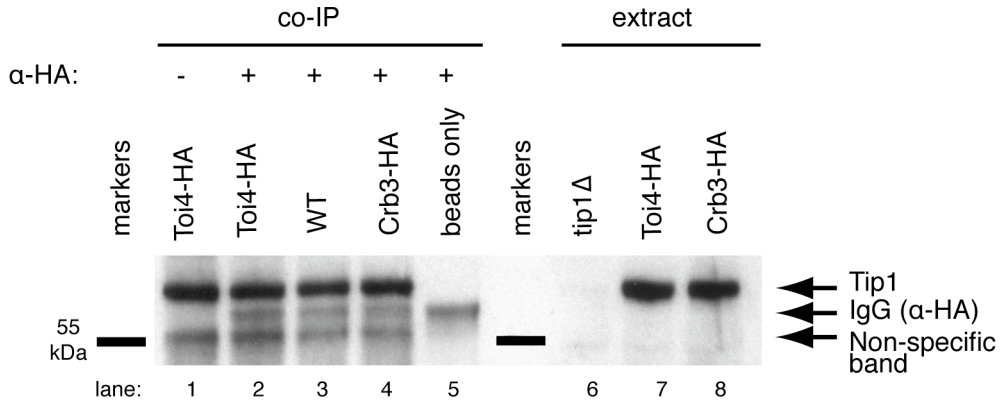

Figure 5.3 Tip1 co-immunoprecipitation

Western blot Tip1 co-immunoprecipitation experiment. Toi4-HA was attached to ProteinG beads using anti-HA and incubated with the soluble extract fraction. Lanes 1-5: Immunoprecipitated protein samples Controls without anti-HA and extract were also included (lanes 1 and 5). Lanes 6-8: Supernatant fraction of extract before incubation with the beads. Tip1 detected using anti-tip1 antibody.

5.3. Toi4-GFP localisation and dynamics

In parallel with testing for an interaction between Toi4 and Tip1, we used the Toi4-GFP strain to examine *in vivo* localisation and dynamic behaviour of Toi4 with the aim of gaining insight into the function of Toi4 in *S. pombe*.

5.3.1. Toi4-GFP localises to discrete patches at the cell periphery

The *in vivo* localisation and dynamics of Toi4-GFP was determined using live cell confocal microscopy. Projection images and analysis of the confocal slices showed that Toi4-GFP localised in bright patches at the cell cortex in the central region of interphase cells, but that the signal was reduced at the cell tips (Figure 5.1; Figure 5.4).

5.3.2. The Toi4-GFP localisation pattern is temperature dependent

During the course of our initial imaging experiments we discovered that the appearance of the Toi4-GFP patches at 25ºC and 30ºC was different: At 25ºC Toi4-GFP patches had the appearance of short rods, but when the cells were cultured at 30ºC Toi4-GFP patches were smaller and more circular (Figure 5.4A). We also tested whether the appearance of the Toi4-GFP patches was different when the cells were grown in rich media (YE5S) or minimal medium (EMM2), however we found that only the temperature determined the Toi4-GFP patch shape (Figure 5.4A).

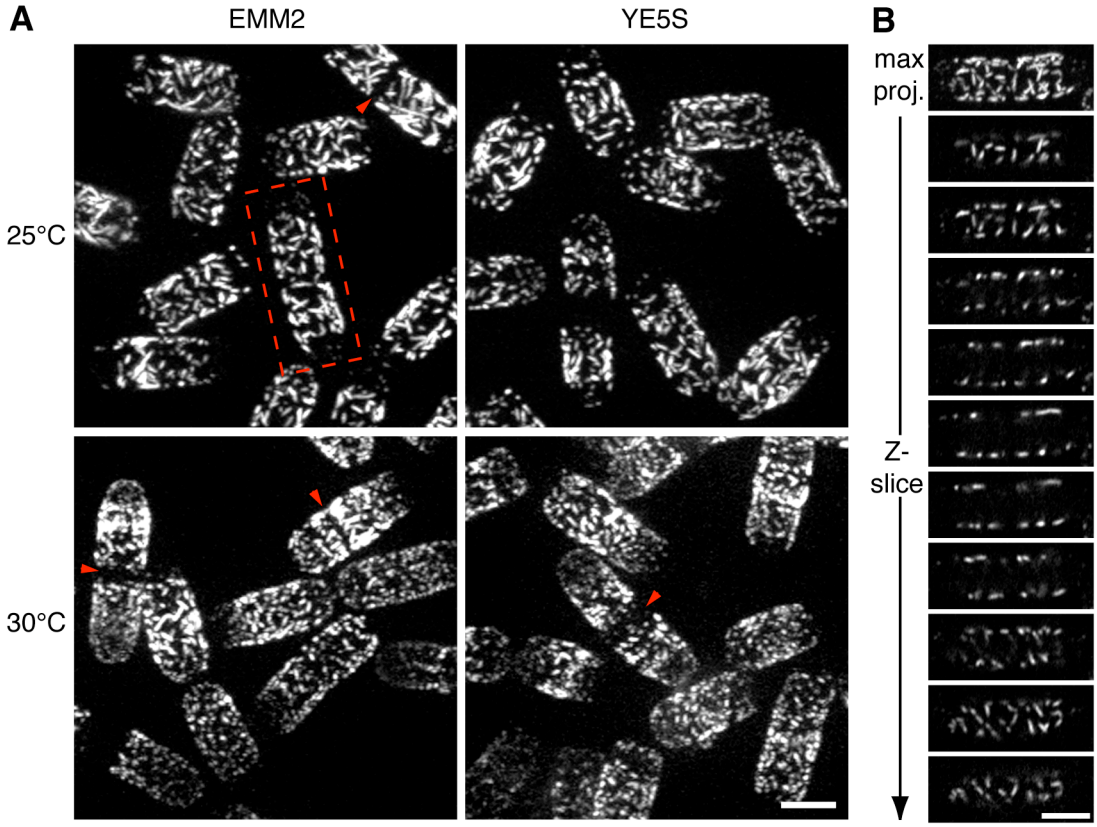

Figure 5.4 The pattern of Toi4-GFP localisation is temperature dependent

(A) Images of Toi4-GFP cells grown at different temperatures and in different media as indicated. Red arrowheads indicate cells in which Toi4-GFP-free stripes are found at the cell centre. Images are projections of confocal sections covering the entire Z-axis of the cell. (B) Single confocal slices of the cell indicated by a red dashed box in (A) showing that Toi4-GFP localisation is confined to the central cell cortex. Bars, 4 μm.

Given this dependence of temperature for Toi4-GFP particle morphology, we were careful to perform all subsequent experiments at 25ºC. We chose this temperature, as is the standard temperature for experiments with *S. pombe* and also for, practical reasons related to our microscope set-ups and cell handling.

5.3.3. Toi4-GFP localisation through the cell cycle

It appeared from the images in Figure 5.4A that the localisation of Toi4-GFP changed through the cell cycle, as cells that appeared to be dividing seemed to have a Toi4-GFP-free region in the cell centre in the region where the septum would be expected to be (arrowheads in Figure 5.4A). We therefore imaged Toi4-GFP-expressing cells over a period of 4 hours to visualise a full cell cycle. The time course of a typical cell is shown in Figure 5.5.

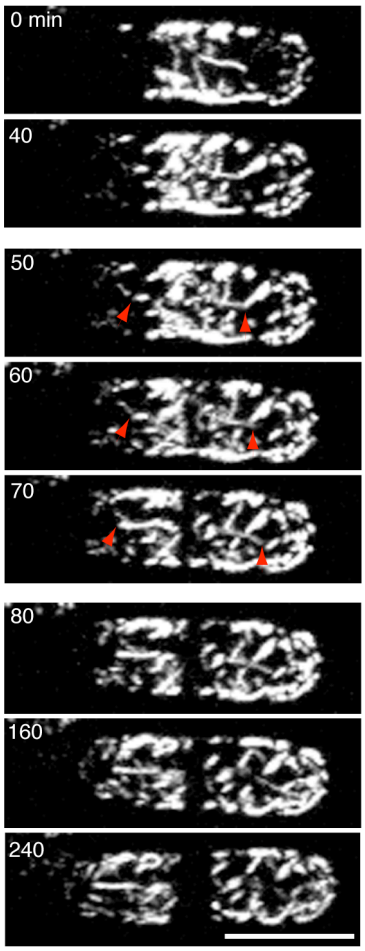

Figure 5.5 Toi4-GFP localisation throughout the cell cycle

Timcourse of Toi4-GFP localisation as the cells proceed through the cell cycle. Red arrowheads indicate stripes of Toi4-GFP moving away from the cell centre. Images are projections of confocal sections covering the entire Z-axis of the cell. Bar, 4 μm.

Initially, during interphase Toi4-GFP localised predominantly to the central cell cortex, although one of the cell ends had some Toi4-GFP staining (Figure 5.5; 0 min). The Toi4-GFP patches in the central cell cortex often had a string-like appearance, being longer than the patches more towards the cell ends. During interphase these central patches appeared to be immobile. As the cell increased in length, the Toi4-GFP signal increased at this cell end and faint Toi4-GFP patches started to appear at the other cell end (Figure 5.5; 40 min). After 50 minutes the bright Toi4-GFP string-like patches at the central region moved apart to leave a stripe across the cell centre entirely free Toi4-GFP (Figure 5.5; 50-70 min). The movement of these patches was striking: rather than all the patches moving together, a number of the patches seemed to slide along the cell cortex (indicated by red arrowheads), a movement that was much faster than that of the other Toi4-GFP patches. The width of the Toi4-GFP free-stripe slowly increased and the cell divided at this point.

In fission yeast, following cytokinesis each daughter cell has an old cell pole that existed in the previous cell cycle and a new cell pole created through separation of the two daughter cells (Mitchison and Nurse, 1985). From the images in Figure 5.5 it seemed likely that the cell ends which had fewer Toi4-GFP patches were the new cell ends. To confirm this we first stained Toi4-GFP-expressing cells with TRITC-lectin, which binds to the cell wall (Horisberger *et al.*, 1978; May and Mitchison, 1986). We washed out the lectin and continued to incubate the cells for a further 45 minutes. We then counterstained the cells with calcofluor, another dye that stains the growing cell wall and septum (Mitchison and Nurse 1985). We found that the cell end that was almost devoid of Toi4-GFP patches was not stained by the TRITC-lectin, indicating that this cell end was the new end, resulting from cell division in the 45 minutes after staining with TRITC-lectin. This cell end was also strongly stained with calcofluor, further showing that this cell wall represented the deposition of new cell wall material (Figure 5.6 top panels). We also observed cells in which there was a Toi4-GFP-free stripe in the cell centre, where we would expect the septum to form. Indeed this Toi4-GFP-free area was stained strongly with calcofluor, confirming that Toi4-GFP is excluded from the site of septum formation. The cell ends were also stained with calcofluor in these cells, indicating, as expected, that they were post NETO (Figure 5.6 bottom panels).

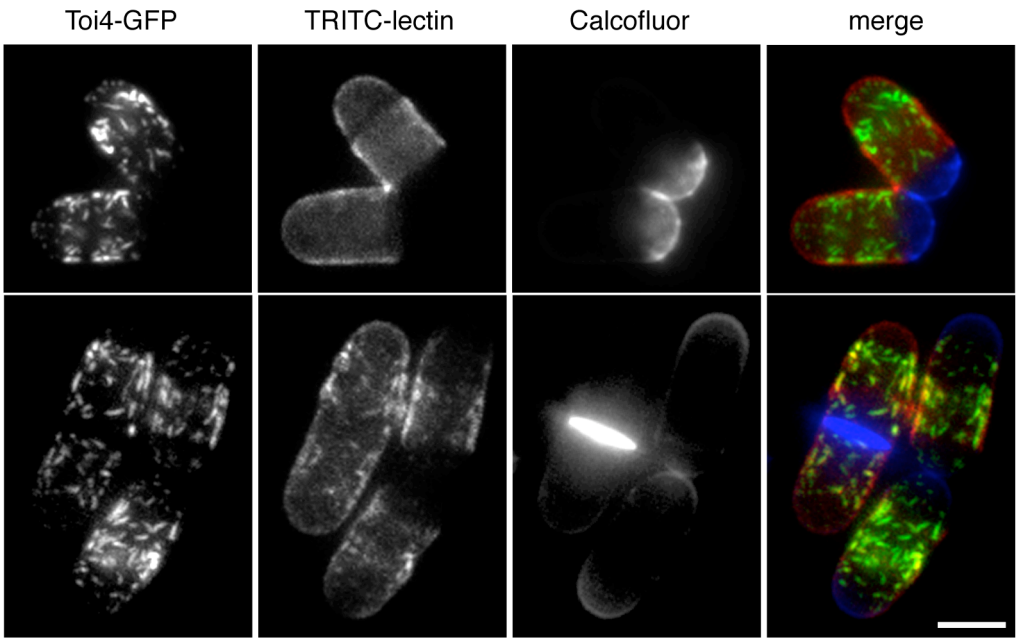

Figure 5.6 Toi4-GFP localisation at the old and new cell ends

Toi4-GFP-expressing cells were stained with TRITC-lectin and then counterstained with calcofluor 45 minutes later and imaged immediately. Images are projections of wide field sections covering the entire Z-axis of the cell. Bar, 4 μm.

5.3.4. Toi4-GFP does not co-localise with actin

The localisation of Toi4 to the central cell cortex and its absence largely from the cell poles and the site of septum formation during mitosis is the inverse localisation of actin, which is concentrated at the cell poles during interphase and the site of division during mitosis (Figure 5.7A (25ºC); Marks and Hyams 1985). We therefore wanted to test whether actin was responsible for the exclusion of Toi4 from the cell ends and cell equator. To do this we made use of the observation that actin rapidly becomes disorganised when the cells are shifted to 36ºC (Figure 5.7A, D. Foethke and I. Aprill, personal communication). This disorganisation is restored after two hours, however we were interested to see if Toi4-GFP localisation was also altered before actin became re-localised. We therefore incubated exponentially growing Toi4-GFP cells for one hour at 25ºC or 36ºC and then rapidly fixed them with paraformaldehyde and stained the actin using Rhodamine-phalloidin. As expected, we found that after one hour at 36ºC the actin was disorganised, however Toi4-GFP maintained its localisation at the central cell cortex (Figure 5.7B). This suggests that Toi4-GFP localisation is not actively restricted to the central cell cortex by actin on a short

timescale, however, given the largely immobile localisation of Toi4-GFP particles it does not exclude that actin organises Toi4-GFP over a timescale longer than one hour.

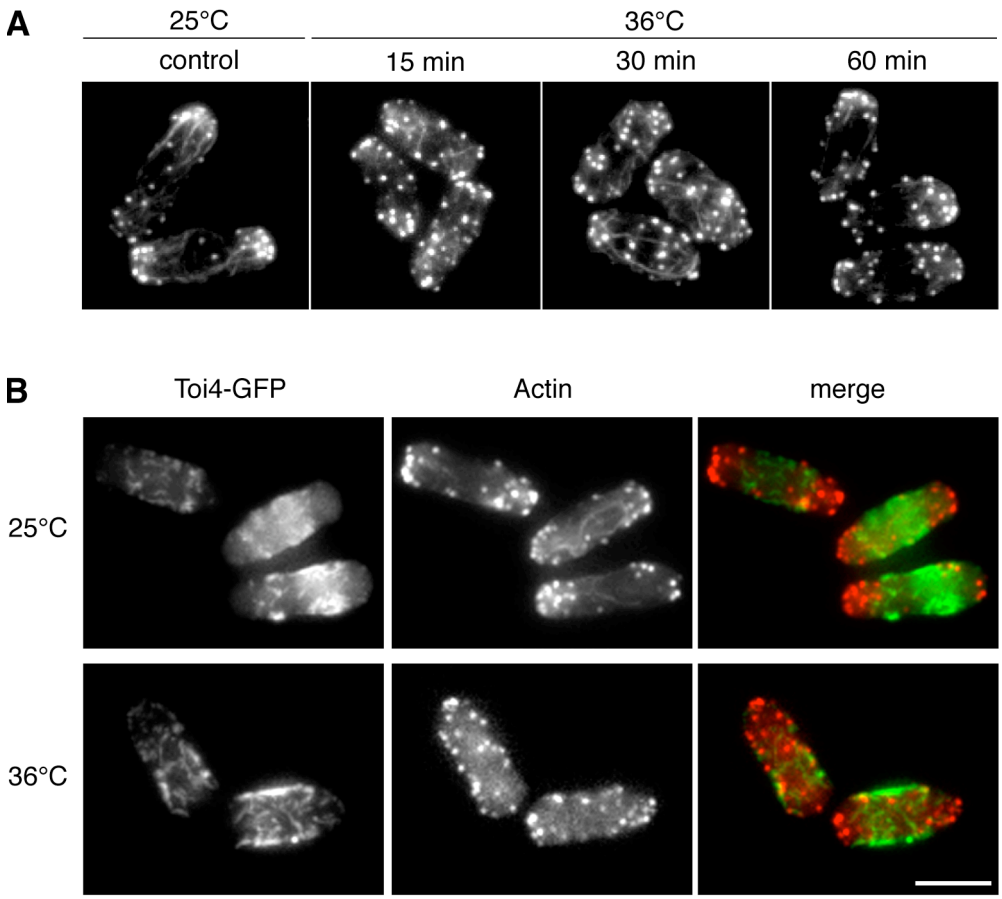

Figure 5.7 Toi4-GFP does not co-localise with actin

(A) Staining of actin in wild type cells with BODIPY-Phallacidin. Shifting to 36ºC results in temporary disorganisation of the actin cytoskeleton. (B) Actin staining of Toi4-GFP cells 1 hour after shifting to 36ºC results in no disorganisation of the Toi4-GFP patches and no co-localisation with actin. Images are projections of wide field sections covering the entire Z-axis of the cell. Bar, 4 μm. Images in (A) were kindly provided by D. Foethke and I. Aprill.

5.3.5. Toi4-localisation in cell cycle and septin mutants

As shown, Toi4-GFP localises to the central cell cortex during interphase and is excluded from the site of septum formation during cell division (Figure 5.5). We were interested to see whether this localisation was maintained in cell cycle and septin mutants.

5.3.5.1. Toi4-GFP in cell cycle mutants

The exclusion of Toi4-GFP from the cell ends appeared, at least in a short timescale, not to be dependent on actin (see Section 5.3.4). Given the gradual increase in Toi4-GFP signal at the cell ends as the cells increased in length when progressing through the cell cycle, we were interested whether Toi4-GFP was actively excluded from the cell ends during interphase. An alternative hypothesis is that Toi4-GFP is passively restricted to the central regions of the cell as a result of the slow dynamics of particle movement; exclusion of Toi4-GFP from the site of septum formation during the previous cell division results in no Toi4-GFP signal at the new ends of the daughter cells. To test this, we used Toi4-GFP strains also containing *cdc25-22* and *cdc10-129* mutations. In these cell cycle mutants, the cells become blocked at the G2/M and G1/S transitions respectively, after shifting to the restrictive temperature of 36ºC and become elongated as a consequence of continued growth. Cells can be released from this block by shifting back to the permissive temperature of 25ºC. Following release, the cells rapidly enter mitosis (Russell and Nurse, 1986; Nurse *et al.*, 1976). Interestingly, after five hours at the restrictive temperature, Toi4-GFP in both cell cycle mutants was still restricted to the central regions of the cell cortex, although this region was broader than in wild type cells, reflecting an increase in cell length, particularly in the *cdc25-22* mutant (Figure 5.8A,B; 1 minute). Upon release of this block Toi4-GFP accumulates at both cell poles and after 40 minutes Toi4-GFP particles are distributed entirely along the cell cortex with only a slight increase in Toi4-GFP signal in the central region of the cell cortex in comparison to the cell poles (Figure 5.8A,B). This suggests that there is an active relocation of Toi4-GFP to the cell poles at the onset of mitosis, as Toi4 particles appear at the cell ends within 10 minutes of shifting back to the restrictive temperature. Interestingly, one cell pole appears to accumulate Toi4-GFP before the other, suggesting that there is still a distinction between the old and new cell poles (Figure 5.8A,B). Further evidence that Toi4-GFP re-location is likely an active rather than a passive diffusion of Toi4-GFP towards the cell poles comes from a comparison of the two mutants: Despite *cdc25-22* cells being double the length of the *cdc10-129* cells, the cell poles of both mutants accumulate Toi4-GFP within 20 minutes of shifting back to the permissive temperature. Additionally, Toi4 appears in all regions of the cell previously lacking Toi4-GFP at the same time, rather than a gradual lengthening of the Toi4-GFP signal from the central regions (Figure 5.8A,B).

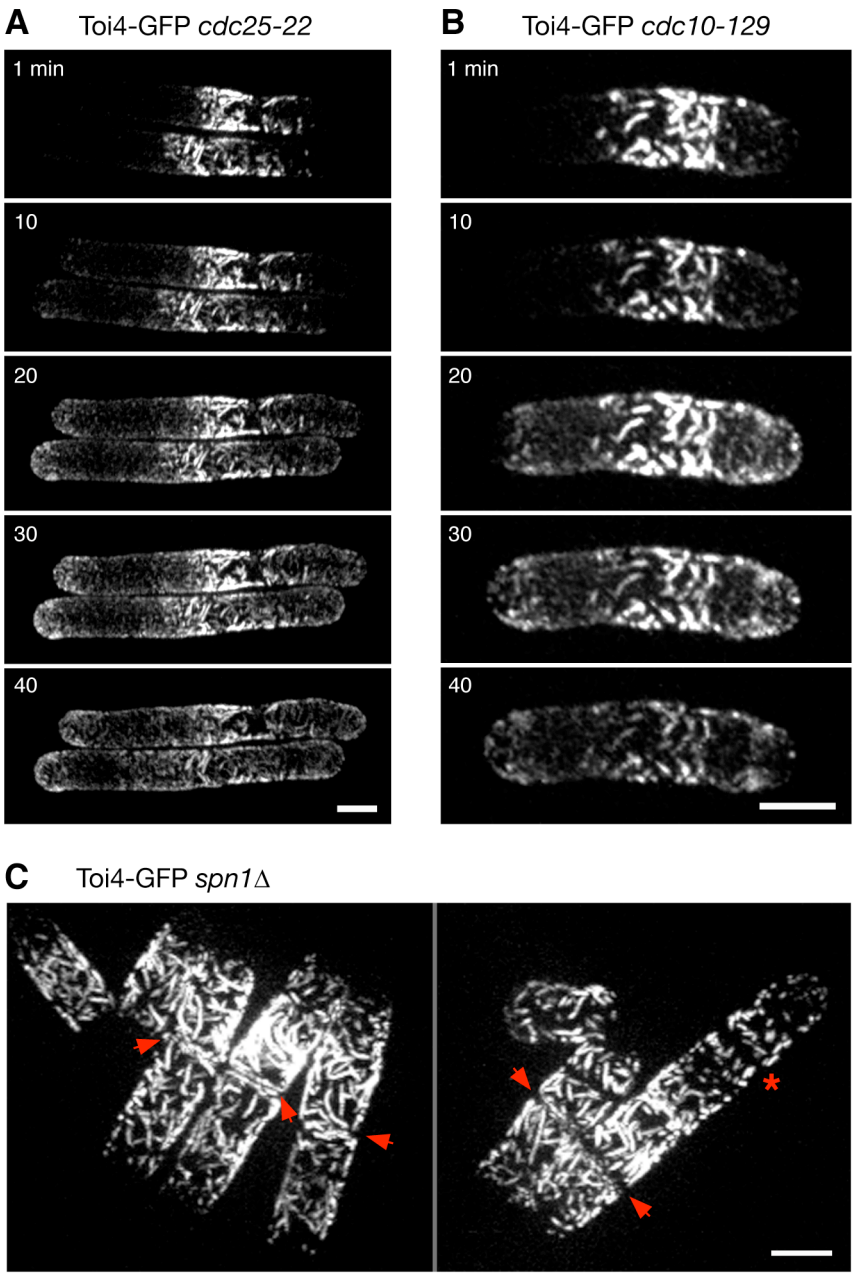

Figure 5.8 Toi4-GFP localisation in cell cycle and septin mutants

(A) and (B) Toi4-GFP localisation in *cdc25-22* (A) and *cdc10-129* (B) mutants. Cells were blocked at the G2/M or G1/S transitions respectively by incubating at 36ºC for 5 hours. Imaging began after shifting back to 25ºC, resulting in release from the cell cycle block as indicated. (C) Toi4-GFP localisation in *spn1Δ* cells in which septum formation is compromised. Arrows indicate failure of the cells to separate following division. Asterisk indicates a site of Toi4-GFP exclusion from the central region of the cell. Images are projections of confocal sections covering the entire Z-axis of the cell. Bars, 4 μm.

5.3.5.2. Toi4-GFP localisation in a septin mutant

To examine the link between septum formation and Toi4 movement away from this site we used a Toi4-GFP strain in which the gene encoding the septin protein, *spn1* was deleted. Spn1 encodes one of four non-essential GTP-binding proteins required for efficient cytokinesis. Mutants lacking any one of these septins show delays in the completion of cell division, resulting in long 'chained' cells with multiple septa (An *et al.*, 2004; Longtine *et al.*, 1996). We examined the localisation of Toi4-GFP in *spn1*Δ cells and found that, as previously published, *spn1*Δ had a chained cell phenotype (Figure 5.8C). Toi4-GFP was still excluded from the site at which the cytokinetic ring formed appeared to proceed as for wild type cells (Figure 5.8C, asterisk). Subsequently, Toi4-GFP strongly labelled the sites where the cells had divided, but failed to physically separate (Figure 5.8C, arrows). This suggests that failure of the cells to separate as a result of aberrant septin ring formation in the *spn1*Δ mutant does not affect Toi4-GFP movement away from the site of cell division, however, in contrast to wild type cells Toi4-GFP is quickly localised to the subsequent "new" cell ends which fail to separate.

5.3.6. Toi4-GFP is associated with the cell membrane

It was clear from the microscopy data that Toi4-GFP localises to the cell cortex, however we were interested to know how Toi4-GFP is attached to the cell cortex and how its localisation maintained in this region. Bioinformatic analysis of the Toi4 sequence revealed no predicted membrane-binding domains, modification sites or trans-membrane sequences, suggesting that Toi4-GFP is either bound to the cell cortex through an indirect interaction with the plasma membrane via interaction with other integral membrane proteins, or directly through a lipid-binding modification. To test whether Toi4 was bound to the plasma membrane, we collected cell extract of cells expressing Toi4-GFP in buffer containing no detergent. As expected, Toi4-GFP was present in both the pellet (Figure 5.9 lane 1) and supernatant fractions (lane 2) after low-speed centrifugation (3,000 xg), which results in sedimentation of non-lysed cells, nuclei and mitochondria. We then re-centrifuged the low-speed supernatant at high speed (100,000 xg), to pellet the membranes. Western blot analysis revealed that although Toi4-GFP was found in the soluble supernatant fraction (Figure 5.9; lane 4), a lot of Toi4-GFP was still present in the membrane-enriched pellet fraction (Figure 5.9; lane 3), indicating an interaction of Toi4-GFP with the cell membrane.

Although no membrane-spanning regions or lipid-binding modification sites were predicted in the Toi4 sequence, not all consensus sites are known. We therefore tested whether the binding of Toi4-GFP to the membrane was through a protein-lipid or protein-protein interaction. To do this, the high-speed pellet fraction was resuspended and incubated in buffer containing chemicals known to disrupt either protein-protein or particular protein-lipid interactions. The sample was then spun again at high speed and the pellet and supernatant samples separated and analysed by Western blot. We found the most Toi4-GFP extraction with 1M urea, 0.1M sodium carbonate and 10 mM DTT respectively. Addition of 0.5M sodium chloride resulted in no release of Toi4-GFP above the levels of the buffer only control (Figure 5.9 lanes 5-14). These assays are normally used to check if a protein is a peripheral membrane protein. Despite low levels of extraction of Toi4-GFP with sodium chloride, based on the results with urea, sodium carbonate and DTT we conclude that Toi4 is a peripheral membrane protein and not an integral membrane protein, in agreement with the bioinformatics analysis.

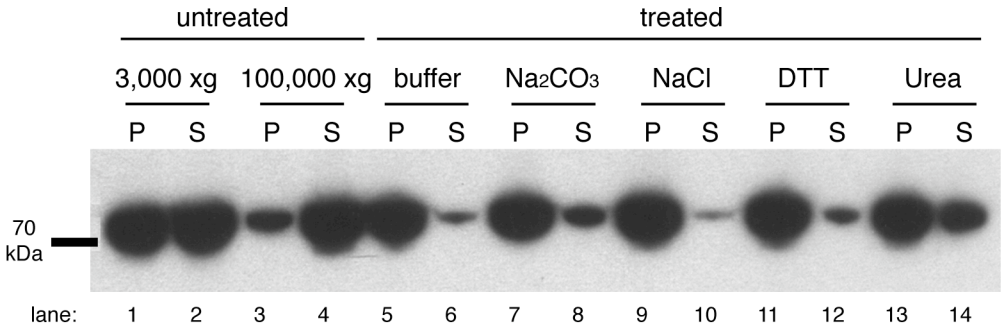

Figure 5.9 Toi4-GFP is associated with the cell membrane

Lanes 1-2: Toi4-GFP is found in both the soluble (S) and pellet (P) fractions of Toi4-GFP cell extract centrifuged at 3,000 xg. Lanes 3-4: The supernatant fraction of the low speed extract (lane 2) was spun at 100,000 xg and the supernatant (S) and membrane (P) fractions isolated. Lanes 5-14: The 100,000 xg membrane fraction was resuspended in buffer containing different chemicals known to disrupt protein-protein and protein-lipid interactions. Samples were then re-centrifuged and the supernatant (S) and membrane (P) fractions collected. Fractions were analysed by SDS-PAGE and Western blotting with an anti-GFP antibody to detect Toi4-GFP.

5.4. *toi4*Δ

The localisation of Toi4-GFP predominantly to the central regions of the cell cortex was particularly interesting in light of the fact that Toi4 was initially identified as a Tip1-interacting protein. Tip1 is known to prevent microtubule bundles from undergoing catastrophe when they contact the cell cortex in the central regions of the cell, such that the bundles slide along the cortex until they reach the cell ends, where they then undergo catastrophe (Brunner and Nurse, 2000). The mechanism by which Tip1 mediates this localised inhibition of catastrophe is unknown, although there are several hypotheses. One of which is that there is a factor(s) localised specifically to the central cell cortex and that interaction of Tip1 with this factor prevents the microtubules from depolymerising. The localisation of Toi4GFP would be consistent with such a role for Toi4. To test for such a role, we generated a *toi4*Δ strain by homologous replacement of the *toi4* open reading frame with an antibiotic resistance gene. We then examined the behaviour of the microtubules and Tip1 during interphase in the absence of *toi4.*

5.4.1. *toi4Δ* cells have normal interphase microtubule arrays

The *toi4*Δ strain was crossed with a wild type strain expressing GFP-tubulin to allow live imaging of the microtubules. We found that the microtubule arrays in projection images of *toi4*Δ cells were indistinguishable from the microtubules in wild type cells (Figure 5.10A). From the single projection images we were unable to see whether there was any change in the behaviour of the microtubules when they contacted the cell wall in the centre of the cell, where Toi4-GFP is enriched in wild type cells (Figure 5.1; Figure 5.4). We therefore made movies of the microtubule dynamics in *toi4*Δ cells. We observed that when they contacted the cell cortex in the central regions of the cell they continued to grow, sliding along the cortex until they reached the cell poles where they then underwent catastrophe. A typical example of such microtubule behaviour in a *toi4*Δ cell is shown in Figure 5.10B. This is in contrast to the behaviour of microtubules in *tip1*Δ cells, which undergo catastrophe when they contact the cell cortex in the central region of the cell, resulting in much fewer microtubules reaching the cell ends (Brunner *et al.*, 2000). From this data we conclude that deletion of *toi4* alone does not affect microtubule organisation and behaviour in interphase cells. If Toi4 does perform a catastrophe-suppressing function then there must necessarily be functional redundancy in the system.

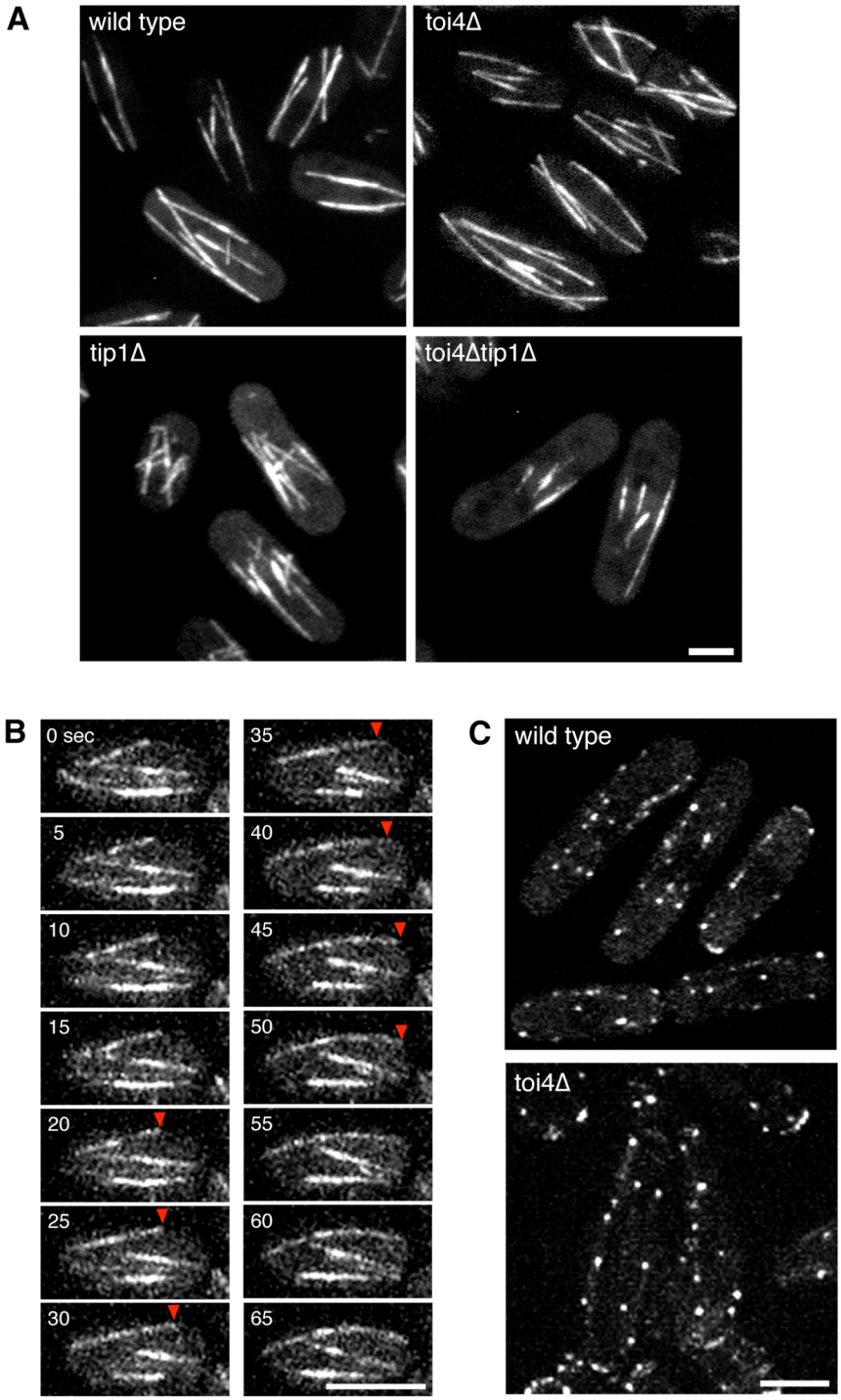

Figure 5.10 Deletion of *toi4* does not affect microtubule organisation or Tip1 localisation

(A) Microtubule organisation in *toi4Δ*, *toi4Δtip1Δ* and control GFP-tubulin-expressing cells. (B) In contrast to *tip1Δ* cells, microtubule bundles contacting the cell cortex in *toi4Δ* cells continue to grow along the cell cortex until they reach the cell ends. Arrowheads indicate the end of one growing bundle. (C) Tip1-GFP localises to the microtubule bundles normally toi4Δ cells. Images are projections of confocal sections covering the entire Z-axis of the cell. Bars, 4 μm.

5.4.2. Tip1-GFP behaviour is not dependent on Toi4

As the microtubules appeared normal in *toi4*Δ cells we wanted to check whether deletion of toi4 results in a subtler phenotype with respect to Tip1 function. We therefore created a *toi4*Δ strain in which Tip1 was C-terminally tagged with GFP. Live imaging of this strain revealed that Tip1-GFP localised normally as particles, which moved outwards from the cell centre towards the cell poles. This localisation and behaviour appeared indistinguishable from wild type cells (Figure 5.10C; Brunner and Nurse, 2000). We therefore conclude that Toi4 is not essential for Tip1 localisation and dynamics.

5.5. The *S. cerevisiae* Toi4 homologues are the major constituents of endocytic organelles termed eisosomes

During the course of the experiments described above, a paper was published that identified the *S. cerevisiae* homologues of Toi4 as components of endocytic organelles the authors termed eisosomes (Walther *et al.*, 2006). Eisosomes in *S. cerevisiae* have a very similar localisation pattern to Toi4-GFP, forming patches at the cell cortex (Figure 5.11A). The closest *S. cerevisiae* homologue of Toi4, Pil1 is required for the proper localisation of the other *S. cerevisiae* Toi4 homologue, Lsp1, to eisosomes and the transmembrane protein Sur7, which when over-expressed suppresses the growth defects of a null mutation of the endocytic effector *RVS161* (Young *et al.*, 2002; Sivadon *et al.*, 1997). Although we were unable to confirm a physical or functional link between Toi4 and Tip1 or Toi4 and microtubules, we decided in light of this publication to see whether there was a link between Toi4 and endocytosis in fission yeast.

5.5.1. Toi4-GFP does not co-localise with sites of endocytosis

In *S. cerevisiae* a sub-population of eisosomes co-localises with patches of the lipophilic dye FM4-64, a marker for endocytosis (Figure 5.11B). Given that Toi4 is homologous to Pil1 and Lsp1 and that they have a similar localisation pattern (Figure 5.9A) we wanted to test whether Toi4 also co-localised with sites of endocytosis. We therefore adapted the FM4-64 experiments performed by Walther *et al.* (2006) for *S.*

pombe and used live confocal imaging to visualise the uptake of FM4-64 in cells expressing Toi4-GFP. We did not find co-localisation between the Toi4-GFP patches and FM4-64 endocytic foci (Figure 5.11C). This implies that Toi4 is not involved in endocytosis of lipid cargo. This is in agreement with the fact that the location of endocytic evens in *S. pombe* are concentrated at the cell poles and the site of cytokinesis (Figure 5.11B; Gachet and Hyams 2005). Thus, it seems that endocytosis occurs predominantly in the regions of the cell from which Toi4-GFP is absent.

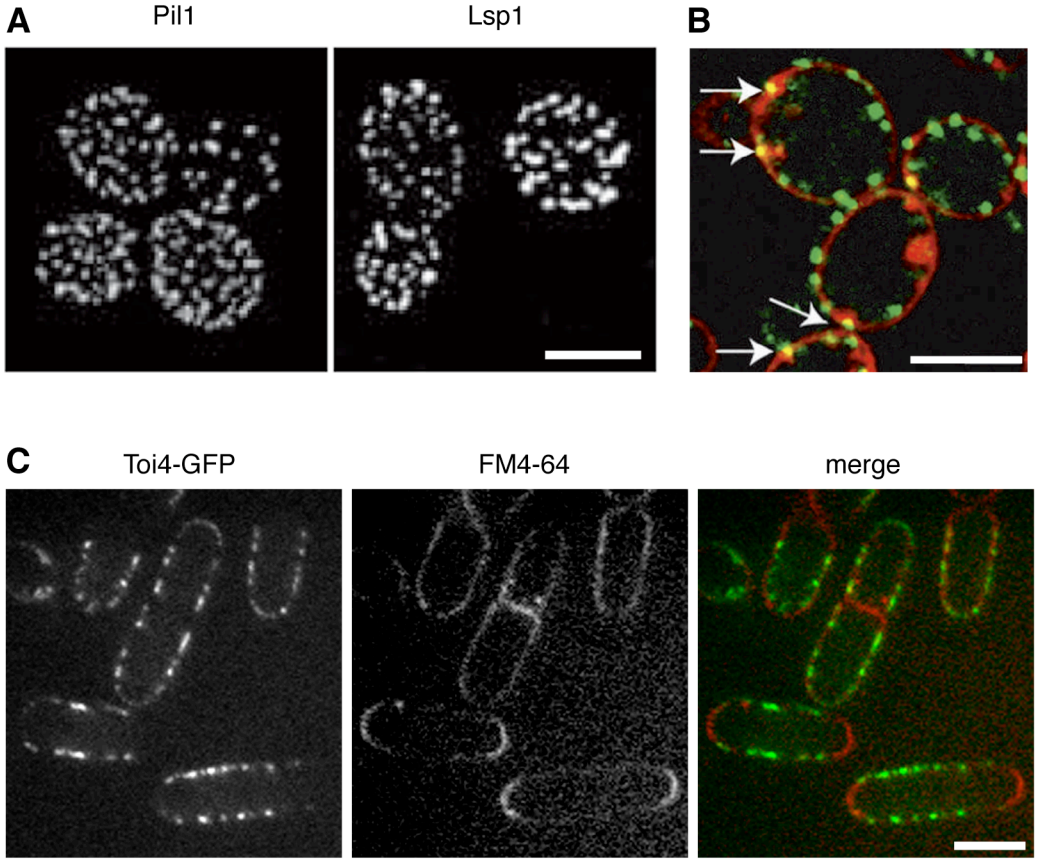

Figure 5.11 Toi4-GFP does appear to mark the sites of endocytosis

(A) Localisation of the *S. cerevisiae* Toi4 homologues, the eisosome components Pil1-GFP and Lsp1-GFP. (B) Pil1-GFP co-localises with a sub-population of endocytic events, monitored by FM4-64 uptake (red), indicated by arrows. (C) FM4-64 endocytic uptake in Toi4-GFP cells. There is no apparent co-localisation between sites of endocytosis and Toi4-GFP. The Toi4-GFP image was acquired before addition of FM4-64 to avoid detection of FM4-64 in the green channel. (A) and (B) taken from Walther *et al.*, 2006 and Swaminathan, 2006. Images in (C) are confocal sections through a central plane of the cell. Bars, 4 μm.

5.5.2. Toi4 is not essential for endocytosis

In *S. cerevisiae*, deletion of Pil1 disrupts the localisation of the other eisosome components Lsp1 and Sur7, resulting in large aberrant membrane invaginations. In addition, the sites of endocytosis are relocated to these structures (Walther *et al.*, 2006). In light of this, and to further test for a link between Toi4 and endocytosis, we wanted to test whether deletion of toi4 affected endocytosis in *S. pombe*. We therefore monitored endocytosis of FM4-64 in a *toi4*Δ strain. Surprisingly, unlike the situation in *S. cerevisiae* for the Toi4 homologue, Pil1, we found that endocytic uptake of FM4-64 was unaffected in the *toi4*Δ strain (Figure 5.12C). This shows that in addition to showing no co-localisation with sites of FM4-64 uptake, Toi4 is not essential for endocytosis of FM4-64.

5.5.3. Depolymerisation of microtubules does not affect endocytosis

Toi4 was identified as a Tip1-interacting protein and although we could not confirm this interaction, we cannot rule out that this occurs only with a small fraction of either protein *in vivo*. Given the link in *S. cerevisiae* between Pil1/Lsp and endocytosis (Walther *et al.*, 2006) and potentially between Tip1 and Toi4, we finally tested whether there was any involvement of microtubules in endocytosis. The known roles of Tip1 to date are related to microtubule regulation (Busch and Brunner, 2004; Niccoli *et al.*, 2004; Brunner and Nurse, 2000) so it would be expected that if Tip1 were involved in endocytosis then its role would also involve microtubules. To test this, we monitored FM4-64 uptake in the presence and absence of the microtubule depolymerising drug methyl-2-benzimidazole carbamate (MBC). Before carrying out the endocytosis assay we first checked that treatment of our MBC stock efficiently depolymerised the microtubules. To do this we used a strain expressing GFP-tubulin to label the microtubules and imaged the cells upon addition of MBC. We found that within 1.5 minutes of MBC addition the microtubules had depolymerised and short microtubule stubs remained at the cell centre, consistent with published results (Figure 5.12A; Tran *et al.*, 2001). Having optimised the conditions for microtubules depolymerisation we monitored endocytic uptake of the lipophilic dye FM4-64 in cells with depolymerised microtubules.

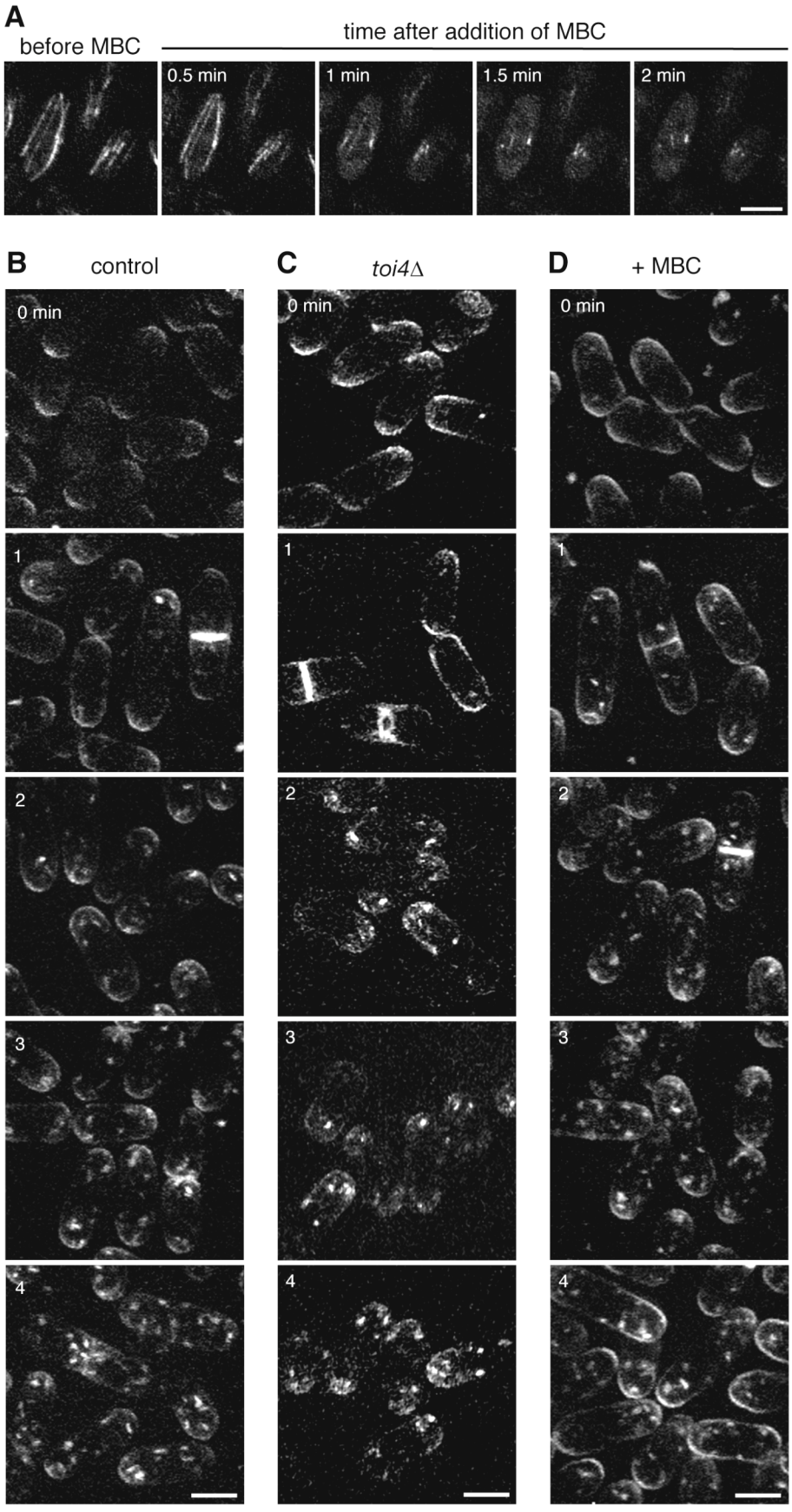
A
before MBC
time after addition of MBC
0.5 min
1 min
1.5 min
2 min
B
control
C
toi4Δ
D
+ MBC
0 min
1
2
3
4

Figure 5.12 Toi4 and microtubules are not essential for endocytosis

(A) Timecourse of microtubule depolymerisation after addition of MBC. The microtubules are completely depolymerised after 2 minutes. Cells are expressing GFP-tubulin. (B), (C) and (D) Endocytosis monitored by the lipophilic dye FM4-64 (B) Wild type cells. (D) Endocytosis in *toi4Δ* cells. (C) FM4-64 was added 2 minutes after addition of MBC. Images are projections of confocal sections covering the entire Z-axis of the cell. Bars, 4 μm.

The FM4-64 was added two minutes after the addition of MBC, when microtubules were depolymerised (Figure 5.12A) and then endocytosis observed by washout of the FM4-64 with medium containing the same concentration of MBC to ensure the microtubules remained depolymerised. We observed that endocytosis was unaffected by addition of MBC when compared to the control where no MBC was added (Figure 5.10B,D). This shows that endocytic uptake of FM4-64 is not dependent on microtubules.

6. Discussion

6.1. Identification of Toi4 as a potential Tip1-interacting protein

The protein product of the uncharacterised open reading frame designated *SPCC736.15* by the *S. pombe* genome sequencing project (Wood *et al.*, 2002) was isolated from a GST-Tip1 pulldown screen to identify new Tip1 interactors (Figure 7.1; Figure 7.2, Appendix). Accordingly, we refer to *SPCC736.15* as Toi4 (**T**ip **o**ne **i**nteracting protein 4). Toi4 was selected for further investigation due to its interesting localisation in patches at the cell cortex in the central regions of the cell, but not at the cell poles (Figure 5.1). This localisation is consistent with that of a hypothetical factor that could interact with Tip1 conferring the ability of Tip1 to suppress microtubule catastrophe specifically at the central cell cortex.

6.2. Is Toi4 a genuine Tip1-interactor?

Toi4 was isolated from a large-scale screen using recombinant GST-Tip1, therefore we first attempted to confirm the interaction between Toi4 and Tip1 *in vivo* using small scale *S. pombe* extract preparations. We were unable to reproducibly detect an interaction between Toi4 and Tip1, possibly as a result of several technical difficulties experienced during the course of these experiments: We found that Tip1 bound non-specifically to the beads used for the co-IPs and pulldowns, resulting in strong background signals in the controls (Figure 5.2). A number of beads and Toi4 tags were tested, but this remained a problem. In addition, and consistent with the *S. cerevisiae* homologues, we found Toi4 to be an extremely abundant protein (Walther *et al.*, 2006; data not shown) thus increasing the likelihood of its detection as a background band. Despite the presence of non-specific binding of Tip1, we still failed to see a reproducible increase in the amount of Tip1 binding to Toi4 relative to the amount binding in the controls. Thus, under our conditions of growth and sample preparation we could not detect and interaction between Toi4 and Tip1. One difference between the large-scale and small-scale screen was that Toi4 was identified

as an interactor of recombinant GST-Tip1. In our small-scale co-IP and pulldown experiments we always used endogenously expressed Tip1 or Tip1-GST. As such, the amount of Tip1 present in the extract was much lower than that used in the large-scale screen. This means that if only a fraction of Toi4 and Tip1 interact might not be detected under our experimental conditions. Additionally, Tip1 could be subject to *in vivo* modifications that were not present on the recombinant GST-Tip1, or the C-terminal tag used in the small-scale experiments could interfere with binding of Toi4, in contrast to the N-terminal tag in the recombinant protein. The latter is probably not the reason, as we also attempted to reproduce the Tip1-Toi4 interaction by co-IP of endogenous non-tagged Tip1, but we cannot exclude that the anti-Tip1 antibodies precluded a Toi4-binding site. A more likely reason that we detected no interaction between Toi4 and Tip1 is that they may interact only during specific cell cycle stages. For example, in meiotic prophase when the microtubules undergo a process known as horse-tail movement, during which pairing of homologous chromosomes and genetic recombination occur (Ding *et al.* 2004; Niwa *et al.* 2000; Yamamoto *et al.* 1999). During this time the microtubules are in contact with the cell cortex through interaction with the cytoplasmic dynein-dynactin complex and Num1 (Yamashita and Yamamoto, 2006; Miki *et al.*, 2002; Yamamoto *et al.*, 1999). Tip1p together with Ssm4p, a p150-Glued protein, regulates dynein heavy chain localisation to the cell cortex (Niccoli *et al.*, 2004), therefore given the localisation of Toi4 it is not implausible that such a meiosis-specific Toi4-Tip1 interaction could occur. In addition, the *S. pombe* Num1 homologue was identified in the ICAT screen as a potential Tip1 interactor (Toi8, Table 5.2). If Toi4 does interact with Tip1 during meiosis, we would not have detected this in our co-IP and pulldown experiments as we always tested for an interaction in extract prepared from exponentially-growing cells, in which very few meiotic cells are found. If the extract for the screen was prepared from cells that were not exponentially growing, the proportion of meiotic cells may have been greater and thus a meiotic-specific interaction could have been detected. This is likely the case, certainly for the ICAT screen, as Num1 is an early meiosis gene and is not expressed in interphase cells, so it would not have been present in the extract if the cells were all growing exponentially (Ohtaka *et al.*, 2007). It would therefore be interesting to test whether an interaction between Toi4 and Tip1 occurs in extract prepared from cells cultured under different conditions, or synchronised such that they are enriched for cells in a specific stage of the cell cycle.

6.3. Toi4-GFP particle dynamics through the cell cycle

In parallel with the co-IP and pulldown experiments to test for an interaction between Toi4 and Tip1, we examined the *in vivo* localisation and dynamic behaviour of Toi4 in more detail. We found that Toi4-GFP localises as bright particles at the cell cortex in the central regions of the cell (Figure 5.1 and Figure 5.4). Interestingly, the shape of these particles depended upon the culture temperature; at 30ºC Toi4-GFP particles are roughly circular similar to the *S. cerevisiae* homologue, Pil1 (Walther *et al.*, 2006), but at 25ºC they have an extended rod-like shape (Figure 5.4A). During interphase the Toi4-GFP particles are largely immobile but at the onset of mitosis, as confirmed by experiments with cell cycle mutants, there is a gradual increase in signal at the cell poles (Figure 5.5; Figure 5.8A,B). The old cell pole seems to acquire Toi4-GFP faster than the new pole, apparently due to formation of new Toi4-GFP particles rather than movement of pre-existing particles (Figure 5.6 and Figure 5.8A,B). There is no apparent cytoplasmic pool of Toi4, so the appearance of new particles probably represents *de novo* synthesis of Toi4-GFP, however we cannot exclude that small amounts of Toi4-GFP are relocated from existing particles to the cell poles. This could be tested by monitoring the total level of Toi4-GFP in synchronised cells at different stages of the cell cycle. Shortly before the cell divides, there is exclusion of Toi4-GFP from a strip across the central region of the cell where the septin and actomyosin rings form (Figure 5.5). The cell subsequently divides, resulting in two daughter cells in which Toi4-GFP is localised predominantly at the central cell cortex. A number of the Toi4-GFP particles move away from this central region, apparently sliding along the cell cortex (Figure 5.5). From examination of Toi4 localisation in a septin mutant we show that this movement is not dependent of septin ring formation (Figure 5.8). There are a number of hypotheses that could explain this movement of the Toi4-GFP particles. The first is that during septum formation there is necessarily an increase in the amount of membrane required. The deposition or synthesis of new membrane components at this site could “push” away the pre-existing cell membrane and cortex components, resulting in an apparent sliding of Toi4-GFP along the cell cortex. Closer examination of the Toi4-GFP particle movement argues against this hypothesis, as only a sub-set of the Toi4-GFP particles show a striking movement and several neighbouring particles only move slightly. This is not consistent with a “pushing” of the entire old cortex away the centre of the cell. Alternatively, there could be an active movement of some of the toi4-GFP particles in this region. This is more consistent with the observed movements, but it is unclear whether this is an intrinsic ability of Toi4 to move along the cortex, or whether this is conferred by an associated factor. Further work is required to understand this.

6.3.1. What confers the cell cortex localisation of Toi4?

There are no predicted transmembrane regions in the amino acid sequence of Toi4. Understanding how Toi4 localises at the cortex might give further insight into its function. When *S. pombe* cell extract was prepared using different detergents we found three distinct molecular weight species of Toi4, indicating that the protein was modified *in vivo* (Figure 5.2). The two highest molecular weight species were extracted efficiently by both the non-ionic and zwitterionic detergents, however, we found that the lowest molecular weight species was solubilised most effectively by the zwitterionic detergent, CHAPS indicating that it may be associated with the membrane via a stronger, possibly protein-lipid interaction. These different molecular weight species of Toi4 may correspond to differentially phosphorylated species. The *S. cerevisiae* homologues of Toi4 are targets of the long-chain base signalling pathway mediated by the Pkh kinases (Zhang *et al.*, 2004) and their phosphorylation regulates the formation and turnover of eisosomes (Luo *et al.*, 2008; Walther *et al.*, 2007). Pkh1 and Pkh2 phosphorylate Pil1 and Lsp1 to produce species B, and heat stress, which activates Pkh1 and Pkh2, generates a more highly phosphorylated species, C. It is therefore possible that the three Toi4 species correspond to the three differentially phosphorylated Pil1/Lsp1 species. *S. pombe* has two Pkh1/2 homologues, Ppk21 and Ksg1, so it would therefore be interesting to investigate whether the same mode of Toi4 regulation exists in *S. pombe* as in *S. cerevisiae*. If all three Toi4 species correspond to different degrees of phosphorylation this implies that differential phosphorylation of Toi4 might regulate its association with the cell membrane. This hypothesis is consistent with the observation in *S. cerevisiae*, that eisosomes did not form in a phosphorylation-null variant of Pil1, in which the phosphorylated serine and threonine residues were changed to alanine (Luo *et al.*, 2008). In the case of Toi4, phosphorylation may not be the only modification contributing to the different molecular weight species. The hyper-phosphorylated species of Pil1/Lsp1 is only detectable following heat stress. As our extracts were not prepared under conditions of heat stress it is therefore possible that only two of the Toi4 species that we observed result from differential phosphorylation. If this is the case, then Toi4 is probably subject to other post-translational modifications *in vivo,* resulting in the additional band. This could be tested by heat shock of the culture prior to extract preparation and treatment with phosphatases.

We further tested whether Toi4 was associated with the plasma membrane via a protein-protein interaction. We found that Toi4-GFP was extracted most efficiently from the membrane fraction of cell extract by treatment with urea and sodium

carbonate (Figure 5.7). Both chemicals are known to disrupt protein-protein interactions therefore we can conclude that Toi4 is a peripheral membrane protein. The high pH of the urea and sodium carbonate can additionally lead to cleavage of fatty acid *S*-acylated modifications, thus we cannot exclude the possibility of association with the plasma membrane through a lipid modification. Our bioinformatics analysis did not reveal any predicted lipid modifications, however not all have a well-defined consensus site, for example palmitoylation of cysteine residues. Mass spectrometry of the different Toi4 species might provide a more detailed insight into the post-translational modifications of Toi4 *in vivo*.

6.4. Is Toi4 involved in endocytosis in *S. pombe*?

During the course of the investigation of Toi4 with respect to Tip1 function, it was published that the *S. cerevisiae* homologues, Pil1 and Lsp1, are the major constituents of a newly identified endocytic organelle termed the eisosome (Walther *et al.*, 2006). Eisosomes show a similar localisation pattern to Toi4-GFP and co-localise with sites of endocytosis of the lipid dye FM4-64 (Figure 5.11A,B). We tested whether Toi4-GFP co-localised with endocytosis of FM4-64. Unsurprisingly, we found no co-localisation, implying that Toi4 is not involved in endocytosis of lipid cargo in *S. pombe* (Figure 5.11C). Further support for this comes from the fact that endocytosis in *S. pombe* occurs predominantly at the cell poles and at the site of cytokinesis, sites where Toi4-GFP is largely absent (Figure 5.12B; Gachet and Hyams, 2005). Transient localisation of actin patch proteins is required for endocytosis in *S. pombe* (Gachet and Hyams, 2005) and *S. cerevisiae* (Kaksonen *et al.*, 2005; Huckaba *et al.*, 2004; Kaksonen *et al.*, 2003; Ayscough *et al.*, 1997) and was shown to be necessary for consumption of FM4-64 foci accumulated at eisosomes (Walther *et al.*, 2006). Unlike in *S. cerevisiae*, we found no co-localisation between Toi4-GFP and actin, rather that actin and Toi4-GFP localised to different regions of the cell (Figure 5.7; Marks and Hyams, 1985). Transient disruption of actin organisation by shifting the cells to 36ºC did not result in a change in Toi4-GFP localisation. Even during the period after shifting to 36ºC, before wild type actin localisation was re-established and actin patches were present in the central regions of the cell, we found no co-localisation between actin and Toi4-GFP (Figure 5.7B). This provides further evidence that Toi4-GFP is not associated with sites of endocytosis in fission yeast. Deletion of *PIL1* in *S. cerevisiae* results in a clustering of eisosome remnants and a re-distribution of endocytosis to these clusters (Walther *et al.*, 2006). As a final test for a link between Toi4 and endocytosis, we repeated the FM4-64 endocytosis assay

in *toi4*Δ strain. We found that FM4-64 was still endocytosed and there appeared to be no difference in the distribution of endocytic events, or a delay in endocytosis compared to wild type cells (Figure 5.12C).

The link between Pil1/Lsp and endocytosis and potentially between Tip1 and Toi4 suggested that Tip1, and therefore microtubules, might be involved in endocytosis. As a final test for a link between Toi4 and Tip1/microtubules in endocytosis we monitored endocytosis in the presence of the microtubule depolymerising drug, MBC. We found no difference between the endocytic uptake of FM4-64 in the presence and absence of MBC (Figure 5.12D). Therefore we conclude that microtubules do not play a role in endocytosis, which additionally indicates that Tip1 is also not required for endocytosis.

6.5. What is the function of Toi4 in *S. pombe*?

From our data we find no direct link between Toi4 or microtubules and endocytosis, suggesting that eisosomes in *S. pombe* are not endocytic organelles. It is possible however, that Toi4 has a non-essential role in endocytosis. Support for this possibility comes from *S. cerevisiae*, which has two Toi4 homologues, both of which are eisosome components, but Pil1 has a more essential role in eisosome organisation than Lsp1 (Walther *et al.*, 2006). Sequence analysis of the *S. pombe* genome database (Wood *et al.*, 2002) revealed that Toi4 has an orthologue, SPAC3C7.02c. The translated sequence of this predicted open reading frame shows less identity to Pil1, the primary eisosome component, than Toi4 (see Appendix Figure 7.3). Despite this, it is possible that SPAC3C7.02c plays a more central role in eisosome organisation and function and that Toi4 plays a more secondary role. This is probably not the case, as Toi4 is more similar to *S. cerevisiae* Pil1 and Lsp1 than it is to SPAC3C7.02c, however if SPAC3C7.02c co-localises with Toi4 this would provide a second marker for *S. pombe* eisosomes and thus allow a more detailed investigation of the *toi4* deletion phenotype. An alternative possibility is that Toi4 is exclusively involved in endocytosis of non-lipid cargo and as such would not be expected to co-localise with FM4-64, the marker for lipid endocytosis. This is highly unlikely, given that eisosomes in *S. cerevisiae* did co-localise with endocytic uptake of proteins, but it remains to be tested.

Hints of other possible roles for Toi4/eisosomes in *S. pombe* can also be found in the literature. For example, eisosomes may constitute a platform for signalling to and from the plasma membrane. Pil1 and Lsp1 are phosphorylated by the Pkh1 and Pkh2

kinases and phosphorylation is required for Pil1 localisation as no, or hyper-phosphorylation results in disorganised eisosomes (Luo *et al.*, 2008; Walther *et al.*, 2007). The Pkc1p-MAP kinase pathway also regulates cell wall maintenance and integrity and repolarisation of the actin cytoskeleton during heat stress in response to activation by sphingolipid long-chain bases (Delley and Hall, 1999; Inagaki *et al.*, 1999; Jenkins *et al.*, 1997; Levin and Bartlett-Heubusch, 1992; Paravicini *et al.*, 1992). Pkh1 and Phk2 homologues also exist in *S. pombe* so it is possible that Toi4 is also subject to such regulation. In addition, a link between the Toi4 homologue of the yeast *Candida albicans* and glucan synthase, the enzyme required for synthesis of fungal cell wall components has been shown. The *C. albicans* Toi4 homologue was identified through a screen to identify proteins interacting with echinocandins (Radding, *et al.*, 1998), naturally occurring lipopeptides that inhibit glucan synthase (Balkovec, 1994). This link with glucan synthase could indicate that Toi4 is involved in the regulation of cell wall synthesis or remodelling. Certainly, Toi4 is optimally positioned for involvement in these processes.

A further possible role of Toi4 could be involvement in the storage of proteins, lipids or membrane. Release of such stored molecules would allow the cell to respond more quickly to external stimuli than if *de novo* synthesis was necessary. Indeed local invaginations of the cell membrane, likely corresponding to eisosomes have been observed by electron microscopy in *S. cerevisiae* (Walther *et al.*, unpublished data). These invaginations could therefore represent stored membrane or membrane enriched in specific lipids or proteins, however further work is required to confirm this.

As we found no apparent link between Tip1 and Toi4 and that Toi4 played no apparent role in endocytosis we decided not to pursue further characterisation of Toi4 at the present time. However, in order to fully characterise the role of Toi4 several experiments are necessary and should be performed for both Toi4 and its orthologue. Not least of which, is to test whether the Pkh protein kinase pathway regulates Toi4, as is the case for the *S. cerevisiae* homologues.

7. Appendix

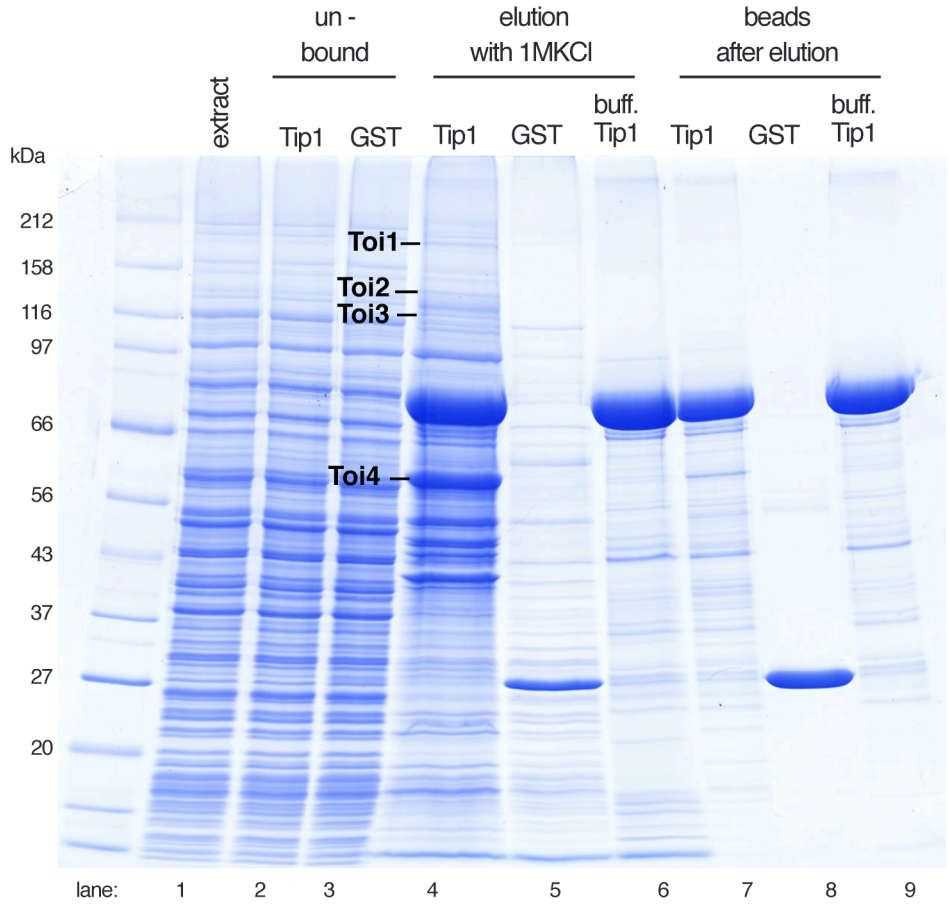

Figure 7.1 Toi proteins identified by GST-pulldown

Toi proteins pulled down by recombinant GST-Tip were separated by SDS-PAGE and stained with coomassie blue. Lane 1, wild type cell extract; lane 2, extract after incubation with GST-Tip1 beads; lane 3, extract after incubation with control GST-beads; lane 4, proteins eluted from GST-Tip1 beads with KCl; lane 5, proteins eluted from control GST beads with KCl; lane 6, proteins eluted from GST-Tip1 beads with buffer only; lane 7-9, proteins remaining on the beads after elution. GST-Tip1 pulldown and analysis performed by M. Toya.

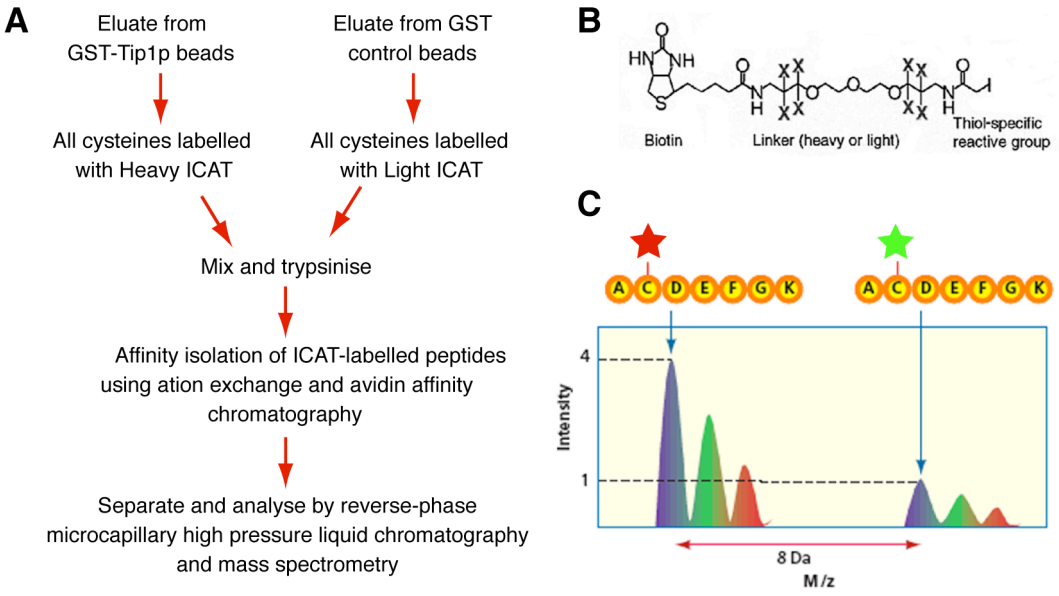

Figure 7.2 ICAT-based identification of Tip1 interacting proteins

(A) Flow diagram indicating the stages in ICAT analysis of proteins pulled down by GST-Tip1 or GST control beads. (B) Isotope-coded affinity tag. The linker residues X are all either isotopically heavy or light. (C) Peptides are measured by mass spectrometry, and otherwise identical peptides can be separated in a mass spectrum by the mass difference between the heavy (green star) and light (red star) reagent. The ratio of a proteins abundance with heavy and light ICAT tags allows proteins specifically pulled down by GST-Tip to be identified. Adapted from Mann (1999) and Gygi *et al.*, (1999)

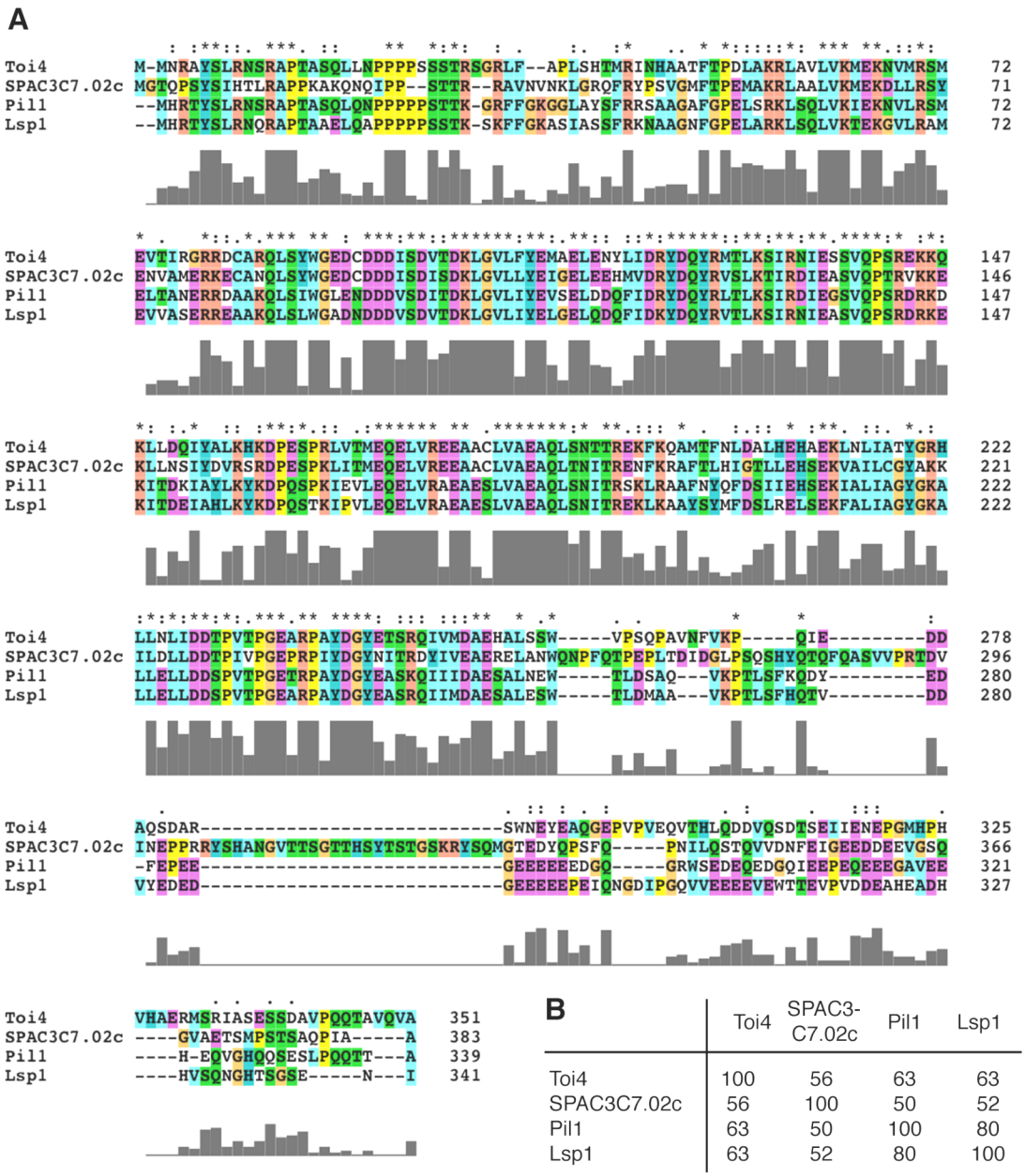

Figure 7.3 Sequence alignment of Toi4 and its homologues

(A) Multiple sequence alignment of *S. pombe* Toi4 and SPAC3C7.02c and *S. cerevisiae* Pil1 and Lsp1 amino acid sequences using the programme MAFFT. (B) A pairwise sequence identity matrix of the N-terminal regions (residue 1-264 in the multiple alignment) of all four proteins, calculated in the context of the MAFFT alignment using ClustalX. **-**, gap characters; *****, identical residues; **:**, conserved residues; **·**, semi-conserved residues. Sequence analysis performed with assistance from A. Budd.

8. References

Akhmanova A, Hoogenraad CC, Drabek K, Stepanova T, Dortland B, Verkerk T, Vermeulen W, Burgering BM, De Zeeuw CI, Grosveld F, Galjart N (2001) Clasps are CLIP-115 and -170 associating proteins involved in the regional regulation of microtubule dynamics in motile fibroblasts. *Cell* **104:** 923-935

Akhmanova A, Steinmetz MO (2008) Tracking the ends: a dynamic protein network controls the fate of microtubule tips. *Nat Rev Mol Cell Biol* **9:** 309-322

Al-Bassam J, van Breugel M, Harrison SC, Hyman A (2006) Stu2p binds tubulin and undergoes an open-to-closed conformational change. *The Journal of cell biology* **172:** 1009-1022

Ali MY, Krementsova EB, Kennedy GG, Mahaffy R, Pollard TD, Trybus KM, Warshaw DM (2007) Myosin Va maneuvers through actin intersections and diffuses along microtubules. *Proc Natl Acad Sci U S A* **104:** 4332-4336

Amos LA, Schlieper D (2005) Microtubules and maps. *Adv Protein Chem* **71:** 257-298

An H, Morrell JL, Jennings JL, Link AJ, Gould KL (2004) Requirements of fission yeast septins for complex formation, localization, and function. *Molecular biology of the cell* **15:** 5551-5564

Andreu JM, Diaz JF, Gil R, de Pereda JM, Garcia de Lacoba M, Peyrot V, Briand C, Towns-Andrews E, Bordas J (1994) Solution structure of Taxotere-induced microtubules to 3-nm resolution. The change in protofilament number is linked to the binding of the taxol side chain. *The Journal of biological chemistry* **269:** 31785-31792

Aoki K, Nakaseko Y, Kinoshita K, Goshima G, Yanagida M (2006) CDC2 phosphorylation of the fission yeast dis1 ensures accurate chromosome segregation. *Curr Biol* **16:** 1627-1635

Arai R, Nakano K, Mabuchi I (1998) Subcellular localization and possible function of actin, tropomyosin and actin-related protein 3 (Arp3) in the fission yeast Schizosaccharomyces pombe. *Eur J Cell Biol* **76:** 288-295

Askham JM, Vaughan KT, Goodson HV, Morrison EE (2002) Evidence that an interaction between EB1 and p150(Glued) is required for the formation and maintenance of a radial microtubule array anchored at the centrosome. *Molecular biology of the cell* **13:** 3627-3645

Ayscough KR, Stryker J, Pokala N, Sanders M, Crews P, Drubin DG (1997) High rates of actin filament turnover in budding yeast and roles for actin in establishment and maintenance of cell polarity revealed using the actin inhibitor latrunculin-A. *The Journal of cell biology* **137:** 399-416

Baas PW, Deitch JS, Black MM, Banker GA (1988) Polarity orientation of microtubules in hippocampal neurons: uniformity in the axon and nonuniformity in the dendrite. *Proc Natl Acad Sci U S A* **85:** 8335-8339

Bahler J, Pringle JR (1998) Pom1p, a fission yeast protein kinase that provides positional information for both polarized growth and cytokinesis. *Genes & development* **12:** 1356-1370

Bahler J, Wu JQ, Longtine MS, Shah NG, McKenzie A, 3rd, Steever AB, Wach A, Philippsen P, Pringle JR (1998) Heterologous modules for efficient and versatile PCR-based gene targeting in Schizosaccharomyces pombe. *Yeast (Chichester, England)* **14:** 943-951

Balkovec JM (1994) Anti-infectives: Lipopeptide antifungal agents. *Expert Opinion on Investigational Drugs* **3:** 65-82

Bartolini F, Gundersen GG (2006) Generation of noncentrosomal microtubule arrays. *Journal of cell science* **119:** 4155-4163

Basi G, Schmid E, Maundrell K (1993) TATA box mutations in the Schizosaccharomyces pombe nmt1 promoter affect transcription efficiency but not the transcription start point or thiamine repressibility. *Gene* **123:** 131-136

Behrens R, Nurse P (2002) Roles of fission yeast tea1p in the localization of polarity factors and in organizing the microtubular cytoskeleton. *The Journal of cell biology* **157:** 783-793

Beinhauer JD, Hagan IM, Hegemann JH, Fleig U (1997) Mal3, the fission yeast homologue of the human APC-interacting protein EB-1 is required for microtubule integrity and the maintenance of cell form. *The Journal of cell biology* **139:** 717-728

Bellanger JM, Gonczy P (2003) TAC-1 and ZYG-9 form a complex that promotes microtubule assembly in C. elegans embryos. *Curr Biol* **13:** 1488-1498

Berrueta L, Tirnauer JS, Schuyler SC, Pellman D, Bierer BE (1999) The APC-associated protein EB1 associates with components of the dynactin complex and cytoplasmic dynein intermediate chain. *Curr Biol* **9:** 425-428

Bieling P, Laan L, Schek H, Munteanu EL, Sandblad L, Dogterom M, Brunner D, Surrey T (2007) Reconstitution of a microtubule plus-end tracking system in vitro. *Nature* **450:** 1100-1105

Bornens M (2002) Centrosome composition and microtubule anchoring mechanisms. *Curr Opin Cell Biol* **14:** 25-34

Bratman SV, Chang F (2007) Stabilization of overlapping microtubules by fission yeast CLASP. *Developmental cell* **13:** 812-827

Brittle AL, Ohkura H (2005) Mini spindles, the XMAP215 homologue, suppresses pausing of interphase microtubules in Drosophila. *The EMBO journal* **24:** 1387-1396

Brouhard GJ, Stear JH, Noetzel TL, Al-Bassam J, Kinoshita K, Harrison SC, Howard J, Hyman AA (2008) XMAP215 is a processive microtubule polymerase. *Cell* **132:** 79-88

Browning H, Hackney DD (2005) The EB1 homolog Mal3 stimulates the ATPase of the kinesin Tea2 by recruiting it to the microtubule. *The Journal of biological chemistry* **280:** 12299-12304

Browning H, Hackney DD, Nurse P (2003) Targeted movement of cell end factors in fission yeast. *Nature cell biology* **5:** 812-818

Brunner D, Nurse P (2000) CLIP170-like tip1p spatially organizes microtubular dynamics in fission yeast. *Cell* **102:** 695-704

Bu W, Su LK (2003) Characterization of functional domains of human EB1 family proteins. *The Journal of biological chemistry* **278:** 49721-49731

Burgess SA, Walker ML, Sakakibara H, Knight PJ, Oiwa K (2003) Dynein structure and power stroke. *Nature* **421:** 715-718

Busch KE, Brunner D (2004) The microtubule plus end-tracking proteins mal3p and tip1p cooperate for cell-end targeting of interphase microtubules. *Curr Biol* **14:** 548-559

Busch KE, Hayles J, Nurse P, Brunner D (2004) Tea2p kinesin is involved in spatial microtubule organization by transporting tip1p on microtubules. *Developmental cell* **6:** 831-843

Carazo-Salas RE, Antony C, Nurse P (2005) The kinesin Klp2 mediates polarization of interphase microtubules in fission yeast. *Science (New York, NY* **309:** 297-300

Carlier MF (1992) Nucleotide hydrolysis regulates the dynamics of actin filaments and microtubules. *Philos Trans R Soc Lond B Biol Sci* **336:** 93-97

Carvalho P, Gupta ML, Jr., Hoyt MA, Pellman D (2004) Cell cycle control of kinesin-mediated transport of Bik1 (CLIP-170) regulates microtubule stability and dynein activation. *Developmental cell* **6:** 815-829

Carvalho P, Tirnauer JS, Pellman D (2003) Surfing on microtubule ends. *Trends Cell Biol* **13:** 229-237

Cassimeris L (1999) Accessory protein regulation of microtubule dynamics throughout the cell cycle. *Curr Opin Cell Biol* **11:** 134-141

Cassimeris L (2002) The oncoprotein 18/stathmin family of microtubule destabilizers. *Curr Opin Cell Biol* **14:** 18-24

Cassimeris L, Gard D, Tran PT, Erickson HP (2001) XMAP215 is a long thin molecule that does not increase microtubule stiffness. *Journal of cell science* **114:** 3025-3033

Cassimeris L, Morabito J (2004) TOGp, the human homolog of XMAP215/Dis1, is required for centrosome integrity, spindle pole organization, and bipolar spindle assembly. *Molecular biology of the cell* **15:** 1580-1590

Caudron M, Bunt G, Bastiaens P, Karsenti E (2005) Spatial coordination of spindle assembly by chromosome-mediated signaling gradients. *Science (New York, NY* **309:** 1373-1376

Chang F, Peter M (2003) Yeasts make their mark. *Nature cell biology* **5:** 294-299

Chang L, Goldman RD (2004) Intermediate filaments mediate cytoskeletal crosstalk. *Nat Rev Mol Cell Biol* **5:** 601-613

Charrasse S, Schroeder M, Gauthier-Rouviere C, Ango F, Cassimeris L, Gard DL, Larroque C (1998) The TOGp protein is a new human microtubule-associated protein homologous to the Xenopus XMAP215. *Journal of cell science* **111 (Pt 10):** 1371-1383

Chen J, Kanai Y, Cowan NJ, Hirokawa N (1992) Projection domains of MAP2 and tau determine spacings between microtubules in dendrites and axons. *Nature* **360:** 674-677

Chikashige Y, Ding DQ, Funabiki H, Haraguchi T, Mashiko S, Yanagida M, Hiraoka Y (1994) Telomere-led premeiotic chromosome movement in fission yeast. *Science (New York, NY* **264:** 270-273

Chikashige Y, Hiraoka Y (2001) Telomere binding of the Rap1 protein is required for meiosis in fission yeast. *Curr Biol* **11:** 1618-1623

Chiron S, Bobkova A, Zhou H, Yaffe MP (2008) CLASP regulates mitochondrial distribution in Schizosaccharomyces pombe. *The Journal of cell biology* **182:** 41-49

Chretien D, Fuller SD, Karsenti E (1995) Structure of growing microtubule ends: two-dimensional sheets close into tubes at variable rates. *The Journal of cell biology* **129:** 1311-1328

Chretien D, Wade RH (1991) New data on the microtubule surface lattice. *Biol Cell* **71:** 161-174

Courtheoux T, Gay G, Reyes C, Goldstone S, Gachet Y, Tournier S (2007) Dynein participates in chromosome segregation in fission yeast. *Biol Cell* **99:** 627-637

Cowan CR, Hyman AA (2004) Asymmetric cell division in C. elegans: cortical polarity and spindle positioning. *Annual review of cell and developmental biology* **20:** 427-453

Cullen CF, Deak P, Glover DM, Ohkura H (1999) mini spindles: A gene encoding a conserved microtubule-associated protein required for the integrity of the mitotic spindle in Drosophila. *The Journal of cell biology* **146:** 1005-1018

Cullen CF, Ohkura H (2001) Msps protein is localized to acentrosomal poles to ensure bipolarity of Drosophila meiotic spindles. *Nature cell biology* **3:** 637-642

Curmi PA, Gavet O, Charbaut E, Ozon S, Lachkar-Colmerauer S, Manceau V, Siavoshian S, Maucuer A, Sobel A (1999) Stathmin and its phosphoprotein family: general properties, biochemical and functional interaction with tubulin. *Cell structure and function* **24:** 345-357

Daga RR, Chang F (2005) Dynamic positioning of the fission yeast cell division plane. *Proc Natl Acad Sci U S A* **102:** 8228-8232

Daga RR, Yonetani A, Chang F (2006) Asymmetric microtubule pushing forces in nuclear centering. *Curr Biol* **16:** 1544-1550

Davis L, Smith GR (2005) Dynein promotes achiasmate segregation in Schizosaccharomyces pombe. *Genetics* **170:** 581-590

Dechat T, Pfleghaar K, Sengupta K, Shimi T, Shumaker DK, Solimando L, Goldman RD (2008) Nuclear lamins: major factors in the structural organization and function of the nucleus and chromatin. *Genes & development* **22:** 832-853

Delley PA, Hall MN (1999) Cell wall stress depolarizes cell growth via hyperactivation of RHO1. *The Journal of cell biology* **147:** 163-174

Desai A, Mitchison TJ (1997) Microtubule polymerization dynamics. *Annual review of cell and developmental biology* **13:** 83-117

Desai A, Verma S, Mitchison TJ, Walczak CE (1999) Kin I kinesins are microtubule-destabilizing enzymes. *Cell* **96:** 69-78

Ding DQ, Chikashige Y, Haraguchi T, Hiraoka Y (1998) Oscillatory nuclear movement in fission yeast meiotic prophase is driven by astral microtubules, as revealed by continuous observation of chromosomes and microtubules in living cells. *Journal of cell science* **111 (Pt 6):** 701-712

Ding DQ, Yamamoto A, Haraguchi T, Hiraoka Y (2004) Dynamics of homologous chromosome pairing during meiotic prophase in fission yeast. *Developmental cell* **6:** 329-341

Ding R, McDonald KL, McIntosh JR (1993) Three-dimensional reconstruction and analysis of mitotic spindles from the yeast, Schizosaccharomyces pombe. *The Journal of cell biology* **120:** 141-151

Ding R, West RR, Morphew DM, Oakley BR, McIntosh JR (1997) The spindle pole body of Schizosaccharomyces pombe enters and leaves the nuclear envelope as the cell cycle proceeds. *Molecular biology of the cell* **8:** 1461-1479

Dionne MA, Sanchez A, Compton DA (2000) ch-TOGp is required for microtubule aster formation in a mammalian mitotic extract. *The Journal of biological chemistry* **275:** 12346-12352

Dogterom M, Kerssemakers JW, Romet-Lemonne G, Janson ME (2005) Force generation by dynamic microtubules. *Curr Opin Cell Biol* **17:** 67-74

Dogterom M, Yurke B (1997) Measurement of the force-velocity relation for growing microtubules. *Science (New York, NY* **278:** 856-860

dos Remedios CG, Chhabra D, Kekic M, Dedova IV, Tsubakihara M, Berry DA, Nosworthy NJ (2003) Actin binding proteins: regulation of cytoskeletal microfilaments. *Physiol Rev* **83:** 433-473

Dragestein KA, van Cappellen WA, van Haren J, Tsibidis GD, Akhmanova A, Knoch TA, Grosveld F, Galjart N (2008) Dynamic behavior of GFP-CLIP-170 reveals fast protein turnover on microtubule plus ends. *The Journal of cell biology* **180:** 729-737

Draviam VM, Shapiro I, Aldridge B, Sorger PK (2006) Misorientation and reduced stretching of aligned sister kinetochores promote chromosome missegregation in EB1- or APC-depleted cells. *The EMBO journal* **25:** 2814-2827

Drechsel DN, Kirschner MW (1994) The minimum GTP cap required to stabilize microtubules. *Curr Biol* **4:** 1053-1061

Drubin DG (1991) Development of cell polarity in budding yeast. *Cell* **65:** 1093-1096

Drummond DR, Cross RA (2000) Dynamics of interphase microtubules in Schizosaccharomyces pombe. *Curr Biol* **10:** 766-775

Dujardin D, Wacker UI, Moreau A, Schroer TA, Rickard JE, De Mey JR (1998) Evidence for a role of CLIP-170 in the establishment of metaphase chromosome alignment. *The Journal of cell biology* **141:** 849-862

Efimov A, Kharitonov A, Efimova N, Loncarek J, Miller PM, Andreyeva N, Gleeson P, Galjart N, Maia AR, McLeod IX, Yates JR, 3rd, Maiato H, Khodjakov A, Akhmanova A, Kaverina I (2007) Asymmetric CLASP-dependent nucleation of noncentrosomal microtubules at the trans-Golgi network. *Developmental cell* **12:** 917-930

Enke C, Zekert N, Veith D, Schaaf C, Konzack S, Fischer R (2007) Aspergillus nidulans Dis1/XMAP215 protein AlpA localizes to spindle pole bodies and microtubule plus ends and contributes to growth directionality. *Eukaryotic cell* **6:** 555-562

Evans L, Mitchison T, Kirschner M (1985) Influence of the centrosome on the structure of nucleated microtubules. *The Journal of cell biology* **100:** 1185-1191

Fodde R, Kuipers J, Rosenberg C, Smits R, Kielman M, Gaspar C, van Es JH, Breukel C, Wiegant J, Giles RH, Clevers H (2001) Mutations in the APC tumour suppressor gene cause chromosomal instability. *Nature cell biology* **3:** 433-438

Folker ES, Baker BM, Goodson HV (2005) Interactions between CLIP-170, tubulin, and microtubules: implications for the mechanism of Clip-170 plus-end tracking behavior. *Molecular biology of the cell* **16:** 5373-5384

Forsburg SL, Rhind N (2006) Basic methods for fission yeast. *Yeast (Chichester, England)* **23:** 173-183

Fujita A, Vardy L, Garcia MA, Toda T (2002) A fourth component of the fission yeast gamma-tubulin complex, Alp16, is required for cytoplasmic microtubule integrity and becomes indispensable when gamma-tubulin function is compromised. *Molecular biology of the cell* **13:** 2360-2373

Funabiki H, Hagan I, Uzawa S, Yanagida M (1993) Cell cycle-dependent specific positioning and clustering of centromeres and telomeres in fission yeast. *The Journal of cell biology* **121:** 961-976

Gachet Y, Hyams JS (2005) Endocytosis in fission yeast is spatially associated with the actin cytoskeleton during polarised cell growth and cytokinesis. *Journal of cell science* **118:** 4231-4242

Galjart N (2005) CLIPs and CLASPs and cellular dynamics. *Nat Rev Mol Cell Biol* **6:** 487-498

Galjart N, Perez F (2003) A plus-end raft to control microtubule dynamics and function. *Curr Opin Cell Biol* **15:** 48-53

Garcia MA, Koonrugsa N, Toda T (2002a) Spindle-kinetochore attachment requires the combined action of Kin I-like Klp5/6 and Alp14/Dis1-MAPs in fission yeast. *The EMBO journal* **21:** 6015-6024

Garcia MA, Koonrugsa N, Toda T (2002b) Two kinesin-like Kin I family proteins in fission yeast regulate the establishment of metaphase and the onset of anaphase A. *Curr Biol* **12:** 610-621

Garcia MA, Vardy L, Koonrugsa N, Toda T (2001) Fission yeast ch-TOG/XMAP215 homologue Alp14 connects mitotic spindles with the kinetochore and is a component of the Mad2-dependent spindle checkpoint. *The EMBO journal* **20:** 3389-3401

Gard DL, Kirschner MW (1987) A microtubule-associated protein from Xenopus eggs that specifically promotes assembly at the plus-end. *The Journal of cell biology* **105:** 2203-2215

Gergely F, Draviam VM, Raff JW (2003) The ch-TOG/XMAP215 protein is essential for spindle pole organization in human somatic cells. *Genes & development* **17:** 336-341

Gigant B, Wang C, Ravelli RB, Roussi F, Steinmetz MO, Curmi PA, Sobel A, Knossow M (2005) Structural basis for the regulation of tubulin by vinblastine. *Nature* **435:** 519-522

Gilbert PF (1972) The reconstruction of a three-dimensional structure from projections and its application to electron microscopy. II. Direct methods. *Proceedings of the Royal Society of London Series B, Containing papers of a Biological character* **182:** 89-102

Goldie KN, Wedig T, Mitra AK, Aebi U, Herrmann H, Hoenger A (2007) Dissecting the 3-D structure of vimentin intermediate filaments by cryo-electron tomography. *J Struct Biol* **158:** 378-385

Goshima G, Nedelec F, Vale RD (2005) Mechanisms for focusing mitotic spindle poles by minus end-directed motor proteins. *The Journal of cell biology* **171:** 229-240

Graf R, Daunderer C, Schliwa M (2000) Dictyostelium DdCP224 is a microtubule-associated protein and a permanent centrosomal resident involved in centrosome duplication. *Journal of cell science* **113 (Pt 10):** 1747-1758

Graf R, Euteneuer U, Ho TH, Rehberg M (2003) Regulated expression of the centrosomal protein DdCP224 affects microtubule dynamics and reveals mechanisms for the control of supernumerary centrosome number. *Molecular biology of the cell* **14:** 4067-4074

Gygi SP, Rist B, Gerber SA, Turecek F, Gelb MH, Aebersold R (1999) Quantitative analysis of complex protein mixtures using isotope-coded affinity tags. *Nature biotechnology* **17:** 994-999

Hagan I, Yanagida M (1995) The product of the spindle formation gene sad1+ associates with the fission yeast spindle pole body and is essential for viability. *The Journal of cell biology* **129:** 1033-1047

Hagan IM (1998) The fission yeast microtubule cytoskeleton. *Journal of cell science* **111 (Pt 12):** 1603-1612

Hayashi I, Ikura M (2003) Crystal structure of the amino-terminal microtubule-binding domain of end-binding protein 1 (EB1). *The Journal of biological chemistry* **278:** 36430-36434

Hayashi I, Wilde A, Mal TK, Ikura M (2005) Structural basis for the activation of microtubule assembly by the EB1 and p150Glued complex. *Mol Cell* **19:** 449-460

Hayles J, Nurse P (2001) A journey into space. *Nat Rev Mol Cell Biol* **2:** 647-656

Helenius J, Brouhard G, Kalaidzidis Y, Diez S, Howard J (2006) The depolymerizing kinesin MCAK uses lattice diffusion to rapidly target microtubule ends. *Nature* **441:** 115-119

Helfand BT, Chang L, Goldman RD (2004) Intermediate filaments are dynamic and motile elements of cellular architecture. *Journal of cell science* **117:** 133-141

Herrmann H, Aebi U (2004) Intermediate filaments: molecular structure, assembly mechanism, and integration into functionally distinct intracellular Scaffolds. *Annu Rev Biochem* **73:** 749-789

Herrmann H, Foisner R (2003) Intermediate filaments: novel assembly models and exciting new functions for nuclear lamins. *Cell Mol Life Sci* **60:** 1607-1612

Hirsh D, Vanderslice R (1976) Temperature-sensitive developmental mutants of Caenorhabditis elegans. *Developmental biology* **49:** 220-235

Hoenger A, Thormahlen M, Diaz-Avalos R, Doerhoefer M, Goldie KN, Muller J, Mandelkow E (2000) A new look at the microtubule binding patterns of dimeric kinesins. *Journal of molecular biology* **297:** 1087-1103

Holmfeldt P, Stenmark S, Gullberg M (2004) Differential functional interplay of TOGp/XMAP215 and the KinI kinesin MCAK during interphase and mitosis. *The EMBO journal* **23:** 627-637

Honnappa S, John CM, Kostrewa D, Winkler FK, Steinmetz MO (2005) Structural insights into the EB1-APC interaction. *The EMBO journal* **24:** 261-269

Hoog JL, Schwartz C, Noon AT, O'Toole E T, Mastronarde DN, McIntosh JR, Antony C (2007a) Organization of interphase microtubules in fission yeast analyzed by electron tomography. *Developmental cell* **12:** 349-361

Hoog JL, Schwartz C, Noon AT, O'Toole ET, Mastronarde DN, McIntosh JR, Antony C (2007b) Organization of interphase microtubules in fission yeast analyzed by electron tomography. *Developmental cell* **12:** 349-361

Horio T, Uzawa S, Jung MK, Oakley BR, Tanaka K, Yanagida M (1991) The fission yeast gamma-tubulin is essential for mitosis and is localized at microtubule organizing centers. *Journal of cell science* **99 (Pt 4):** 693-700

Horisberger M, Vonlanthen M, Rosset J (1978) Localization of alpha-galactomannan and of wheat germ agglutinin receptors in Schizosaccharomyces pombe. *Archives of microbiology* **119:** 107-111

Hotani H, Miyamoto H (1990) Dynamic features of microtubules as visualized by dark-field microscopy. *Advances in biophysics* **26:** 135-156

Howard J, Hyman AA (2007) Microtubule polymerases and depolymerases. *Curr Opin Cell Biol* **19:** 31-35

Huckaba TM, Gay AC, Pantalena LF, Yang HC, Pon LA (2004) Live cell imaging of the assembly, disassembly, and actin cable-dependent movement of endosomes and actin patches in the budding yeast, Saccharomyces cerevisiae. *The Journal of cell biology* **167:** 519-530

Inagaki M, Schmelzle T, Yamaguchi K, Irie K, Hall MN, Matsumoto K (1999) PDK1 homologs activate the Pkc1-mitogen-activated protein kinase pathway in yeast. *Molecular and cellular biology* **19:** 8344-8352

Irazoqui JE, Lew DJ (2004) Polarity establishment in yeast. *Journal of cell science* **117:** 2169-2171

Janson ME, de Dood ME, Dogterom M (2003) Dynamic instability of microtubules is regulated by force. *The Journal of cell biology* **161:** 1029-1034

Janson ME, Dogterom M (2004) A bending mode analysis for growing microtubules: evidence for a velocity-dependent rigidity. *Biophysical journal* **87:** 2723-2736

Janson ME, Setty TG, Paoletti A, Tran PT (2005) Efficient formation of bipolar microtubule bundles requires microtubule-bound gamma-tubulin complexes. *The Journal of cell biology* **169:** 297-308

Jenkins GM, Richards A, Wahl T, Mao C, Obeid L, Hannun Y (1997) Involvement of yeast sphingolipids in the heat stress response of Saccharomyces cerevisiae. *The Journal of biological chemistry* **272:** 32566-32572

Jones RH, Moreno S, Nurse P, Jones NC (1988) Expression of the SV40 promoter in fission yeast: identification and characterization of an AP-1-like factor. *Cell* **53:** 659-667

Joseph J, Dasso M (2008) The nucleoporin Nup358 associates with and regulates interphase microtubules. *FEBS letters* **582:** 190-196

Kabsch W, Vandekerckhove J (1992) Structure and function of actin. *Annual review of biophysics and biomolecular structure* **21:** 49-76

Kaksonen M, Sun Y, Drubin DG (2003) A pathway for association of receptors, adaptors, and actin during endocytic internalization. *Cell* **115:** 475-487

Kaksonen M, Toret CP, Drubin DG (2005) A modular design for the clathrin- and actin-mediated endocytosis machinery. *Cell* **123:** 305-320

Kaneko T, Itoh TJ, Hotani H (1998) Morphological transformation of liposomes caused by assembly of encapsulated tubulin and determination of shape by microtubule-associated proteins (MAPs). *Journal of molecular biology* **284:** 1671-1681

Kawamura E, Himmelspach R, Rashbrooke MC, Whittington AT, Gale KR, Collings DA, Wasteneys GO (2006) MICROTUBULE ORGANIZATION 1 regulates structure and function of microtubule arrays during mitosis and cytokinesis in the Arabidopsis root. *Plant physiology* **140:** 102-114

Keating TJ, Borisy GG (2000) Immunostructural evidence for the template mechanism of microtubule nucleation. *Nature cell biology* **2:** 352-357

Kemphues KJ, Wolf N, Wood WB, Hirsh D (1986) Two loci required for cytoplasmic organization in early embryos of Caenorhabditis elegans. *Developmental biology* **113:** 449-460

Khodjakov A, Copenagle L, Gordon MB, Compton DA, Kapoor TM (2003) Minus-end capture of preformed kinetochore fibers contributes to spindle morphogenesis. *The Journal of cell biology* **160:** 671-683

King MC, Drivas TG, Blobel G (2008) A network of nuclear envelope membrane proteins linking centromeres to microtubules. *Cell* **134:** 427-438

Kirschner MW (1978) Microtubule assembly and nucleation. *International review of cytology* **54:** 1-71

Komarova Y, Lansbergen G, Galjart N, Grosveld F, Borisy GG, Akhmanova A (2005) EB1 and EB3 control CLIP dissociation from the ends of growing microtubules. *Molecular biology of the cell* **16:** 5334-5345

Kosco KA, Pearson CG, Maddox PS, Wang PJ, Adams IR, Salmon ED, Bloom K, Huffaker TC (2001) Control of microtubule dynamics by Stu2p is essential for spindle orientation and metaphase chromosome alignment in yeast. *Molecular biology of the cell* **12:** 2870-2880

Kremer JR, Mastronarde DN, McIntosh JR (1996) Computer visualization of three-dimensional image data using IMOD. *J Struct Biol* **116:** 71-76

Kudo N, Wolff B, Sekimoto T, Schreiner EP, Yoneda Y, Yanagida M, Horinouchi S, Yoshida M (1998) Leptomycin B inhibition of signal-mediated nuclear export by direct binding to CRM1. *Experimental cell research* **242:** 540-547

La Carbona S, Le Goff C, Le Goff X (2006) Fission yeast cytoskeletons and cell polarity factors: connecting at the cortex. *Biol Cell* **98:** 619-631

Laan L, Husson J, Munteanu EL, Kerssemakers JW, Dogterom M (2008) Force-generation and dynamic instability of microtubule bundles. *Proc Natl Acad Sci U S A* **105:** 8920-8925

Laemmli UK. (1970) Cleavage of structural proteins during the assembly of the head of bacteriophage T4. *Nature*, Vol. 227, pp. 680-685.

Larkin MA, Blackshields G, Brown NP, Chenna R, McGettigan PA, McWilliam H, Valentin F, Wallace IM, Wilm A, Lopez R, Thompson JD, Gibson TJ, Higgins DG (2007) Clustal W and Clustal X version 2.0. *Bioinformatics (Oxford, England)* **23:** 2947-2948

Lawrence CJ, Dawe RK, Christie KR, Cleveland DW, Dawson SC, Endow SA, Goldstein LS, Goodson HV, Hirokawa N, Howard J, Malmberg RL, McIntosh JR, Miki H, Mitchison TJ, Okada Y, Reddy AS, Saxton WM, Schliwa M, Scholey JM, Vale RD, Walczak CE, Wordeman L (2004) A standardized kinesin nomenclature. *The Journal of cell biology* **167:** 19-22

Lee H, Engel U, Rusch J, Scherrer S, Sheard K, Van Vactor D (2004) The microtubule plus end tracking protein Orbit/MAST/CLASP acts downstream of the tyrosine kinase Abl in mediating axon guidance. *Neuron* **42:** 913-926

Lee L, Tirnauer JS, Li J, Schuyler SC, Liu JY, Pellman D (2000) Positioning of the mitotic spindle by a cortical-microtubule capture mechanism. *Science (New York, NY* **287:** 2260-2262

Lee MJ, Gergely F, Jeffers K, Peak-Chew SY, Raff JW (2001) Msps/XMAP215 interacts with the centrosomal protein D-TACC to regulate microtubule behaviour. *Nature cell biology* **3:** 643-649

Levin DE, Bartlett-Heubusch E (1992) Mutants in the S. cerevisiae PKC1 gene display a cell cycle-specific osmotic stability defect. *The Journal of cell biology* **116:** 1221-1229

Liakopoulos D, Kusch J, Grava S, Vogel J, Barral Y (2003) Asymmetric loading of Kar9 onto spindle poles and microtubules ensures proper spindle alignment. *Cell* **112:** 561-574

Ligon LA, Shelly SS, Tokito MK, Holzbaur EL (2006) Microtubule binding proteins CLIP-170, EB1, and p150Glued form distinct plus-end complexes. *FEBS letters* **580:** 1327-1332

Lim HWG, Huber G, Torii Y, Hirata A, Miller J, Sazer S (2007) Vesicle-like biomechanics governs important aspects of nuclear geometry in fission yeast. *PLoS ONE* **2:** e948

Loiodice I, Staub J, Setty TG, Nguyen NP, Paoletti A, Tran PT (2005) Ase1p organizes antiparallel microtubule arrays during interphase and mitosis in fission yeast. *Molecular biology of the cell* **16:** 1756-1768

Longtine MS, DeMarini DJ, Valencik ML, Al-Awar OS, Fares H, De Virgilio C, Pringle JR (1996) The septins: roles in cytokinesis and other processes. *Curr Opin Cell Biol* **8:** 106-119

Lu C, Srayko M, Mains PE (2004) The Caenorhabditis elegans microtubule-severing complex MEI-1/MEI-2 katanin interacts differently with two superficially redundant beta-tubulin isotypes. *Molecular biology of the cell* **15:** 142-150

Luo G, Gruhler A, Liu Y, Jensen ON, Dickson RC (2008) The sphingolipid long-chain base-Pkh1/2-Ypk1/2 signaling pathway regulates eisosome assembly and turnover. *The Journal of biological chemistry* **283:** 10433-10444

Maiato H, Rieder CL, Khodjakov A (2004) Kinetochore-driven formation of kinetochore fibers contributes to spindle assembly during animal mitosis. *The Journal of cell biology* **167:** 831-840

Maiato H, Sampaio P, Lemos CL, Findlay J, Carmena M, Earnshaw WC, Sunkel CE (2002) MAST/Orbit has a role in microtubule-kinetochore attachment and is essential for chromosome alignment and maintenance of spindle bipolarity. *The Journal of cell biology* **157:** 749-760

Mandelkow EM, Schultheiss R, Rapp R, Muller M, Mandelkow E (1986) On the surface lattice of microtubules: helix starts, protofilament number, seam, and handedness. *The Journal of cell biology* **102:** 1067-1073

Mann M (1999) Quantitative proteomics? *Nature biotechnology* **17:** 954-955

Marklund U, Larsson N, Gradin HM, Brattsand G, Gullberg M (1996) Oncoprotein 18 is a phosphorylation-responsive regulator of microtubule dynamics. *The EMBO journal* **15:** 5290-5298

Marks J, Hyams JS (1985) Localization of F-actin through the cell division cycle of Schizosaccharomyces pombe. *European Journal of Cell Biology* **39:** 27-32

Martin SG, Chang F (2006) Dynamics of the formin for3p in actin cable assembly. *Curr Biol* **16:** 1161-1170

Martin SG, McDonald WH, Yates JR, 3rd, Chang F (2005) Tea4p links microtubule plus ends with the formin for3p in the establishment of cell polarity. *Developmental cell* **8:** 479-491

Marx A, Muller J, Mandelkow E (2005) The structure of microtubule motor proteins. *Adv Protein Chem* **71:** 299-344

Mastronarde DN (1997) Dual-axis tomography: an approach with alignment methods that preserve resolution. *J Struct Biol* **120:** 343-352

Mastronarde DN (2005) Automated electron microscope tomography using robust prediction of specimen movements. *J Struct Biol* **152:** 36-51

Mata J, Nurse P (1997) tea1 and the microtubular cytoskeleton are important for generating global spatial order within the fission yeast cell. *Cell* **89:** 939-949

Matsuyama A, Arai R, Yashiroda Y, Shirai A, Kamata A, Sekido S, Kobayashi Y, Hashimoto A, Hamamoto M, Hiraoka Y, Horinouchi S, Yoshida M (2006) ORFeome cloning and global analysis of protein localization in the fission yeast Schizosaccharomyces pombe. *Nature biotechnology* **24:** 841-847

Matthews LR, Carter P, Thierry-Mieg D, Kemphues K (1998) ZYG-9, a Caenorhabditis elegans protein required for microtubule organization and function, is a component of meiotic and mitotic spindle poles. *The Journal of cell biology* **141:** 1159-1168

May JW, Mitchison JM (1986) Length growth in fission yeast cells measured by two novel techniques. *Nature* **322:** 752-754

McCarthy EK, Goldstein B (2006) Asymmetric spindle positioning. *Curr Opin Cell Biol* **18:** 79-85

Miki F, Okazaki K, Shimanuki M, Yamamoto A, Hiraoka Y, Niwa O (2002) The 14-kDa dynein light chain-family protein Dlc1 is required for regular oscillatory nuclear movement and efficient recombination during meiotic prophase in fission yeast. *Molecular biology of the cell* **13:** 930-946

Miki H, Okada Y, Hirokawa N (2005) Analysis of the kinesin superfamily: insights into structure and function. *Trends Cell Biol* **15:** 467-476

Mimori-Kiyosue Y, Shiina N, Tsukita S (2000) The dynamic behavior of the APC-binding protein EB1 on the distal ends of microtubules. *Curr Biol* **10:** 865-868

Mitchison JM, Nurse P (1985) Growth in cell length in the fission yeast Schizosaccharomyces pombe. *Journal of cell science* **75:** 357-376

Mitchison T, Kirschner M (1984) Dynamic instability of microtubule growth. *Nature* **312:** 237-242

Moon W, Hazelrigg T (2004) The Drosophila microtubule-associated protein mini spindles is required for cytoplasmic microtubules in oogenesis. *Curr Biol* **14:** 1957-1961

Moores CA, Hekmat-Nejad M, Sakowicz R, Milligan RA (2003) Regulation of KinI kinesin ATPase activity by binding to the microtubule lattice. *The Journal of cell biology* **163:** 963-971

Moores CA, Yu M, Guo J, Beraud C, Sakowicz R, Milligan RA (2002) A mechanism for microtubule depolymerization by KinI kinesins. *Mol Cell* **9:** 903-909

Moreno S, Klar A, Nurse P (1991) Molecular genetic analysis of fission yeast Schizosaccharomyces pombe. *Methods in enzymology* **194:** 795-823

Moritz M, Braunfeld MB, Guenebaut V, Heuser J, Agard DA (2000) Structure of the gamma-tubulin ring complex: a template for microtubule nucleation. *Nature cell biology* **2:** 365-370

Morrison EE, Wardleworth BN, Askham JM, Markham AF, Meredith DM (1998) EB1, a protein which interacts with the APC tumour suppressor, is associated with the microtubule cytoskeleton throughout the cell cycle. *Oncogene* **17:** 3471-3477

Moseley JB, Bartolini F, Okada K, Wen Y, Gundersen GG, Goode BL (2007) Regulated binding of adenomatous polyposis coli protein to actin. *The Journal of biological chemistry* **282:** 12661-12668

Musch A (2004) Microtubule organization and function in epithelial cells. *Traffic* **5:** 1-9

Nabeshima K, Kurooka H, Takeuchi M, Kinoshita K, Nakaseko Y, Yanagida M (1995) p93dis1, which is required for sister chromatid separation, is a novel microtubule and spindle pole body-associating protein phosphorylated at the Cdc2 target sites. *Genes & development* **9:** 1572-1585

Nabeshima K, Nakagawa T, Straight AF, Murray A, Chikashige Y, Yamashita YM, Hiraoka Y, Yanagida M (1998) Dynamics of centromeres during metaphase-anaphase transition in fission yeast: Dis1 is implicated in force balance in metaphase bipolar spindle. *Molecular biology of the cell* **9:** 3211-3225

Nakaseko Y, Goshima G, Morishita J, Yanagida M (2001) M phase-specific kinetochore proteins in fission yeast: microtubule-associating Dis1 and Mtc1 display rapid separation and segregation during anaphase. *Curr Biol* **11:** 537-549

Nakaseko Y, Nabeshima K, Kinoshita K, Yanagida M (1996) Dissection of fission yeast microtubule associating protein p93Dis1: regions implicated in regulated localization and microtubule interaction. *Genes Cells* **1:** 633-644

Nathke IS, Adams CL, Polakis P, Sellin JH, Nelson WJ (1996) The adenomatous polyposis coli tumor suppressor protein localizes to plasma membrane sites involved in active cell migration. *The Journal of cell biology* **134:** 165-179

Neuwald AF, Hirano T (2000) HEAT repeats associated with condensins, cohesins, and other complexes involved in chromosome-related functions. *Genome research* **10:** 1445-1452

Niccoli T, Yamashita A, Nurse P, Yamamoto M (2004) The p150-Glued Ssm4p regulates microtubular dynamics and nuclear movement in fission yeast. *Journal of cell science* **117:** 5543-5556

Niethammer P, Kronja I, Kandels-Lewis S, Rybina S, Bastiaens P, Karsenti E (2007) Discrete states of a protein interaction network govern interphase and mitotic microtubule dynamics. *PLoS biology* **5:** e29

Niwa O, Shimanuki M, Miki F (2000) Telomere-led bouquet formation facilitates homologous chromosome pairing and restricts ectopic interaction in fission yeast meiosis. *The EMBO journal* **19:** 3831-3840

Nogales E, Wolf SG, Downing KH (1998) Structure of the alpha beta tubulin dimer by electron crystallography. *Nature* **391:** 199-203

Nurse P, Thuriaux P, Nasmyth K (1976) Genetic control of the cell division cycle in the fission yeast Schizosaccharomyces pombe. *Mol Gen Genet* **146:** 167-178

O'Toole ET, McDonald KL, Mantler J, McIntosh JR, Hyman AA, Muller-Reichert T (2003) Morphologically distinct microtubule ends in the mitotic centrosome of Caenorhabditis elegans. *The Journal of cell biology* **163:** 451-456

O'Toole ET, Winey M, McIntosh JR (1999) High-voltage electron tomography of spindle pole bodies and early mitotic spindles in the yeast Saccharomyces cerevisiae. *Molecular biology of the cell* **10:** 2017-2031

Ohkura H, Garcia MA, Toda T (2001) Dis1/TOG universal microtubule adaptors - one MAP for all? *Journal of cell science* **114:** 3805-3812

Ohtaka A, Saito TT, Okuzaki D, Nojima H (2007) Meiosis specific coiled-coil proteins in Shizosaccharomyces pombe. *Cell division* **2:** 14

Oliferenko S, Balasubramanian MK (2002) Astral microtubules monitor metaphase spindle alignment in fission yeast. *Nature cell biology* **4:** 816-820

Omary MB, Coulombe PA, McLean WH (2004) Intermediate filament proteins and their associated diseases. *The New England journal of medicine* **351:** 2087-2100

Otterbein LR, Graceffa P, Dominguez R (2001) The crystal structure of uncomplexed actin in the ADP state. *Science (New York, NY* **293:** 708-711

Paluh JL, Nogales E, Oakley BR, McDonald K, Pidoux AL, Cande WZ (2000) A mutation in gamma-tubulin alters microtubule dynamics and organization and is synthetically lethal with the kinesin-like protein pkl1p. *Molecular biology of the cell* **11:** 1225-1239

Paravicini G, Cooper M, Friedli L, Smith DJ, Carpentier JL, Klig LS, Payton MA (1992) The osmotic integrity of the yeast cell requires a functional PKC1 gene product. *Molecular and cellular biology* **12:** 4896-4905

Pardo M, Nurse P (2003) Equatorial retention of the contractile actin ring by microtubules during cytokinesis. *Science (New York, NY* **300:** 1569-1574

Pasqualone D, Huffaker TC (1994) STU1, a suppressor of a beta-tubulin mutation, encodes a novel and essential component of the yeast mitotic spindle. *The Journal of cell biology* **127:** 1973-1984

Perez F, Diamantopoulos GS, Stalder R, Kreis TE (1999) CLIP-170 highlights growing microtubule ends in vivo. *Cell* **96:** 517-527

Pierre P, Pepperkok R, Kreis TE (1994) Molecular characterization of two functional domains of CLIP-170 in vivo. *Journal of cell science* **107 (Pt 7):** 1909-1920

Pierre P, Scheel J, Rickard JE, Kreis TE (1992) CLIP-170 links endocytic vesicles to microtubules. *Cell* **70:** 887-900

Pollard TD, Borisy GG (2003) Cellular motility driven by assembly and disassembly of actin filaments. *Cell* **112:** 453-465

Popov AV, Severin F, Karsenti E (2002) XMAP215 is required for the microtubule-nucleating activity of centrosomes. *Curr Biol* **12:** 1326-1330

Pruyne D, Legesse-Miller A, Gao L, Dong Y, Bretscher A (2004) Mechanisms of polarized growth and organelle segregation in yeast. *Annual review of cell and developmental biology* **20:** 559-591

Quinlan RA, Pogson CI, Gull K (1980) The influence of the microtubule inhibitor, methyl benzimidazol-2-yl-carbamate (MBC) on nuclear division and the cell cycle in Saccharomyces cerevisiae. *Journal of cell science* **46:** 341-352

Radding JA, Heidler SA, Turner WW (1998) Photoaffinity analog of the semisynthetic echinocandin LY303366: identification of echinocandin targets in Candida albicans. *Antimicrobial agents and chemotherapy* **42:** 1187-1194

Ravelli RB, Gigant B, Curmi PA, Jourdain I, Lachkar S, Sobel A, Knossow M (2004) Insight into tubulin regulation from a complex with colchicine and a stathmin-like domain. *Nature* **428:** 198-202

Rehberg M, Graf R (2002) Dictyostelium EB1 is a genuine centrosomal component required for proper spindle formation. *Molecular biology of the cell* **13:** 2301-2310

Rickard JE, Kreis TE (1990) Identification of a novel nucleotide-sensitive microtubule-binding protein in HeLa cells. *The Journal of cell biology* **110:** 1623-1633

Rogers SL, Rogers GC, Sharp DJ, Vale RD (2002) Drosophila EB1 is important for proper assembly, dynamics, and positioning of the mitotic spindle. *The Journal of cell biology* **158:** 873-884

Rowat AC, Lammerding J, Herrmann H, Aebi U (2008) Towards an integrated understanding of the structure and mechanics of the cell nucleus. *Bioessays* **30:** 226-236

Russell P, Nurse P (1986) cdc25+ functions as an inducer in the mitotic control of fission yeast. *Cell* **45:** 145-153

Sagolla MJ, Uzawa S, Cande WZ (2003) Individual microtubule dynamics contribute to the function of mitotic and cytoplasmic arrays in fission yeast. *Journal of cell science* **116:** 4891-4903

Saitoh S, Takahashi K, Yanagida M (1997) Mis6, a fission yeast inner centromere protein, acts during G1/S and forms specialized chromatin required for equal segregation. *Cell* **90:** 131-143

Samso M, Radermacher M, Frank J, Koonce MP (1998) Structural characterization of a dynein motor domain. *Journal of molecular biology* **276:** 927-937

Sandberg K, Mastronarde DN, Beylkin G (2003) A fast reconstruction algorithm for electron microscope tomography. *J Struct Biol* **144:** 61-72

Sandblad L, Busch KE, Tittmann P, Gross H, Brunner D, Hoenger A (2006) The Schizosaccharomyces pombe EB1 homolog Mal3p binds and stabilizes the microtubule lattice seam. *Cell* **127:** 1415-1424

Sato M, Dhut S, Toda T (2005) New drug-resistant cassettes for gene disruption and epitope tagging in Schizosaccharomyces pombe. *Yeast (Chichester, England)* **22:** 583-591

Sato M, Koonrugsa N, Toda T, Vardy L, Tournier S, Millar JB (2003) Deletion of Mia1/Alp7 activates Mad2-dependent spindle assembly checkpoint in fission yeast. *Nature cell biology* **5:** 764-766; author reply 766

Sato M, Toda T (2007) Alp7/TACC is a crucial target in Ran-GTPase-dependent spindle formation in fission yeast. *Nature* **447:** 334-337

Sato M, Vardy L, Angel Garcia M, Koonrugsa N, Toda T (2004) Interdependency of fission yeast Alp14/TOG and coiled coil protein Alp7 in microtubule localization and bipolar spindle formation. *Molecular biology of the cell* **15:** 1609-1622

Satterwhite LL, Pollard TD (1992) Cytokinesis. *Curr Opin Cell Biol* **4:** 43-52

Sawin KE, Lourenco PC, Snaith HA (2004) Microtubule nucleation at non-spindle pole body microtubule-organizing centers requires fission yeast centrosomin-related protein mod20p. *Curr Biol* **14:** 763-775

Sawin KE, Tran PT (2006) Cytoplasmic microtubule organization in fission yeast. *Yeast (Chichester, England)* **23:** 1001-1014

Schiff PB, Fant J, Horwitz SB (1979) Promotion of microtubule assembly in vitro by taxol. *Nature* **277:** 665-667

Schneider SQ, Bowerman B (2003) Cell polarity and the cytoskeleton in the Caenorhabditis elegans zygote. *Annual review of genetics* **37:** 221-249

Shaw RM, Fay AJ, Puthenveedu MA, von Zastrow M, Jan YN, Jan LY (2007) Microtubule plus-end-tracking proteins target gap junctions directly from the cell interior to adherens junctions. *Cell* **128:** 547-560

Shirasu-Hiza M, Coughlin P, Mitchison T (2003) Identification of XMAP215 as a microtubule-destabilizing factor in Xenopus egg extract by biochemical purification. *The Journal of cell biology* **161:** 349-358

Sivadon P, Peypouquet MF, Doignon F, Aigle M, Crouzet M (1997) Cloning of the multicopy suppressor gene SUR7: evidence for a functional relationship between the yeast actin-binding protein Rvs167 and a putative membranous protein. *Yeast (Chichester, England)* **13:** 747-761

Slep KC, Rogers SL, Elliott SL, Ohkura H, Kolodziej PA, Vale RD (2005) Structural determinants for EB1-mediated recruitment of APC and spectraplakins to the microtubule plus end. *The Journal of cell biology* **168:** 587-598

Squire JM (1997) Architecture and function in the muscle sarcomere. *Curr Opin Struct Biol* **7:** 247-257

Srayko M, Quintin S, Schwager A, Hyman AA (2003) Caenorhabditis elegans TAC-1 and ZYG-9 form a complex that is essential for long astral and spindle microtubules. *Curr Biol* **13:** 1506-1511

Steinmetz MO, Stoffler D, Hoenger A, Bremer A, Aebi U (1997) Actin: from cell biology to atomic detail. *J Struct Biol* **119:** 295-320

Strelkov SV, Herrmann H, Aebi U (2003) Molecular architecture of intermediate filaments. *Bioessays* **25:** 243-251

Su LK, Burrell M, Hill DE, Gyuris J, Brent R, Wiltshire R, Trent J, Vogelstein B, Kinzler KW (1995) APC binds to the novel protein EB1. *Cancer Res* **55:** 2972-2977

Swaminathan S (2006) Eisosomes: endocytic portals. *Nature cell biology* **8:** 310

Takahashi K, Chen ES, Yanagida M (2000) Requirement of Mis6 centromere connector for localizing a CENP-A-like protein in fission yeast. *Science (New York, NY* **288:** 2215-2219

Tange Y, Fujita A, Toda T, Niwa O (2004) Functional dissection of the gamma-tubulin complex by suppressor analysis of gtb1 and alp4 mutations in Schizosaccharomyces pombe. *Genetics* **167:** 1095-1107

Tange Y, Hirata A, Niwa O (2002) An evolutionarily conserved fission yeast protein, Ned1, implicated in normal nuclear morphology and chromosome stability, interacts with Dis3, Pim1/RCC1 and an essential nucleoporin. *Journal of cell science* **115:** 4375-4385

Thevenaz P, Ruttimann UE, Unser M (1998) A pyramid approach to subpixel registration based on intensity. *IEEE Trans Image Process* **7:** 27-41

Tilney LG, Bryan J, Bush DJ, Fujiwara K, Mooseker MS, Murphy DB, Snyder DH (1973) Microtubules: evidence for 13 protofilaments. *The Journal of cell biology* **59:** 267-275

Tirnauer JS, Bierer BE (2000) EB1 proteins regulate microtubule dynamics, cell polarity, and chromosome stability. *The Journal of cell biology* **149:** 761-766

Tirnauer JS, Grego S, Salmon ED, Mitchison TJ (2002) EB1-microtubule interactions in Xenopus egg extracts: role of EB1 in microtubule stabilization and mechanisms of targeting to microtubules. *Molecular biology of the cell* **13:** 3614-3626

Tirnauer JS, O'Toole E, Berrueta L, Bierer BE, Pellman D (1999) Yeast Bim1p promotes the G1-specific dynamics of microtubules. *The Journal of cell biology* **145:** 993-1007

Torosantucci L, De Luca M, Guarguaglini G, Lavia P, Degrassi F (2008) Localized RanGTP Accumulation Promotes Microtubule Nucleation at Kinetochores in Somatic Mammalian Cells. *Molecular biology of the cell* **19:** 1873-1882

Tournebize R, Popov A, Kinoshita K, Ashford AJ, Rybina S, Pozniakovsky A, Mayer TU, Walczak CE, Karsenti E, Hyman AA (2000) Control of microtubule dynamics by the antagonistic activities of XMAP215 and XKCM1 in Xenopus egg extracts. *Nature cell biology* **2:** 13-19

Tran PT, Doye V, Chang F, Inoue S (2000) Microtubule-dependent nuclear positioning and nuclear-dependent septum positioning in the fission yeast Schizosaccharomyces [correction of Saccharomyces] pombe. *The Biological bulletin* **199:** 205-206

Tran PT, Marsh L, Doye V, Inoue S, Chang F (2001) A mechanism for nuclear positioning in fission yeast based on microtubule pushing. *The Journal of cell biology* **153:** 397-411

Tulu US, Fagerstrom C, Ferenz NP, Wadsworth P (2006) Molecular requirements for kinetochore-associated microtubule formation in mammalian cells. *Curr Biol* **16:** 536-541

Uzawa S, Li F, Jin Y, McDonald KL, Braunfeld MB, Agard DA, Cande WZ (2004) Spindle pole body duplication in fission yeast occurs at the G1/S boundary but maturation is blocked until exit from S by an event downstream of cdc10+. *Molecular biology of the cell* **15:** 5219-5230

Vale RD (2003) The molecular motor toolbox for intracellular transport. *Cell* **112:** 467-480

Vardy L, Toda T (2000) The fission yeast gamma-tubulin complex is required in G(1) phase and is a component of the spindle assembly checkpoint. *The EMBO journal* **19:** 6098-6111

Vasquez RJ, Gard DL, Cassimeris L (1999) Phosphorylation by CDK1 regulates XMAP215 function in vitro. *Cell motility and the cytoskeleton* **43:** 310-321

Vaughan KT (2005) TIP maker and TIP marker; EB1 as a master controller of microtubule plus ends. *The Journal of cell biology* **171:** 197-200

Vaughan KT, Tynan SH, Faulkner NE, Echeverri CJ, Vallee RB (1999) Colocalization of cytoplasmic dynein with dynactin and CLIP-170 at microtubule distal ends. *Journal of cell science* **112 (Pt 10):** 1437-1447

Venkatram S, Tasto JJ, Feoktistova A, Jennings JL, Link AJ, Gould KL (2004) Identification and characterization of two novel proteins affecting fission yeast gamma-tubulin complex function. *Molecular biology of the cell* **15:** 2287-2301

Vida TA, Emr SD (1995) A new vital stain for visualizing vacuolar membrane dynamics and endocytosis in yeast. *The Journal of cell biology* **128:** 779-792

Wacker IU, Rickard JE, De Mey JR, Kreis TE (1992) Accumulation of a microtubule-binding protein, pp170, at desmosomal plaques. *The Journal of cell biology* **117:** 813-824

Wade RH, Chretien D, Job D (1990) Characterization of microtubule protofilament numbers. How does the surface lattice accommodate? *Journal of molecular biology* **212:** 775-786

Walczak CE, Mitchison TJ, Desai A (1996) XKCM1: a Xenopus kinesin-related protein that regulates microtubule dynamics during mitotic spindle assembly. *Cell* **84:** 37-47

Walther TC, Aguilar PS, Frohlich F, Chu F, Moreira K, Burlingame AL, Walter P (2007) Pkh-kinases control eisosome assembly and organization. *The EMBO journal* **26:** 4946-4955

Walther TC, Brickner JH, Aguilar PS, Bernales S, Pantoja C, Walter P (2006) Eisosomes mark static sites of endocytosis. *Nature* **439:** 998-1003

Wang PJ, Huffaker TC (1997) Stu2p: A microtubule-binding protein that is an essential component of the yeast spindle pole body. *The Journal of cell biology* **139:** 1271-1280

Wani MC, Taylor HL, Wall ME, Coggon P, McPhail AT (1971) Plant antitumor agents. VI. The isolation and structure of taxol, a novel antileukemic and antitumor agent from Taxus brevifolia. *J Am Chem Soc* **93:** 2325-2327

Wegner A, Isenberg G (1983) 12-fold difference between the critical monomer concentrations of the two ends of actin filaments in physiological salt conditions. *Proc Natl Acad Sci U S A* **80:** 4922-4925

West RR, Malmstrom T, McIntosh JR (2002) Kinesins klp5(+) and klp6(+) are required for normal chromosome movement in mitosis. *Journal of cell science* **115:** 931-940

West RR, Malmstrom T, Troxell CL, McIntosh JR (2001) Two related kinesins, klp5+ and klp6+, foster microtubule disassembly and are required for meiosis in fission yeast. *Molecular biology of the cell* **12:** 3919-3932

White SR, Evans KJ, Lary J, Cole JL, Lauring B (2007) Recognition of C-terminal amino acids in tubulin by pore loops in Spastin is important for microtubule severing. *The Journal of cell biology* **176:** 995-1005

Whittington AT, Vugrek O, Wei KJ, Hasenbein NG, Sugimoto K, Rashbrooke MC, Wasteneys GO (2001) MOR1 is essential for organizing cortical microtubules in plants. *Nature* **411:** 610-613

Wiese C, Zheng Y (2000) A new function for the gamma-tubulin ring complex as a microtubule minus-end cap. *Nature cell biology* **2:** 358-364

Wittmann T, Bokoch GM, Waterman-Storer CM (2004) Regulation of microtubule destabilizing activity of Op18/stathmin downstream of Rac1. *The Journal of biological chemistry* **279:** 6196-6203

Wittmann T, Desai A (2005) Microtubule cytoskeleton: a new twist at the end. *Curr Biol* **15:** R126-129

Wolff B, Sanglier JJ, Wang Y (1997) Leptomycin B is an inhibitor of nuclear export: inhibition of nucleo-cytoplasmic translocation of the human immunodeficiency virus type 1 (HIV-1) Rev protein and Rev-dependent mRNA. *Chemistry & biology* **4:** 139-147

Wolyniak MJ, Blake-Hodek K, Kosco K, Hwang E, You L, Huffaker TC (2006) The regulation of microtubule dynamics in Saccharomyces cerevisiae by three interacting plus-end tracking proteins. *Molecular biology of the cell* **17:** 2789-2798

Wood V, Gwilliam R, Rajandream MA, Lyne M, Lyne R, Stewart A, Sgouros J, Peat N, Hayles J, Baker S, Basham D, Bowman S, Brooks K, Brown D, Brown S, Chillingworth T, Churcher C, Collins M, Connor R, Cronin A, Davis P, Feltwell T, Fraser A, Gentles S, Goble A, Hamlin N, Harris D, Hidalgo J, Hodgson G, Holroyd S, Hornsby T, Howarth S, Huckle EJ, Hunt S, Jagels K, James K, Jones L, Jones M, Leather S, McDonald S, McLean J, Mooney P, Moule S, Mungall K, Murphy L, Niblett D, Odell C, Oliver K, O'Neil S, Pearson D, Quail MA, Rabbinowitsch E, Rutherford K, Rutter S, Saunders D, Seeger K, Sharp S, Skelton J, Simmonds M, Squares R, Squares S, Stevens K, Taylor K, Taylor RG, Tivey A, Walsh S, Warren T, Whitehead S, Woodward J, Volckaert G, Aert R, Robben J, Grymonprez B, Weltjens I, Vanstreels E, Rieger M, Schafer M, Muller-Auer S, Gabel C, Fuchs M, Dusterhoft A, Fritzc C, Holzer E, Moestl D, Hilbert H, Borzym K, Langer I, Beck A, Lehrach H, Reinhardt R, Pohl TM, Eger P, Zimmermann W, Wedler H, Wambutt R, Purnelle B, Goffeau A, Cadieu E, Dreano S, Gloux S, Lelaure V, Mottier S, Galibert F, Aves SJ, Xiang Z, Hunt C, Moore K, Hurst SM, Lucas M, Rochet M, Gaillardin C, Tallada VA, Garzon A, Thode G, Daga RR, Cruzado L, Jimenez J, Sanchez M, del Rey F, Benito J, Dominguez A, Revuelta JL, Moreno S, Armstrong J, Forsburg SL, Cerutti L, Lowe T, McCombie WR, Paulsen I, Potashkin J, Shpakovski GV, Ussery D, Barrell BG, Nurse P (2002) The genome sequence of Schizosaccharomyces pombe. *Nature* **415:** 871-880

Xiao H, Verdier-Pinard P, Fernandez-Fuentes N, Burd B, Angeletti R, Fiser A, Horwitz SB, Orr GA (2006) Insights into the mechanism of microtubule stabilization by Taxol. *Proc Natl Acad Sci U S A* **103:** 10166-10173

Yamamoto A, West RR, McIntosh JR, Hiraoka Y (1999) A cytoplasmic dynein heavy chain is required for oscillatory nuclear movement of meiotic prophase and efficient meiotic recombination in fission yeast. *The Journal of cell biology* **145:** 1233-1249

Yamashita A, Yamamoto M (2006) Fission yeast Num1p is a cortical factor anchoring dynein and is essential for the horse-tail nuclear movement during meiotic prophase. *Genetics* **173:** 1187-1196

Yarbro JW (1992) Mechanism of action of hydroxyurea. *Seminars in oncology* **19:** 1-10

Yeh E, Yang C, Chin E, Maddox P, Salmon ED, Lew DJ, Bloom K (2000) Dynamic positioning of mitotic spindles in yeast: role of microtubule motors and cortical determinants. *Molecular biology of the cell* **11:** 3949-3961

Yildiz A, Selvin PR (2005) Kinesin: walking, crawling or sliding along? *Trends Cell Biol* **15:** 112-120

Young ME, Karpova TS, Brugger B, Moschenross DM, Wang GK, Schneiter R, Wieland FT, Cooper JA (2002) The Sur7p family defines novel cortical domains in Saccharomyces cerevisiae, affects sphingolipid metabolism, and is involved in sporulation. *Molecular and cellular biology* **22:** 927-934

Zhang X, Lester RL, Dickson RC (2004) Pil1p and Lsp1p negatively regulate the 3-phosphoinositide-dependent protein kinase-like kinase Pkh1p and downstream signaling pathways Pkc1p and Ypk1p. *The Journal of biological chemistry* **279:** 22030-22038

Zheng L, Schwartz C, Wee L, Oliferenko S (2006) The fission yeast transforming acidic coiled coil-related protein Mia1p/Alp7p is required for formation and maintenance of persistent microtubule-organizing centers at the nuclear envelope. *Molecular biology of the cell* **17:** 2212-2222

Zimmerman S, Chang F (2005) Effects of {gamma}-tubulin complex proteins on microtubule nucleation and catastrophe in fission yeast. *Molecular biology of the cell* **16:** 2719-2733

Zimmerman S, Tran PT, Daga RR, Niwa O, Chang F (2004) Rsp1p, a J domain protein required for disassembly and assembly of microtubule organizing centers during the fission yeast cell cycle. *Developmental cell* **6:** 497-509

Zumbrunn J, Kinoshita K, Hyman AA, Nathke IS (2001) Binding of the adenomatous polyposis coli protein to microtubules increases microtubule stability and is regulated by GSK3 beta phosphorylation. *Curr Biol* **11:** 44-49